NASA CR-66346

STUDY AND PRELIMINARY DESIGN OF AN ISOTOPE-HEATED CATALYTIC OXIDIZER SYSTEM (U)

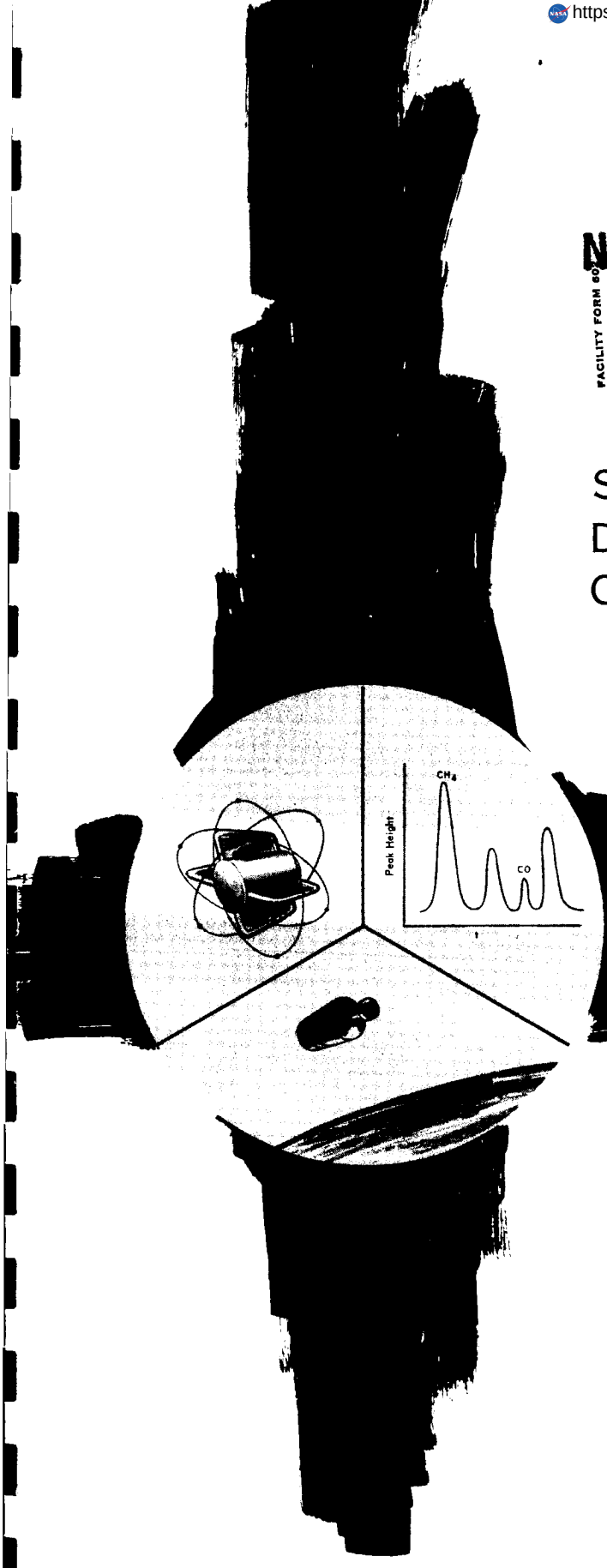

PREPARED UNDER CONTRACT NAS 1-6256
by BIOTECHNOLOGY
Lockheed Missiles & Space Company
Sunnyvale, California

NATIONAL AERONAUTICS AND SPACE ADMINISTRATION
LANGLEY RESEARCH CENTER, LANGLEY STATION ● HAMPTON, VIRGINIA

NASA CR-66346

STUDY AND PRELIMINARY DESIGN OF AN ISOTOPE-HEATED CATALYTIC OXIDIZER SYSTEM (U)

Prepared Under Contract No. NAS 1-6256
by
Biotechnology Organization
Lockheed Missiles & Space Company
Sunnyvale, California

Thomas M. Olcott

NATIONAL AERONAUTICS AND SPACE ADMINISTRATION
Langley Research Center
Langley Station
Hampton, Virginia

PRECEDING PAGE BLANK NOT FILMED.

LOCKHEED MISSILES & SPACE COMPANY

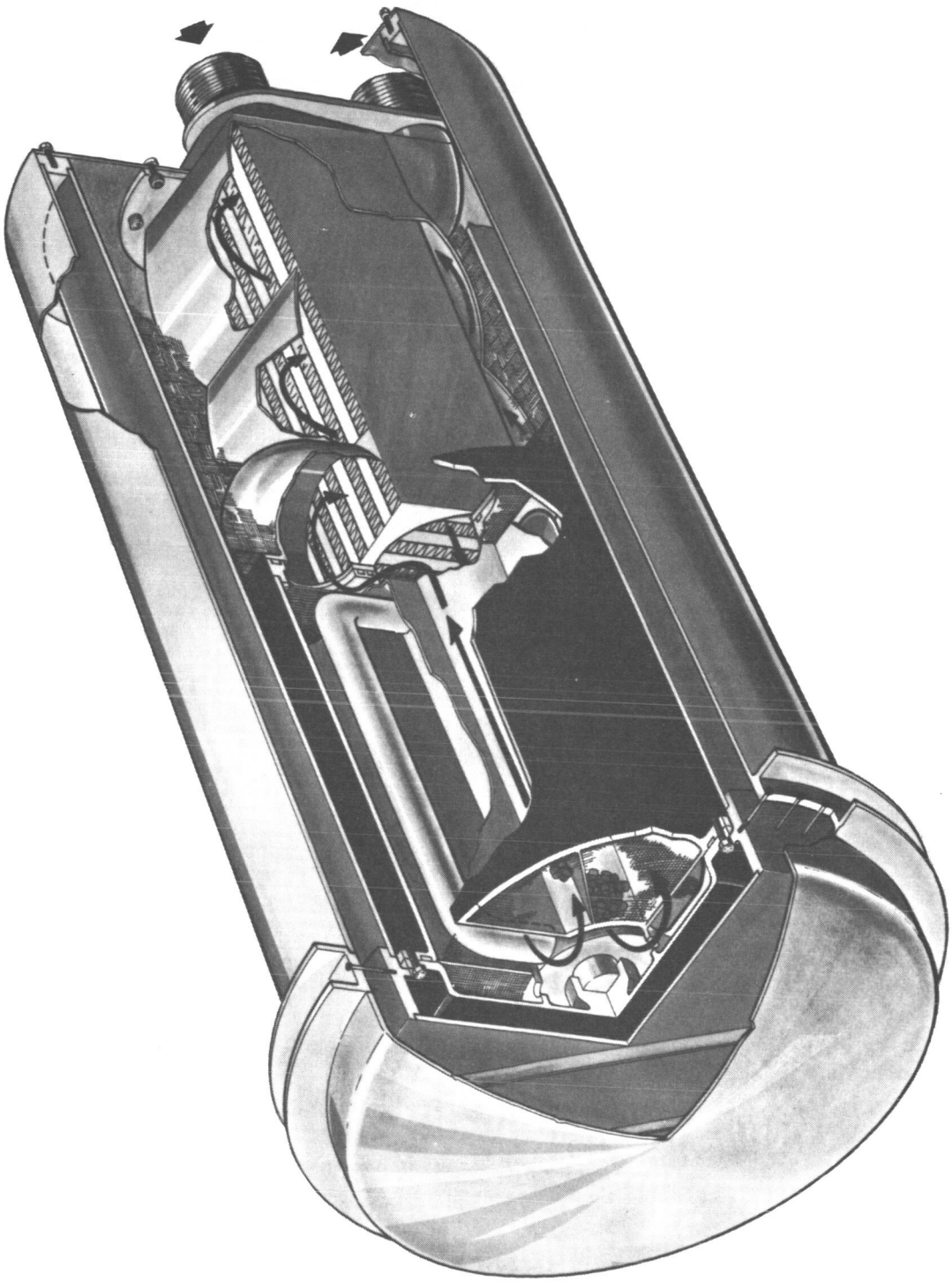

Isotope Heated Catalytic Oxidizer – Moist Gas Version

LIST OF CONTRIBUTORS

Name	Area of Contribution
T. M. Olcott	Project Direction
R. W. Joy	System Design
R. A. Lamparter	Analysis and Optimization
E. H. Kawasaki	Catalyst Evaluation
O. T. Leong	Catalyst Evaluation
R. J. Jaffe	Radiation Analysis
T. E. Adamson	Report Integration

Subcontract – TRW Systems

A. P. Shlosinger	TRW Project Direction
J. C. Stansel	Heat Source Design
H. Lurie	Heat Source Design

NASA TECHNICAL MONITOR

Rex Martin

Life Support Section
Flight Instrument Division
NASA Langley Research Center

CONTENTS

ILLUSTRATIONS

TABLES

STUDY AND PRELIMINARY DESIGN OF AN ISOTOPE-HEATED CATALYTIC OXIDIZER SYSTEM

By Thomas M. Olcott
Biotechnology
Lockheed Missiles & Space Company

SUMMARY

A design study was performed to develop an isotope-heated catalytic oxidizer system (IHCOS). The design was based on the requirements of a typical early space station which should have a high probability of implementation within the next decade. A crew size of nine men and mission duration of 180 days was selected for this study. The contaminant load anticipated for this spacecraft was determined and the results indicated a need for a catalytic oxidizer capable of controlling methane, carbon monoxide, hydrogen and a number of hydrocarbons.

A study was made to establish the radioisotope most suitable for use in IHCOS. Conceptual designs of alternative radioisotope heat sources were accomplished in order to determine approximate weights of the isotope capsules. A comparative study was then performed and the final radioisotope selection was based on minimum system weight commensurate with mission objectives, availability, cost, and safety constraints. The selected isotope fuel is Pu-238.

A number of candidate catalysts were experimentally evaluated to determine their relative effectiveness for methane oxidation. The results of this effort indicated that for a particular dispersion technique, catalyst activity increased with increasing metal weight up to a point of nearly complete coverage. The 0.5 percent and 1.0 percent palladium catalysts manufactured by Engelhard had the highest activity of any of the catalysts evaluated. The 0.5 percent palladium was selected for use in IHCOS since its performance was essentially the same as the 1.0 percent palladium, and its cost and availability are much more favorable.

Following the selection of a catalyst for use in IHCOS, an experimental effort was conducted to parametrically establish the performance of this catalyst to support the analysis and optimization task. In this effort, data were obtained on methane conversion efficiency in a background of competing contaminants, as a function of space velocity and catalyst bed temperature.

The data on catalyst performance was used to perform an analysis and optimization study in order to define the optimum configuration for IHCOS. This optimization study was based on establishing a unit resulting in a minimum total equivalent weight. However, the final design configuration was also influenced by economic considerations. The results of this study dictated the insulation, power, heat exchanger effectiveness, operating temperature, and catalyst volume requirements for IHCOS.

Once the operating parameters for IHCOS were established, a long-term test of the catalyst was initiated. The objective of this test was to determine if the catalyst performance degrades with time. During the test, the catalyst was operated with a representative background gas, including a number of competing contaminants. This test revealed that catalyst degradation did occur and that this degradation could be attributed to the presence of water vapor in the background gas stream. It was concluded that the two operating regions existed, one with normal cabin moisture in the gas stream (moist gas), and the other with a very low dew point (dry process gas).

The optimization study previously performed was valid for the dry process gas unit. A second optimization study, utilizing trends established in the first study, was performed to define the configuration of the moist gas unit.

A design of the isotope heat source and catalyst canister was performed for both the moist and dry process gas versions of IHCOS. This design effort resulted in layout drawings of both the moist and dry process gas units. The design effort also included a radiation dose analysis for each configuration. The results of this effort indicated that for either version of IHCOS the radiation dose level is considerably less than 5 percent of the total allowable accumulated for a 1.5 meter average separation distance.

A development plan was prepared to furnish a planning document for implementing the detailed design fabrication and evaluation of a space flight qualifiable isotope-heated catalytic oxidizer system. Phase II of this effort deals with a unit utilizing a resistively heated-simulated isotope, and Phase III describes the effort required to complete the isotopically heated unit.

INTRODUCTION

The NASA-Langley Research Center, recognizing future manned space program requirements, directed the Lockheed Missiles & Space Company (LMSC) to initiate the development of a flight qualifiable isotope-heated catalytic oxidizer for control of trace contaminants. Trace contaminant control by catalytic oxidation has received attention under other programs such as NAS 9-3415, "Contaminant Removal System for Apollo." However, these prior programs dealt only with electrically heated catalytic oxidizers, and did not include any long-term catalyst performance evaluation tests. This program involved the study and design of an isotope heat source, and the selected catalyst was evaluated experimentally for the full mission duration (180 days).

The specific purpose of this investigation was to conduct a preliminary design to establish the feasibility and desirability of an isotope-heated catalytic oxidizer.

The tasks involved in the program were to:

- Define the mission or missions for which an isotope-heated catalytic oxidizer is desirable
- Describe expected contaminant types and production rates for the mission of greatest interest
- Select a preferred isotope based on a study of all critical aspects of the isotope fuel element including, but not limited to, cost, availability, weight, volume, aerospace safety, and reliability
- Conduct catalyst screening tests and select a preferred catalyst for this application
- Perform catalyst tests to obtain necessary data for the oxidizer analysis, optimization, and design
- Perform an analysis and optimization study to determine the configuration having the least penalty and to establish that this configuration will function satisfactorily under flow shut-down and other "off-design" conditions
- Perform an extended-duration (180-day) test of the selected catalyst under expected operating conditions of flow and temperature, to determine if significant degradation of catalyst performance occurs
- Design the isotope heat source, including considerations of containment, configuration, compatibility with the fuel, heat transfer, logistics, and other critical factors

- Prepare layout-type drawings to define the optimum isotope-heated catalytic oxidizer, in sufficient depth to allow subsequent detailed manufacturing drawings to be prepared

- Prepare in detail the development plan to carry this program through prototype development and evaluation; provide manpower estimates on subsequent phases required for flight qualification.

This report describes in detail the results of the effort conducted for each of the above tasks. The results of these efforts will permit the immediate implementation of the subsequent phases of this program described in the development plan.

Information relating to the power density, specific materials of construction, and radiation intensity of the isotope heat source, are described in a classified summary of this report.

MISSION DEFINITION

This section presents the results of a brief study of potential mission and spacecraft characteristics to ascertain how these characteristics influence the IHCOS design and to select a mission and spacecraft model.

Mission and Spacecraft Characteristics Affecting Design

Mission and spacecraft characteristics will have an effect on the relative advantages of the use of an isotope-heated catalytic trace contaminant oxidizer. A summary of the effects of mission characteristics is provided here. In the next section, the specific model mission and spacecraft selected for IHCOS design is discussed with the rationale for the selected parameters.

Mission duration. – Duration of a mission affects the total amount of thermal energy required for the operation of a catalytic trace contaminant oxidizer. As thermal energy can be provided by an isotope heat source at a lower weight penalty than by another energy source, the savings attained by the use of the isotope heat source will increase when mission length increases, provided that the competing power source uses expendables as a source of energy. Typical for this type of situation is a tradeoff between an isotope heat source and electric heating, with fuel cells as power source.

Where the source of electric power is of a type not requiring expendables for power generation as, for example, would be the case with the use of solar cells, the tradeoff would be made relative to the installed weight of the electric power generating system, and mission duration would have a lesser influence.

The power emission characteristics of the isotope will require matching to the duration of the mission. An isotope heat source decays exponentially. In order to have a reasonable constant energy output, the isotope half-life should be long relative to mission duration. On the other hand, as the weight of the isotope heat source per unit of energy available from it is relatively constant, selection of an isotope with a half-life which is excessively long will increase the isotope weight, because too large a fraction of energy will not be used and will still be available at the end of the mission.

Prelaunch considerations. – The time between isotope manufacture and launch date will require consideration in isotope selection. Decay of the isotope starts immediately after its manufacture and the time span prior to launch must be included in the mission duration from the viewpoint of isotope half-life selection. Launch date uncertainties must, therefore, be allowed for when the half-life is stipulated. Because of the peculiarities of available isotopes, usually half-lives considerably in excess of those required will be selected and an adequate leeway in launch date will exist.

Crew size. – Since man is one of the sources of contaminants, the contaminant production rate and, hence, the power requirement and size of IHCOS will depend strongly on the crew size. In general, the larger the crew size, the larger the unit; however, the weight savings will be greater by using an isotope heat source over a resistance heat source. Excessively large power requirements may limit the choice of isotopes which can be used due to availability considerations.

Atmosphere. – The effects of the spacecraft atmosphere on the IHCOS design include fan power and heat transfer. As the gas density in the cabin increases, the fan power and quantity of heat transfer surface required for a given contaminant removal capability tends to increase. Thus, the IHCOS design is somewhat sensitive to the spacecraft atmosphere. However, this is probably not a major effect.

Leakage. – One of the primary criteria concerning the profitable use of IHCOS is the relationship between vehicle leakage rate, the production rate, and allowable concentration of contaminants that are primarily removed by catalytic oxidation.

Figure 1 indicates this relationship between vehicle leakage, contaminant production, and allowable concentration. If vehicle leakage exceeds the amount indicated for a given production rate and allowable concentration, no active removal system is required; if, on the other hand, it is less, an active removal system is required. The operating temperature of IHCOS is established by the contaminant most difficult to oxidize for which an active removal system is required. Therefore, if an active removal system is required for methane (the most difficult contaminant to oxidize) the operating temperature of the oxidizer is then set by methane removal requirements.

Vehicle power penalty. – The vehicle power source and thus, vehicle power penalty, has an effect on the weight-saving to be realized by utilizing an isotope source for heating. However, since the weight penalty for electrical power is quite high for all types of spacecraft electrical power systems compared to the approximate 20 lb/kw for an isotope heater, the decision to utilize an isotope heat source is not strongly dependent upon the nature of the spacecraft electrical power system.

Environmental requirements. – Like all other spacecraft components, IHCOS must be designed to withstand the effects of launch, acceleration, shock, and vibration. The impact of this, in terms of design, is not major; however, as the environmental requirements become more rigorous, the unit weight will tend to increase.

Selected Mission and Spacecraft Model

A discussion of the selection of a specific mission and vehicle model follows. Study results are summarized in Table 1; the rationale for the selected mission and spacecraft parameters is presented in the discussion. In selection of the mission model, consideration has been given to the probability of an actual mission as well as the suitability of the mission for the IHCOS application. The assumed mission is one which should have a high probability of implementation within the next decade.

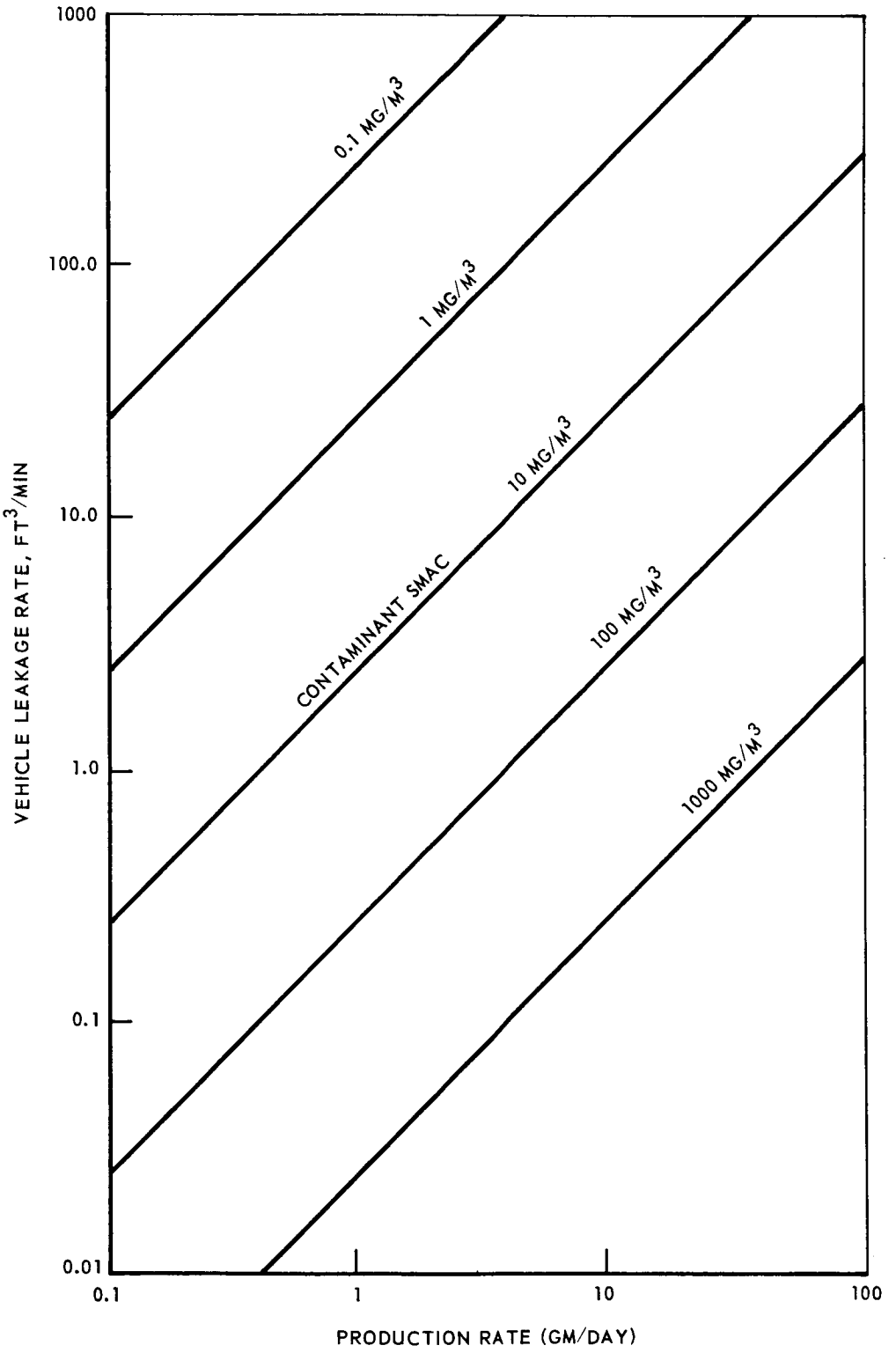

Fig. 1 Contaminant Concentration vs Leakage and Production Rates

TABLE 1

SUMMARY OF SELECTED MISSION AND SPACECRAFT MODEL

Spacecraft Mission	
Purpose	Earth-Orbiting Laboratory
Duration	180-Days
Orbit Geometry	Earth Orbit
Prelaunch Considerations	90-day Prelaunch Time Interval
Spacecraft Model	
Atmosphere	10 psia total pressure, 31% O_2 – 69% N_2
Leakage	2.9 pounds per day at 10 psia
Power Available	28 volt dc or 115 volt ac 400 cps
Power Penalty	400 pounds per kilowatt
Environmental Requirements	Temperature, acceleration, vibration and shock as defined in the discussion

Spacecraft mission. – The selected spacecraft mission includes discussion of the mission purpose, mission duration, orbit geometry, and prelaunch considerations.

Purpose: The mission purpose is assumed to be an earth-orbiting laboratory used for experimental investigation, such as a test bed for evaluation of advanced mission systems. It will be assumed that no experiments will require special radiation-sensitive experiment protection.

Duration: Space station studies have indicated a variety of mission durations. Among these appropriate for IHCOS are the AES Independent Module with proposed mission durations of 48 days to 1 year; MORL, with proposed durations of 1 to 10 years; and the Langley ILSS, which was designed for missions of 6 months to 1 year. Since most of these space station studies have indicated missions of 180 days or greater, and the range of missions spelled out in the Work Statement is 90 to 180 days, the maximum limit of 180 days is selected.

Orbit parameters: The spacecraft will be assumed to be in earth orbit. The radiation dose from IHCOS will be maintained at a low level, such as 1– 20 rem/ 180 days, so as to not significantly limit the vehicle in orbit altitude or inclination by preempting the allowable dose.

Prelaunch considerations: A number of activities must transpire between isotope manufacture and launch date. The isotope source will have to be checked out, transported to the launch site, installed in the spacecraft prior to spacecraft system checkout, and then remain onboard until launch time. This time period will include any uncertainties in the launch date. It appears that this period of time could be as great as 90 days; therefore, a 90-day prelaunch interval will be assumed for the IHCOS study.

Spacecraft model. – The spacecraft is assumed to be an orbiting laboratory used for experimental investigation. The selected spacecraft characteristics include crew size, atmosphere, vehicle leakage, type of vehicle power, power penalty, and environmental requirements.

Crew size: A crew of 9 is selected for the IHCOS design study for two reasons: (1) space station studies such as MORL and the AES Independent Module have indicated crew sizes up to 9 men, usually in multiples of three; (2) it is near the mean of the range of crew sizes indicated in the Work Statement.

Atmosphere: A total pressure of 10 psia with 31 percent O_2 and the balance N_2 is selected as the nominal design atmosphere. This atmosphere has been selected to be compatible with the Langley ILSS, and would thus allow IHCOS to be installed in ILSS for evaluation purposes. Consideration will be given to the impact of operating IHCOS at the MORL atmosphere of 7 psia 50 percent O_2, 50 percent N_2, and the AES atmosphere of 5 psia 70 percent O_2, 30 percent N_2.

Leakage: Proposed spacecraft leakage rates vary widely. The NASA AES space station consisting of the Apollo CSM and Independent Module, has a leakage rate at 10 psia of approximately 18.0 pounds per day. This leakage rate was agreed upon by NASA and NAA for the NAA study of this vehicle (NAS 9-5017). The MORL space station has a proposed leakage rate of 2.9 pounds per day at 10 psia (NAS 1-3612).

The proposed MORL leak rate is considerably below the Apollo CSM and Independent Module. This is because it is an integral vehicle whereas AES is an Apollo, docked with another vehicle, and thus includes the Apollo leakage, the docking interface leakage, and the Independent Module leakage.

It appears that the MORL leak rate is more conservative in increasing the load on the trace contaminant removal system, and more nearly represents an advanced space station. For these reasons, a leakage rate of 2.9 pounds per day is selected for the IHCOS development.

Power available: Electrical power required for controls and instrumentation for the simulated electrically-heated isotope source will be considered to be available at either 28 volts dc, or 115 volts ac 400 cps. These two power services represent the type of source most likely to be found on a spacecraft.

Vehicle power penalty: Proposed spacecrafts utilizing solar cell power sources, such as MORL and MOL, have power penalties in the range of 500 to 600 pounds per kilowatt. Vehicles with isotope sources and Rankine, or other proposed fluid cycles such as the Langley ILSS and AES, have power penalties in the range of 300 to 400 lb/kw. Since direct isotope heating at approximately 10 lb/kw is quite competitive with any of the above penalties, a representative yet conservative penalty of 400 lb/kw is selected for use in the IHCOS design study.

Environmental requirements: The critical environmental requirements for IHCOS are temperature, acceleration, and vibration, applied during boost and shock loads. During the design effort consideration, but not a complete analysis, will be given to the strength of construction materials for the following environmental requirements:

Temperature:

Boost – Maximum $150^{o}F$
– Minimum $0^{o}F$

Acceleration:

Boost – Along x-x axis 7 g for 5 minutes
Space operation – None

Vibration:

The following vibration levels are imposed on three mutually perpendicular axes for 30 minutes each axis:

Launch

Sinusoidal Vibration Levels – 0.30 g at 5 cps with linear increase to 8.5 at 100 cps; 8.5 g from 100 cps to 300 cps with linear decrease to 5 g at 2000 cps.

Random Vibration Levels – 0.0063 g^2/cps at 5 cps, with linear increase to 0.095 g^2/cps at 50 cps; 0.095 g^2/cps from 50 cps to 150 cps with a linear decrease to 0.0035 g^2/cps at 2000 cps.

Space Operation

Sinusoidal Vibration Levels – 0.16 g at 5 cps, with a linear increase to 3.5 g at 300 cps; 3.5 g at 300 cps with a linear decrease to 2.5 g at 2000 cps.

Random Vibration Levels – 0.007 g^2/cps at 5 cps with a linear increase to 0.04 g^2/cps at 100 cps; 0.04 g^2/cps at 100 cps to 200 cps with a linear decrease to 0.015 g^2/cps at 2000 cps.

Shock:

Boost and space operation any direction for 11 milliseconds – -70 g

The above loads are taken from the Apollo Saturn vehicles, and are considered typical for the IHCOS design study.

CONTAMINANT LOAD DEFINITION

The contaminant types and production rates for the IHCOS design study are based on data obtained from recent manned space flights, ground test data, and space station studies. The allowable concentration data are based on values established by toxicologists working in the field of spaceflight toxicology. These concentrations are considered to be appropriate for continuous exposure up to 180 days. The contaminant load data is presented in Appendix A. The appendix includes (1) the contaminants considered to be appropriate for the mission selected for the IHCOS study; (2) the biological, nonbiological, and total contaminant production rates; (3) the allowable contaminant concentrations; (4) the data source on both production rate and allowable concentration; (5) whether or not the contaminant is primarily removed by oxidation; and (6) the catalytic oxidizer flow rate required for removal of the contaminant.

Selected Contaminants

A study was made to establish what contaminants might be expected to exist in the model spacecraft selected for the IHCOS Program. The contaminants selected are presented in Appendix A, and were obtained from the following sources: (1) outgassing products from materials testing of space cabin qualified materials as measured by Lockheed Missiles & Space Company (ref. 1), North American Aviation (ref. 2), and Minneapolis Honeywell (ref. 3), (2) contaminants detected in Mercury and Gemini (through GT7) charcoal beds (ref. 4), (3) contaminants detected in the AF Biosatellite 30-day test (ref. 5), (4) contaminants reported by Toliver and Morris in the manned 30-day test at the AF Aerospace Medical Research Laboratory (ref. 6), (5) contaminants detected in a 27-day manned test at the AF School of Aerospace Medicine (ref. 7), (6) contaminants detected during Apollo breadboard testing (ref. 8) and, (7) candidates likely to result from experiments onboard space stations such as MORL and AES (ref. 9). A list of some pertinent chemical synonyms is also presented in Appendix A.

Contaminant Production Rates

The major source of quantitative information on nonbiological (equipment and materials) contaminant production rates was the contaminant identification program conducted by NAA for the Apollo Program. In this effort, the outgassing rate of materials within the Apollo was determined experimentally and indicated that the total quantity of contaminants produced by equipment in Apollo is 2.5 grams/day. This work was accomplished by placing spacecraft materials in a 5 psia oxygen environment for 14 days. The material was kept at its expected operating temperature for the entire period. At the end of the 14 days, the atmosphere within the closed test chamber was analyzed to determine the type and quantity of contaminants evolved. These data were then used, based upon the total quantity of the material tested within the spacecraft, to estimate contaminant production rates. At the present time, approximately 25 percent of the materials within the Apollo spacecraft have been tested. The 2.5 gram/day estimate is four times the production rate determined for 25 percent of the materials in the Apollo command module.

As a preliminary design estimate it can be assumed that the mass of internal materials and equipment within a spacecraft is proportional to the total gross weight of the spacecraft. Based on this assumption, an estimate of the equipment contaminant production for the model spacecraft can be made by multiplying the 2.5 grams/day by the ratio of the model spacecraft weight to the Apollo Command Module weight. A space station placed in a 300-mile orbit by a Saturn C5 booster is expected to weigh approximately 220,000 pounds. Since the Apollo Command Module weighs 11,000 pounds, the model spacecraft would be 20 times the weight of an Apollo Command Module. Based on this ratio, a total equipment contaminant production rate of 50 grams per day is estimated for the model spacecraft.

To determine the individual equipment contaminant production rates, the contaminant distribution (i.e., percentage of total) from the NAA Program was utilized with the exception that no primary contaminant was considered to be produced at a rate less than 5 percent of the total and no secondary contaminant was considered to be produced at a rate less than 0.5 percent of the total. Primary contaminants are those where a known large source exists or where the contaminant has been identified in several systems. The remaining contaminants are defined as secondary contaminants.

The majority of production rates for contaminants indicated as metabolic products were based on reported quantitative production rates for humans. Where no quantitative data were available, a minimum production capability of 0.25 gm/day was assumed.

Allowable Concentration

Contaminant allowable concentration estimates are needed to establish the required performance characteristics of IHCOS. The footnotes listed in Appendix A indicate the basis of estimation for each contaminant. In some instances these are based on gross approximations. The major data sources for allowable concentrations, listed in the order of preference are:

(1) Submarine Habitability Handbook values. – These concentrations for 90-day exposure in a normal atmosphere are based on long-term exposure studies of animals at 760 mmHg pressure and are believed to be the most applicable data available as a basis for conversion to extended space station atmosphere purity specifications.

(2) 1965 Threshold Limit Values (TLV) of the American Conference of Governmental Industrial Hygienists. – These values "represent concentrations under which it is believed that nearly all workers may be repeatedly exposed, day after day, without adverse effect," on the basis of an 8-hour work-day for five working days per week. For application to space station atmosphere purity specification, LMSC recommends 0.1 of the TLV as the maximum allowable space cabin atmosphere contaminant concentration (Space – MAC). This reduction is an attempt to account for the added stresses of continuous exposure and other factors, such as zero or low-g, unusual atmosphere, radiation, and mixtures of contaminants that would be encountered onboard a spacecraft. The numerical value of 0.1 is somewhat arbitrary. Others have proposed values from 0.3 to 0.02 for individual contaminants. The average ratio of the submarine limits to the TLVs is about 0.06.

(3) Analogy to chemical compounds with established TLV. – Utilizing homolog analogies, which are valid for chemical reaction studies, is probably a valid approximation method. It has been used where necessary.

(4) Vapor pressure limitation. – For substances for which no industrial TLV has been determined, or no other toxicological data exist, it seems desirable to set a limit on the vapor pressure of the compound. For this work, a low vapor pressure of 0.02 torr was used. This arbitrary limit was used in NAS 9-3415 (ref. 10).

The estimates presented in Appendix A for maximum allowable concentrations have been reviewed by Lockheed Missiles & Space Company toxicologists and are considered appropriate for the design of a trace contaminant removal system for the selected mission.

Contaminants to be Removed by Oxidation

In determining the contaminants to be removed by oxidation, consideration was given to the following factors:

- Ease of oxidation
- Sorbents required for control of potential catalyst poisons or contaminants whose oxidation produces noxious or toxic products.
- Removal of contaminants by other components of the life support systems.

Since the catalytic oxidizer will be operating at a temperature high enough to oxidize methane, it is estimated that it will oxidize all of the remaining contaminants listed in Appendix A. However, many of the contaminants listed will be removed by other processes existing within the life support system, such as water condensation within the humidity control system, sorption in the CO_2 removal system, vehicle leakage, or by the presorbent provided to remove those contaminants that product undesirable products or poison the catalyst.

Thus the process used in establishing the contaminants to be removed by oxidation was as follows: The contaminant removal capability of the other life support systems was estimated to determine what contaminants they would control. This removal capability was then compared with the total load indicated in Appendix A, to determine what fraction of the total load can be handled by removal systems other than oxidation. The contaminants not controlled to suitable levels by these methods were then considered to be removed by oxidation.

Catalytic Oxidizer Flow

A tentative estimate of the IHCOS flow rate required for removal of the contaminants indicated to be removed by oxidation is presented in Appendix A. This flow rate estimate was based on an IHCOS removal efficiency per pass of 80 percent for all contaminants considered except methane.

$$\text{Removal Efficiency (\%)} = \frac{\text{Inlet Concentration} - \text{Outlet Concentration}}{\text{Inlet Concentration}} \times 100$$

The 80 percent removal efficiency is based on oxidation efficiency tests performed at LMSC with multiple contaminants (ref. 11). Utilizing the maximum required IHCOS flow rate, from Appendix A, of approximately 3 cfm, the removal efficiency required for methane is 27 percent. The flow rate estimates include the effect of the 2.9 pounds per day of vehicle leakage, established under the mission definition task previosuly completed.

Requirements for Pre- and Post-Sorbents

If all of the contaminants listed in Appendix A were exposed to a catalytic oxidizer, it is possible that certain gases might react to more harmful substances which could be injurious to man or to the catalyst.

Catalytic oxidation of compounds containing nitrogen, sulphur, or the halogens may lead to the formation of new compounds of greater toxicity or of acid that would deteriorate equipment. For example, NRL studies of Hopcalite-catalyzed oxidation of Freon-11, -12, and -114 have indicated halogen and acid products formation, and the formation of vinylidine chloride and trichloroethylene from methyl chloroform (ref. 12). LMSC tests have detected SO_2 and NO_2 in the outlet stream of an oxidizer-fed Freon-114, H_2S, and monomethyl hydrazine; the absence of HC1 and HF was attributed to reaction with the monomethyl hydrazine (ref. 13).

To minimize the occurrence of harmful products of oxidation, presorbent material should be provided to reduce the extent to which undesirable contaminants reach the catalytic oxidizer. A majority of the contaminants that produce undesirable products are removed by basic sorbents such as lithium hydroxide. Ammonia, however, is one exception that requires an acidic sorbent for removal.

To further ensure that undesirable products do not reach the cabin, a postsorbent bed should be provided. Previous consideration of this problem (ref. 10) has lead to the conclusion that all of the new toxic species formed are acidic. Tests also showed that H_2S or stronger acids were well-absorbed on LiOH. (The carbonate form is equally effective for these acid-base removal reactions.) It is doubtful whether HCN would be well-absorbed by a base, as it is a weaker acid than H_2S or H_2CO_3. It is felt

that carbonyl chloride and fluoride would be absorbed and decomposed on a basic sorption bed, as it is reported that carbonyl chloride is decomposed by activated charcoal. The other possible toxic species – halogens, halogen acids, NO_2, and SO_2, are effectively removed by a basic sorbent.

It is recommended that a basic sorption medium be used in a postoxidizer bed. Availability of reaction data and of the material itself leads to the use of LiOH as the medium.

ISOTOPE STUDY AND SELECTION

The primary objective of this task was to evaluate alternative isotopic fuel forms, and select the one best suited for application to the catalytic oxidizer system. Conceptual designs of alternative radioisotope heat sources were accomplished in order to determine approximate weights of both isotope capsules and shielding. A comparative study was then performed and the final radioisotope selection was based on minimum system weight commensurate with mission objectives, availability, cost, and safety constraints.

Requirements and Assumptions

The mission and spacecraft requirements pertinent to the comparative analysis are as follows:

- Manned earth-orbiting laboratory
- Mission duration of six months, and a minimum capsule design of two years
- Radioisotope heat source located within the manned cabin
- Prelaunch time delay of approximately 90 days
- An allowable radiation dose to personnel in the range of 1–20 rem over a 180-day period.

In evaluating alternative radioisotope fuel forms, a detailed consideration of isotope half-life, cost, availability, and radiation levels eliminated from further consideration all candidates except Pm-147, Pu-238, and Cm-244. Sr-90 was also included in the study for comparison purposes because of its availability and low cost relative to the other isotopes, even though its radiation dose rate is quite high. The reasons for eliminating Po-210 and Th-171 are also discussed briefly. Aerospace safety dictates that all radioisotopes must be fully contained, not only during the proposed mission life but also in case of a mission abort and return of the spacecraft through the earth's atmosphere. The radioisotope must, therefore, be enclosed in a capsule designed to withstand both operating and possible abort conditions, such as launch pad explosion, reentry, impact, and postimpact corrosive environments. The conceptual capsule and shielding designs for each of the four candidate isotopes were based on the assumption that:

- Fuel loading was 300 watts.
- Encapsulating material was either TZM (Mo-0.5Ti-0.08Zr) or Haynes 25 (Co-10Ni-20Cr-15W) in all cases. Allowable stress for both materials = 50,000 psi, based on a stress-rupture criterion of 1000°F for 2 years.
- Wall thicknesses were based on those required to survive impact.

- Capsule was considered to be a right circular cylinder with flat end caps and an outside L/D = 3.

- Four π radiation shielding was located external to the catalytic burner assembly.

- Attenuation of neutron and gamma radiation by the catalytic material or other structural material between the capsule and shielding was not considered. However, the capsule wall thickness was considered in determining the total shielding thickness required.

- For comparative shielding calculations, an allowable dose rate of 4 mrem/hr was selected at distances of 1 and 3 meters from the centerline of the capsule.

Isotope Comparison

The assumed system configuration is shown in fig. 2, and the results of the conceptual design study are summarized in Table 2. It is clear that the use of plutonium fuel forms result in the lightest weight system. However, the following paragraphs include discussions of the pertinent findings for each of the four isotope systems considered in the study.

Sr-90. – Although the cost and availability of strontium-90 were highly favorable, this isotope was eliminated from further study on the basis of the excessive shielding weight (ref. 14) required to attenuate the bremsstrahlung radiation to acceptable levels.

Pu-238. – The only radioisotope that has been flight-qualified and used operationally in spacecraft power systems is Pu-238. This isotope has the advantage of low radiation levels (and shield weights) relative to those for Pm-147 and Cm-244, and has an attractive half-life (88 years) for long-lived missions.

Recent investigations at Mound Laboratory on PuO_2 (ref. 15), indicated that this fuel form can be produced in microspheres whose sizes are well above the respirable size range. This property, coupled with the extreme insolubility and inertness to chemical attack, tends to make it one of the most biologically safe fuel forms available.

Although alpha decay of the Pu-238 isotope results in a pressure buildup within the capsule, the void resulting from the mechanical packing of the microspheres is sufficiently large to keep the pressure at acceptable small values to insure the two-year ($1000^{o}F$) design life of the capsule. At this temperature and pressure, stress-rupture (creep) of either the TZM or Haynes-25 encapsulating material is not a problem and capsule wall thicknesses are, in fact, governed by the thickness necessary to survive impact.

The principal types of nuclear radiation which contribute to the external radiation field associated with the PuO_2 fuel form are gammas, neutrons, and alpha particles. The shielding required to reduce this radiation field to tolerable levels was calculated

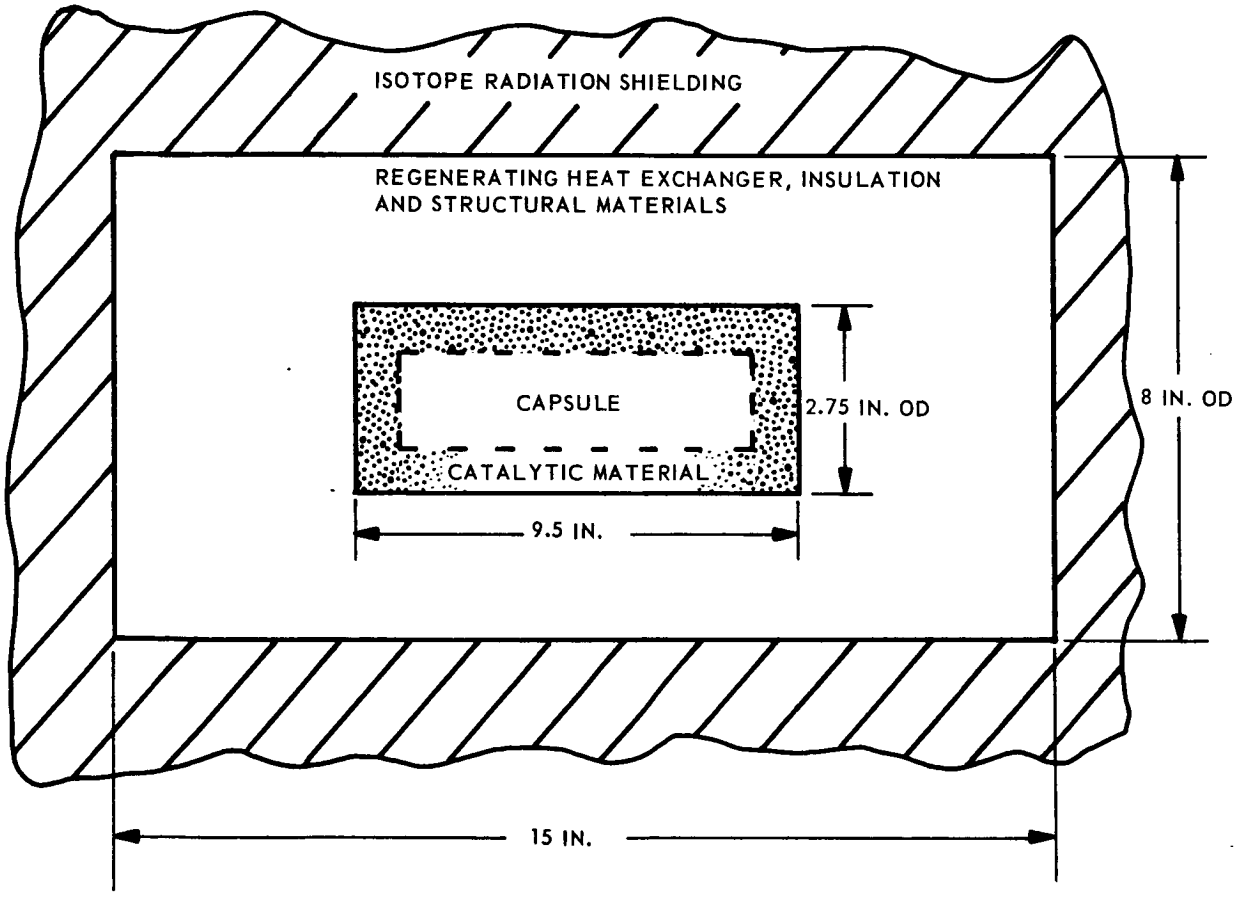

Fig. 2 System Configuration Used in Comparative Analysis

TABLE 2

COMPARATIVE ANALYSIS OF SELECTED RADIOISOTOPES
BASED ON FIG. 2 CONFIGURATION

	Sr-90	Pu-238	Pm-147	Cm-244	
Half-life (yrs)	28	88	2.7	18	
Availability	Available	Available	Limited	Limited	
Status of Development	Not Developed for Space Application	Highly Developed for Space Application	Limited	Limited	
Present Cost ($/watt) (ref. 16)	19	894	90	357	
Fuel Form	$SrTiO_3$ (or SrO_2)	PuO_2	Pm_2O_3	Cm_2O_3	
Capsule Dimensions (in.)					
Length	7.5	5.2	5.8	2.8	
Diameter	2.5	1.7	1.85	1.0	
Wall Thicknesses	0.20	0.15	0.15	0.15	
Type of Radiation	β, bremss	α, γ, n	β, γ, bremms	α, γ, n	
Shielding					
Material	Pb	LiH	Pb	Pb	LiH
Thickness (in.)					
4 mrem/hr at:					
100 cm	5.5	1.3	1.0	2.35	7.5
300 cm	4.2	0	0.13	0.5	3.5
System Weights (lb)					
Capsule	5.1	3.2	2.9		0.75
Shielding (4π)					
4 mrem/hr at:					
100 cm	2700	21	240	1212	
300 cm	1705	0	27	201	

on the basis of the latest information obtained from the AEC's Division of Isotopes Development.* The alpha particles are completely contained within the capsule, and the gamma radiation level is significantly reduced by the capsule wall thickness required to survive impact. However, to attenuate the neutron flux to safe levels, lithium hydride (LiH) having a neutron removal cross-section of 0.15 cm^{-1} was assumed. At 300 cm from the source, no LiH shielding is required since the dose rate at this location is less than 4 mrem/hr. At 100 cm, a LiH shield weight of 21 pounds is required to obtain a dose rate of 4 mrem/hr. Using either criteria, a PuO_2 system is superior to the other candidate isotopic systems and nonisotopic heat sources.

It is estimated that the cost of Pu-238 in 1971 will be $550 per watt.

Pm-147. – The Pm_2O_3 fuel form is presently considered to be not as well-developed for heat source applications as PuO_2 due to limited supply and experience with this fuel form. Promethium is a pure beta emitter, thus avoiding the problems of pressure buildup in the capsule. Sizing the capsule on the basis of fuel volume and wall thickness required to survive impact results in the dimensions listed in Table 2. At present, only very limited data on the characteristics of this fuel form at high temperatures are available. Its chemical compatibility with molybdenum is reported good but some evidence of chemical attack has been observed with the cobalt-based alloys.

Although the radiation field associated with pure Pm-147 is very small, minute quantities (5×10^{-5} percent) of Pm-146 with a half-life of 1.94 years are present and contribute to a significant gamma radiation field. Capsule material thickness was sufficient to attenuate the bremsstrahlung radiation in the comparative design, but additional high-density shielding (ref. 14) was necessary to reduce the gamma flux to a dose level of 4 mrem/hr at 100 cm. This additional shielding increased the total system weight (less reentry aids) to 240 pounds assuming 4π shielding. Obviously little weight advantage over nonisotopic heat sources can be realized in this case. Sufficient aging to reduce the Pm-146 gamma level would reduce the shielding weight but would also decrease the specific power, thereby increasing capsule weight and volume.

Cm-244. – Curium-244 has been considered for several spacecraft missions, including OAO and NIMBUS (ref. 17), but the high neutron radiation background from spontaneous and (alpha, n) reactions with the oxygen in Cm_2O_3 has been a deterrent. Its development has been limited by availability, but present production schedules indicate sufficient quantities will be available to meet mission requirements in 1967 (ref. 18). The void volume generated from the mechanical packing of the fuel into the capsule is sufficient, as with PuO_2, to maintain the helium pressure resulting from alpha decay at acceptable levels.

*Personal communication with Dr. James Powers, Branch Chief, Division of Isotopes Development, U. S. Atomic Energy Commission.

Extensive shielding (ref. 14) will be required to reduce the neutron and gamma flux to tolerable levels unless the heat source is placed external to the spacecraft. As shown in Table 2, the radiation shielding weight is high relative to both Pm-147 and Pu-238.

Po-210. – A comparison of Po-210 was not presented in Table 2 due to its short half-life (0.379 year) relative to the IHCOS mission requirements. With this half-life, a source capable of dissipating 300 watts at the end of the mission would have to dissipate approximately 1155 watts initially. This would involve a considerable amount of active thermal regulation of the unit which would add weight and complexity.

Thulium-171. – A fuel recently proposed for use in heating underwater diving suits is Tm-171. Preliminary performance numbers indicate that this fuel is competitive with Pu-238. It was eliminated from consideration, however, because of the following factors:

- Thulium-171, and its oxide fuel form, Tm_2O_3, are presently not undergoing any significant development for aerospace heat source applications. The chemical compatibility with encapsulating materials at high temperatures is presently unknown. The determination of high-temperature stability characteristics of the Tm_2O_3 fuel form must also be determined and requires a considerable developmental effort.

- Only small research quantities of Tm-171 have been produced by Savannah River, although increased production is probably possible if warranted by demand.

- The cost (in dollars per watt) is excessive for Thulium-171, due to higher radiation costs associated with the target material (Erbium-170), and the high purity level requirements in order to avoid excessive radiation from trace contaminants.

Isotope Selection

Based on the comparative analysis presented in Table 2, Pu-238 was selected on the isotope heat source best suited for use in IHCOS. The Pu-238 fuel form, PuO_2, is more highly developed for space application and requires considerably less shielding than any of the other fuel forms. PuO_2 is also available in sufficient quantities to meet the mission requirements.

CATALYST SELECTION

The catalyst selection tests were performed from 24 May 1966 through 24 June 1966. This section presents the objectives of the test, apparatus and procedures used, the results obtained and a discussion of the results.

Objectives

The objectives of the tests were to establish the ability of various catalysts to oxidize methane to determine the catalyst preferred for IHCOS. The catalysts were to be screened on the basis of catalyst activity and durability for the selected mission.

Apparatus

The apparatus utilized in performing the catalyst selection tests is shown in figs. 3, 4, and 5. The major test equipment includes the following:

- Cylinder for gaseous contaminant, oxygen and carbon dioxide supply
- Flowmeter to monitor total flow rate
- Pressure gauges to measure system pressures
- Catalytic oxidizer tube to contain catalyst
- Oven to control catalyst bed temperature
- Pressure regulator to control system pressure
- Control valves to control system flow
- Septa for taking gas samples with a syringe
- F&M gas chromatograph equipped with flame ionization detectors for gas analysis

Procedure

During the catalyst selection tests, the following six catalysts, each deposited on 1/8" alumina pellets, were evaluated:

- 0.5 percent palladium
- 1.0 percent palladium
- 1.0 percent platinum
- 1.0 percent palladium
- 2.0 percent platinum – 2.0 percent palladium
- 4.0 percent palladium

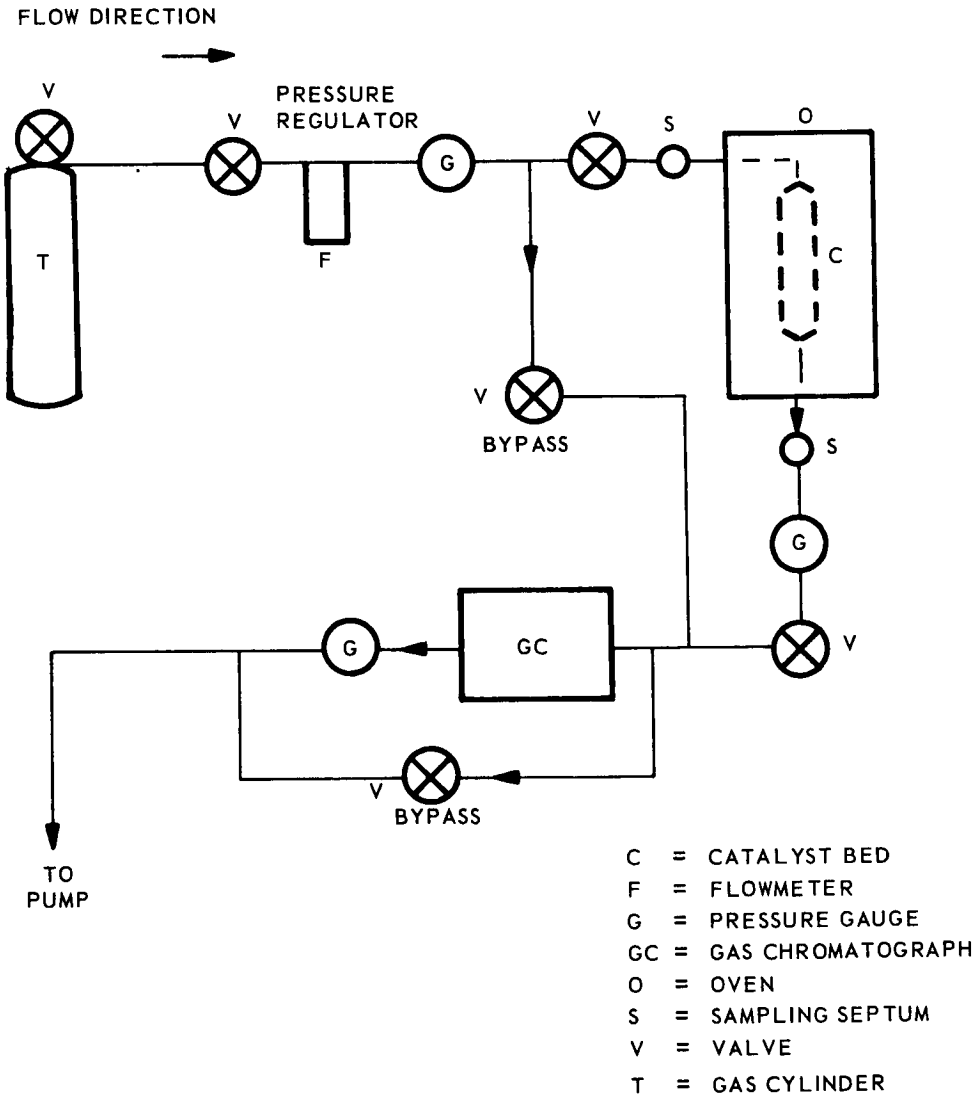

Fig. 3 Schematic Diagram of System Apparatus

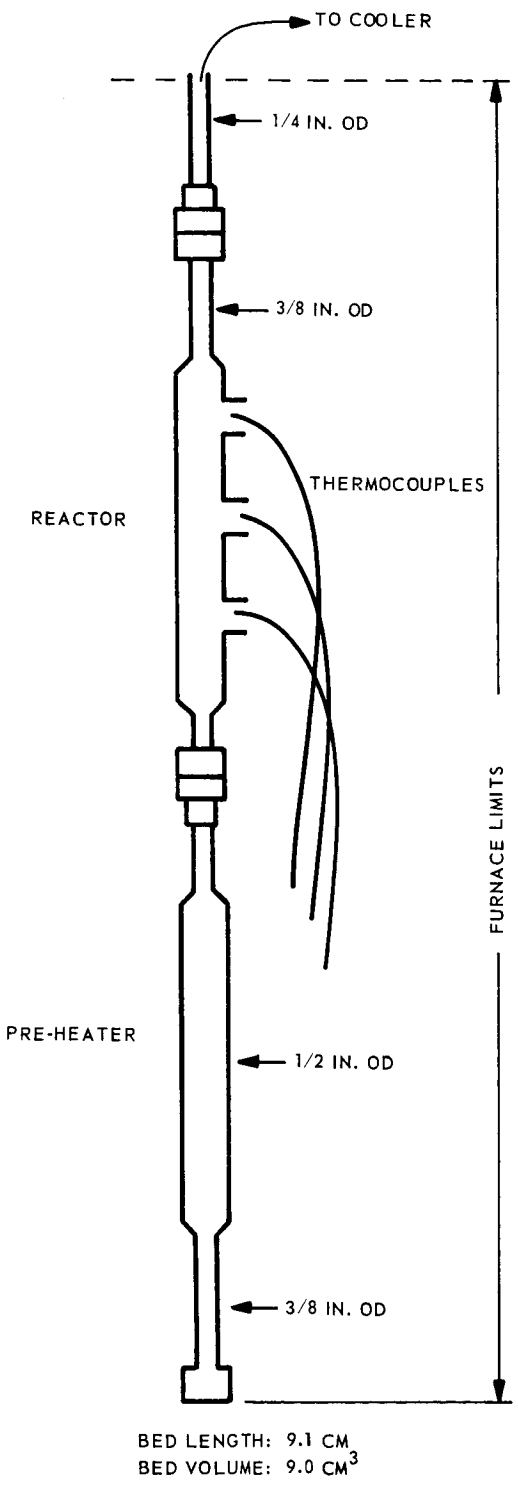

Fig. 4 Diagram of Catalyst Reactor

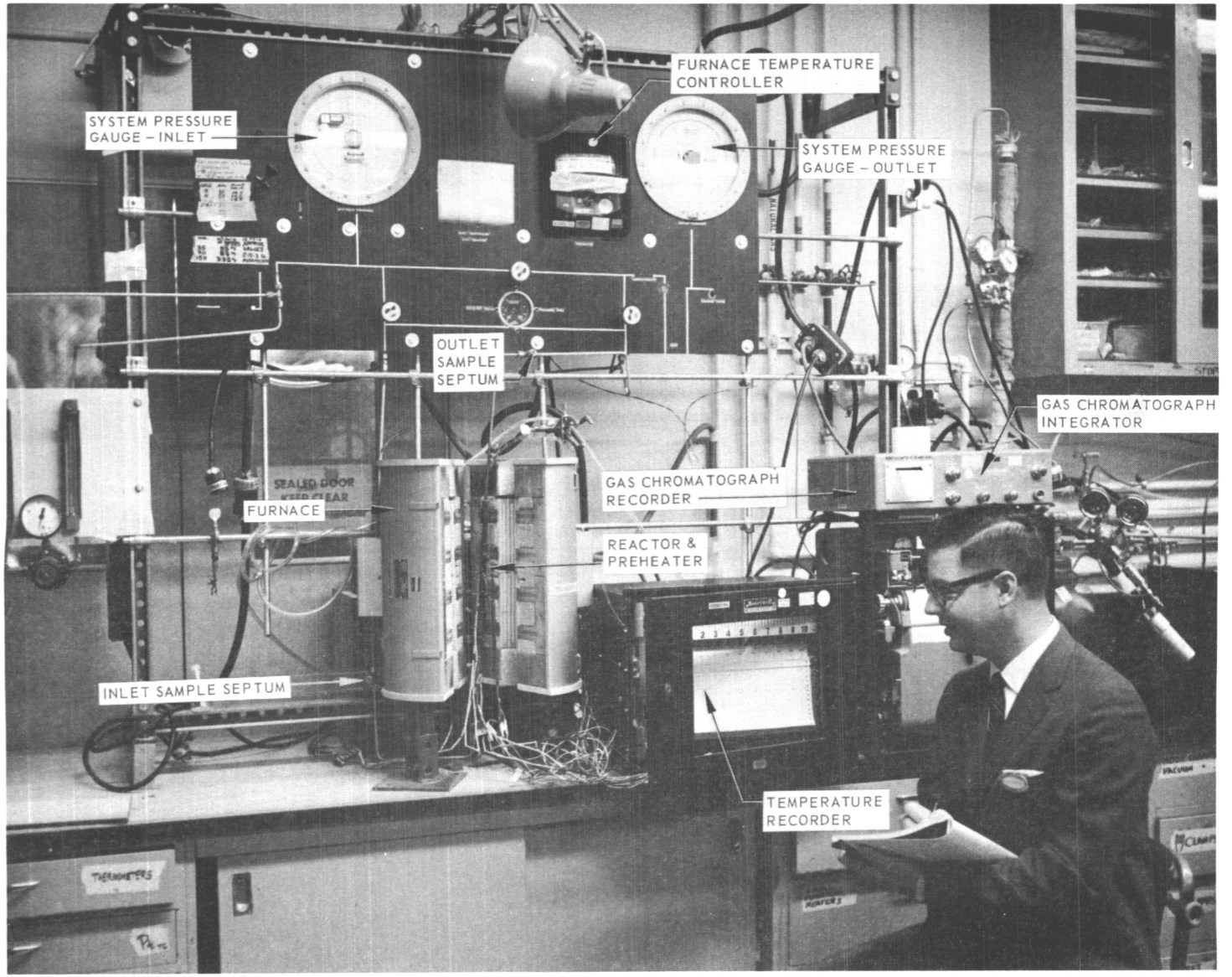

Fig. 5 System Apparatus

The 0.5 percent, and one of the 1.0 percent palladium catalysts were manufactured by Engelhard Industries, and the remaining catalysts by J. Bishop and Company. The experiments were performed at an actual space velocity of 15,000 hours^{-1}, a pressure of 10 psia, and at temperatures from 200°C to 600°C. Methane conversion efficiency was measured and physical changes noted.

The tests were performed by flowing a mixture of gases (0.34 percent methane, 0.75 percent CO_2, 32.7 percent O_2 and the balance nitrogen) through the catalyst bed at the desired flow rate and temperature. The catalyst bed was allowed to equilibrate at each temperature before gas samples were taken. Sampling was performed at both the inlet and outlet of the catalyst bed with a 2.5 cc gas-tight syringe. Gas samples were also taken through a Beckman solenoid-operated gas sampling valve to verify the validity of the results obtained with the gas-tight syringe.

Results

Data were obtained for a range of methane conversion efficiences from less than 25 percent to greater than 75 percent. These results are tabulated in Table 3, and plotted in fig. 6, for the six catalysts tested.

Figure 6 also includes data from two tests performed during the LMSC development of a trace contaminant removal system for Apollo (NAS 9-3415). These evaluations were of a 1 percent Pt - 1 percent Pd catalyst dispersed by LMSC, and the 0.5 percent Pd catalyst prepared by Engelhard. Both of these tests were performed at 5 psia in a predominantly oxygen atmsophere.

The results of the comparison between data sampling with a gas-tight syringe and the chromatograph sampling valve are shown in Table 4, and indicate that methane conversion efficiency agreement of the two sampling techniques is within a few percent.

The data listed in Table 3 were obtained with the gas-tight syringe technique. Inspection of the catalysts after each run indicated that the palladium catalysts underwent color changes from an original grey-black to a ferrous brown. The platinum catalyst showed no change in color and the mixed Pt-Pd showed a slight color change. The catalysts manufactured by Bishop exhibited greater powdering and friability than the Engelhard catalyst.

Comparison of the test data obtained during this program with data obtained during the development of a trace contaminant removal system for Apollo, indicate a slight increase in catalytic activity for 5 psia, 100 percent oxygen as compared to 31 percent oxygen, 10 psia.

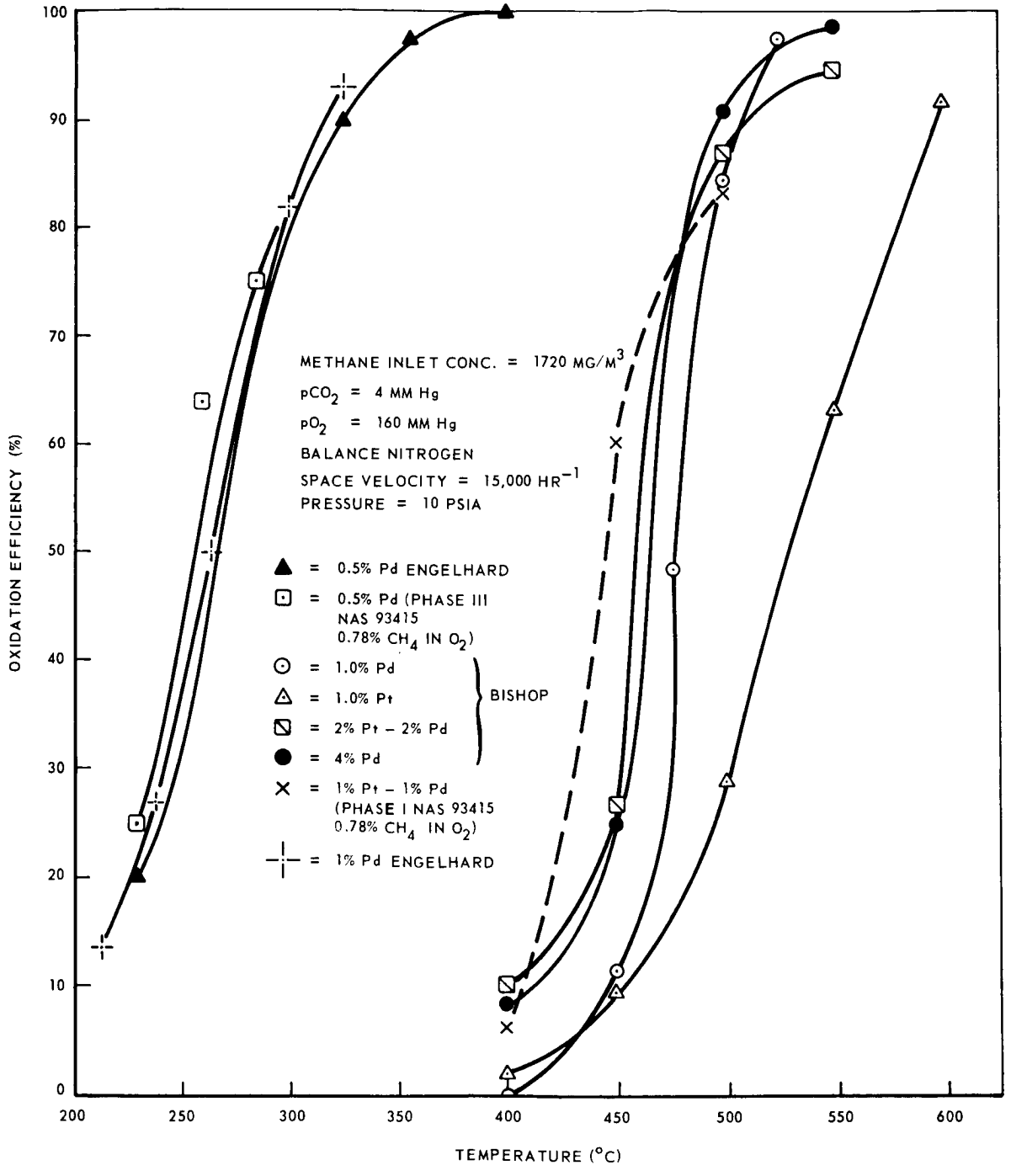

Fig. 6 Percent Conversion of Methane vs Temperature

TABLE 3

CONVERSION OF METHANE VS TEMPERATURE

Catalyst	Temperature (^{o}C)	Conversion (%)
1% Pd (Bishop)	400	0
	450	12.0
	475	48.5
	500	84.5
	525	97.5
1% Pt (Bishop)	400	2.0
	450	9.5
	500	29.0
	550	63.5
	600	91.5
2% Pt (Bishop) 2% Pd	400	9.5
	450	27.0
	500	87.0
	550	94.5
4% Pd (Bishop)	400	8.0
	450	25.0
	500	90.5
	550	98.5
0.5% Pd (Engelhard)	235	19.5
	325	90.0
	360	97.5
	400	99.5
1% Pd (Engelhard)	215	14.9
	240	29.5
	265	54.5
	300	81.3
	325	93.0

Notes:

Actual Space Velocity = 15,000 hr^{-1}
Methane Inlet Concentration = 1720 mg/m^3
CO_2 Concentration = 4 mmHg
O_2 Concentration = 160 mmHg
Balance Nitrogen
Total Pressure = 10 psia

TABLE 4

COMPARISON OF DATA OBTAINED BY USING HAMILTON SYRINGE AND BECKMEN SAMPLING VALVE FOR 2 PERCENT Pd CATALYST

Temperature (^{o}C)	Methane Conversion % (Syringe Method)	Methane Conversion % (Beckman Sampling Valve Method)	Difference %
400	9.6 ±1	11.5 ±0.1	1.9
450	26.5 ±0.2	29.0 ±0.2	2.5
500	86.6 ±0.3	87.7 ±0.3	1.1
550	94.6 ±0.3	95.1 ±0.3	0.5

Discussion of Results

The catalyst selection for IHCOS was to be based on catalyst activity and durability* under mission requirements. Catalyst durability and activity should increase by increasing the number of active catalyst sites. The original hypothesis was that the number of active sites would be increased by increasing the noble metal surface area which implies an increased weight in dispersed metal. Catalyst manufacturers were contacted, and it was determined that Bishop offered dispersions up to 4 percent metal by weight, whereas Engelhard normally only offers dispersions to up 0.5 percent. Catalysts were obtained from Bishop ranging from 1 to 4 percent in metal and evaluated. The results of the evaluation indicated that the increased metal weight did increase the catalytic activity and thus the number of active sites. Evaluation of the 0.5 percent palladium Engelhard catalyst, however, indicated a far greater activity than any of the Bishop catalysts. This implies that Engelhard has superior dispersion techniques or utilizes a higher area substrate, resulting in a greater number of active sites with a smaller mass of noble metal. Durability should be related to the number of active sites, consequently to activity.

After these tests were performed, Engelhard was contacted and they agreed to make a special 1 percent Pd dispersion. Evaluation of this catalyst revealed no appreciable difference between the performance of Engelhard's 1 percent and 0.5 percent dispersion. Engelhard feels this is due to the fact that the coverage of the 0.5 percent catalyst is nearly complete and thus no significant benefit can be realized from additional metal dispersion.

Conclusions

The results of the testing indicated that the 0.5 percent and 1.0 percent palladium catalysts manufactured by Engelhard has the highest activity of any of the catalysts evaluated. It is concluded that these catalysts should also have a higher resistance to deactivation due to the greater number of active catalyst sites present. The 0.5 percent palladium catalyst was selected for use in the IHCOS over the 1.0 percent due to the slight difference in performance, its lower cost, and greater availability.

*Resistance to deactivation.

PERFORMANCE DATA ON SELECTED CATALYST

Performance data on the selected 0.5 percent palladium catalyst, manufactured by Engelhard Industries, were obtained from 1 July 1966 through 27 July 1966. This section presents the objectives, apparatus and procedures used, the results obtained and a discussion of the results.

Objectives

The objectives of the performance data tests with the 0.5 percent palladium catalyst were to determine methane conversion efficiencies vs temperatures and space velocities in the presence of selected competing contaminants. The data obtained will be used to select optimum operating parameters for IHCOS.

Apparatus

The test apparatus used to obtain the performance data is illustrated in figs. 7 through 11. Listed below are the major items of test equipment used:

- Cylinders for gaseous contaminants and background gas
- Motorized syringe for methanol introduction
- Pressure gauges and regulator to measure and control system pressure
- Inlet and exit sampling septa for obtaining gas samples
- Preheater for heating incoming gas to catalyst bed
- Catalytic oxidizer tube to contain catalyst (catalyst volume = 57 cc)
- Furnace and temperature controller to control catalyst bed temperature
- Temperature recorder to obtain catalyst bed temperature data
- Air-cooled heat exchanger for cooling exit gas from catalyst bed
- Diaphragm pump and flow control valves for maintaining pressure and for varying system flow rate
- Flowmeter and wet test meter to determine system flowrates
- F&M gas chromatographs Models 720, 1609, 810, 700A and 700B, equipped with flame ionization and thermal conductivity detectors for contaminant analysis

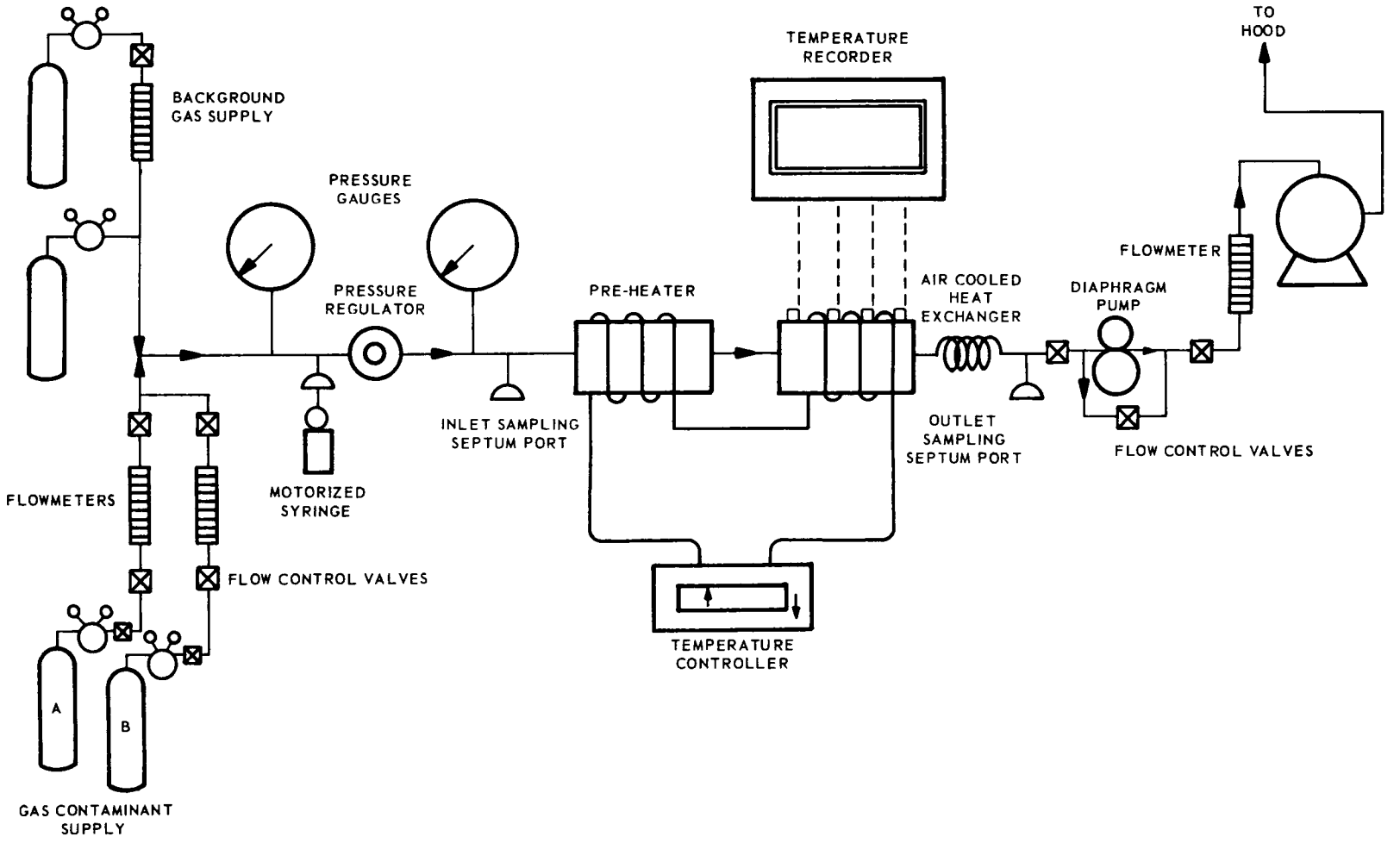

Fig. 7 Catalyst Performance Data Test Apparatus Schematic Diagram

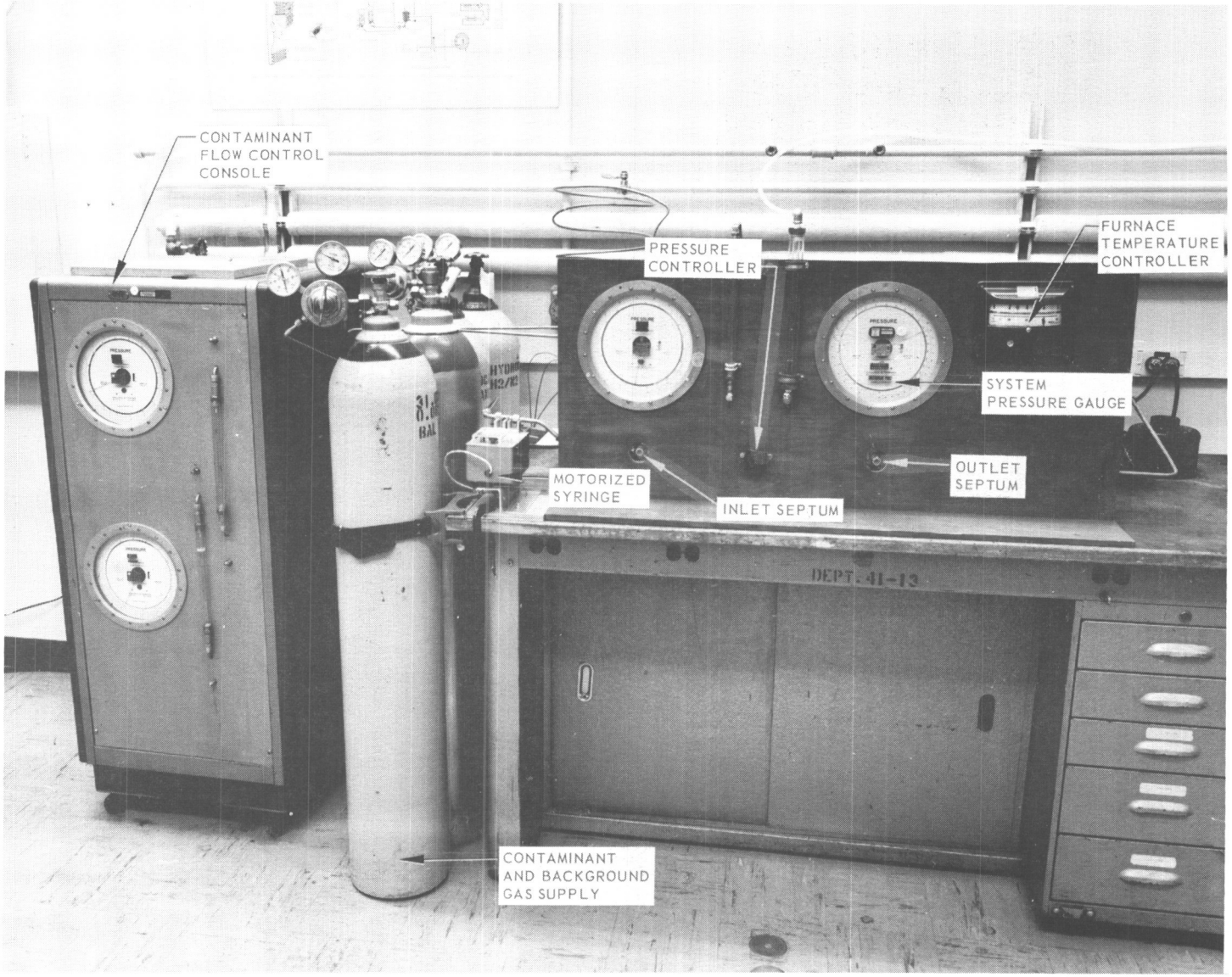

Fig. 8 Catalyst Performance Data Test Apparatus

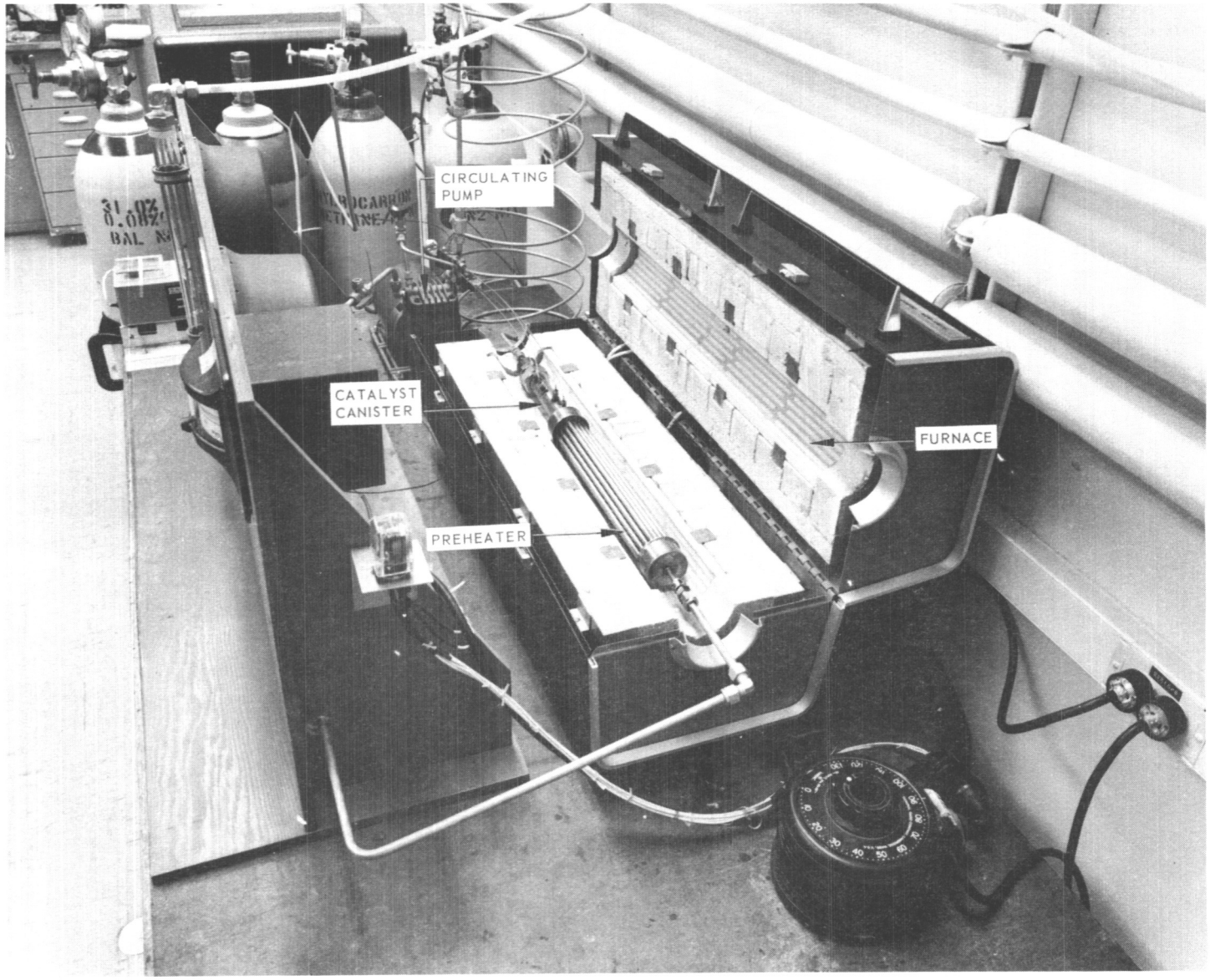

Fig. 9 Oven, Preheater, and Catalyst Bed

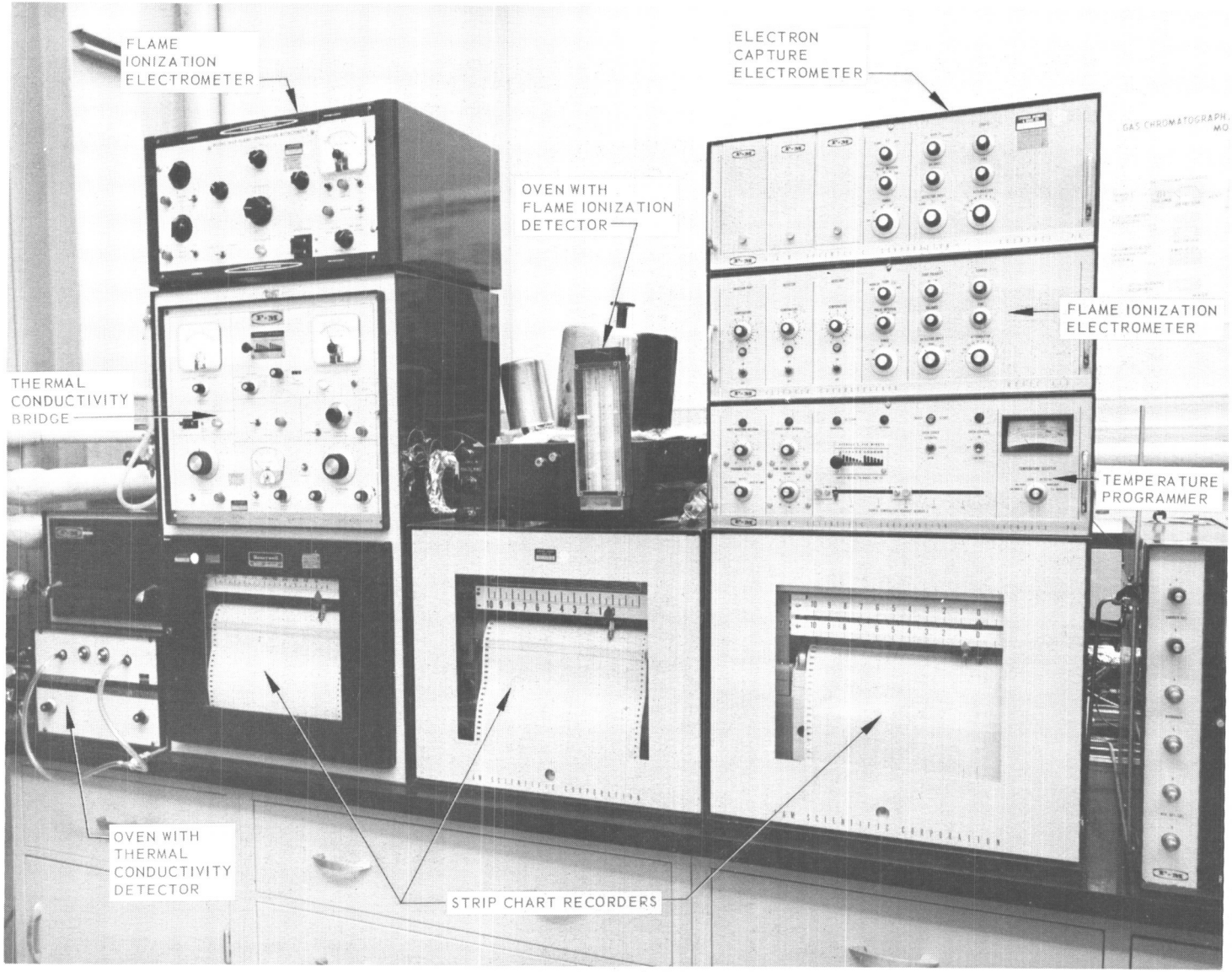

Fig. 10 Gas Chromatographs Used for Contaminant Monitoring

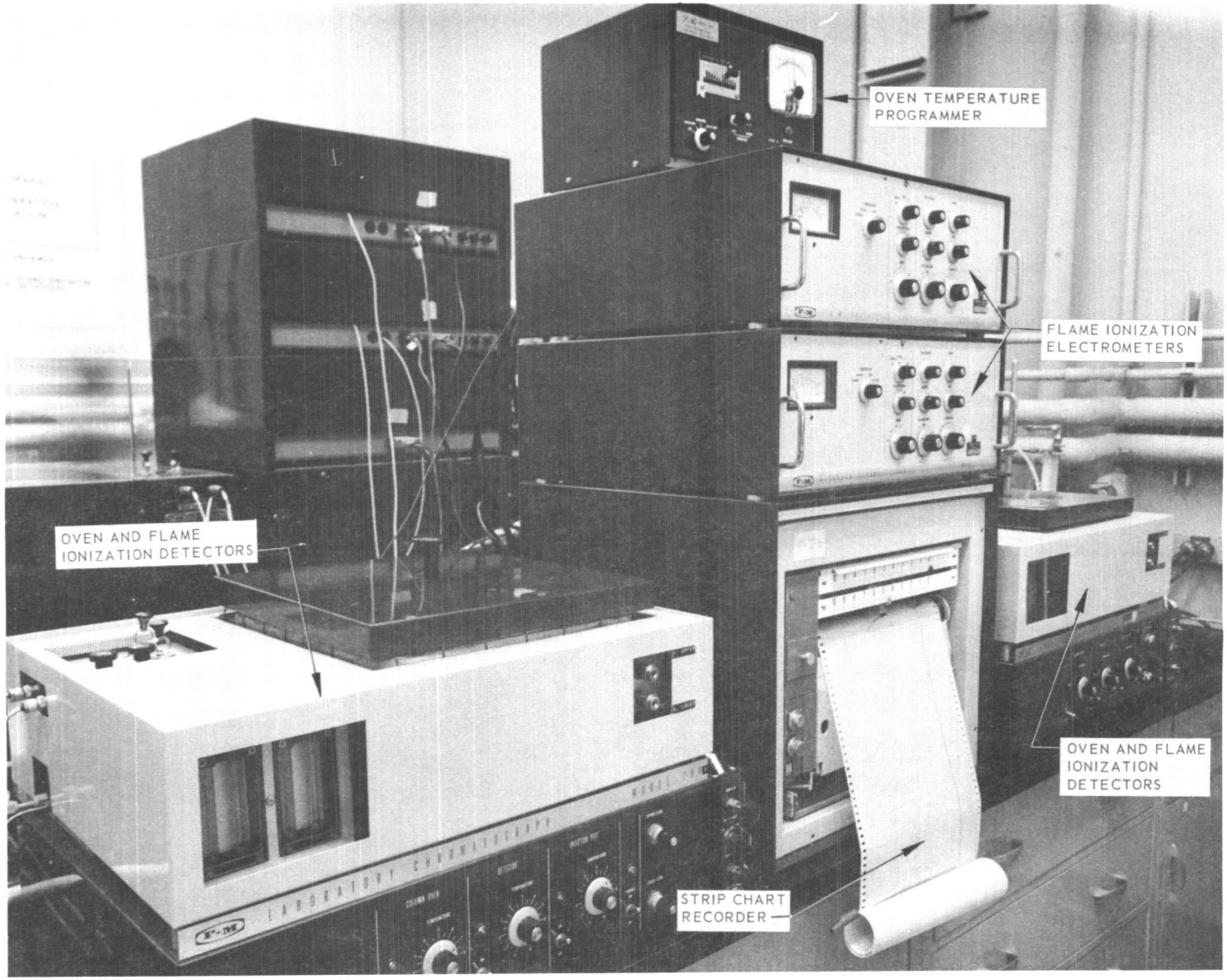

Fig. 11 Additional Gas Chromatographs Used for Contaminant Monitoring

Procedure

The performance data on the 0.5 percent Pd catalyst were obtained with the system operating at space velocities of 2090 hrs^{-1}, 5000 hrs^{-1}, 15,000 hrs^{-1}, and 30,000 hrs^{-1}. Catalyst bed temperatures were maintained at four temperature settings to produce methane conversion efficiency data ranging from less than 25 percent to greater than 75 percent. Total system pressure was held at 10 psia with a background gas consisting of the contaminants listed in Table 5, 159 mm oxygen (30.9 vol %), 4 mm carbon dioxide (0.779 vol %), and the balance nitrogen.

TABLE 5

CONTAMINANTS INTRODUCED IN METHANE CONVERSION EFFICIENCY TESTS

Acetylene	Hydrogen
n-Butane	Methane
Butene – 1	Methyl alcohol
trans-Butene – 2	Propane
Carbon Monoxide	Propylene
Ethane	

Sampling was performed at both the inlet and outlet of the catalyst bed with a 2.5 cc gas-tight syringe after the catalyst bed was allowed to equilibrate at each temperature setting.

The methane inlet and outlet concentration was determined for each space velocity and temperature. The inlet concentrations for the other contaminants were determined twice at each space velocity, at the highest and lowest catalyst bed temperature.

Results

The results on methane conversion efficiency are tabulated in Table 6 and plotted in fig. 12. Contaminant inlet concentrations determined at each space velocity at the lowest and highest temperatures are tabulated in Table 7.

The data reported represent the average value of three or more analyses. The determinate error indicated for each average value reported is the mean deviation of the individual measurements.

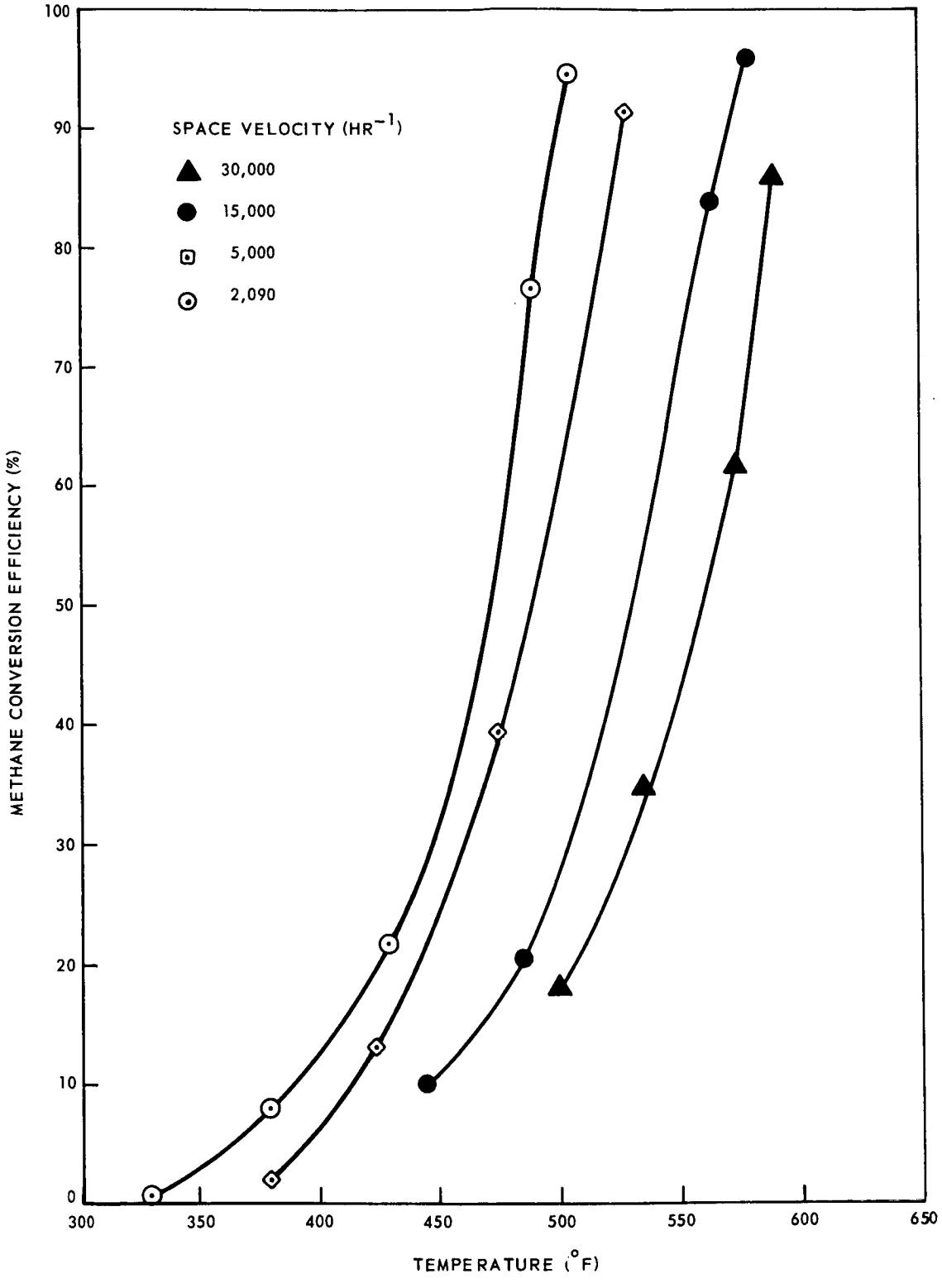

Fig. 12 Methane Conversion Efficiency

TABLE 6

METHANE CONVERSION EFFICIENCY

Space Velocity Hrs^{-1}	Temp. °F	Methane Conc.* Mg/M^3 Inlet	Outlet	Methane Conversion Efficiency, %
2,090	380	1660	1530	7.8 ±2.3
	430	1638	1290	21.3 ±0.8
	490	1550	356	76.9 ±3.3
	510	1750	97	94.6 ±1.6
5,000	380	1690	1657	2.0 ±1.3
	420	1683	1467	12.9 ±2.6
	475	1720	1036	39.5 ±2.4
	530	1720	145	91.6 ±0.1
15,000	445	1605	1445	9.9 ±1.6
	485	1503	1193	20.6 ±0.8
	565	1710	282	83.6 ±1.3
	580	1710	96	95.9 ±0.9
30,000	505	1740	1430	18.3 ±2.2
	535	1750	1133	35.2 ±1.0
	575	1730	680	61.7 ±3.3
	590	1730	241	86.1 ±1.5

*Average of three.

Discussion

Methane conversion efficiency. – The methane conversion efficiencies were calculated by the following equation:

$$\eta r = \frac{C_i - C_o}{C_i}$$

where

C_i = methane inlet concentration

C_o = methane outlet concentration

ηr = removal efficiency

The values obtained were the average of three or more outlet concentrations as reported in Table 6.

TABLE 7

CONTAMINANT INLET CONCENTRATION AT THE LOWEST AND HIGHEST TEMPERATURE FOR EACH SPACE VELOCITY (Mg/M^3)

Contaminant	Space Velocity							
	2090 Hrs^{-1}		5000 Hrs^{-1}		15,000 Hrs^{-1}		30,000 Hrs^{-1}	
	380°F	510°F	380°F	530°F	445°F	580°F	505°F	590°F
Acetylene	52.2 ±0.6	57.4 ±4.5	53.3 ±1.0	48.8 ±3.6	49.2 ±3.4	50.7 ±0.8	46.2 ±0.2	45.6 ±3.5
n-Butane	30.5 ±1.7	32.2 ±0	25.2 ±0.5	23.2 ±0.3	24.7 ±0.4	25.5 ±0.4	25.5 ±0.3	25.4 ±0.3
Butene-1	73.1 ±2.1	70.3 ±1.3	59.7 ±0.9	48.3 ±2.6	55.6 ±0.8	63.3 ±0.4	55.7 ±0.1	55.9 ±0.2
t-Butene-2	64.4 ±3.1	59.2 ±2.7	53.4 ±1.6	43.7 ±2.1	50.7 ±0.6	58.1 ±1.0	49.2 ±0.4	49.3 ±0.3
Carbon Monoxide	17.3 ±0.8	14.4 ±0.4	15.4 ±1.5	17.5 ±0.7	23.1 ±2.8	20.5 ±0.6	15.3 ±1.2	14.9 ±0.7
Ethane	37.8 ±0.1	41.3 ±2.8	40.3 ±1.9	40.0 ±1.7	42.3 ±2.0	40.0 ±2.0	38.6 ±0.9	36.1 ±1.3
Hydrogen	229 ±2	227 ±3	235 ±8	204 ±3	207 ±7	210 ±1	236 ±0	218 ±0
Methyl Alcohol	40.5 ±2.0	69.8 ±2.4	53.7 ±9.2	62.6 ±5.4	38.7 ±0.5	55.1 ±2.8	42.1 ±1.7	40.1 ±0.7
Propane	53.2 ±0.6	52.9 ±1.0	40.2 ±0.7	37.2 ±2.1	47.9 ±0.2	52.2 ±2.8	39.9 ±1.7	37.9 ±0.7
Propylene	48.2 ±0.1	48.3 ±0	45.0 ±0.7	43.5 ±2.6	48.0 ±2	45.4 ±4.3	43.8 ±0.2	43.8 ±1.5
Methane	1660 ±0	1750 ±9	1690 ±0	1720 ±7	1605 ±16	1710 ±13	1740 ±8	1730 ±27

The results plotted in fig. 12 follow the expected trends of increase in methane conversion efficiency with increasing catalyst bed temperature and a decreasing conversion efficiency with increasing space velocity.

Competing contaminant inlet concentration. – The competing contaminant inlet concentrations listed in Table 7 were obtained at the lowest and highest temperature for each space velocity and with the exception of methyl alcohol were fairly consistent throughout the test.

Methyl alcohol inlet concentrations fluctuated because of variations in the speed of the motorized syringe used for the introduction of this contaminant. The remainder of the contaminants were introduced in the gaseous state in premixed contaminant blends.

When the contaminant blends were ordered for this task, it was originally assumed that the 0.02 Torr limit on contaminant partial pressure would be imposed for certain contaminants. It was necessary to order the contaminant blends early in the program due to the long lead time (approximately 8 weeks) required for delivery. Refinement of the contaminant load definition indicated that the 0.02 Torr arbitrary limit could be relaxed on contaminants where a homolog to a contaminant for which toxicological data existed could be identified. As a result of this, the inlet concentrations for some of the contaminants used in the background were not at the maximum limit specified in the contaminant load definition phase. The inlet concentrations of methane and hydrogen were at the maximum limit specified in the contaminant load definition phase.

Based on the assumed removal efficiency per pass of 80 percent for contaminants other than methane, the inlet concentrations of the background contaminants would be well below the level used during the test. Therefore, the test levels represented conservative values based on what would exist in a space station when removal capability of the oxidizer is considered.

Conclusions

The performance tests generated the data necessary to support the analysis and design of IHCOS. From these data, a selection of the optimum operating temperature and space velocity can be made.

The performance data obtained during this test compares well with the data taken during the catalyst selection phase of this contract and Phase III of NAS 9-3415. *

There is a reduction in methane conversion efficiency in these data, with a background of competing contaminants, as compared to the data with methane as the only contaminant. This was anticipated as a result of the work done under NAS 9-3415, and was the reason for utilizing a background of competing contaminants in these tests.

*NAS 9-3415 – Design and Fabrication of a Trace Contaminant Removal System for Apollo

ANALYSIS AND OPTIMIZATION

After the tests to obtain design data on the selected catalyst were completed, an analysis and optimization effort was initiated. The purpose of this effort was to define an optimum configuration for IHCOS. This analysis and optimization effort occurred in several phases, all of which are described herein. The first phase dealt with the results of the catalyst design data tests described in the preceding section. During this effort a conceptual design was developed and its configuration optimized. This resulted in a unit with an operating temperature of 517°F requiring 98 watts of thermal power and having a total equivalent weight of approximately 18.5 lb. The steps leading to this selection are described in the following pages.

With the design operating conditions established, a long-term catalyst performance test was initiated. The objective of this effort, described in the section following the analysis and optimization, was to establish if the performance characteristics of the catalyst changed over long-term periods. The early results of this test had an impact on the established design. It developed that two regions of operation exist for IHCOS.

One region is with a very low dew point inlet gas stream and the other with moderate dew points typical of spacecraft cabins. The established design was valid for the low dew point situation and is termed the dry process gas version. At this point in the program a second optimization was performed for the high dew point or moist gas version of IHCOS. This optimization effort was brief and was based on trends established during the optimization of the dry process gas unit. The resulting moist gas unit requires 125 watts of thermal power and operates at 680°F. The results of the moist gas optimization effort are described following the dry process gas optimization.

At the conclusion of the long-term catalyst test, parametric performance data were again obtained. At this point the two design configurations, moist gas and dry process gas, were examined to establish off-design performance and to determine if the design point was affected by the final catalyst performance data. The results of this effort are described following the moist gas optimization.

The design point for this optimization study of a catalytic oxidizer was established by the requirements for a nine-man vehicle. The production rates and allowable concentration levels for each of the contaminants expected to be encountered are discussed in the contaminant load definition study. Results of that study established the flow rate of the oxidizer at 3 cfm to control the maximum concentration of carbon monoxide at an acceptable level. With 3 cfm, the required methane conversion efficiency is 27 percent. This conversion and the selected space velocity will set the operating temperature of the oxidizer. All other contaminants will be below their allowable concentration levels at the flow and temperature levels set by these two contaminants. The exothermic heat of reaction of the contaminants being oxidized was not considered as available energy. This was because the presence of contaminants should not be required to achieve the desired operating temperature. This energy amounts to a maximum of 25 watts.

One constraint placed on the design of IHCOS is that during a flow shutdown with a depressurized cabin, the catalyst bed temperature shall not exceed 1000°F. This constraint was imposed due to uncertainties in catalyst behavior after exposure to temperatures above 1000°F. The flow-shutdown depressurized-cabin situation results in the highest possible internal temperature.

Optimization Plan and Procedure

The objective of the optimization study was to establish design data for a catalytic oxidizer using an isotope heat source. These data would define a design that is optimum based on total equivalent weight and cost considerations. The method of approach was to:

- Establish a baseline concept for the system
- Develop parametric data for each of the components of the system
- Integrate the parametric data to develop curves of system penalty
- Evaluate the penalty data to establish a final design point.

The optimization procedure consisted of the following steps which are summarized here and discussed in detail in the balance of the report.

(1) The heat exchanger characteristics of volume, weight, energy loss and pressure drop were plotted as a function of effectiveness with catalyst bed temperature and heat exchanger core length as parameters.

(2) From the above curves, total equivalent weight (including fixed weight, fan power, and the isotope weight associated with the heat exchanger energy loss) was plotted as a function of heat exchanger core length with effectiveness and catalyst bed temperature as parameters. For each effectiveness assumed, a minimum total equivalent weight occurred at a specific heat exchanger core length.

(3) The family of minimum total equivalent weights was then plotted as a function of catalyst bed temperature and effectivness. This plot resulted in a minimum total equivalent weight at a specific effectiveness for each of the assumed catalyst bed temperatures. At this point, optimum heat exchanger configuration is defined as a function of catalyst bed temperature.

(4) The isotope heat source characteristics (weight, length and diameter) were plotted as a function of isotope power level.

(5) The catalytic oxidizer canister and catalyst bed characteristics (space velocity, volume and pressure drop) were plotted as a function of catalyst bed temperature with catalyst bed length as a parameter.

(6) From the data developed in Step 5, the catalyst canister total equivalent weight was plotted as a function of catalyst bed temperature with catalyst bed length as a parameter.

(7) The next step combined the heat exchanger total equivalent weight, isotope weight, and catalyst canister total equivalent weight with various insulation thicknesses. This developed a complete total equivalent weight for IHCOS as a function of insulation thickness, with catalyst bed temperature as a parameter. Inspection of these curves revealed that a minimum total equivalent weight occurred at a specific insulation thickness for each temperature considered, and that the lowest weight minimum occurred at a particular temperature. In this way, minimum total equivalent weight, IHCOS configuration, and operating temperature were defined.

(8) The optimum design defined in Step 7 was further investigated with respect to two major economic considerations. The isotope heating element cost and the cost of boost vehicle and launch operations associated with placing an IHCOS on orbit were estimated as a function of IHCOS weight and power. These total costs were plotted as a function of IHCOS power. Minimum cost occurred with a lower power and higher weight than the optimum resulting from Step 7.

The minimum cost unit was compared with the unit optimized purely on a weight basis, and a final selection was made.

The remaining discussions define the baseline concept and present the optimization procedure in greater detail.

Baseline Concept

At the outset of this study it was assumed that an optimum IHCOS would include the following major components as shown in fig. 13:

- Regenerative heat exchanger
- Isotope heat source
- Catalyst canister
- Internal structural supports
- Thermal insulation

Concepts to meet each of these functional requirements were examined in terms of:

- Fixed weight
- Electrical power penalty
- Thermal power penalty
- Reliability
- Cost

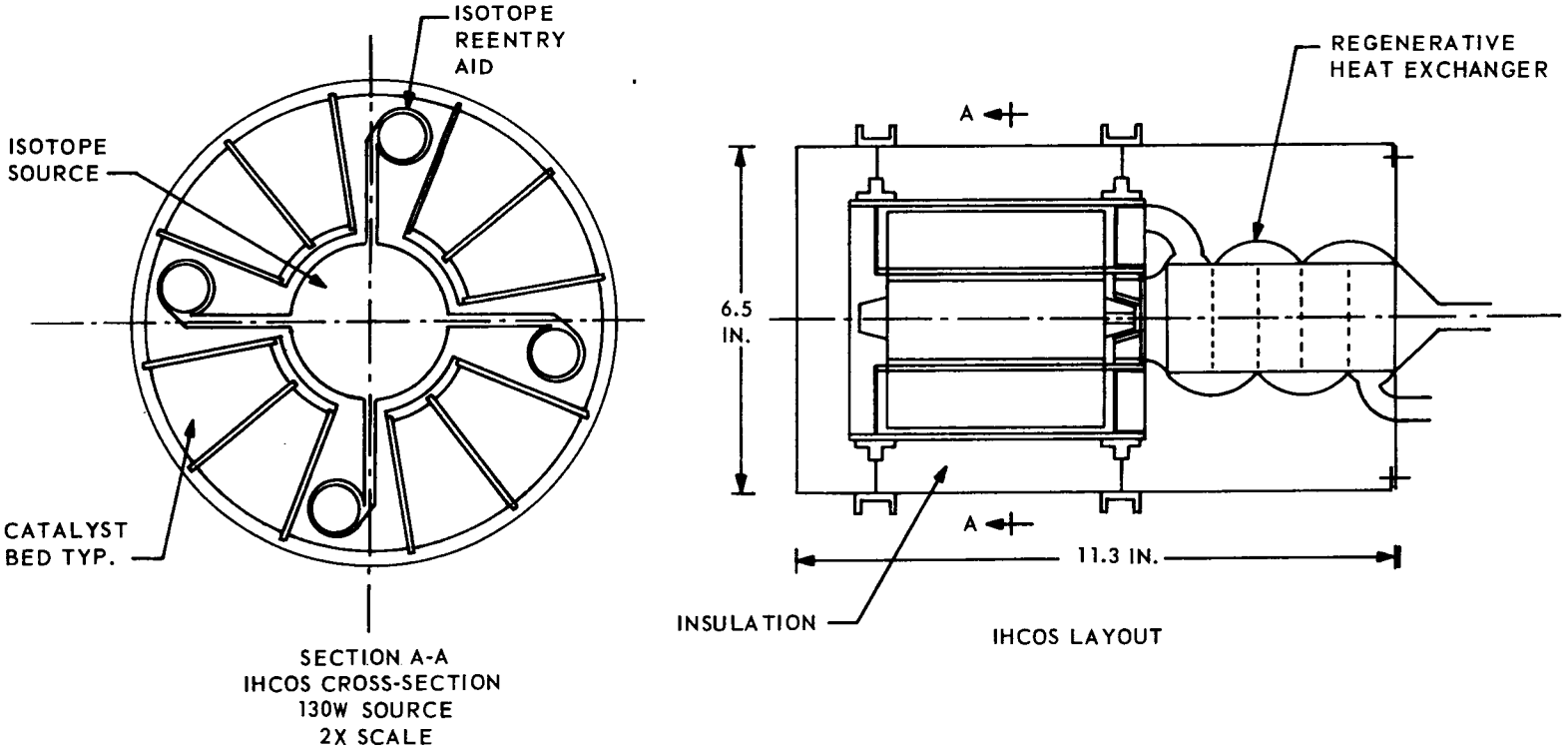

Fig. 13 Selected IHCOS Baseline Configuration

Description. – The heat exchanger is the largest single consumer of power in this unit, with the major loss being loss of heat to the air with secondary losses through conduction down the metal core and from the surface. A minimum-penalty heat exchanger will have a high transfer rate with low volume and fixed weight. A plate-fin type heat exchanger exhibits these desirable characteristics. The high heat transfer rate will minimize the core volume for a given effectiveness. This reduces the heat conduction losses along the core to the lowest possible levels. Further, the small volume will present the lowest surface area for heat loss through the insulation. As a result, a plate-fin heat exchanger was chosen for the baseline concept.

The design of the isotope heat source is constrained by a requirement for intact reentry through the earth's atmosphere. The isotope design section of this report discusses several possible methods of accomplishing this.

The configuration chosen for the isotope heat source is a cylindrical core containing the isotope and having four radial fins with beads on the ends to stabilize and protect the capsule during reentry. A layout of a catalyst canister surrounding the isotope source (fig. 13), showed these two components to be compatible in this configuration in the range of power levels and space velocities being considered. As the integration of these two components into one compact package yields the minimum surface area for thermal loss and the lowest volume penalty, as opposed to a series arrangement of catalyst bed and isotope source, this match was chosen for the baseline system.

A series placement of the oxidizer-isotope and heat exchanger was chosen for minimum heat loss and simplicity of integration. This combined package is wrapped with insulation which is retained by an outer canister. The selection of the insulation type will depend on complete system evaluations of different types of conventional insulation, vacuum insulations and thermal radiation shields.

The oxidizer section is supported by a spoked wheel which is representative of a low-conduction, high-strength support. Using this concept, conduction loss through the supporting members is reduced to a second-order effect.

Method of operation. – During normal operation, cabin air passes through the regenerative heat exchanger where it is heated by the gases leaving the catalyst bed. The incoming gas flows into the passage between the isotope heat source and catalyst canister to the end of the unit. Some heat transfer from the isotope to the air occurs in this passage. After passing over the isotope heat source, the gas flow direction is reversed and the gas then passes through the catalyst bed. The bulk of the gas heating will take place in the catalyst bed. The gas then flows from the catalyst bed into a collector at the end of the canister, and then into the regenerative heat exchanger before returning to the cabin. When the unit is depressurized, heat which is normally lost to the gas leaving the unit must be dissipated through the conduction paths. This results in a higher temperature of the unit.

The heat generated by the isotope is dissipated through two flow paths. The major portion is transferred directly to the catalyst container by radiation, and conduction through the isotope supports. During normal operation, the remaining energy is transferred directly to the gas flowing through the system. During depressurized operation, all of the heat is transferred by radiation and conduction to the catalyst container.

Heat Exchanger Optimization

It is possible to define an optimum heat exchanger for the IHCOS knowing the required gas flow rate and penalties for thermal and electrical power. The procedure used in the heat exchanger optimization was to define the core size, weight, air loss, and direct heat transfer loss in terms of the effectiveness, core length, and temperature parameters. These data were then combined to relate to total heat exchanger equivalent weight and to heat exchanger core length for given effectiveness. When the total equivalent weight at each optimum length was plotted as a function of effectiveness, an optimum effectiveness and geometry resulted.

This optimum is for the assumed power penalties of 20 lb/kw thermal and 400 lb/kw electrical. In the event that the thermal power penalty for the isotope source should change, the optimum effectiveness will vary.

Heat exchanger effectiveness vs volume (fig. 14). – Preliminary calculations on typical heat exchangers indicated very low Reynolds numbers. In this operating region, the heat transfer coefficients were in the minimum Nusselt number range. The assumption was made that the Nusselt number was constant over the entire range, thus setting the heat transfer coefficient as a constant for all heat exchanger geometries. Upon completion of the calculations, this assumption was checked on the final design and found to be valid. When this assumption is made, the heat transfer coefficient is not dependent upon Reynolds number. As a result, the volume may be directly related to effectiveness.

Effectiveness vs weight (fig. 15). – The volume of the heat exchanger core and weight of the complete unit with headers and mounting brackets are closely related for a given fin material. This curve is based upon a core density factor for the particular fin chosen and adding a weight allowance for headering and supporting structure. This establishes the fixed weight of the heat exchanger.

Effectiveness vs air heat loss (fig. 16). – A major thermal loss from the IHCOS unit is the heat carried away by hot air leaving the unit. The energy level of this air is directly related to the effectiveness of the heat exchanger and the specified operation temperatures. The air inlet temperature is assumed constant at $75^{\circ}F$ for all conditions. This leaves the hot inlet, or oxidizer temperature, as the only temperature parameter.

Effectiveness vs core conduction and surface losses (fig. 17). – Second-order heat exchanger thermal losses result from conduction down the metal of the core and from conduction from the surface of the heat exchanger through the insulation. These losses are normally neglected in heat exchanger design but must be considered in units with high-temperature gradients and low flow rates such as the IHCOS unit. These losses will be a function of the core length and oxidizer temperature. Of these parameters, the oxidizer temperature is a second-order effect in the range of temperatures being considered around a nominal level of $530^{\circ}F$. The core length is the major parameter and is plotted as a parameter over the values of interest.

For the shorter cores, the conduction losses down the core represent the major heat loss. In longer units, heat transfer from the surface and conduction loss are of the same magnitude.

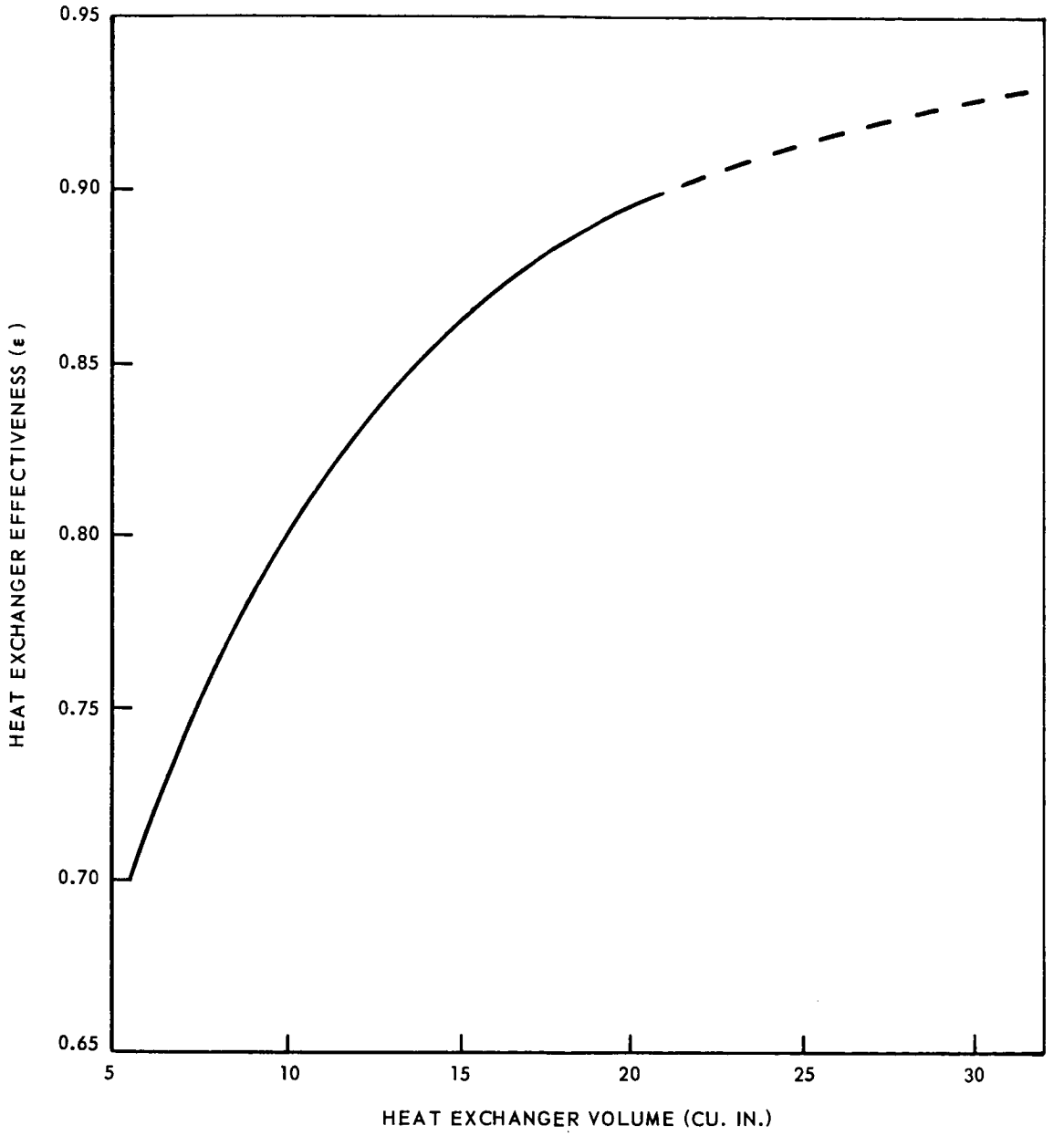

Fig. 14 Heat Exchanger Effectiveness vs Volume

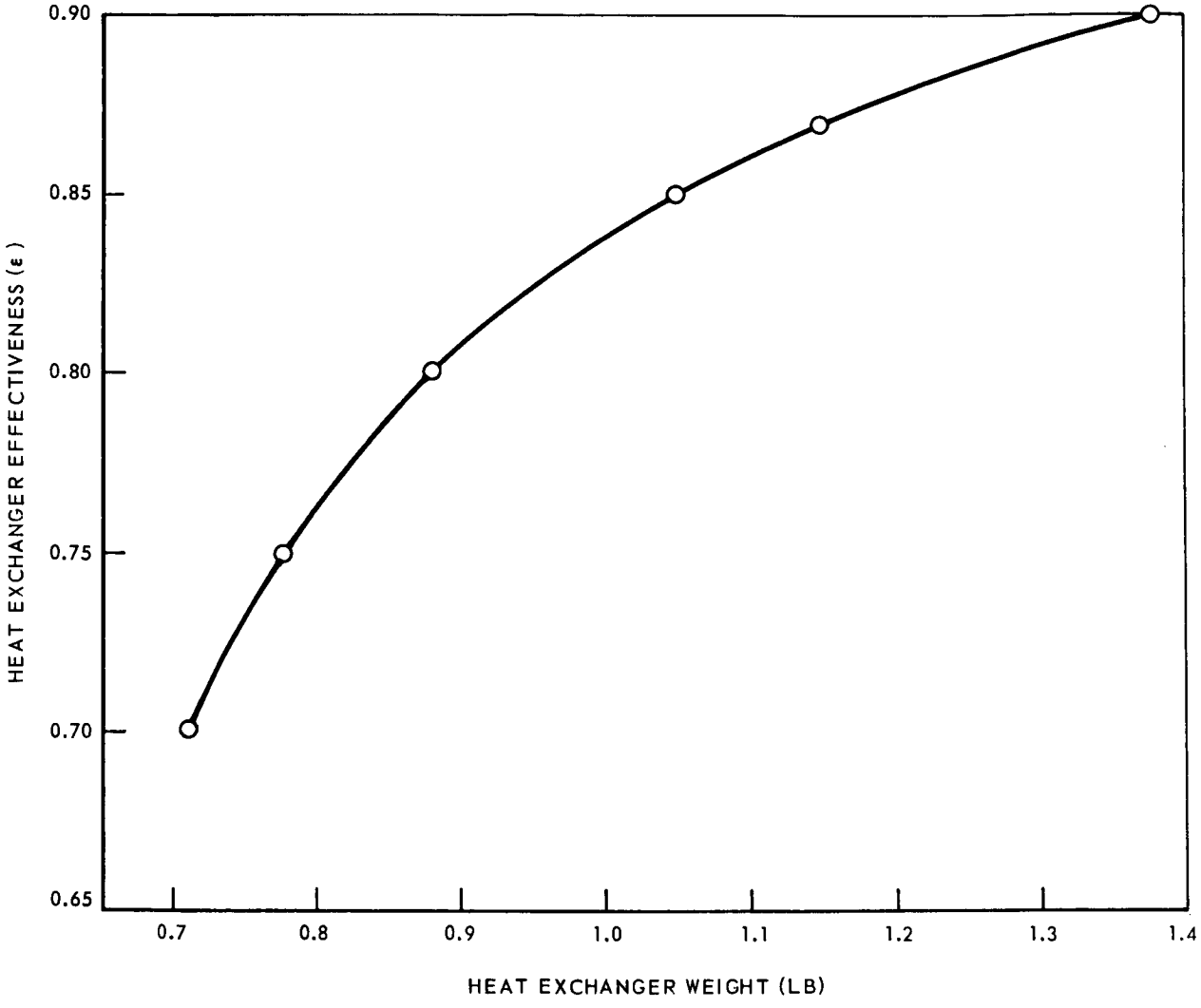

Fig. 15 Effectiveness vs Weight

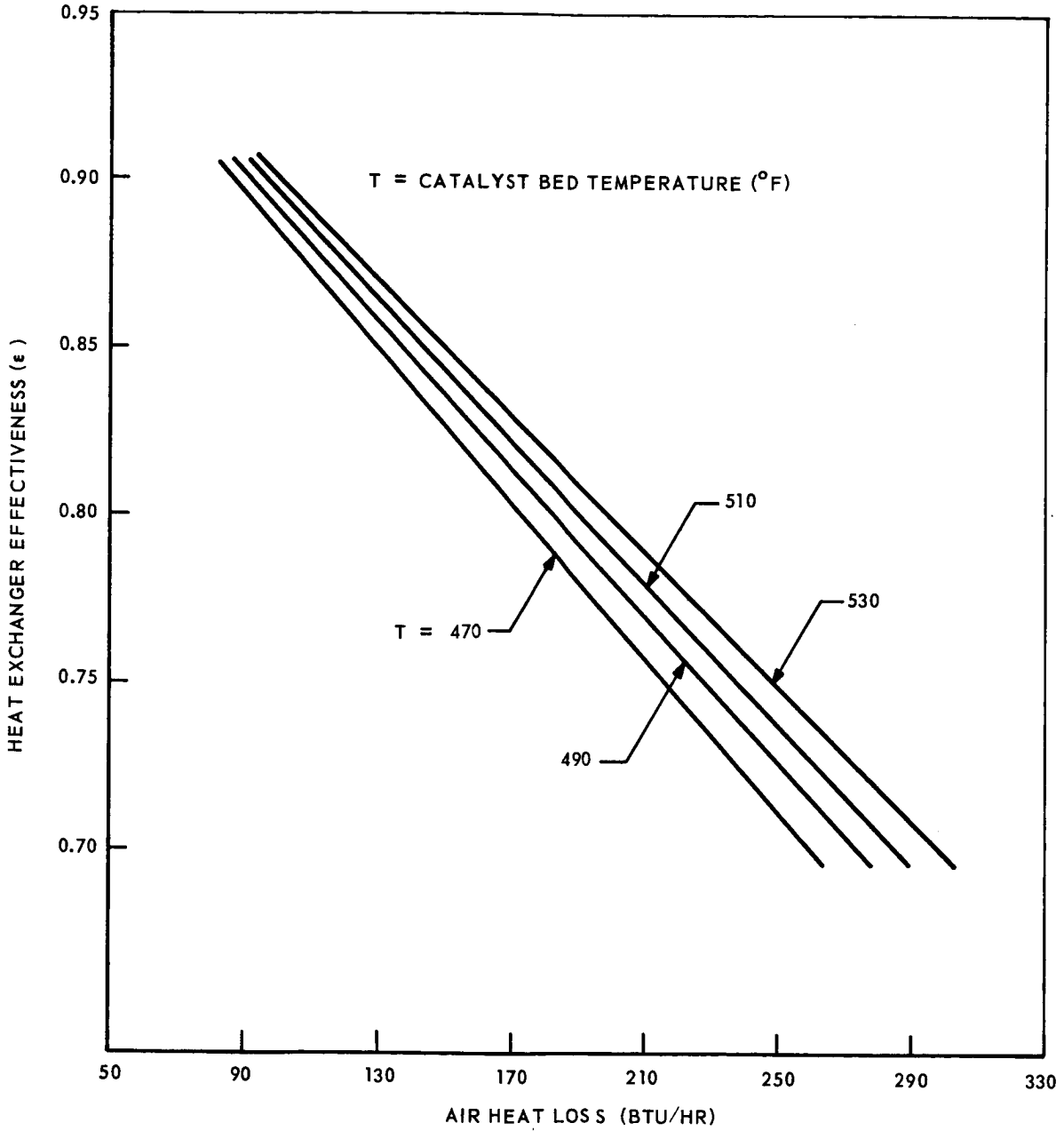

Fig. 16 Effectiveness vs Air Heat Loss

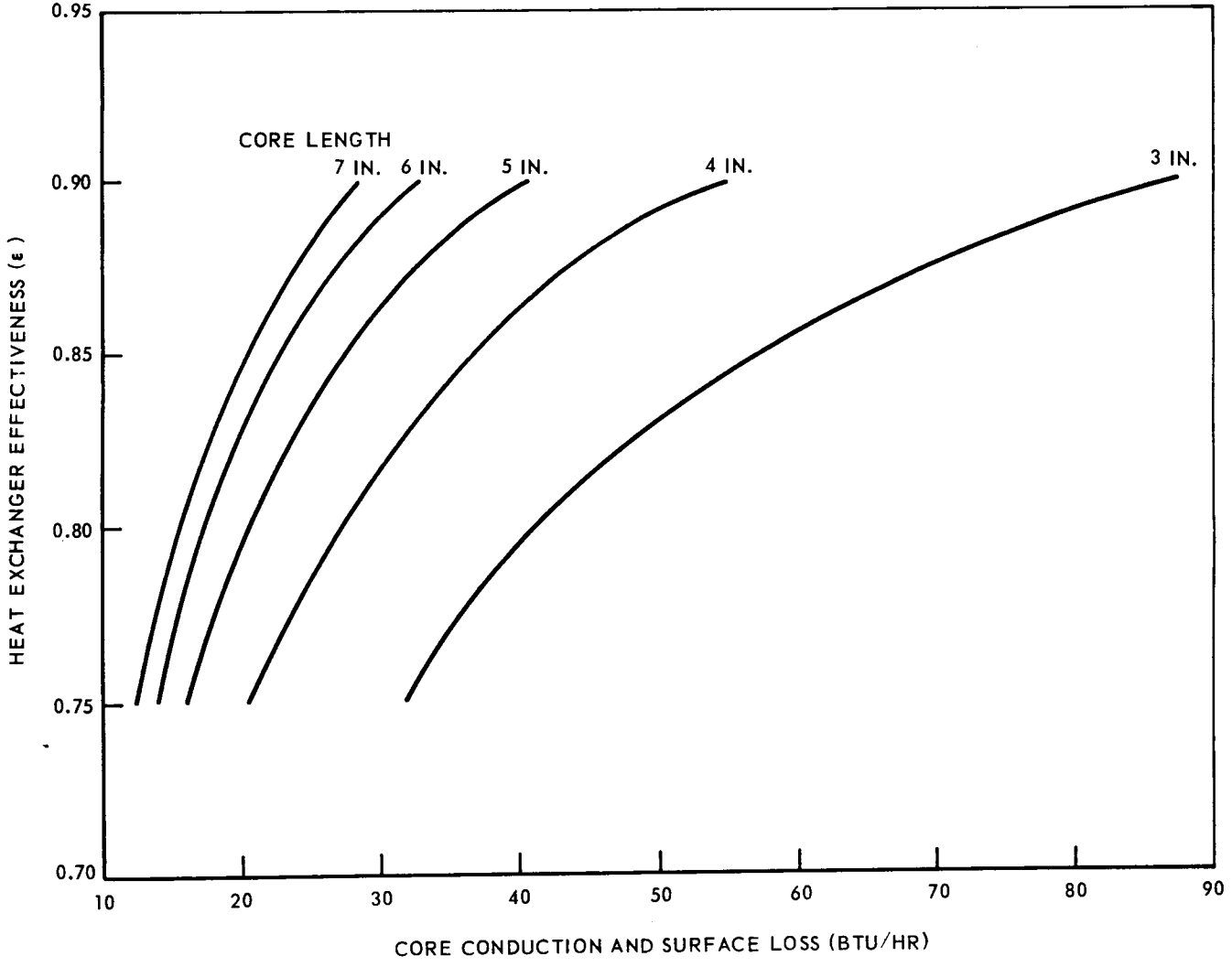

Fig. 17 Effectiveness vs Core Conduction and Surface Losses

Effectiveness vs pressure drop (fig. 18). – The pressure loss for the heat exchanger is an important factor as it relates to the electrical pumping power. This factor is shown as a function of effectiveness for core lengths of interest.

As core length increases, the flow area decreases, resulting in significantly higher losses in long cores. The importance of this effect is seen as pressure loss in proportion to the square of the length in the IHCOS operating region where laminar flow prevails.

Total equivalent weight vs core length and effectiveness (figs. 19 through 22). – The previously developed curves of weight, thermal losses and pressure loss can now be combined using the assumed power penalties, at a given effectiveness, to yield total equivalent weight as a function of core length.

In general, the low core lengths result in high core conduction thermal losses and high penalty while the higher length results in a significant pressure loss penalty. The result is a minimum penalty at a unique optimum core length for each effectiveness.

Total equivalent weight vs effectiveness (fig. 23). – When the total equivalent weight is plotted as a function of effectiveness at the optimum lengths (obtained from figs. 19 through 22), an optimum effectiveness (which results in a minimum total equivalent weight) is indicated at 87 percent (for all temperatures in the region of interest) for IHCOS conditions. At lower values of effectiveness, the thermal losses result in high penalties. Fixed weight is the dominant factor at the higher values of effectiveness.

Heat exchanger effectiveness vs optimum core length (fig. 24). – As effectivness is increased, the core face area increases for a given core length. This reduces the pressure loss factor and increases the core conduction penalty. As a result, the optimum length for a given effectiveness will increase with efficiencies to balance these two factors. This relation is shown in this curve.

Heat Exchanger Selection

The final heat exchanger configuration can now be obtained from the curves developed in the optimization study. The optimum effectiveness of 87 percent is obtained from fig. 23 at the minimum total equivalent weight. For an effectiveness of 87 percent, the optimum heat exchanger core length is found on fig. 24 as 4.3 inch. The core volume is 16 cubic in., and is found in fig. 14. For the assumed geometry of a square inlet face, the resultant heat exchanger core dimensions will be:

Cold flow length	–	4.3 in.
Hot flow length	–	1.93 in.
No flow length	–	1.93 in.

The total fixed weight of this unit including headers is obtained from fig. 15, at 1.15 lb. The pressure drop for the heat exchanger can be found by entering fig. 18 at a length of 4.3 in., yielding 0.5 in. of water. The selection of this heat exchanger is valid for the entire range of operating temperatures being considered for IHCOS since the optimum effectiveness and core geometry were independent of operating temperature.

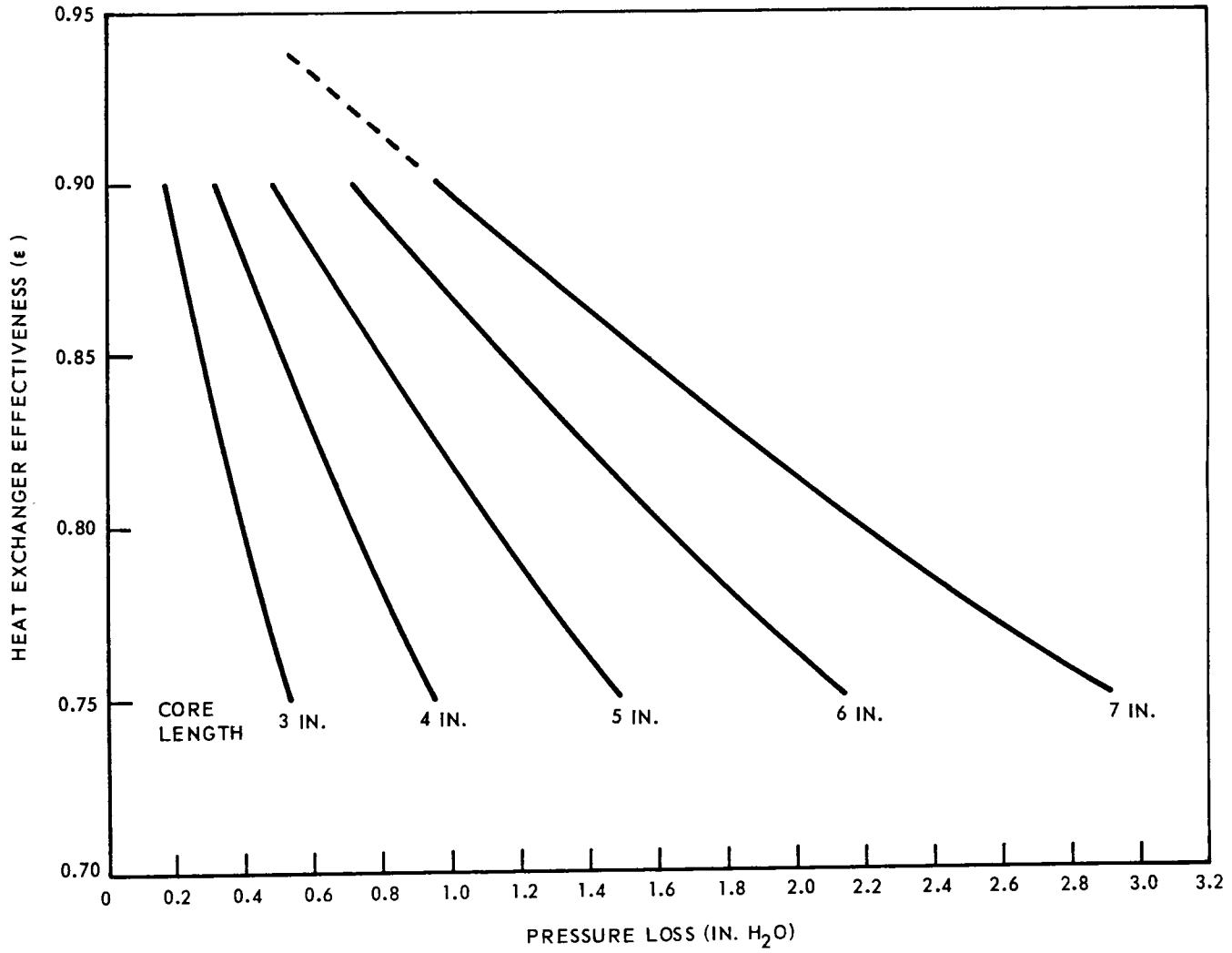

Fig. 18 Effectiveness vs Pressure Drop

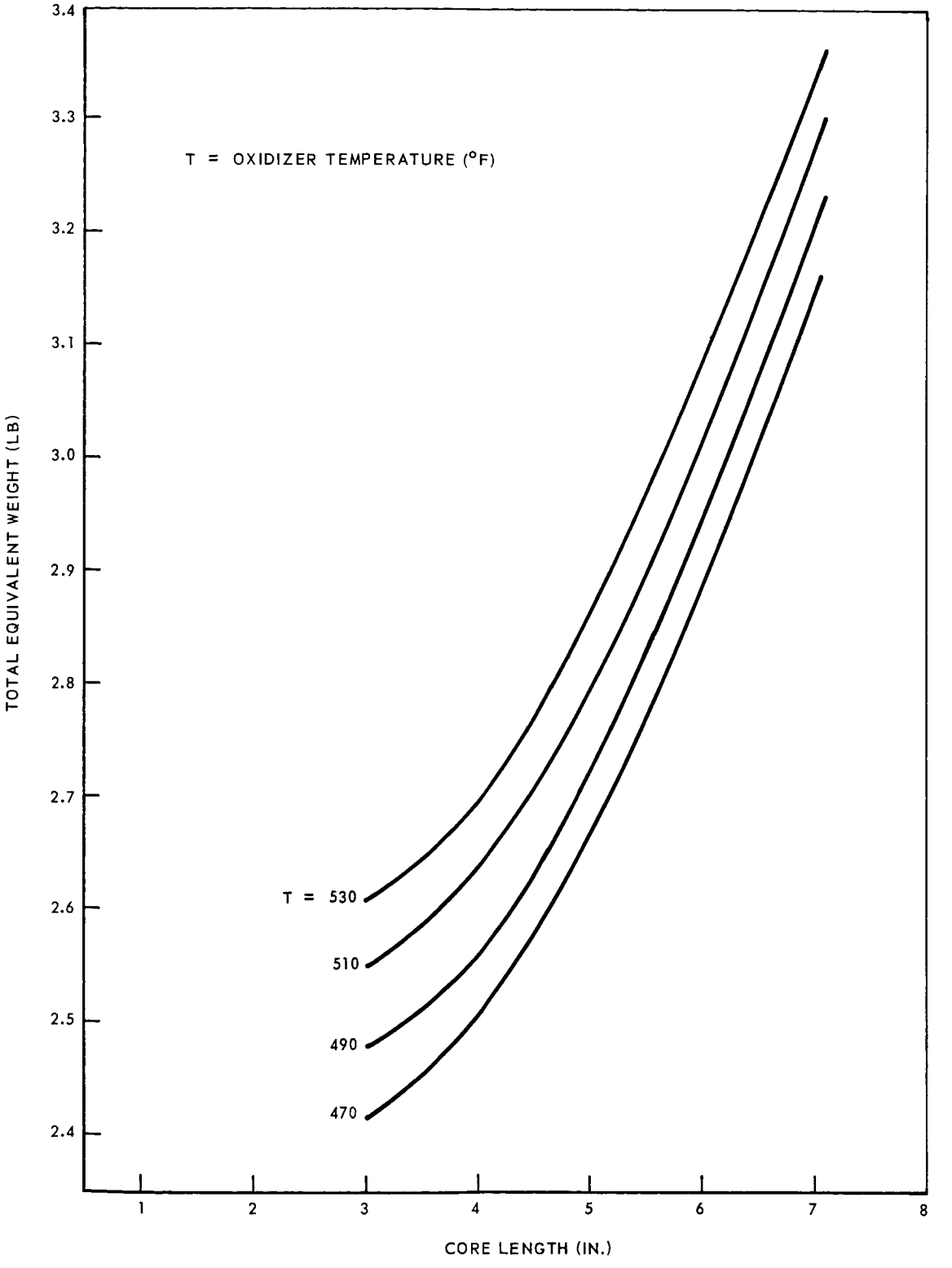

Fig. 19 Total Equivalent Weight vs Core Length and Effectiveness (ϵ = .75)

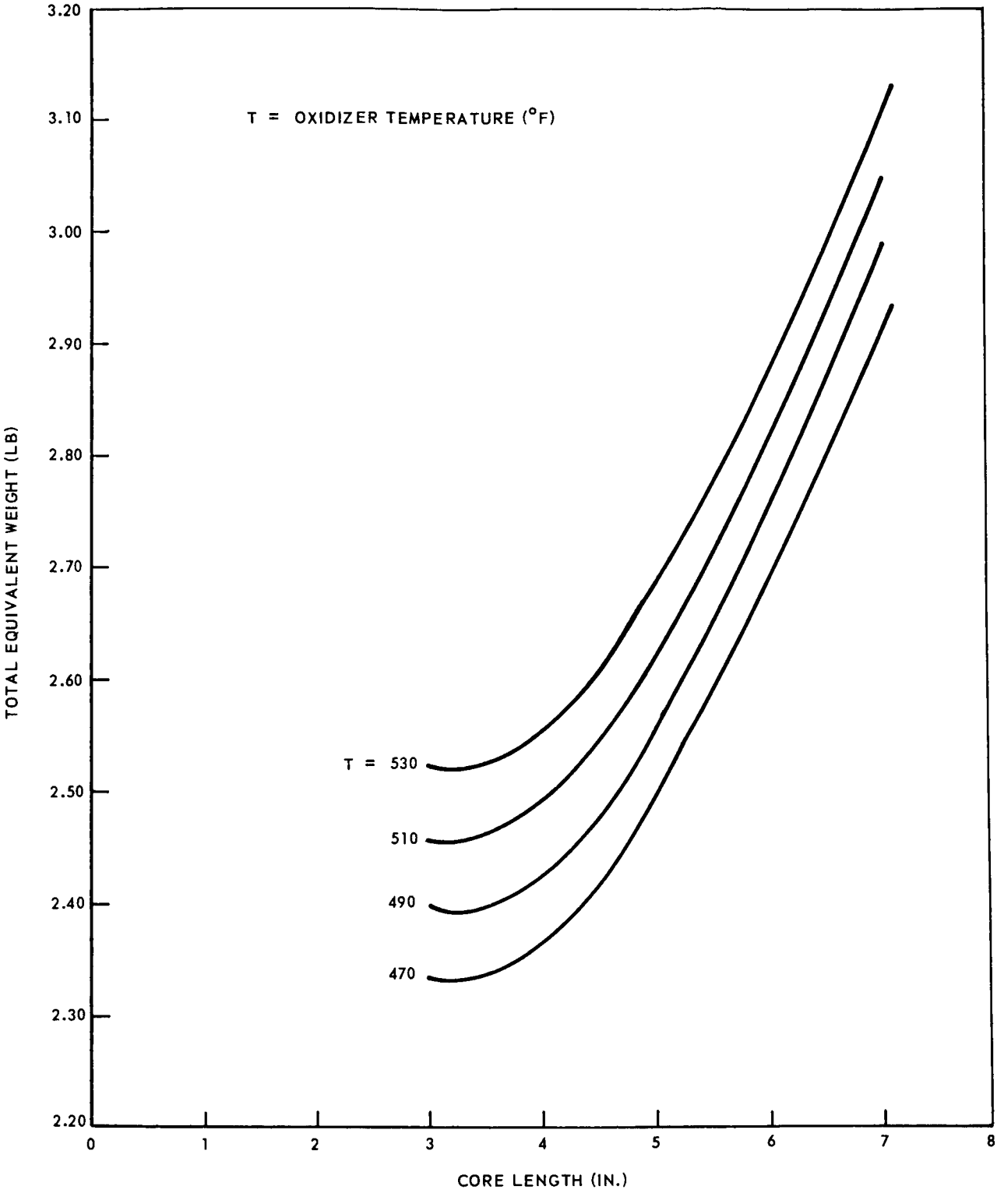

Fig. 20 Total Equivalent Weight vs Core Length and Effectiveness (ϵ = .80)

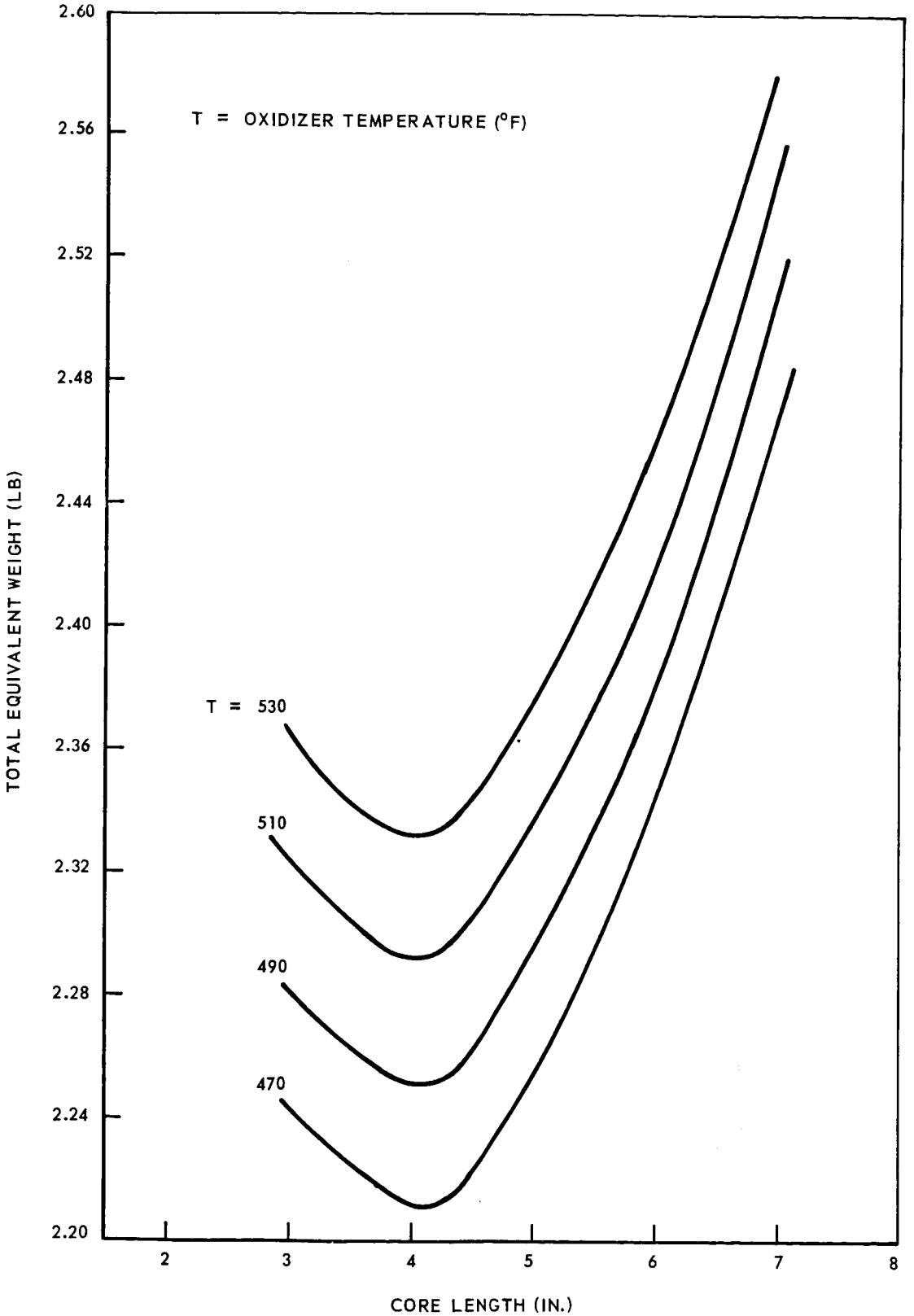

Fig. 21 Total Equivalent Weight vs Core Length and Effectiveness (ϵ = .85)

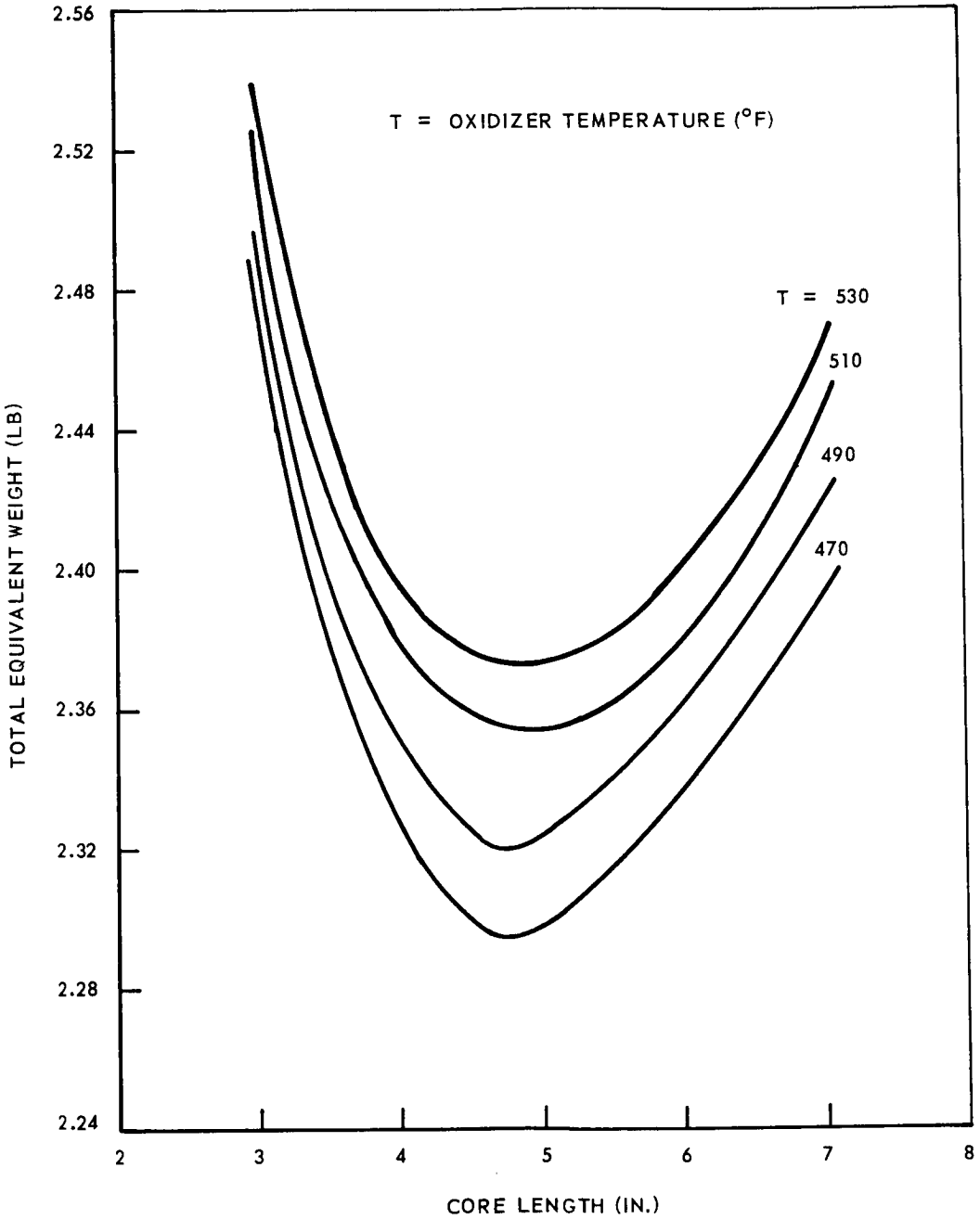

Fig. 22 Total Equivalent Weight vs Core Length and Effectivness ($\varepsilon = .90$)

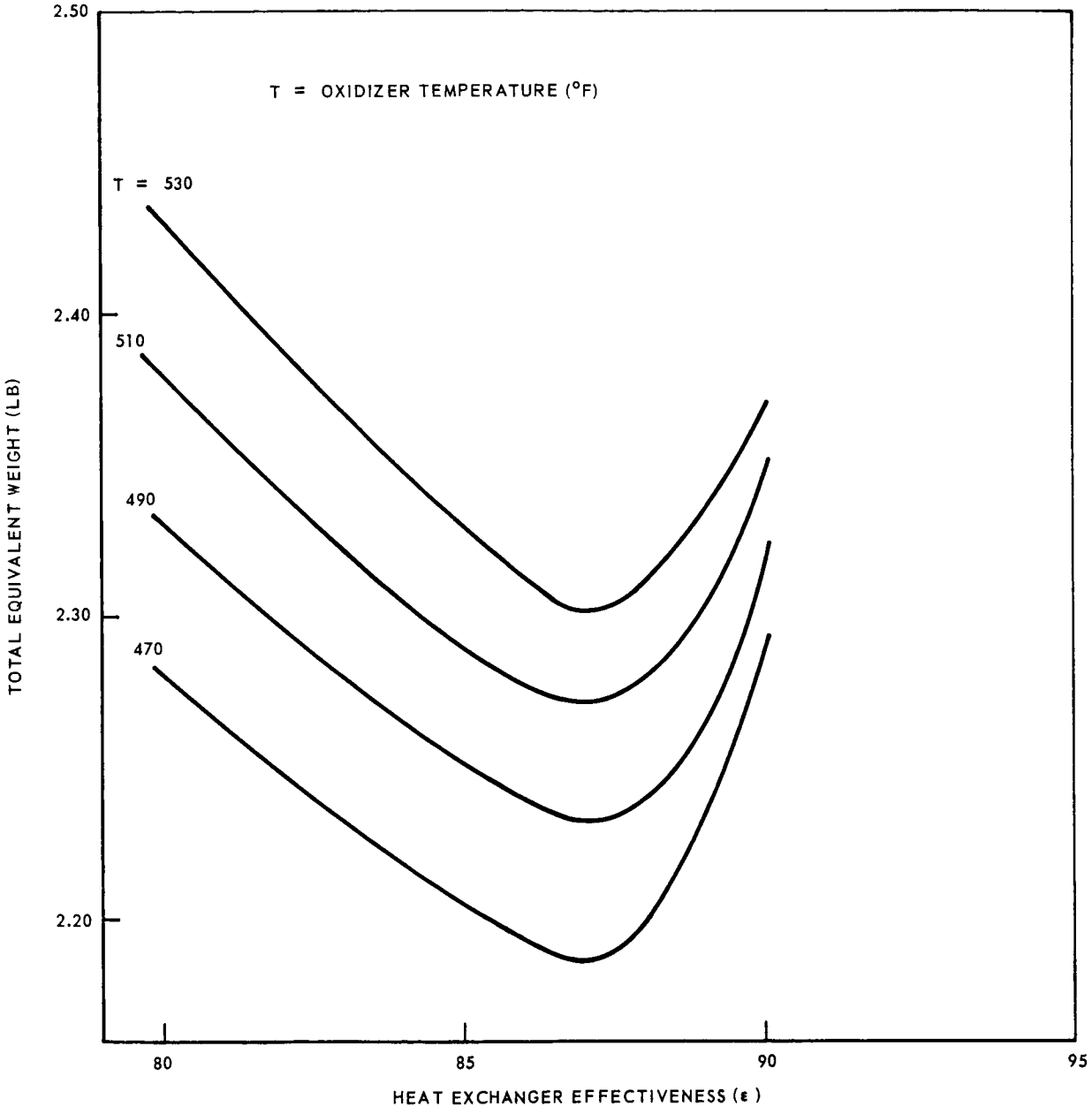

Fig. 23 Total Equivalent Weight vs Effectiveness for Optimum Core Length

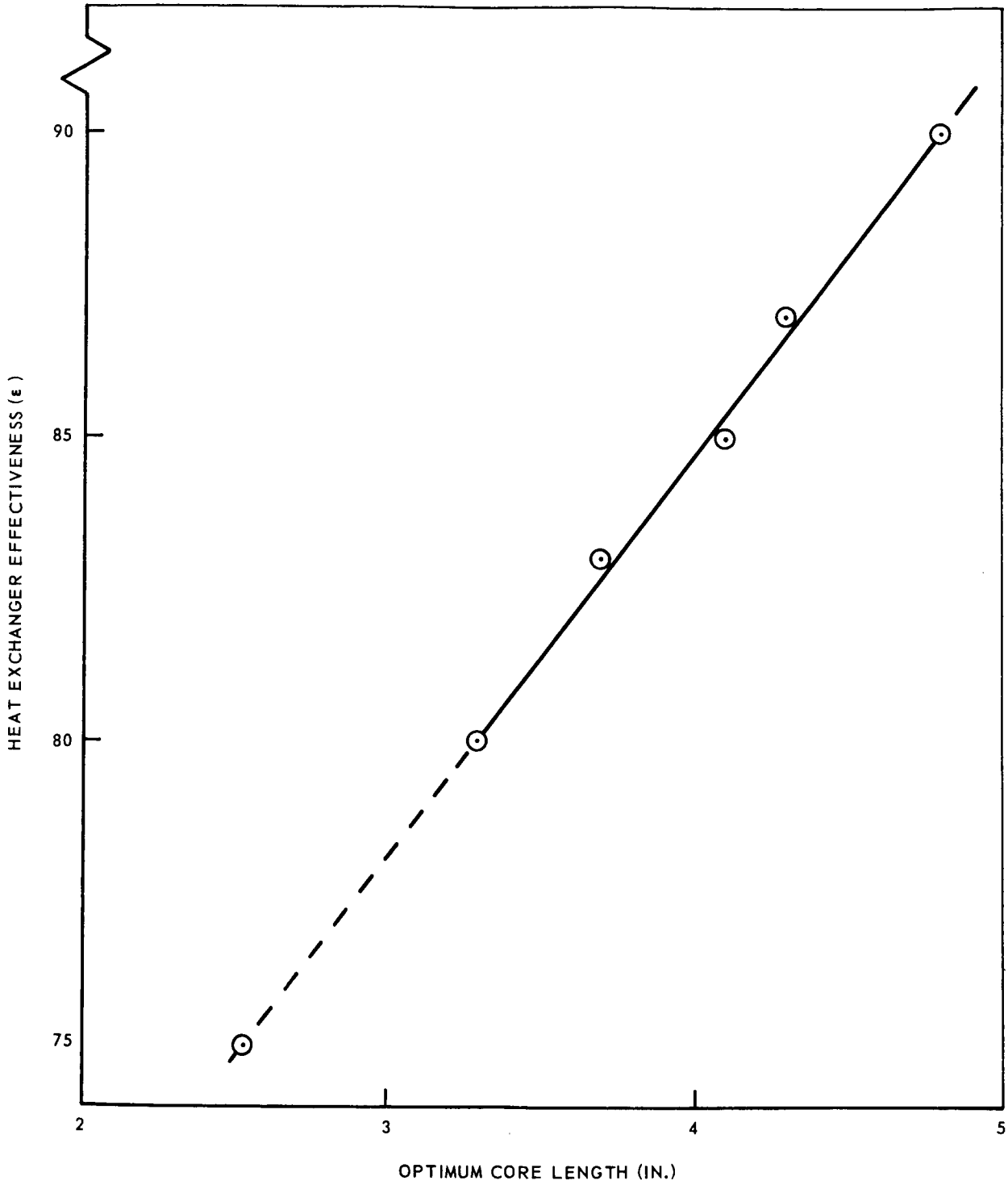

Fig. 24 Heat Exchanger Effectiveness vs Optimum Core Length

If the penalty factors for electrical and thermal energy are changed, the results of this optimization study will vary. An increase in thermal power penalty will result in increased core lengths to reduce core conduction loss factors. An increase in the electrical penalty increases the importance in pumping power with a resulting decrease in core length. Unfortunately for the heat exchanger optimization, the true thermal power penalty will depend upon the final isotope power level and design configuration which is, as might be expected, unavailable at the onset of the optimization study.

For the purpose of this heat exchanger optimization, a predicted power penalty of 20 lb/kw was assumed. If this value of power penalty does not change much, the results of this optimization will remain valid. This effect will be checked after the final step of the system optimization is completed.

Following the heat exchanger optimization effort the performance characteristics of the selected heat exchanger were reviewed by potential heat exchanger suppliers. The results of their analyses indicated a slightly different core geometry to achieve the desired performance. This heat exchanger will have an overall effectiveness of 0.83, including core and surface heat transfer losses, and will have core dimensions of:

Cold flow length	–	5.0 in.
Hot flow length	–	2.0 in.
No flow length	–	3.0 in.

The effect of the new core geometry is not included in the optimization study results presented herein; however, they have been examined and were found to be minor.

Isotope Heat Source Characterization

During early stages of the IHCOS study, sizes and weights on a number of isotope heat sources of different power levels were developed by TRW. Data from these preliminary calculations were plotted to present size and weight parameters for the IHCOS optimization. The results are shown in figs. 25 through 27.

Thermal energy level vs source diameter (fig. 25). – This figure gives the overall diameter of the heat source including the fuel, container, impact resistant structural material, nickel metal cladding and base for reentry fins. This is the diameter which is used in determining the inside dimension of the catalyst bed.

Thermal energy level vs source length (fig. 26). – This curve shows the total length of the isotope heat source as a function of thermal energy level. This dimension will be used to set the length of the catalyst bed.

Thermal energy level vs source weight (fig. 27). – This curve presents the total weight of the isotope source, including the reentry aids, as a function of thermal energy level. The result of this curve is a power penalty of about 28 lb/kw, rather than 20 lb per kw assumed in the heat exchanger study. This small change in penalty will have a negligible effect in the heat exchanger optimization. These data will be used in the final optimization to obtain a more accurate power penalty.

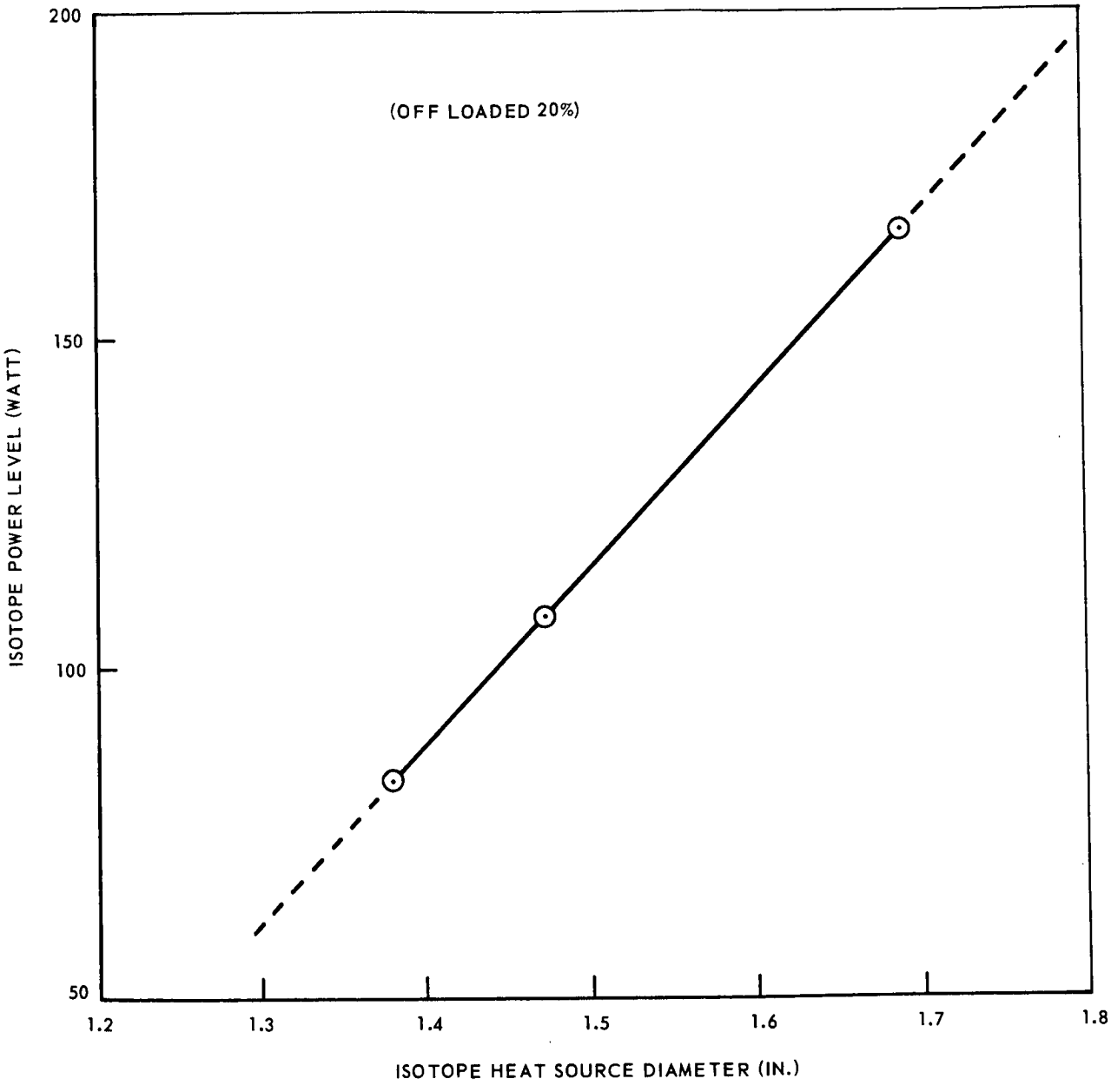

Fig. 25 Thermal Energy Level vs Heat Source Diameter

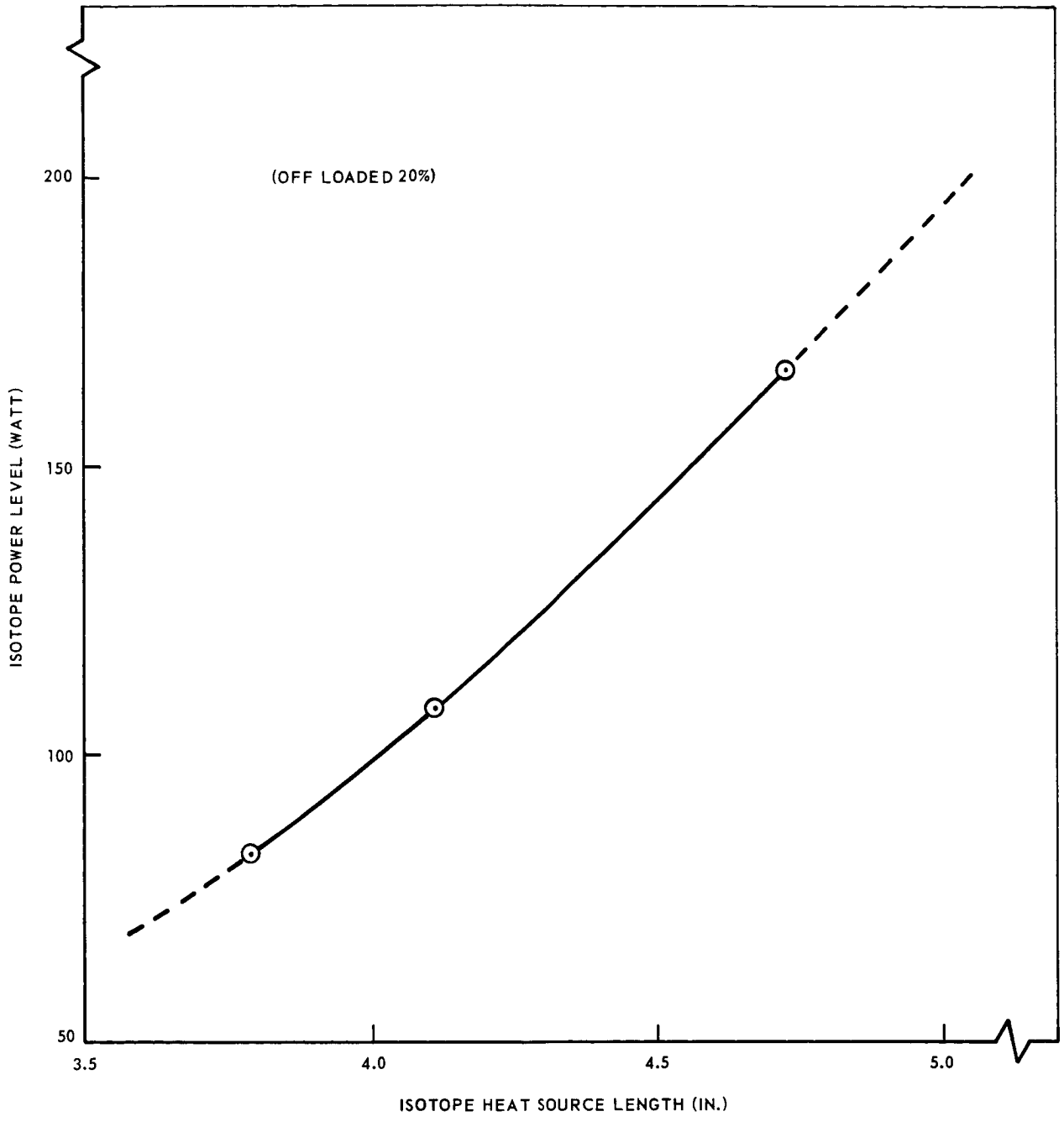

Fig. 26 Thermal Energy Level vs Heat Source Length

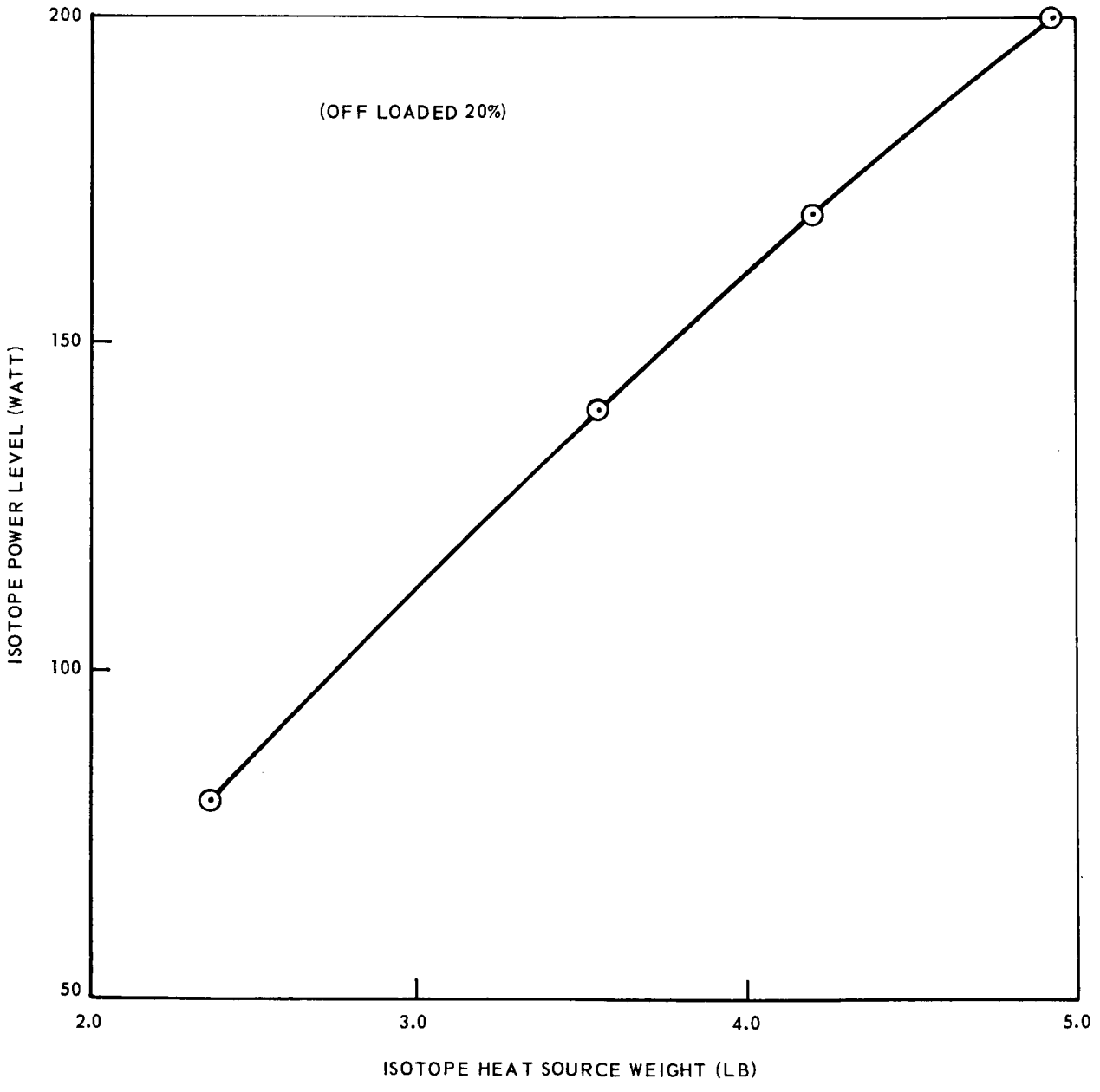

Fig. 27 Thermal Energy Level vs Heat Source Weight

Catalyst Canister Characteristics

The configuration chosen for the catalyst canister in the baseline system was based on a minimum penalty system. A design constraint of the isotope source requires that no material contact the reentry aid fins during normal operation. To maintain a clearance to prevent contact and minimize the size and weight of the catalyst canister, a minimum clearance of 0.1 in. from the heat source was established. This will set the internal diameter of the catalyst bed and the minimum outside diameter.

The metal structure which contains the catalyst must perform a dual function. It must constrain the catalyst, and distribute the heat throughout the bed to minimize thermal gradients during normal operation. Further, it must also provide the major heat flow path to the oxidizer surface during the no-flow depressurized condition. Nickel was chosen as the material for this piece since it has good thermal conductivity and strength at the temperatures encountered. An analysis of the heat transfer required sets the thickness of the radial fins at .050 in., and the inner and outer wall at .100 in. The fins were assumed radial for simplicity in fabrication. Contouring of the fins would result in a negligible advantage in bed size and weight compared to the added complexity.

Space velocity vs temperature (fig. 28). – As previously discussed, the operating temperature of the catalyst oxidizer is set by a requirement for 27 percent conversion of methane at 3 cfm. The catalyst test data relating conversion efficiency as a function of temperature and space velocity were used to establish fig. 28. This figure is a plot of temperature vs the space velocity required for 30 percent conversion of methane. These data are used in establishing the catalyst volume.

Required catalyst volume vs temperature (fig. 29). – This figure is generated from the specified flow of 3 cfm and the data shown in fig. 28. It is used to define the catalyst weight and the geometry of the catalyst container as a function of the bed length.

Oxidizer pressure loss vs temperature (fig. 30). – The pressure loss in the catalyst bed is a contributor to the penalty of IHCOS because of the electrical energy required for the blower. Figure 30 shows increased pressure loss with increasing temperature at fixed values of catalyst bed length. This is due to the smaller cross-section for flow resulting in higher velocities. Further, an increase in length also results in higher pressure loss because of the lower cross-section for flow at a constant temperature (or volume).

Catalyst canister weight penalty vs temperature (fig. 31). – This figure combines the pressure loss penalty with catalyst and metal weight for the catalyst canister. This is done as a function of bed temperature and bed length. Fixed weight is the major factor in setting the penalty of this component. Only at the highest temperatures does the effect of pressure drop become an important contributor to the total penalty. This curve gives a strong indication that, with a relatively low power penalty, it is desirable to operate at the highest possible level of bed temperature and space velocity.

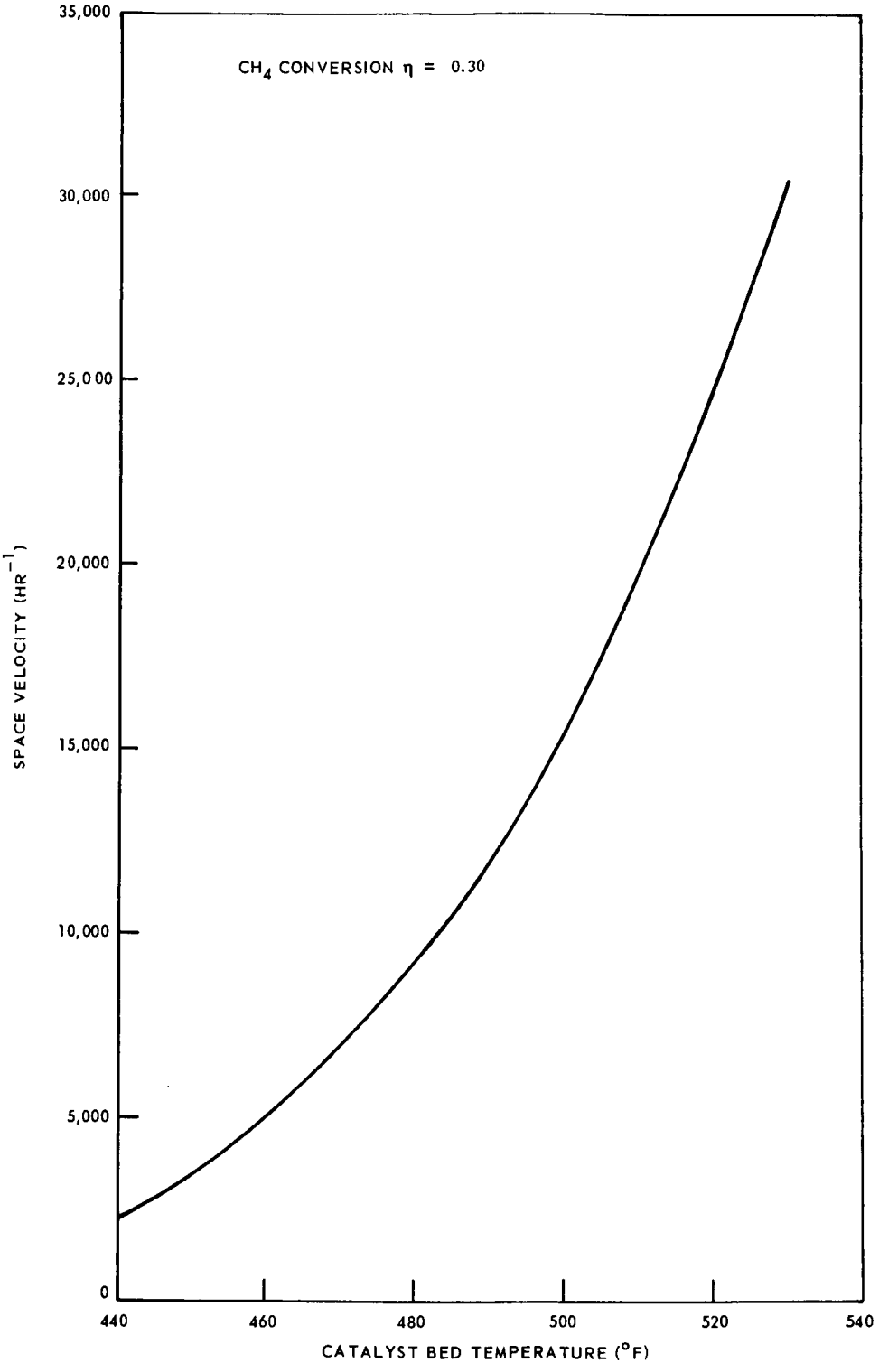

Fig. 28 Space Velocity vs Temperature

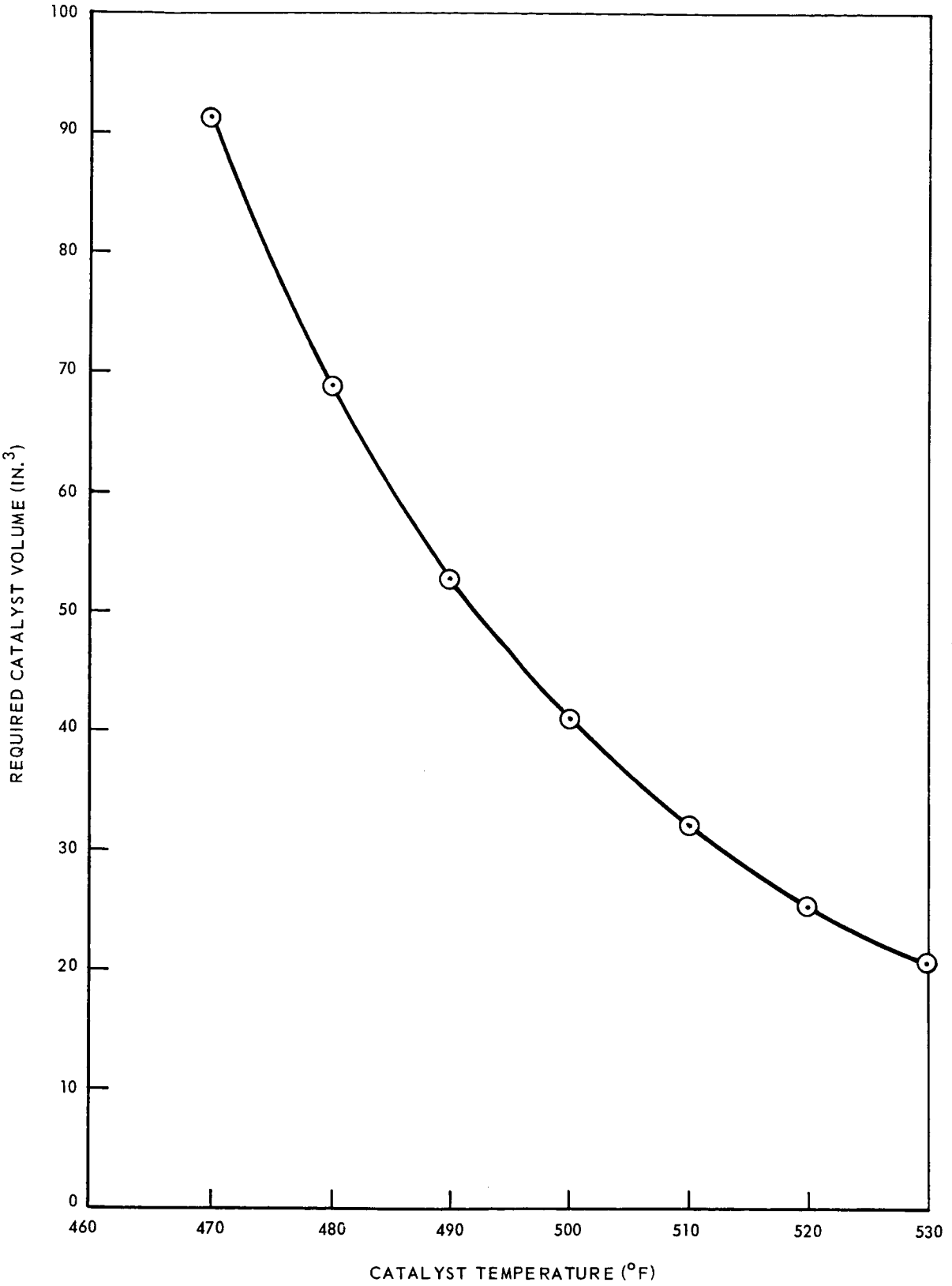

Fig. 29 Catalyst Volume vs Temperature

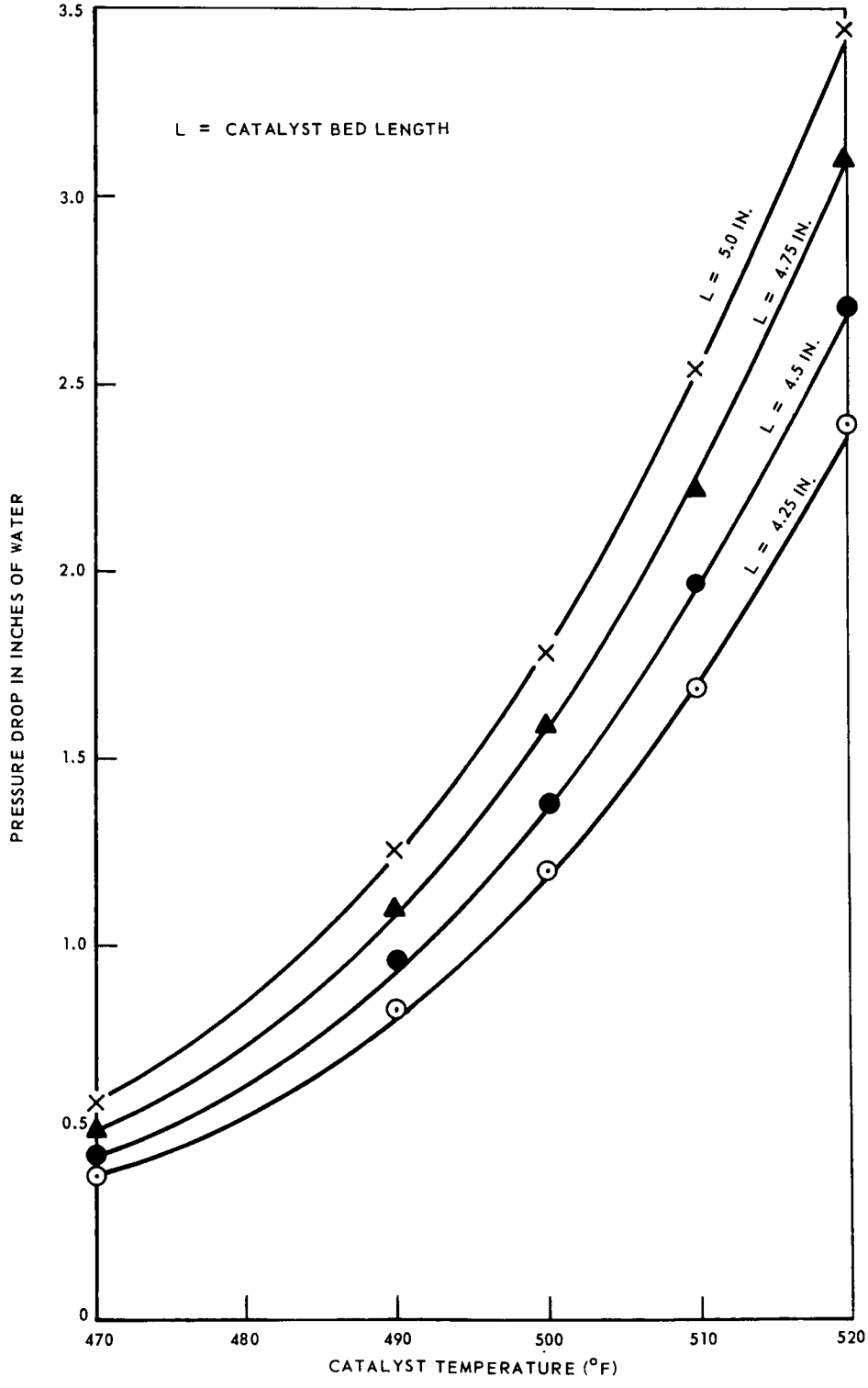

Fig. 30 Catalyst Bed Pressure Loss vs Temperature

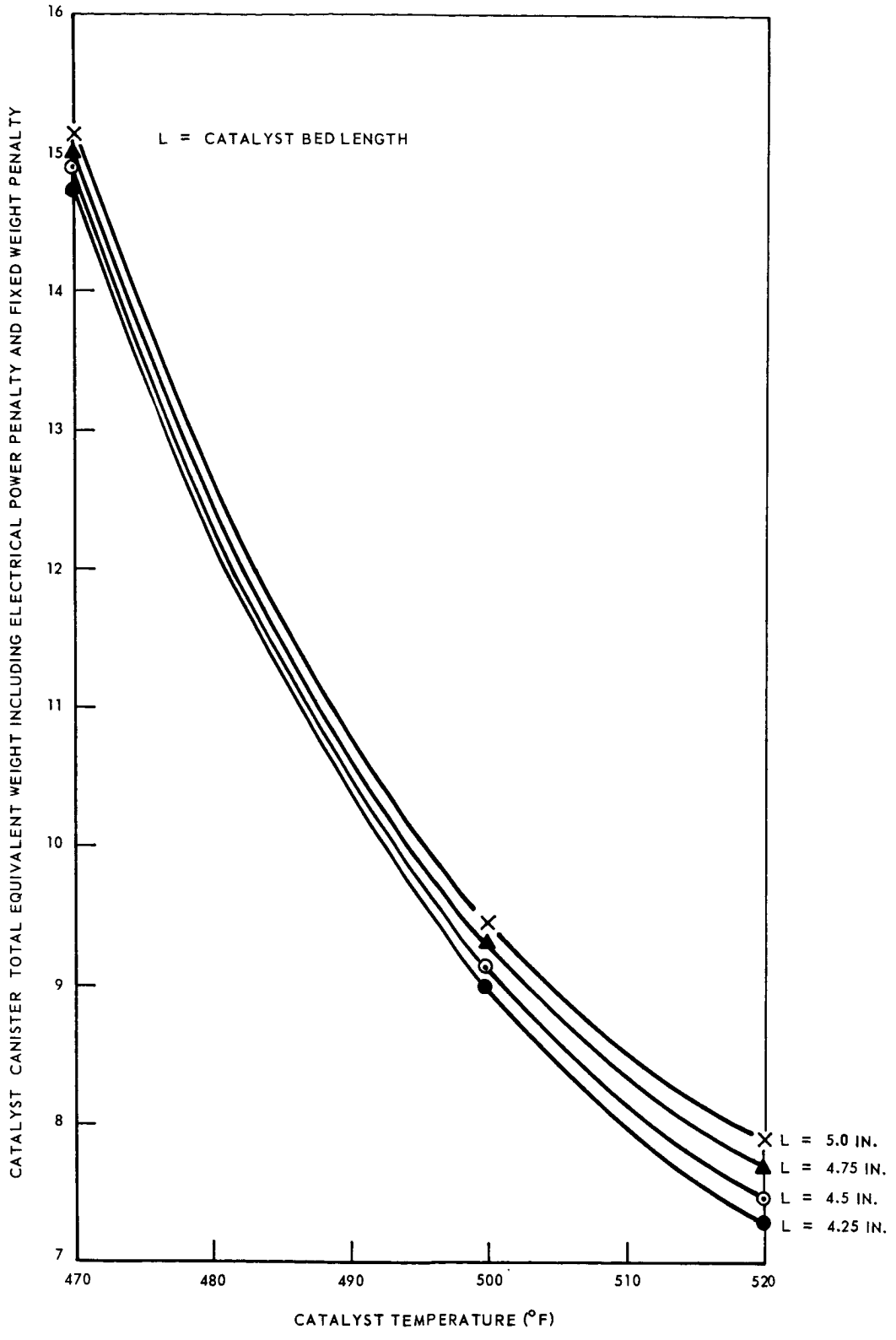

Fig. 31 Catalyst Canister Weight Penalty vs Temperature

Integration of Parametric Data

The final step in the total equivalent weight optimization of IHCOS combines the heat exchanger optimization and the parametric data on the isotope source and catalyst canister with an insulation type and thickness. The assumed configuration for IHCOS is a core consisting of the heat exchanger and isotope heat source catalyst bed section surrounded by a layer of insulation which is encased in an outside can. In this section of the optimization, insulation types are assumed and the heat loss from the system as a function of insulation thickness for various values of bed temperature are determined. With the heat losses and oxidizer temperature specified, the penalties of the heat exchanger, isotope thermal energy source, catalyst bed, insulation, supports, and outside canister can be summed to yield a total equivalent weight for IHCOS.

Figures 32 through 34 present isotope power level and total equivalent weight as a function of insulation thickness for Johns-Manville Min-K insulation at various catalyst bed temperatures. Each of the curves shows a minimum total equivalent weight at a low insulation thickness and relatively high power level. This results from the low weight penalty for thermal energy from an isotope compared to insulation weight.

The insulation thickness for which the no-flow depressurized cabin case will result in a 1000°F catalyst-canister temperature is shown on the curves for the Min-K insulation.

The minimum total equivalent weight experienced is 17.95 lb and occurs at a temperature of 510°F with a corresponding insulation thickness of 0.85 in. These data were also developed for heat-felted fiberglass insulation; however, a higher weight penalty and considerably higher power resulted.

Economic considerations. – It is important to examine the effect of power and booster costs on the IHCOS optimization. The predicted value of isotope costs for a typical mission using IHCOS is $550 per watt of thermal power. A projected on-orbit cost figure is $1500 per pound of payload weight. We may now add these cost penalties to find the point at which the booster and launch penalty of placing insulation in orbit is greater than the savings in power achieved by increasing the insulation thickness of the unit. Figure 35 shows the sum of isotope and booster plus launch costs as a function of insulation thickness. This curve shows a cost penalty optimum of about 1.5 in. of insulation.

An IHCOS design point was chosen at the total minimum cost point, not at the minimum total equivalent weight. This yields a final design configuration of a 98-watt thermal power level, 517°F operating temperature and 1.5 in. of insulation resulting in a total equivalent weight of 19.5 lb, which is only about 1.5 lb greater than a unit optimized on a weight penalty basis only.

The isotope and booster costs associated with a purely weight-optimized unit are approximately $98,000, whereas these costs are about $83,000 for the cost optimized unit. Thus, the selected unit is only 1.5 lb greater than minimum possible total equivalent weight but $15,000 cheaper per unit.

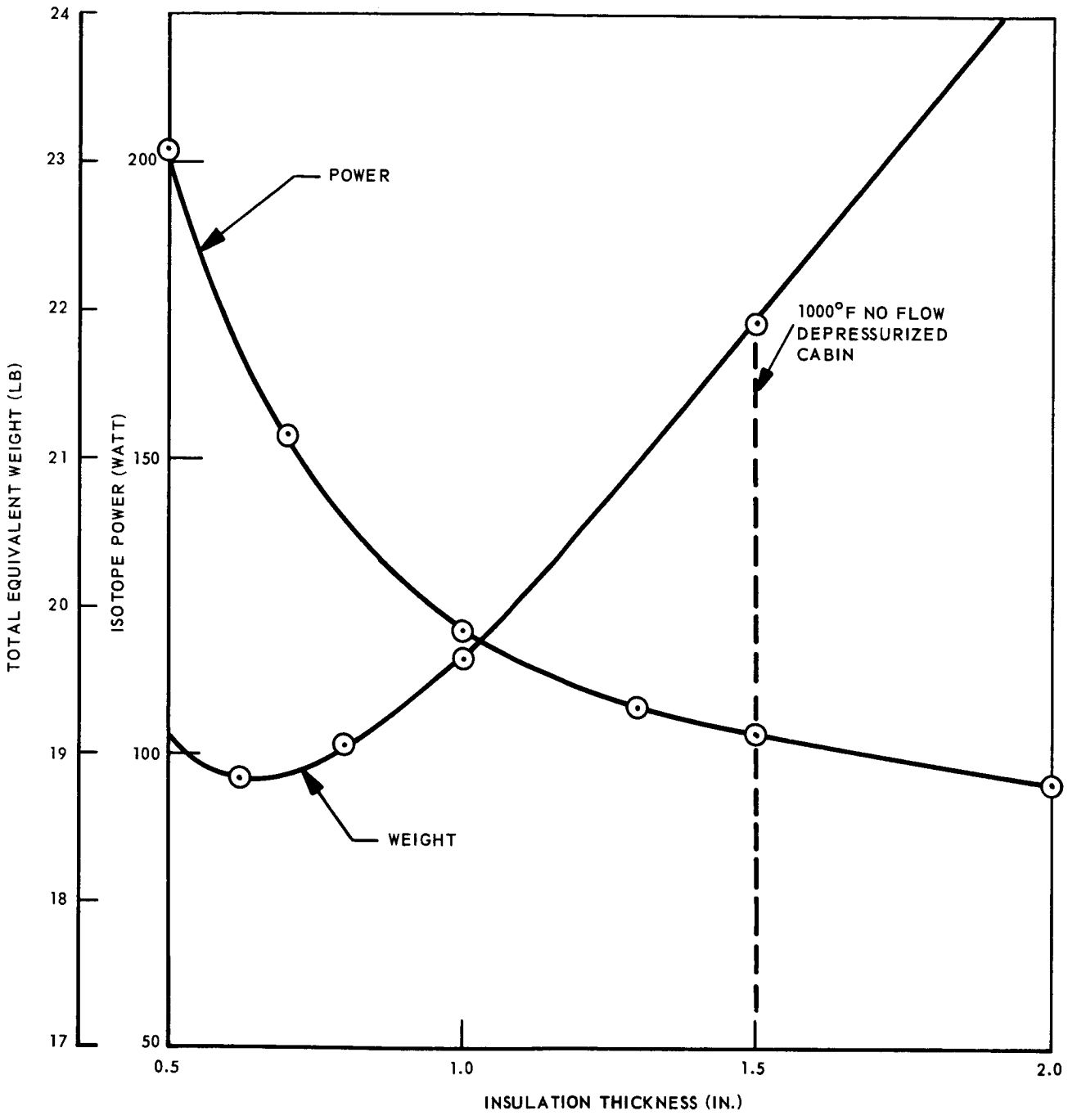

Fig. 32 Isotope Power Level and TEW vs Insulation Thickness at Temperature of 505°F

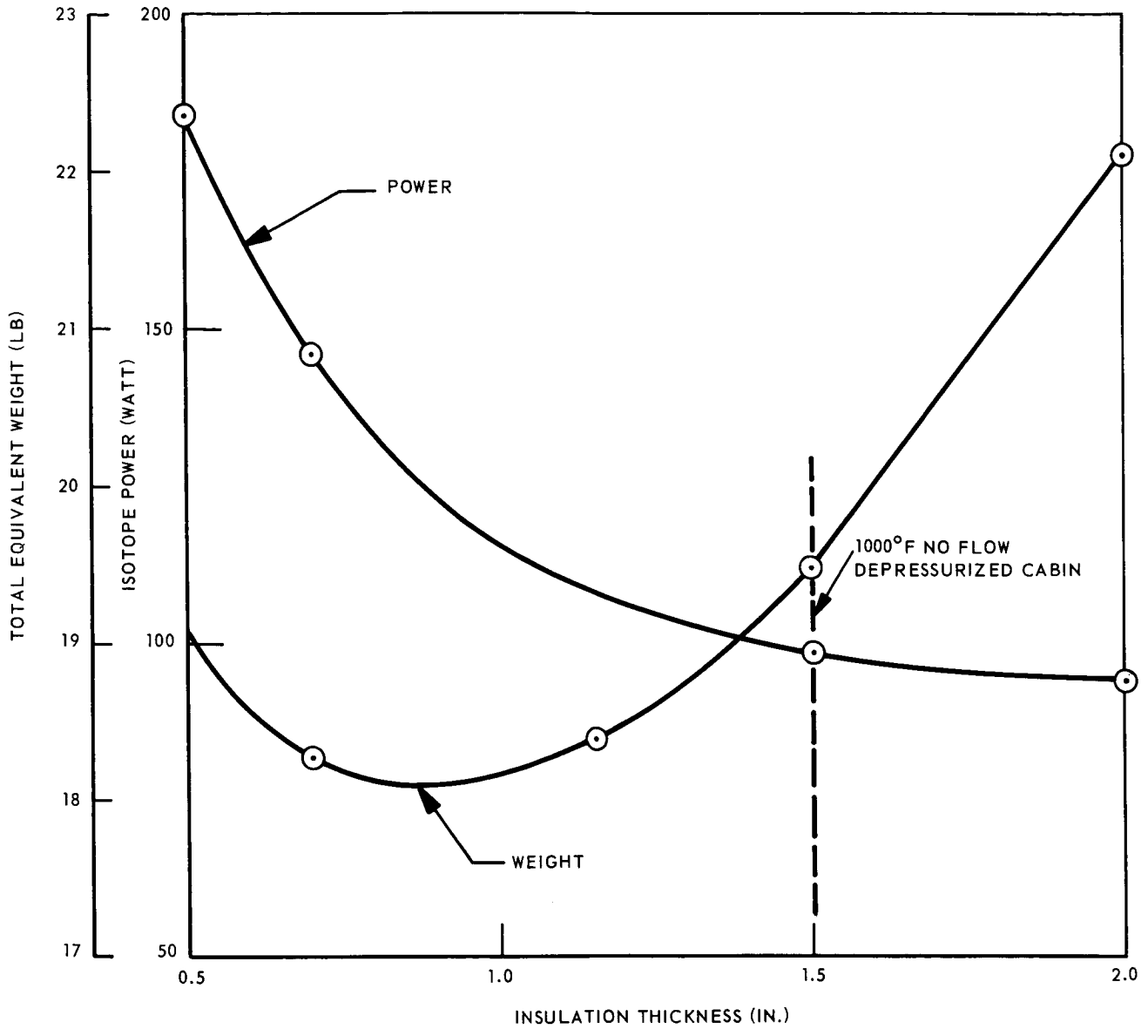

Fig. 34 Isotope Power Level and TEW vs Insulation Thickness at Temperature of 517°F

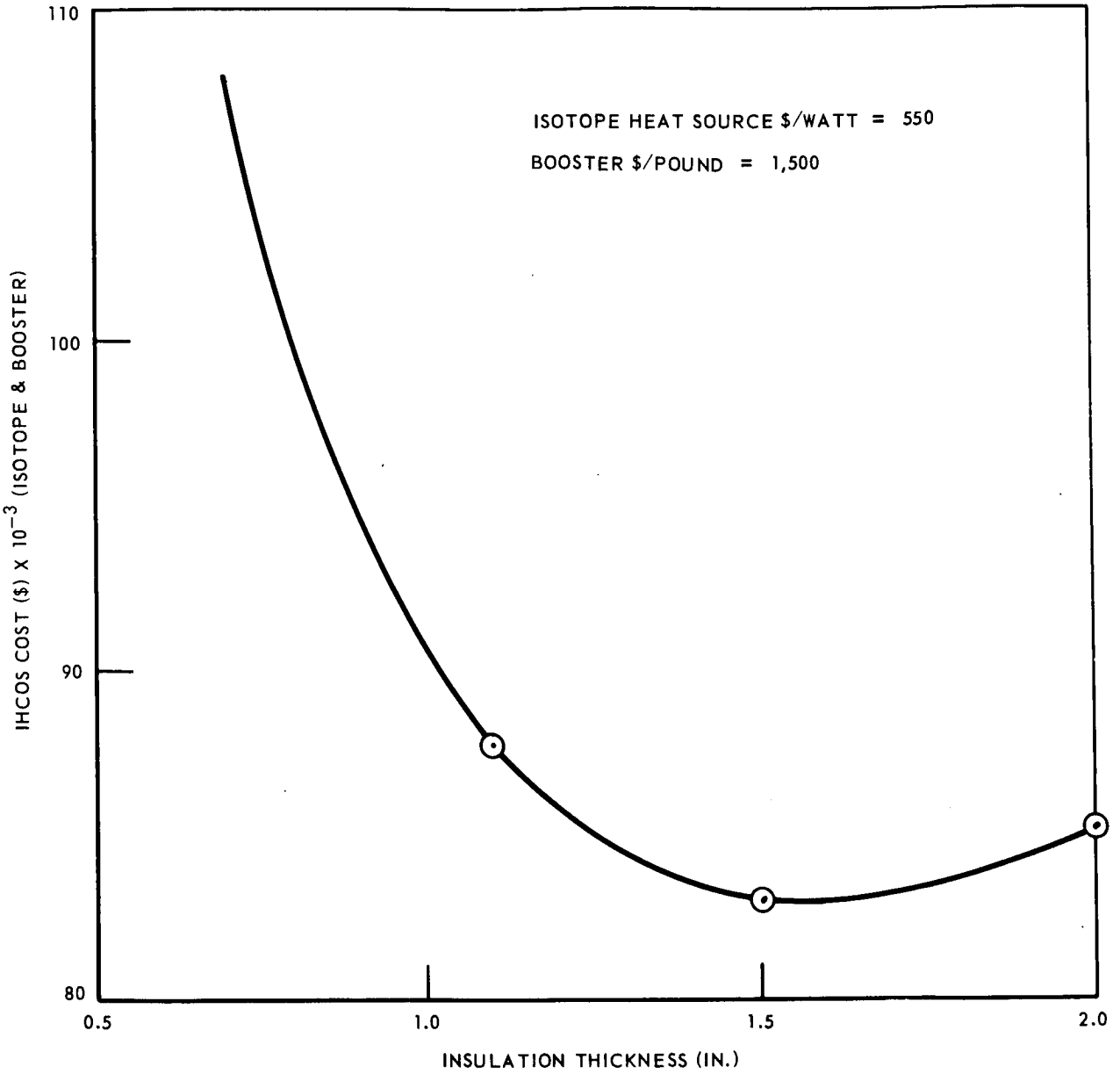

Fig. 35 IHCOS Cost (Isotope and Booster) vs Insulation Thickness

The final power penalty for this unit is 27 lb/kw. A check of the effect of this penalty on the heat exchanger optimization showed a negligible effect.

Active vs passive temperature control. – The choice between active and passive temperature control for IHCOS depends upon the potential weight savings of an actively controlled unit as compared to the simplicity and reliability of a passively controlled unit. The heat exchanger weight will be the same for each method of temperature control. Further, the type of supporting structure chosen is typical of low heat loss supports, and little weight savings can be expected from further reducing losses in this area. The only area where a significant savings can be made is in the heat losses from the surface of the catalytic oxidizer and the heat exchanger. If passive control is used where losses are by thermal conductivity through the insulation, the minimum loss will be established by the 1000°F maximum temperature limit on the oxidizer surface during the no-flow depressurized cabin condition. This results in a loss of 44 watts through the insulation for the selected configuration, resulting in an insulation penalty of 9.04 lb. These losses could be reduced by using a different type of passive temperature control. If the mode of heat loss from the oxidizer and heat exchanger surface is by radiation only, the loss could be reduced to 36 watts by using hard vacuum and polished gold surfaces to obtain low emissivity. This represents the limiting case for passive temperature control. With this configuration, weight of the vacuum can and power penalty will be 5.96 lb. This represents a potential savings over the selected conventional insulation schemes of 3.08 lb. The use of active temperature control allows the power level to be reduced even further, since thermal resistance can be altered to satisfy the 1000°F limitation on catalyst bed temperature. To achieve these lower powers, super insulation will be required. This type of insulation may reduce, under ideal conditions, the heat loss through the insulation to as little as 7 watts with a power penalty of 0.2 lb. The weight of the insulation and vacuum can are 5.7 lb for a total penalty of 5.9 lb.

Table 8 summarizes the differences of these three methods of temperature control and insulation.

TABLE 8

TEMPERATURE CONTROL AND INSULATION

Insulation Method	Conduction	Radiation	Super
Temperature control	Passive	Passive	Active
Insulation losses (watts)	44.0	36.0	7.0
Total insulation weight penalty (lb)	9.04	5.96	5.7
Vacuum required	No	Yes	Yes

The added complexity, and the resulting increased development costs and decreased reliability of the vacuum insulation techniques or active temperature control method, seem to offset the advantages of the 3 to 4 lb weight savings that could be realized. Therefore, passive temperature control utilizing conventional insulation techniques is the selected approach to the IHCOS design.

Selected System

The final design configuration utilizes passive temperature control with conventional insulation. It requires 98 watts of thermal power, operates at 517°F, and has a total equivalent weight of 19.5 lb.

This optimization study shows that an isotope heat source with a thermal power penalty of only 27.5 lb/kw can significantly reduce the penalty of a catalytic oxidizer system for contaminant control. In addition to reducing the equivalent weight of the system, the low penalty of isotope power makes possible the use of passive temperature control and conventional insulation methods at a minimum sacrifice in equivalent weight. This results in reduced complexity and improved reliability.

Moist Gas Design

The long-term test results on the catalyst selected for IHCOS indicate two possible regions of operation depending on the humidity level of the inlet gas. If the inlet gas has a very low dew point, such as the exit of a molecular sieve canister, satisfactory conversion of the methane is achieved at a catalyst bed operating temperature of 517°F. This dry process gas condition served as the basis for the initial IHCOS optimization study. When the inlet gas humidity is raised to a level which might be expected in a typical cabin atmosphere, results show that the catalyst temperature must be raised to 680°F to obtain the required methane conversion efficiency. As a result of this test data, a new design was generated which would provide the required performance with the higher humidity cabin air.

The analysis of the dry process gas unit resulted in considerable insight into the important parameters involved in optimizing IHCOS and clearly showed trends which can be used to generate a new optimized design without repetition of the detail involved in the initial task. The success of the previously selected baseline configuration in generating a straightforward design with a low weight and volume penalty resulted in the use of this basic configuration for the higher temperature unit.

In establishing the configuration of the moist gas unit the heat exchanger, catalyst canister, isotope heat source and insulation were reevaluated.

The heat exchanger optimization study indicated that the optimum heat exchanger is dependent primarily on the heat source power penalty, which is nearly the same for the moist and dry process gas units. As a result, the same heat exchanger configuration has been used in both configurations.

The catalyst canister study showed that an optimum, at the highest possible space velocity, results when the isotope heat source fin height is held at the minimum possible value. Discussions with TRW systems indicated that the previously used isotope fin height of one inch represented the lowest possible value. It was further established that scaling of the isotope heat source should be done by changing the length only. As a result, the catalyst canister diameter was set, and a close estimate of the length could be made by estimating the total power required. The accuracy with which this estimate could be made resulted in a rapidly converging interaction between the power level and length when the insulation calculation was made.

The major difference between the two designs lies in the method of insulating the unit. The temperature must remain between the normal operating temperature and the 1000°F flow shutdown limit during all operating conditions. The two major paths of heat loss during normal operation are (1) losses due to the ineffectiveness of the heat exchanger, and (2) losses through the supporting structure and insulation. During the flow shutdown condition, all of the heat which is normally lost due to the heat exchanger ineffectiveness must be transferred through the insulation and supports. This is possible because of the higher temperature difference (ΔT) between the interior of the unit and ambient during the flow shutdown condition. In the dry process and moist gas units these differences are:

	Normal ΔT	No Flow ΔT
Dry process gas unit	445	785
Moist gas unit	605	785

As can be seen, the increase in ΔT available between the normal and no-flow conditions in the moist gas unit is significantly less than the dry process gas unit. As a result, the use of conventional insulation will require that a larger portion of the losses be through the insulation and supports in the moist gas unit. The power consumption of a moist gas unit using Min-K will be 223 watts. In view of this high power level, a vacuum insulation, whose heat loss varies as the fourth power of temperature, was evaluated. Using this type of insulation, the power level can be reduced to 125 watts and still meet the flow shutdown temperature requirement. In order to achieve this low-power level the emissivities of the vacuum surfaces must be carefully controlled. A gold surface with an emissivity of 0.10 has been selected for the hot surface of the vacuum jacket and a silver surface with an emissivity of 0.05 has been selected for the cold surface. With these surface finishes, both the normal operation and flow shutdown conditions will be met.

In summary, the moist gas design is similar to the unit using dry process gas except for an increase in power from 98 to 125 watts, an increase in operating temperature from 517°F to 680°F, and substitution of a vacuum insulation on the moist gas unit for the conventional insulation for the dry process gas unit.

Off-Design Performance

Upon completion of the long term catalyst test program, parametric catalyst performance was established as a function of temperature, for both dry process and moist gas feed streams. These data were then used to perform a final evaluation of the two designs and establish performance at off-design conditions with varying flow and power level.

Examination of these data revealed that the performance degraded when using a dry inlet feed stream, resulting in a required inlet temperature of 560°F versus the initial design point of 517°F. This higher operating temperature can be achieved by decreasing the isotope off-loading and raising the power level to 107 watts. For the purposes of the off-design performance evaluation, a power level of 107 watts has been used.

After the establishment of 680°F as the design value for the moist gas unit operating temperature, a chemical presorbent was added to the long-term test apparatus to remove unwanted contaminants from the gas stream. The installation of this unit resulted in slightly improved catalyst performance. The improved performance allowed a power reduction, through increased isotope off-loading, to 117 watts. For the purposes of the off-design performance evaluation, the increased performance characteristic was maintained and the 125 watt design power level used.

In establishing the off-design performance characteristics, new performance maps were generated for both the moist and dry process gas units. With these data, the operating temperature for the moist gas and dry process gas units was determined as a function of flow rate and power level. From this, the variation in methane removal with gas flow was established. These off-design performance characteristics are described below.

IHCOS catalyst performance. – The final catalyst performance data were taken at a space velocity of 21,000 hr^{-1} for both dry process and moist gas feed streams. These data were scaled in accordance with the following relationship to obtain values of removal efficiency at other space velocities.

$$\eta\phi = 1 - \left(1 - \eta_{21,000}\right)^2$$

where

$n = \frac{21,000}{\phi}$

ϕ = space velocity

η = removal efficiency

This relation is based on the assumption that a total bed of some particular space velocity has the same performance as a bed made up of n beds of a space velocity for which performance is known. This technique was checked back against the original performance map which was more extensive and found to be a valid extrapolation technique. The results are plotted in figs. 36 and 37 as conversion efficiency vs effective catalyst temperature with space velocity as a parameter.

Operating temperature vs gas flow rate: As the gas flow rate through IHCOS is varied, the heat exchanger losses will change. With the isotope power level held constant at 107 and 125 watts for the dry process and moist gas units, respectively, the relation between operating temperature and flow can be determined from the thermal characteristics of each unit. This variation of operating temperature with flow is presented in fig. 38.

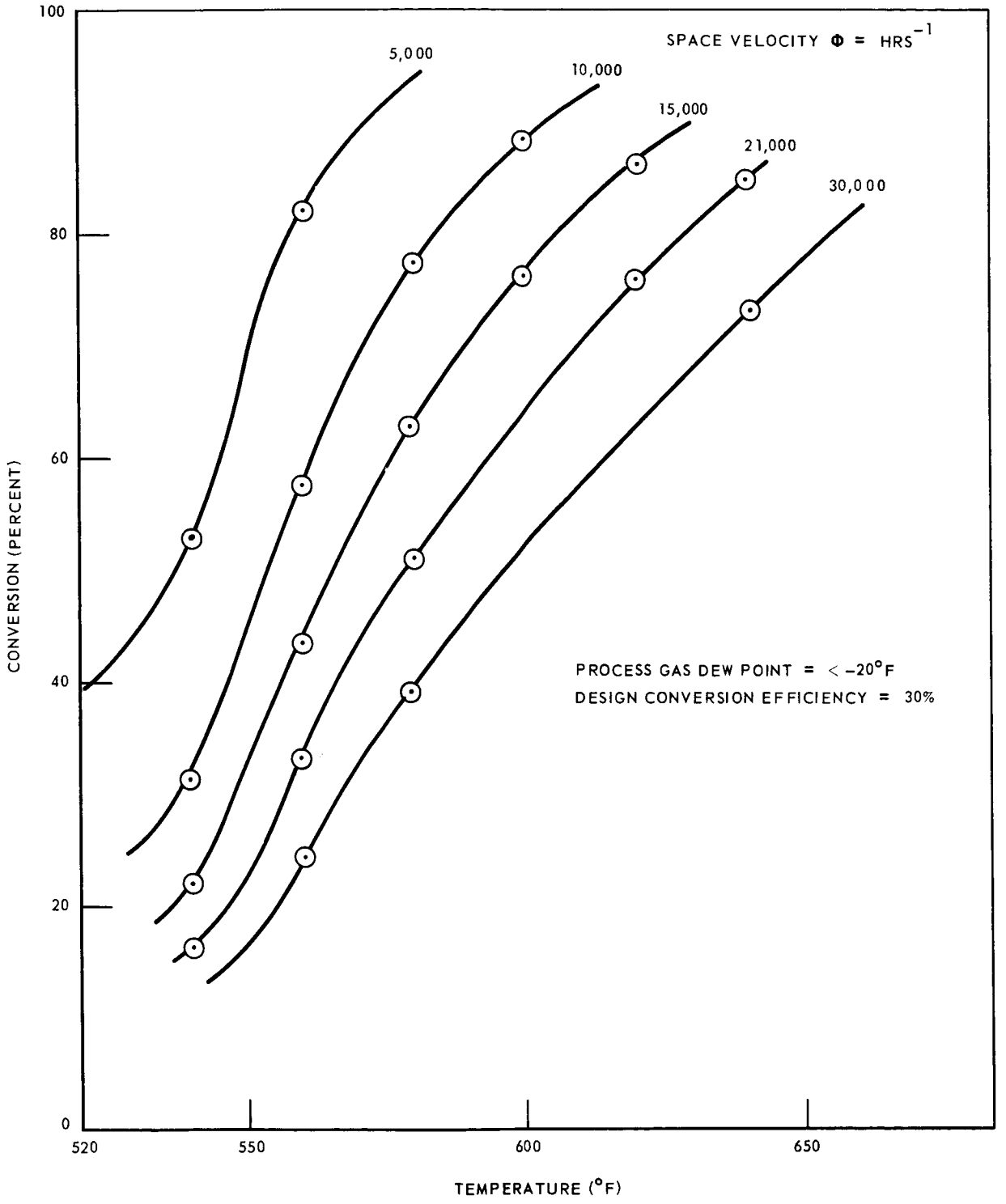

Fig. 36 IHCOS Catalyst Performance – Dry Process Inlet Gas (After 180-Day Endurance Test)

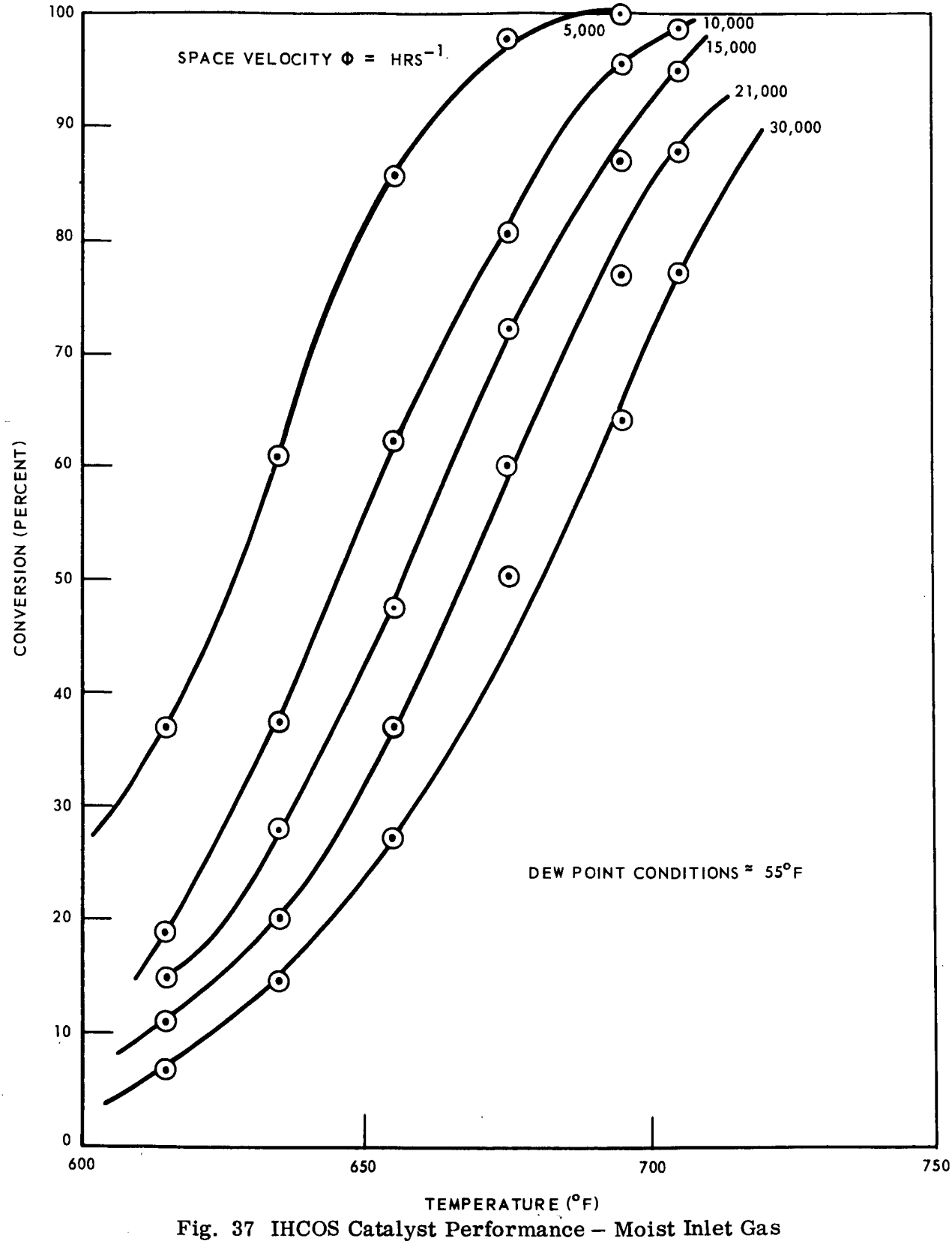

Fig. 37 IHCOS Catalyst Performance – Moist Inlet Gas

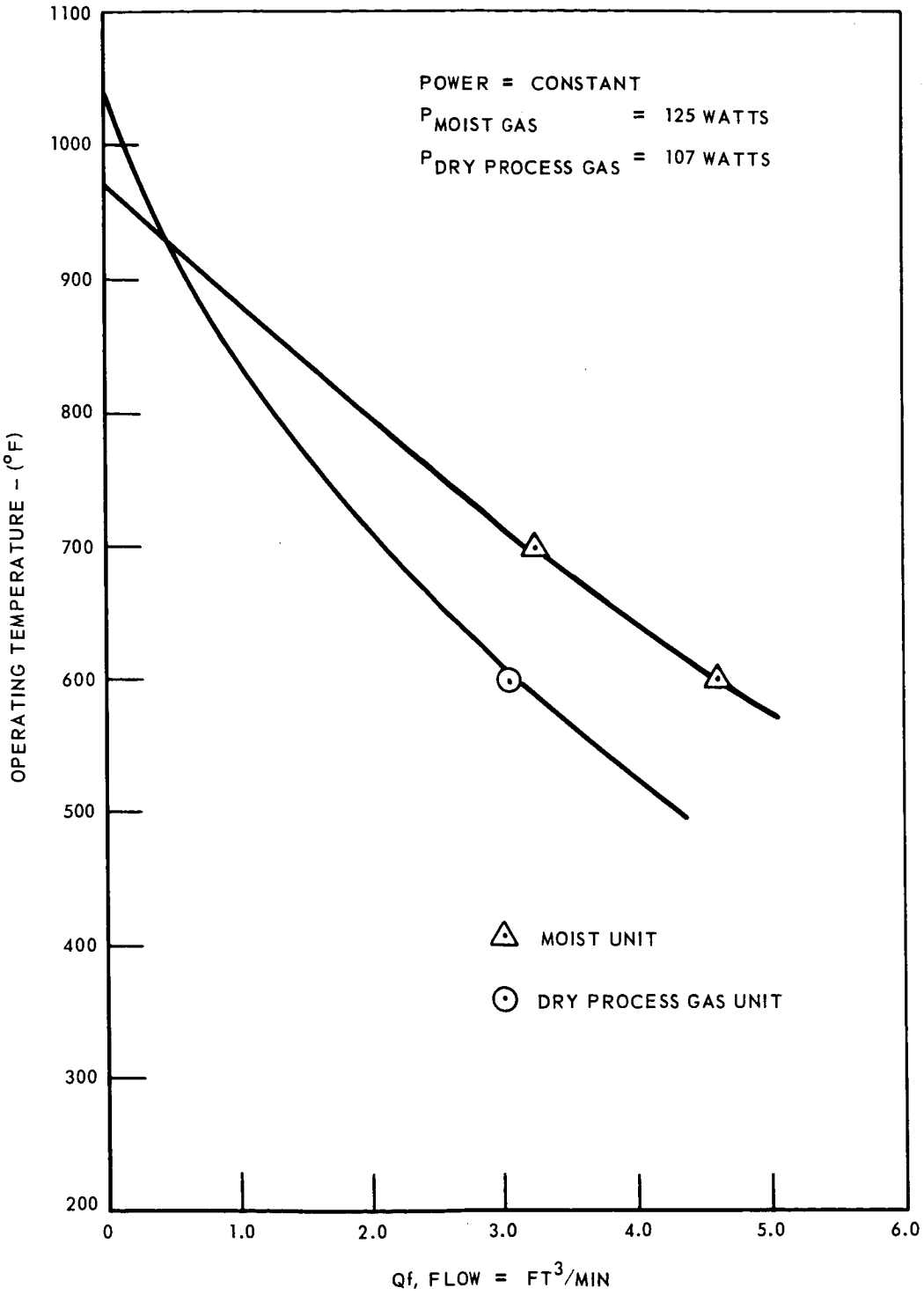

Fig. 38 IHCOS Operating Temperature vs Flow

Operating temperature vs power level: The power level of IHCOS can be varied by changing the off loading of the isotope heat source. The range of interest will vary from a fully loaded capsule of 122 watts for the dry process gas capsule and 157 watts for the moist gas capsule to power levels resulting in temperatures with limited methane conversion. As power level is varied, the no-flow temperature must also be checked for the 1000°F limit. Figure 39 presents the flow and no-flow temperatures as a function of power level for both the dry process and moist gas units. It is observed from these curves that the dry process gas unit at 107 watts exceeds the 1000°F limit by a small amount.

Methane removal capability: The gas flow rate through IHCOS was set by a requirement of 3 cfm for carbon monoxide removal. The IHCOS temperature level is established by a methane removal requirement of 27 percent at 3 cfm. If the required gas flow rate should vary, the methane removal capabilities of the unit will change. This removal capability can be characterized by the product of removal efficiency and flow. The efficiency variation can be found from the operating temperature, space velocity, and catalyst performance variations as established in the previously discussed figures. These data were combined to yield a curve of methane removal capability with flow variation (fig. 40). This curve shows the unit capability varying directly with flow to slightly over 2 cfm. Throughout this region the conversion efficiency is near 100 percent. At about 2 cfm the efficiency starts to drop rapidly due to a drop in temperature with flow and the capability drops to near zero at about 4 cfm.

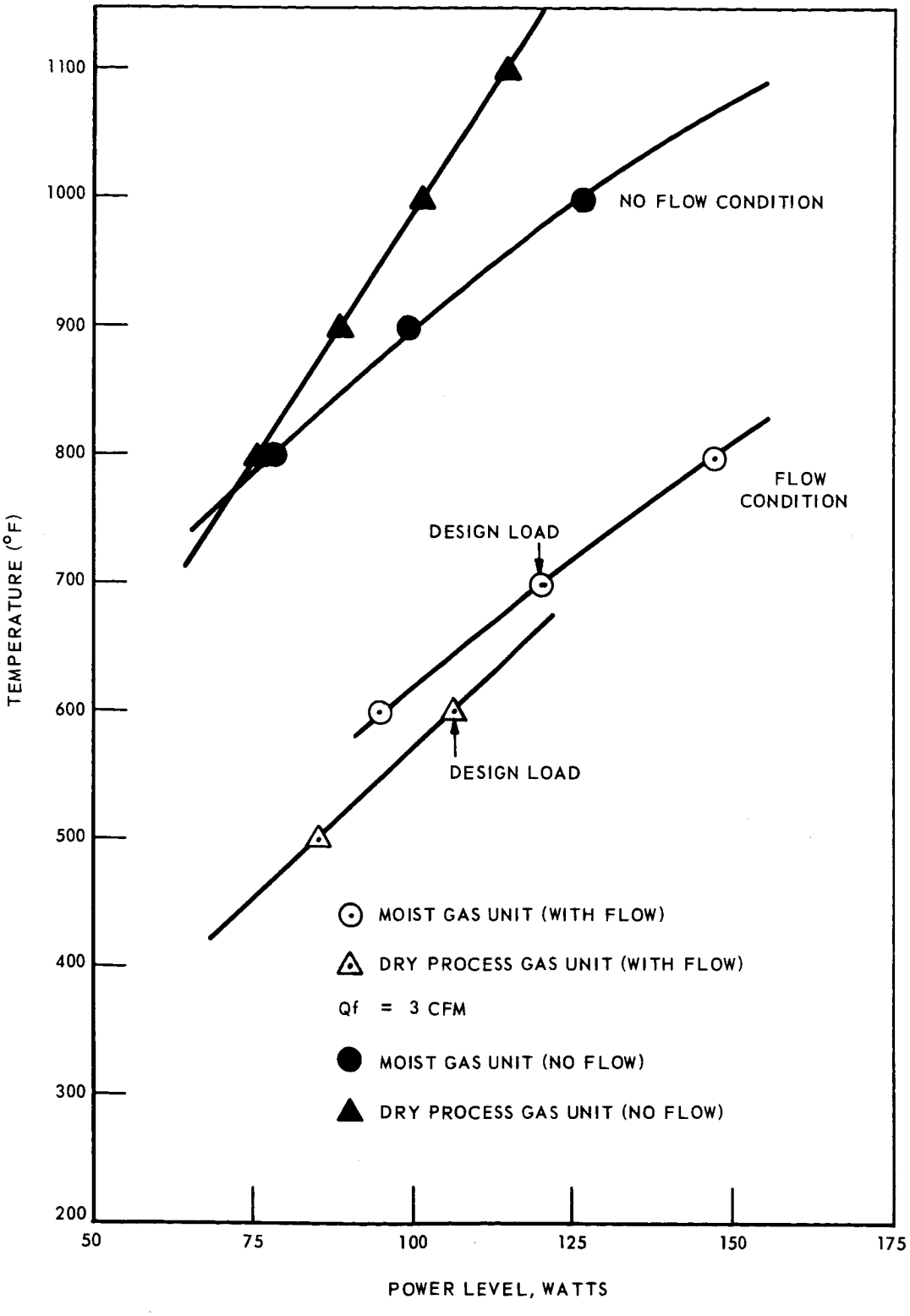

Fig. 39 IHCOS Off-Design Performance – Temperature vs Power Level

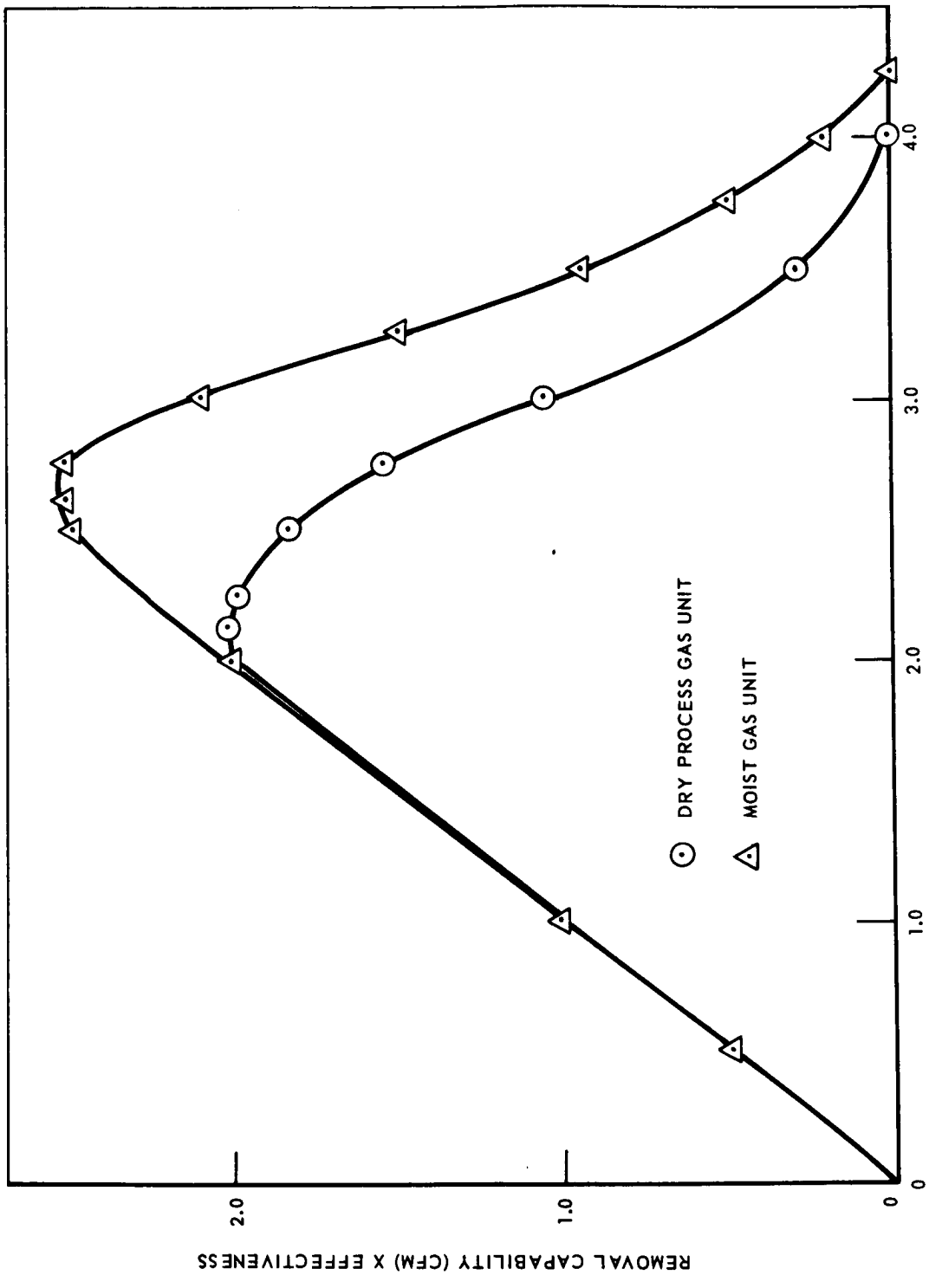

Fig. 40 Methane Removal Capability

LONG TERM CATALYST EVALUATION

Long-term testing of the Isotope Heated Catalytic Oxidizer System, utilizing the selected 0.5 percent palladium catalyst manufactured by Engelhard Industries, was performed for 180 days, beginning on 12 September 1966 and ending on 10 March 1967. This section presents the objectives, apparatus, and procedures used, the results obtained, and a discussion of the results.

Objective

The objective of this test effort was to observe long-term performance characteristics of the selected catalyst under the conditions established in the optimization study. This effort would be accomplished by monitoring the removal efficiency for methane and various other competing contaminants for a 180-day period.

Apparatus

The test apparatus used to obtain the performance data is illustrated in fig. 41. Listed below are the major items of test equipment used.

- Cylinders for gaseous contaminants and a portion of the background gas
- Pressure gauges and regulator to measure and control system pressure
- Inlet and exit sampling septa for obtaining gas samples
- Preheater for heating incoming gas to catalyst bed
- Catalytic oxidizer tube to contain catalyst (catalyst volume = 57 cc)
- Furnace and temperature controller to control catalyst bed temperature
- Air-cooled heat exchanger for cooling exit gas from catalyst bed
- Diaphragm pump and flow control valves for maintaining pressure and for varying system flow rate
- Flowmeter and wet test meter to determine system flowrates
- F&M gas chromatographs Models 720, 1609, 810, 700A and 700B, equipped with flame ionization and thermal conductivity detectors for contaminant analysis
- Water bubbler for humidifying inlet gas stream (added on 29th day)
- Presorbent bed of lithium hydroxide and activated charcoal to remove contaminants present in room air (added on 88th day).

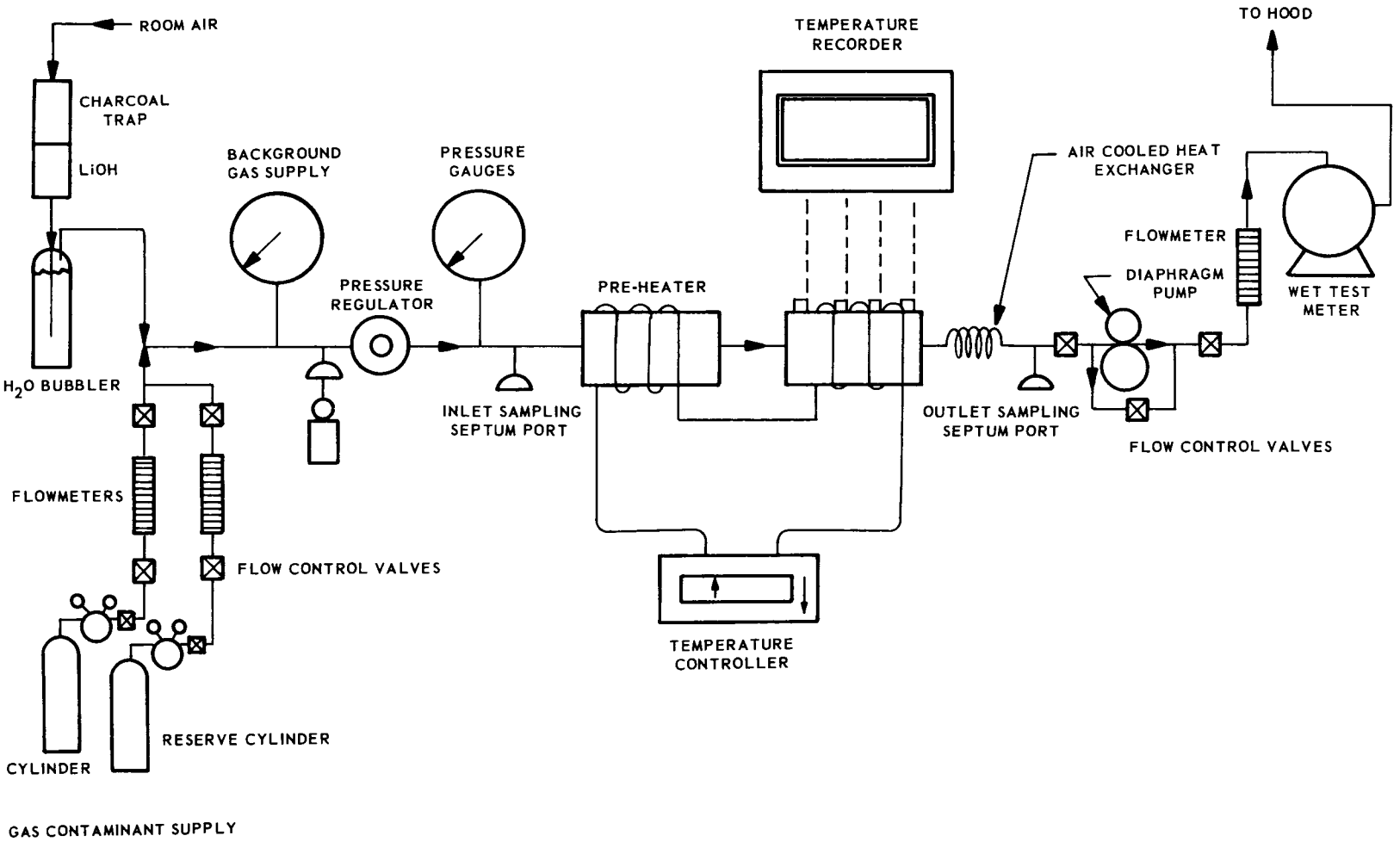

Fig. 41 Schematic Diagram for Long-Term Catalyst Evaluation

Procedure

The long-term performance data on the 0.5 percent Pd catalyst were obtained with the system operating at a space velocity of 21,000 hr^{-1}. Catalyst bed temperatures were maintained at temperature settings varying from 552°F to 692°F to maintain methane conversion efficiency at approximately the required value of 30 percent. Total system pressure was held at 10 psia with a background gas consisting of the contaminants listed in Table 9, 160 mm Hg oxygen, 4 mm Hg carbon dioxide, and the balance nitrogen. Gas supplies were from cylinders, with the exception of the background gas, a portion of which was drawn from the room.

TABLE 9

CONTAMINANTS INTRODUCED IN 180 DAY TEST

Compound	Desired Inlet Concentration (mg/m^3 at 10 psia)
Acetylene	180.0
n-Butane	180.0
Carbon monoxide	29.0
Ethane	180.0
Methane	1720.0
Propylene	180.0

Sampling was performed at both the inlet and outlet of the catalyst bed with a Hamilton 2.5 cc gas-tight syringe and analyzed by a F&M Model 700B gas chromatograph. The inlet and outlet concentrations of methane and carbon monoxide were determined daily, and once weekly, for all other contaminants.

System modifications were made at different times to study the effect of moisture and possible contaminants present in the room air. A humidity sensor was installed on September 28 (17th day). On October 10 (29th day) a water bubbler was installed to increase the dew point of the inlet gas stream to approximately 55°F. On December 7 (88th day) a bed of activated charcoal and lithium hydroxide (first half charcoal, second LiOH) was placed in the room air inlet to remove possible contaminants present in the room air.

The water bubbler was removed on December 12 (123rd day), and was replaced with two canisters of molecular sieve in parallel. This arrangement made it possible for one canister to be on-stream continuously while the molecular sieve in the other was desorbed. A dew point of approximately -20°F was maintained with this arrangement.

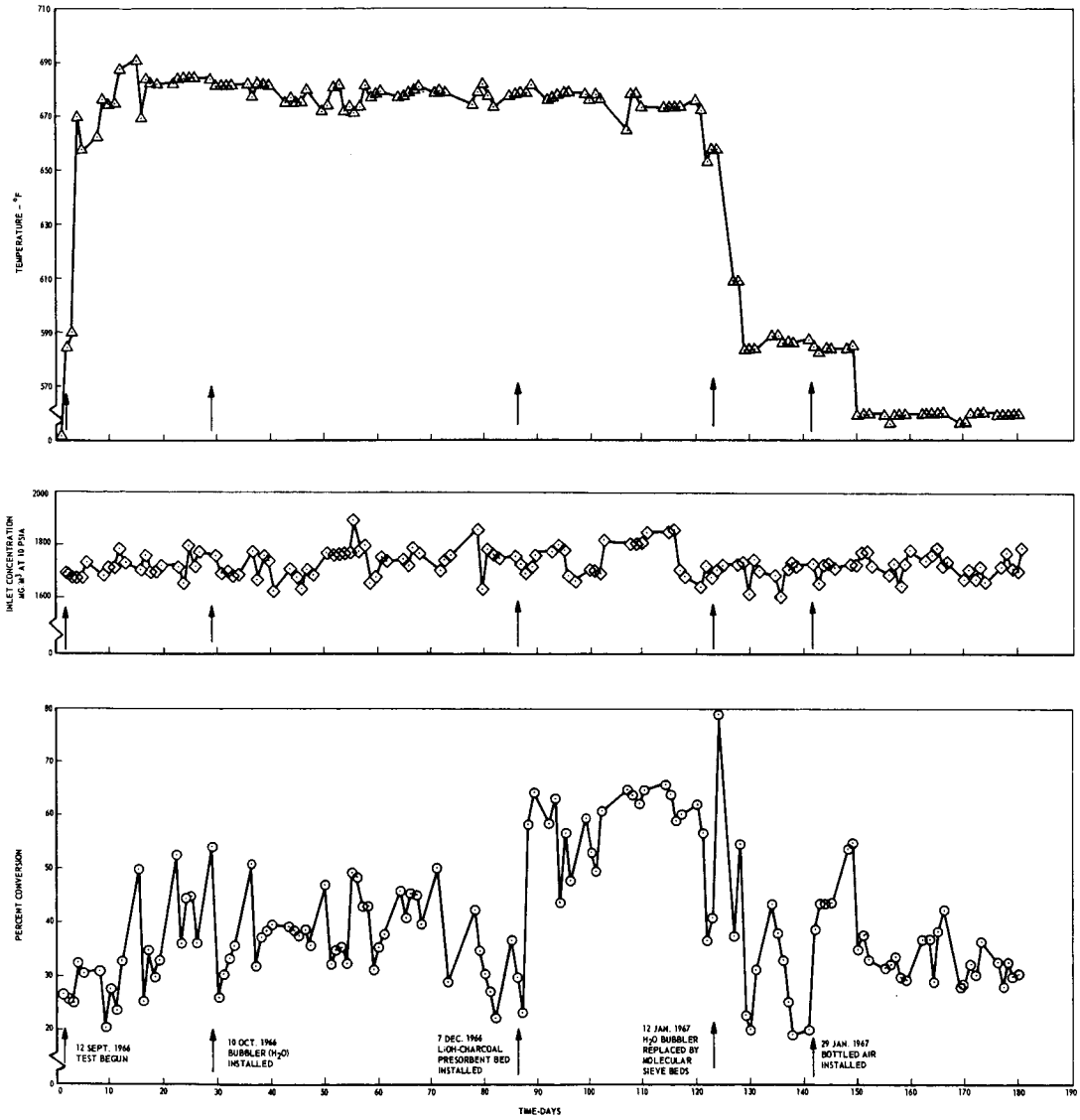

Fig. 42 Daily Methane Conversion Efficiency

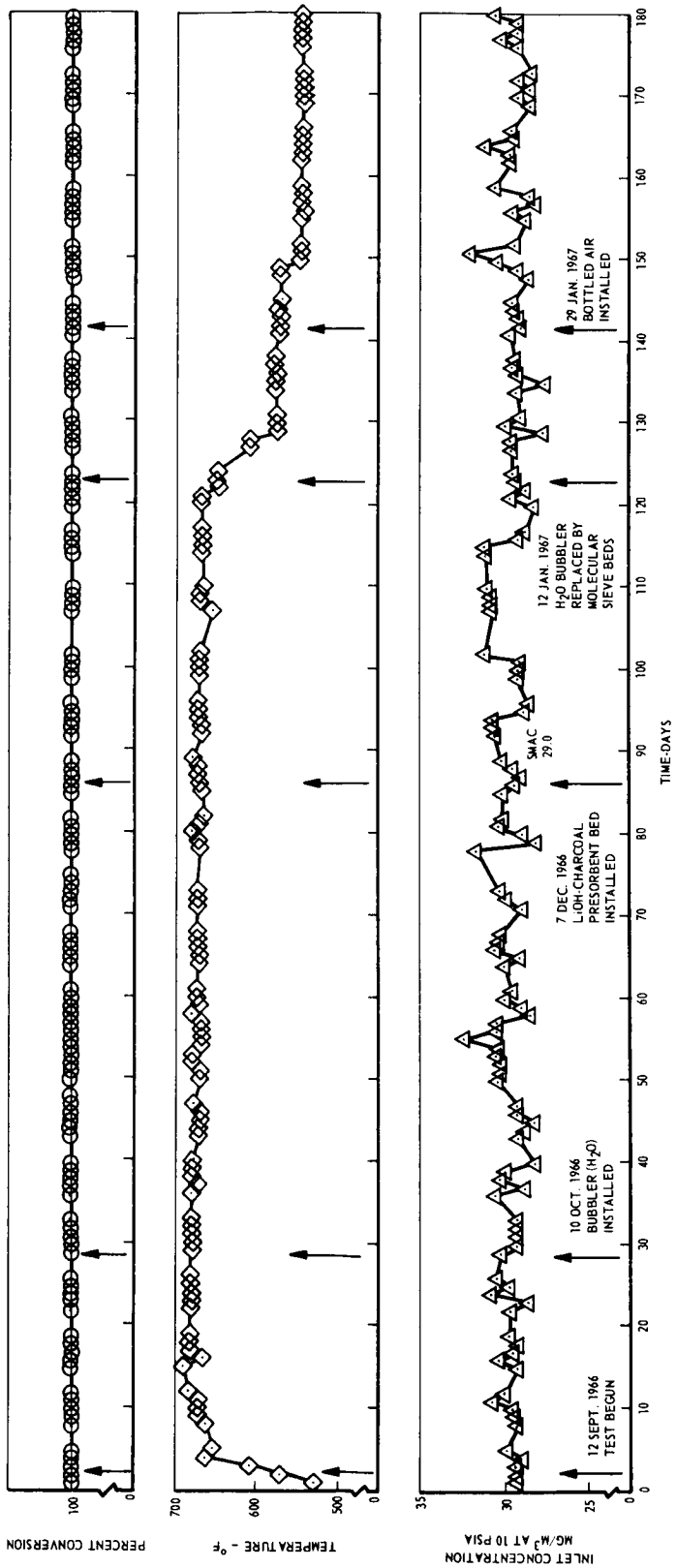

Fig. 43 Daily CO Conversion Efficiency

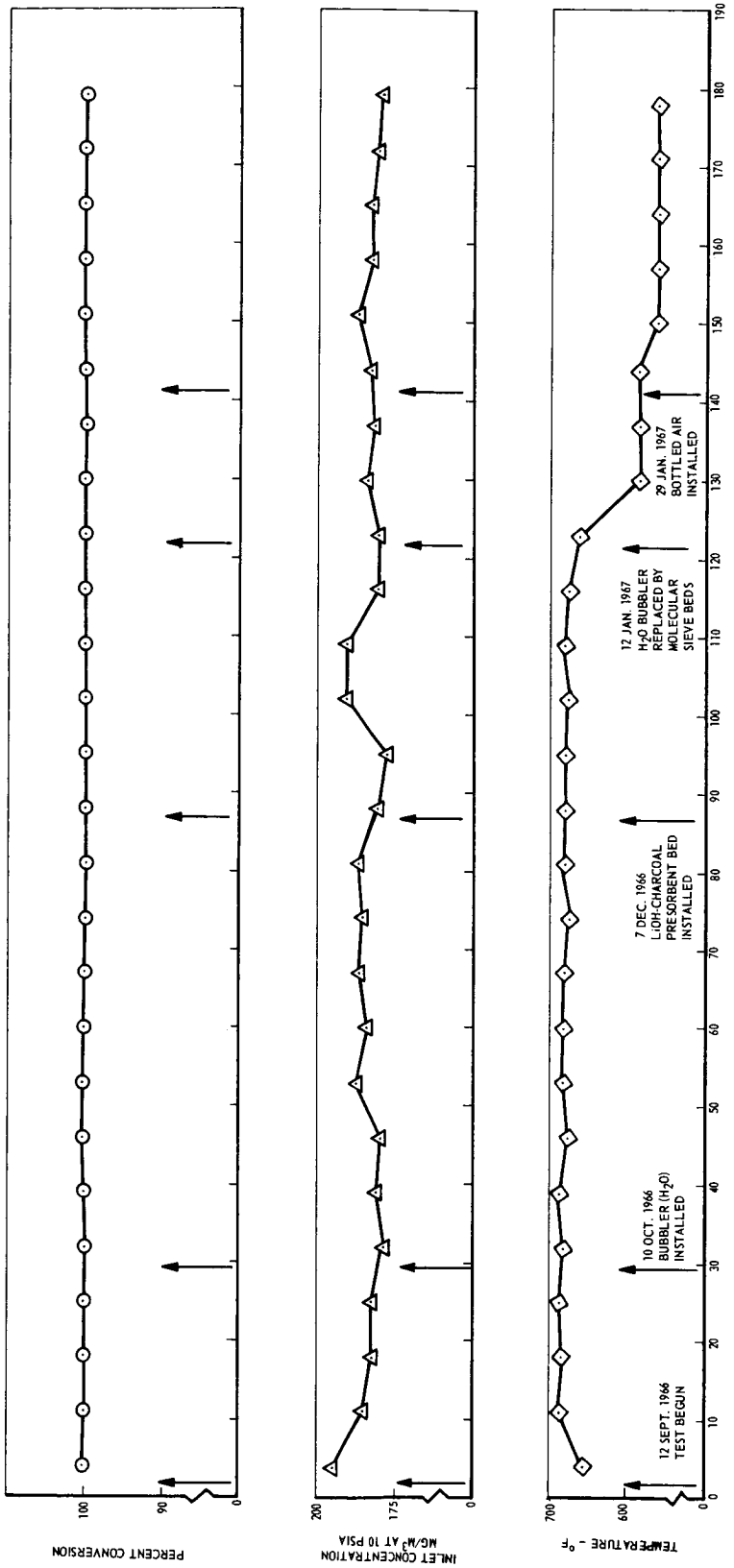

Fig. 44 Daily Acetylene Conversion Efficiency

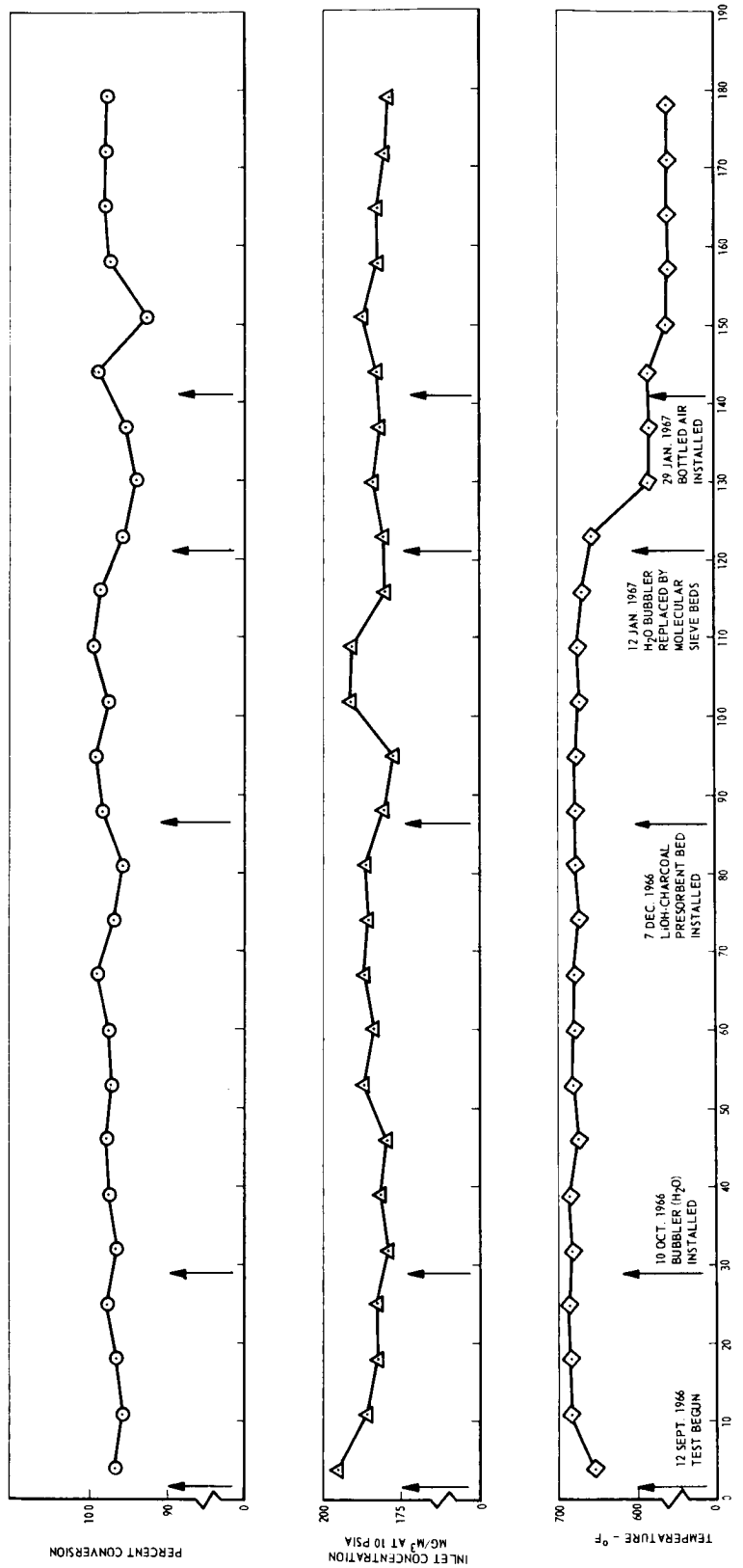

Fig. 45 Daily Butane Conversion Efficiency

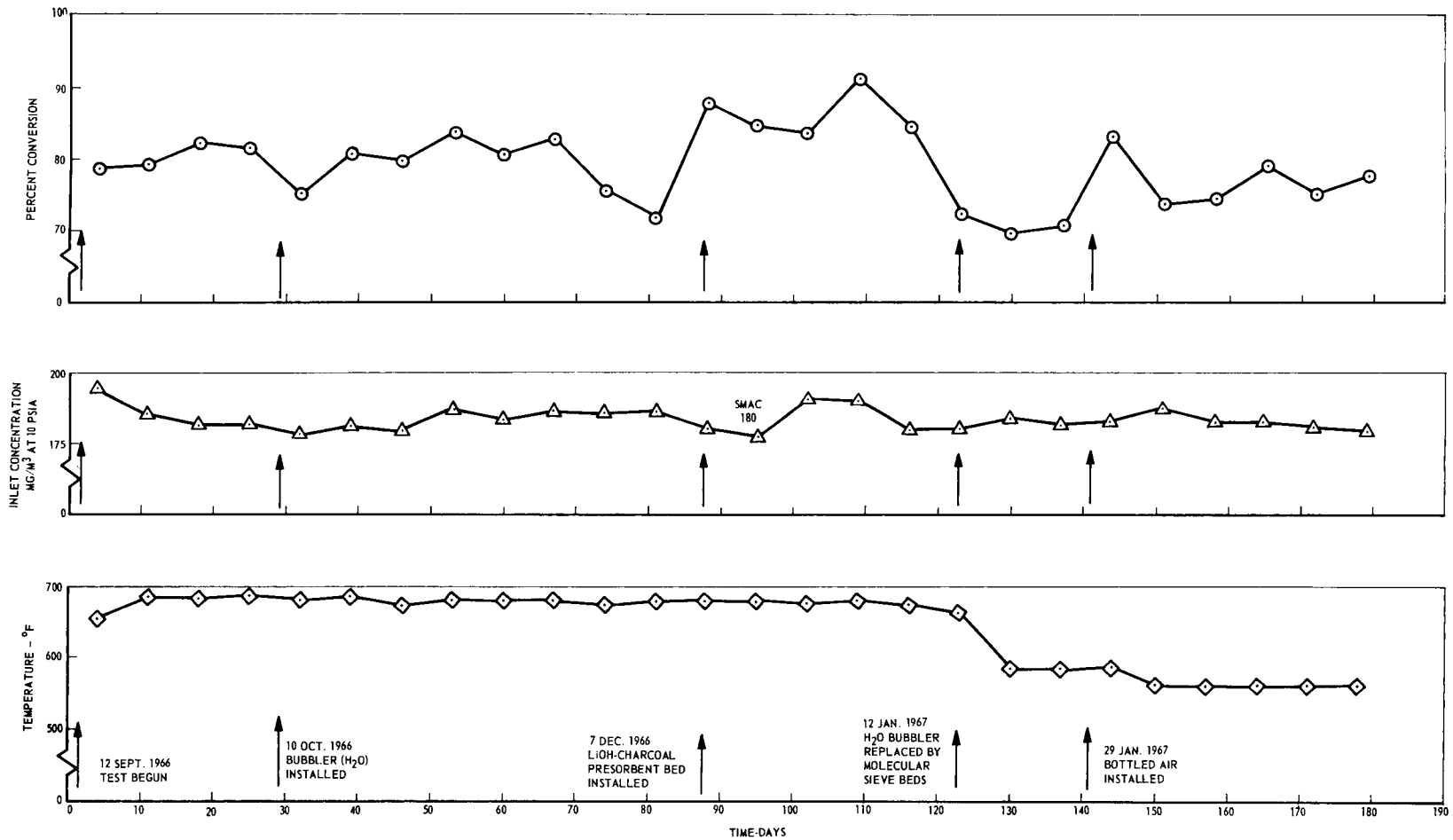

Fig. 46 Daily Ethane Conversion Efficiency

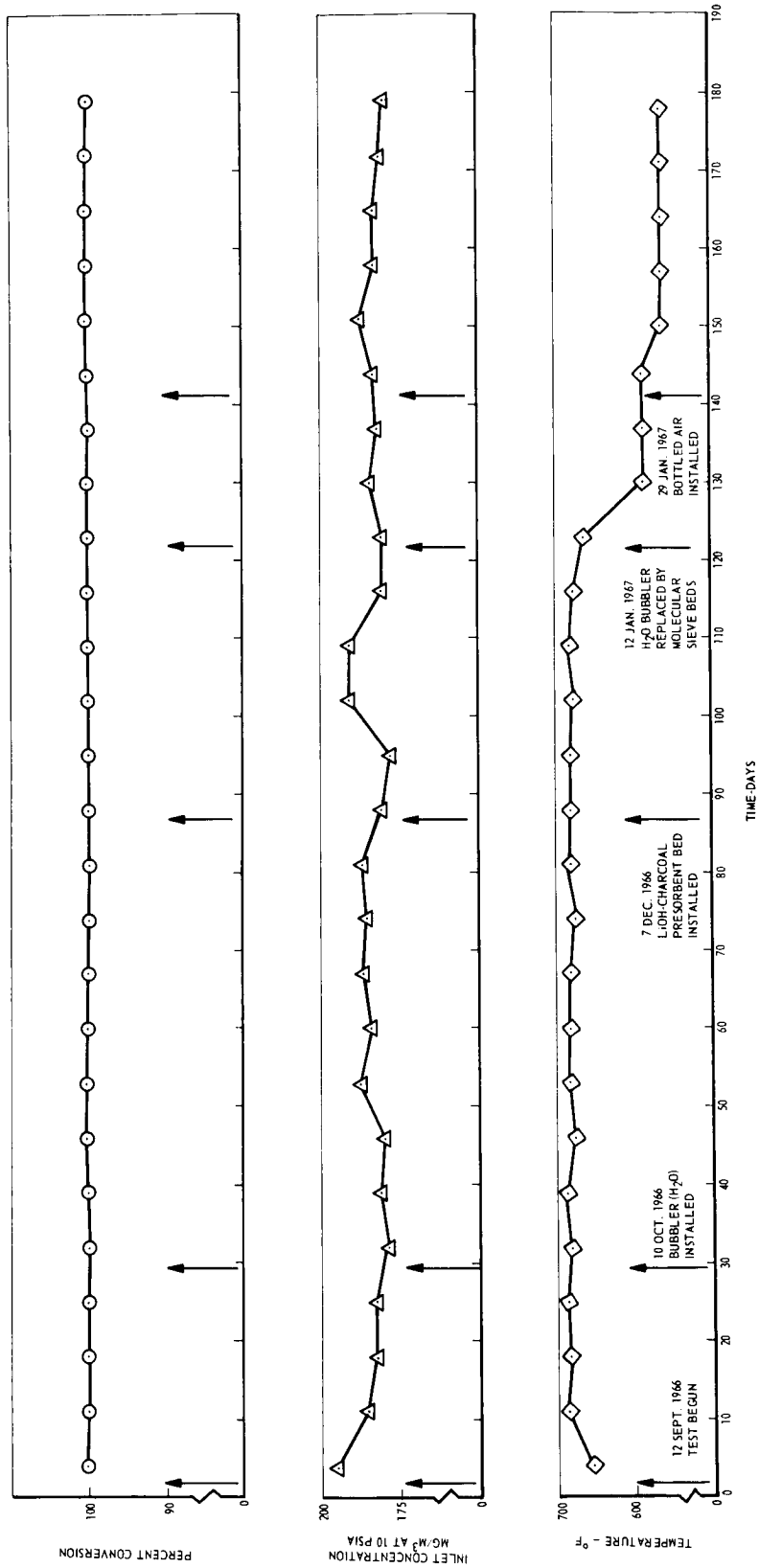

Fig. 47 Daily Propylene Conversion Efficiency

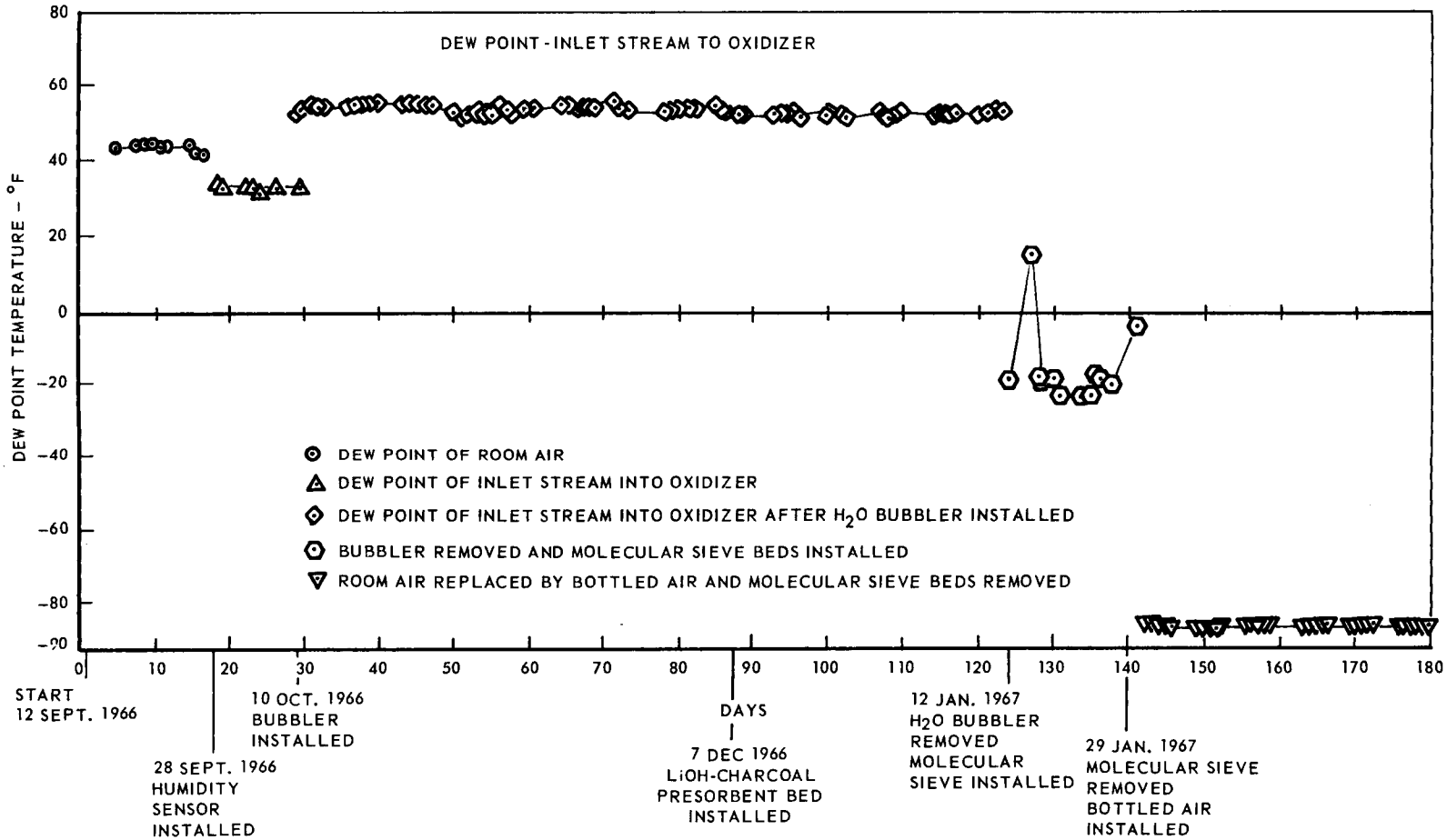

Fig. 48 Daily Record of Dew Point Inlet Stream to Oxidizer

At this point it was apparent that two operating regions existed with this catalyst. One was with a very low dew point, or dry process gas, and the other with a normal cabin dew point, or moist gas. It was decided to continue the test at this point with the high dew point gas stream, and at the end of the test period return to the low dew point gas stream. Two designs would then be developed, a dry process gas and a moist gas version.

During the first 88 days, it was noticed that methane conversion was higher on Mondays, and declined during the following week days, constituting a noticeable weekend effect. Since a portion of the background gas for this test is drawn from the room, it was concluded that variations in the contaminant level in the room air could be causing this effect. Attempts were made to quantify a difference between the contaminant level in room air between week days and weekends. No conclusive results were obtained in this effort.

On the 88th day of the test, a presorbent bed (lithium hydroxide and charcoal) was placed in the system to remove any contaminants that might be present in the room air being introduced to the system. The results of this were that the weekend effect appeared to be eliminated and a slight rise occurred in the contaminant removal efficiencies. Methane removal efficiency increased from a range near 40 percent to a range near 60 percent as a result of this change.

From the end of the first week of the test to the 120th day, the catalyst bed temperature was maintained at approximately 680°F. On the 121st day, the temperature was lowered to reduce the methane conversion efficiency from the 60 percent range to nearer 30 percent. This reduced temperature was approximately 660°F.

At this point in the test, it was decided to return to the very low dew point (dry process gas) condition to verify system performance under dry process gas conditions after long-term operation.

On the 123rd day (12 December), the water bubbler was removed and molecular sieve canisters were placed in the inlet gas stream to reduce the dew point to approximately -20°F. The system remained in this configuration for approximately 20 days, during which time the temperature required for 30 percent methane conversion was approximately 585°F. The -20°F dew point was not as low as would be anticipated from the outlet of a spacecraft silica gel-molecular sieve type carbon dioxide removal system. To simulate this dew point situation, bottled gas was utilized for the background gas stream. The dew point in this mode of operation was about -80°F. The catalyst bed temperature required for 30 percent methane conversion during this period was about 565°F. On the 162nd and 163rd days, the catalyst bed temperature was varied to obtain conversion efficiency data at 520°F, 540°F, 610°F, and 660°F. These data were used with data taken previously at 560°F and 585°F, to yield a methane conversion vs temperature plot for dry process gas after long-term exposure. This curve is presented in fig. 49. After these data points were taken, the catalyst bed temperature was returned to 560°F for the remainder of the test.

Removal efficiency of competing contaminants. – The competing contaminants, carbon monixide, acetylene, n-butane, ethane, and propylene, were introduced in the gaseous state in premixed contaminant blends to yield the desired levels in the

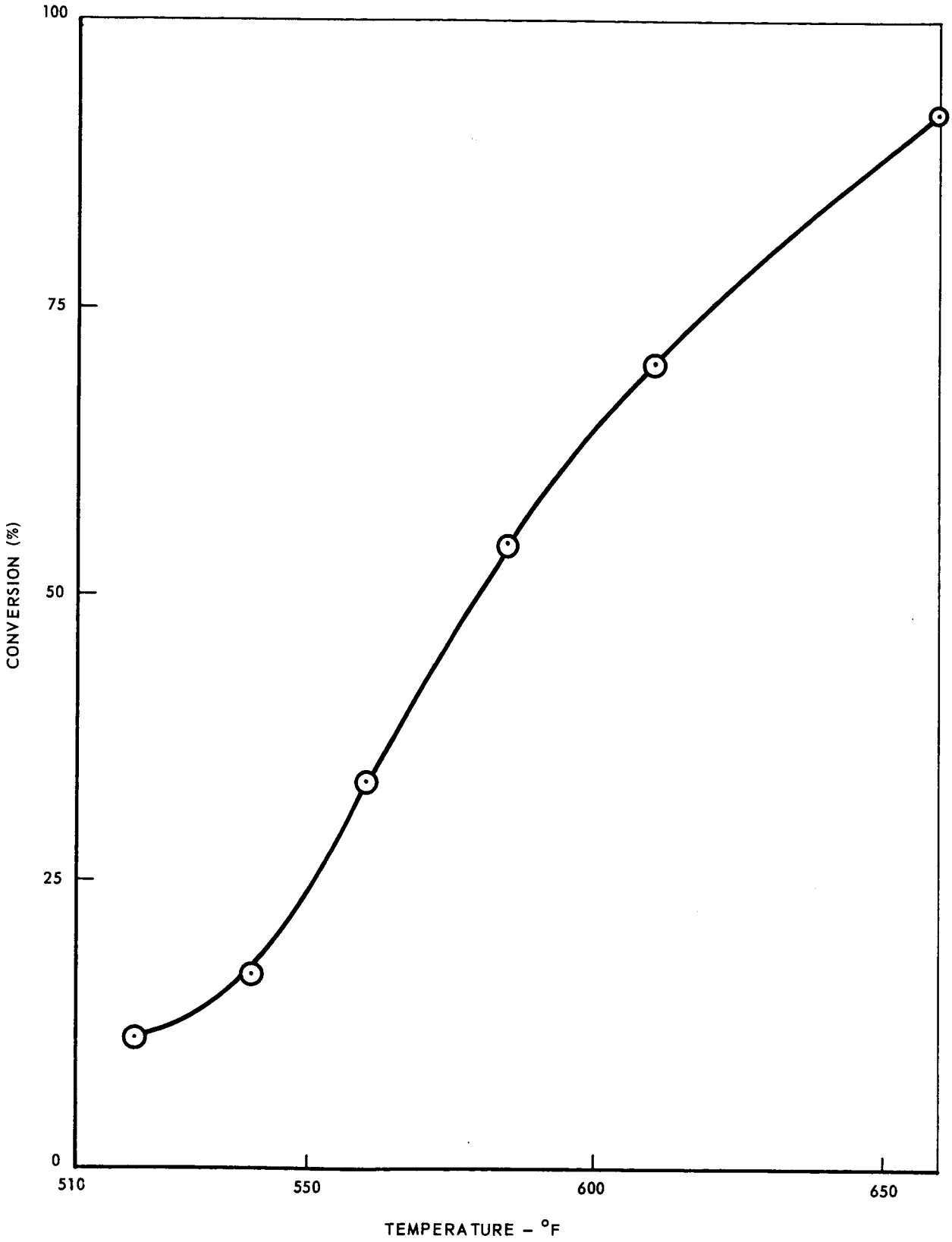

Fig. 49 Methane Conversion vs Temperature for Dry Process Gas

inlet gas stream. The conversion efficiency of each contaminant was calculated in the same way as methane. Carbon monoxide was monitored daily, whereas the other contaminants were monitored once weekly. The results are tabulated in Appendices B-1 and B-3, and are plotted in figs. 43, 44, 45, 46, and 47.

Carbon monoxide, acetylene, and propylene were converted at 100 percent efficiency throughout the test. Ethane reached a high of 92.5 percent, and a low of 58.5 percent. n-Butane reached a high of 98.5 percent, and a low of 93.5 percent.

ISOTOPE HEAT SOURCE DESIGN

The following section describes the work accomplished in the design of the radioisotope heat source for IHCOS. This effort includes the detailed design conducted on the dry process gas version (98 watt nominal) of the isotope heat source as well as the design of the moist gas version (125 watt nominal). The design of the 125 watt isotope was scaled from the 98 watt design.

Design Criteria

To establish the heat source design criteria, it was first necessary to review the mission and life support system characteristics and then define an acceptable aerospace safety philosophy. The pertinent design parameters obtained from this analysis are summarized in the following paragraphs:

Mission characteristics. – IHCOS was designed to satisfy the following typical mission requirements:

- Manned earth-orbiting laboratory (such as MORL)
- Crew size: nine men
- Mission duration: six months
- Continuous operation of IHCOS over entire mission duration
- Radioisotope heat source located within the manned cabin
- Maximum time delay between isotope encapsulation and launch: 90 days

In addition, the effect of the following typical boost vehicle environment (ref. 19) on the heat source integrity was considered in designing the heat source:

- Vibration – sinusoidal: 7.5 g peak (50 sec)
  random above 300 cps: 0.42 g^2/cps peak (50 sec)
- Acoustic (overall): 155 db (up to 2 min)
- Steady-stage acceleration: 30 g (3 min)
- Shock: 60 g in boost direction

Operational system requirements. – System analyses were performed to determine the design contraints for the radioisotope heat source. The results of these studies are summarized below:

- Maximum capsule surface temperature: 1300^{o}F
- Nominal isotope power loading: 98 watts (dry process gas version)

- Maximum isotope power loading: 123 watts (dry process gas version)
- Minimum capsule design life: 10 years
- Encapsulation materials chemically compatible with cabin atmosphere and contaminants
- A total allowable radiation dose to an astronaut of 185 rem. Of this total, IHCOS may contribute 5 to 10 percent.

Aerospace nuclear safety requirements. – The following aerospace nuclear safety criteria were established for the IHCOS heat source:

- Complete containment of the isotope during ground handling and launch pad operations
- Encapsulation materials chemically compatible with potential launch and space abort environments
- Intact reentry capability
- Capsule survival in the event of earth-impact.

Since the methods analyzed in aerospace safety analyses have not heretofore been discussed; the general approach utilized in arriving at these criteria is given in the following paragraphs. Specific environments which depend in part on the heat source geometry, such as reentry heating and temperature, are discussed in later sections of this report.

The use of radioisotopes requires consideration of safety in all phases of operation, from initial encapsulation of the isotope through mission completion. Concurrent with the heat source design, it is necessary to determine the accidental environments to which the heat source might be subjected and to evaluate the effects of these environments on capsule integrity. Safety criteria are then established and adhered to in order to assure a final design capable of hazard-free operation.

Traditionally, the AEC has required the demonstration of safe containment of all radioisotopes during source fabrication, handling, and use. The development and use of radioisotope heat sources for applications in the national space program have resulted in the evolution of a new series of hostile environments to which the isotope system might be exposed, including the severe environments associated with reentry into the earth's atmosphere, followed by earth-impact at terminal velocity. Presently, demonstration of complete isotope containment in these environments appears to be the most widely accepted safety criteria.

The potential abort environments associated with each of the following phases of a typical mission were considered, and the design requirements imposed upon the radioisotope capsule were established: ground transportation and handling, launch pad operations, suborbital flight, and orbital flight. A brief summary of the general findings of this study (ref. 19) are presented in the following paragraphs.

Ground transportation. – The possible impact, fire, and explosion characteristics of ground transportation accidents have been found in previous studies to be less severe than those which may be experienced by the radioisotope heat source after installation aboard the launch vehicle. Suitable shipping containers, fabricated in compliance with the AEC and ICC Standards, are adequate to prevent damage to the assembly while in transit.

Launch pad operations. – One of the most severe accident environments which may be experienced at the launch site is that associated with a propellant tank rupture, resulting from booster fallback or early destruct. When a liquid propellant booster fails in this manner on the launch pad, the propellants mix, burn, and form a fireball. The most complete and quantitative treatment of the thermal and chemical environment encountered inside or near the fireball is contained in reports summarizing work accomplished by TRW Systems under contract to NASA and Sandia Corporation (refs. 20 and 21). Instantaneous fireball temperatures of approximately 5000°F, lasting for several seconds, are typical of nonhypergolic propellant explosions. Hypergolic propellant peak temperatures are somewhat lower, approximately 4000°F. These temperatures decrease rapidly to steady-state combustion temperatures of 1800-2500°F, lasting for periods possibly up to an hour. Because of the interior location of the radioisotope capsule, both within the spacecraft and IHCOS, the extreme fireball thermal environment will not seriously affect the capsule integrity. However, experimental results have indicated that the reactions of refractory metals with the combustion gases CO, CO_2, and H_2O, will be rapid at the expected temperatures. To insure the survivability of these materials, they must be protected with a suitable high-temperature, noncorroding clad such as a noble metal.

Suborbital flight. – Booster malfunctions prior to achieving earth-orbit result in exposure of the radioisotope heat source to reentry environments of varying severity, depending upon where the booster aborts in the ascent trajectory. The most probable abort locations will depend upon specific booster configurations, and may be established for a given mission profile by carefully studying the ascent trajectories and booster abort probabilities. To prevent isotope dispersion into the atmosphere during descent, the heat source subsystem must be designed to survive the most severe reentry environments and subsequent earth-impact.

It has been determined in previous programs (ref. 22) that the explosive potential of rocket propellants decreases rapidly with increasing altitude and that above 200,000 feet, explosive aborts are virtually impossible. In the event of abort at the high altitudes, the propellants mix and burn rapidly; however, due to the extremely low atmospheric pressure, the strong shock front normally associated with explosions does not develop. Hence, the explosive forces are not sufficient to either seriously damage the heat source or remove the capsule from it.

Orbital flight. – In many of the missions for which radioisotope-power life-support components are attractive, a commonly used booster trajectory technique is to first place the payload and a secondary propulsion system into a low-to-medium earth-orbit. The secondary propulsion system is then fired at the appropriate time to achieve the final orbit. If the secondary propulsion system fails to inject the payload into the proper final orbit, the radioisotope heat source will be subjected to an orbital decay reentry environment. This environment produces the highest total heat input to the system, as well as a large heating rate, and was considered in detail in the reentry aid design discussed previously.

Radioisotope Capsule Design

Since no single material can presently satisfy all the physical and chemical requirements imposed by mission, performance, and safety considerations, multiwall capsule configuration (fig. 50) is required.

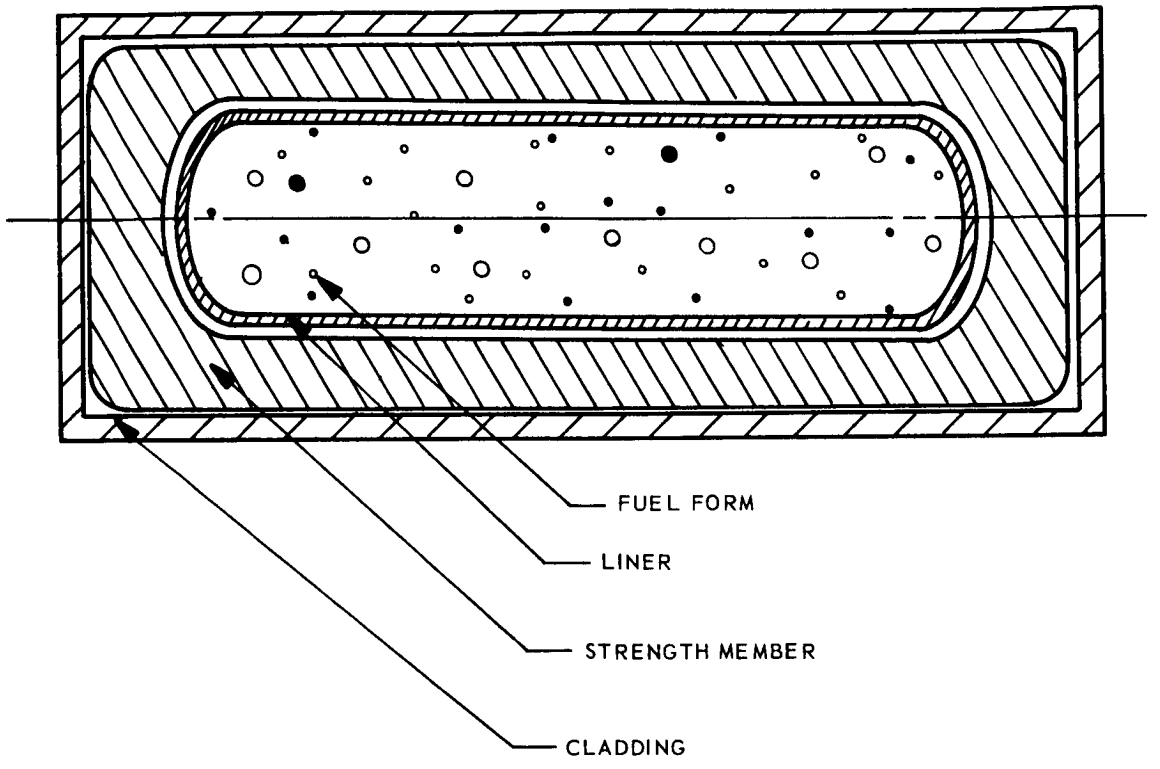

Fig. 50 Basic Capsule Configuration

As determined by this design study, the composite radioisotope capsule is composed of the following components, listed in order from the capsule centerline: fuel form, fuel liner, strength member, and protective cladding. The components external to the protective cladding are considered as part of the reentry aid design. The specific materials of construction for the radioisotope capsule are delineated in a Classified Supplement to this report. During the following discussion, those materials will be referred to as the selected liner, the selected strength member, and the selected cladding material.

Fuel. – Four radioisotopes, Sr-90, Pm-147, Cm-244, and Pu-238, were initially selected as possible candidate heat source materials for IHCOS. A detailed comparative analysis (ref. 23) of these radioisotopes was performed in which factors such as half-life, availability, cost, state of development as a heat source material for space application, and shielding requirements were considered. This analysis resulted in the selection of plutonium dioxide, PuO_2, as the most applicable fuel form.

Liner material. – The liner material was selected on the basis of chemical compatibility with both the fuel form and strength member. Numerous materials have been placed in contact with the selected fuel and tested at Mound Laboratory. The experimental results indicated that two of the candidate liner materials appeared to be satisfactory at temperatures up to 2000°F for time periods in excess of 30 days. Longer-duration tests are presently underway. Based on these data and the requirement of withstanding high reentry temperatures, one of the candidates was selected as the liner material for the IHCOS capsule.

Experiments at TRW Systems (ref. 21) on the interdiffusion of the selected liner with candidate strength member materials have shown that the materials are compatible, experiencing only slight interdiffusion. Interdiffusion behavior between the selected liner and a candidate strength member material was investigated at 2000°F for varying periods of time. The width of the interdiffusion zone after long periods of exposure can be predicted from the following relationship:

$$X^n = kt$$

where

X = diffusion zone width
t = time
n, k = constants

The lowest observed value of n in any system is approximately two. On this basis, a conservative diffusion zone thickness of 12.6 mils after ten years of operation at 2000°F was computed. Since the rate of interdiffusion decreases rapidly with decreasing temperature, the use of a 20-mil liner appears adequate to satisfy both interdiffusion and capsule assembly requirements at the substantially lower temperatures expected for the IHCOS capsule.

Strength member material selection. – Due to the alpha decay of the plutonium fuel, resulting in the continuous generation of helium gas, the strength member, or pressure vessel, must be designed to contain the internal pressure buildup. In case of mission abort, such as launch pad explosion or premature reentry, the strength member must also be designed to completely contain the isotope through the entire reentry environment, and both during and after impact with the ground.

A number of refractory alloys were evaluated as potential capsule strength member materials. One of the refractory materials was selected for consideration over candidate refractory material because it possessed the best compromise of desirable properties, including high-temperature strength, low density, good impact resistance, and favorable creep characteristics. In addition, superalloys were considered, and a superalloy was selected for detailed comparison with the selected refractory because of its high-strength and chemical stability at temperatures in the range of 1500-2000°F. The following considerations were taken into account in selecting the final material for the capsule structural member:

Fabricability: Studies indicated that both the selected refractory and superalloy could be machined by conventional techniques. Conventional joining techniques currently being used by the aerospace industry can be employed satisfactorily with the selected superalloy. Welding of the selected refractory is somewhat more difficult because of embrittlement of the weld zone due to minute amounts of oxygen and nitrogen. Electron beam fusion welding techniques can, however, be used and result in high-quality welds. The selected refractory alloy can also be brazed with a large variety of materials, the choice of which depends on the particular service conditions.

Creep: Creep is the phenomena of time-dependent deformation of a material under stress. In this case, the stress is produced by helium pressure buildup from the decaying plutonium fuel. To allow a comparison between the two materials and to allow extrapolation of creep-strain data between various times and temperatures, plots of rupture stress versus the Larson-Miller parameter were made for the selected superalloy and refractory, and are shown in fig. 51. For the selected superalloy, previous calculations indicated that a value of 19 for the Larson-Miller constant afforded a good correlation of the available data. Similar calculations for the selected refractory resulted in a value of 20 for the Larson-Miller constant. Using the Larson-Miller correlation, and fully realizing the problems associated with extrapolating short-term data to longer times, ten-year allowable creep rupture stresses for the selected refractory and superalloy, corresponding to a temperature of 1300°F, were computed to be 44,000 and 21,000 psi, respectively (fig. 51). On this basis, the refractory is clearly much superior to the superalloy.

Strength to density ratio: An important consideration in optimizing the selection of structural materials for aerospace (weight-limited) applications is the strength-to-density ratio. In cases where the materials are subjected to elevated temperatures, such as in the IHCOS capsule design, this property takes on paramount importance. Since the selected superalloy has only a slightly lower density than the selected refractory, the strength-to-density ratio of the selected refractory at predicted operational and abort temperatures is nearly twice that of the selected superalloy.

Impact: Other programs (ref. 24) concerned with the impact characteristics of the selected superalloy and refractory capsules at elevated temperatures have been and are presently being conducted. Impact velocities, in the range of 190 to 250 feet per second, correspond to those achieved by an actual radioisotope heat source prior to earth impact. Impact temperatures in this test series range from 1700°F to 2000°F, and impact angles vary from zero degrees, corresponding to end-on impact, to 90 degrees, corresponding to broadside impact. The effect of these factors on different joint preparations was also evaluated. From this series of impact tests, it was concluded that a strength member thickness of approximately 0.100 inch is sufficient to maintain capsule integrity upon impact regardless of which of the two candidate strength member materials is ultimately chosen.

Oxidation: The oxidation of alloys such as the selected refractory, has been studied extensively (ref. 21). At 1400°F (the closest data point to 1300°F available), the oxidation is linear having an oxidation rate of 83.5 mils per year. Hence, the use of the selected refractory as a strength member material necessitates a protective coating or cladding of some type to insure capsule integrity under normal operating conditions and abort environments.

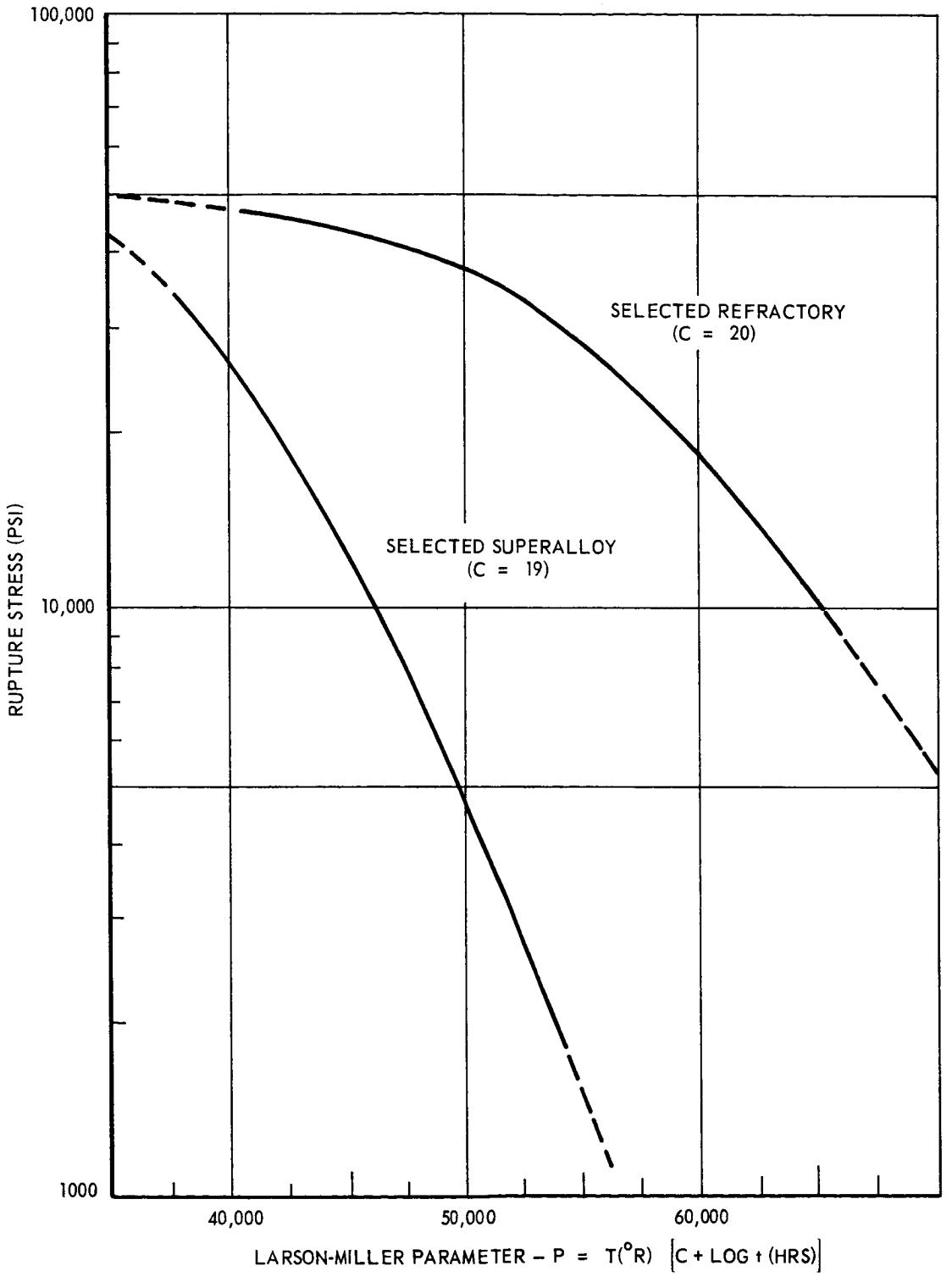

Fig. 51 Rupture Stress vs Larson-Miller Parameter

The selected superalloy forms a protective oxide film in the presence of an air or oxygen environment at elevated temperatures up to 2000°F. At 1600°F and one atmosphere pressure, the oxidation rate is 7.8 mils per year. Assuming a wall thickness of 0.100 inch, it is probable that the capsule would survive unprotected for 10 years in an oxidizing environment at the 1300°F maximum design temperature. However, because of the extreme temperatures which could be encountered during a nominal orbital decay reentry, it is extremely doubtful that this strength member would survive, even though the time period of peak heating experienced during reentry is short.

Evaluation of the above factors resulted in the selection of the refractory for the capsule strength member. It was chosen primarily because of (1) high strength-to-density ratio (even in the recrystallized state) resulting in a low capsule weight, (2) advanced state of development as a capsule strength member, (3) favorable long-term stress-rupture characteristics, (4) high-temperature strength, and (5) high melting point required to survive predicted reentry temperatures.

Strength member design. – As previously mentioned, the use of an alpha emitting fuel, such as Pu-238, results in a pressure buildup within the capsule. The strength member, or pressure vessel, must, therefore, be properly designed to withstand the effects of long-term creep. The void resulting from the mechanical packing of the selected fuel is often large enough to keep the pressure at a sufficiently small value to assure capsule survivability for a long time period. Although 1300°F is a fairly low temperature when considering plastic deformation or creep in a refractory metal, the ten-year design life criterion necessitated the consideration of creep in determining the strength member wall thickness. It is assumed in all creep calculations that the internal volume of the capsule was completely filled with radioisotope fuel, except for the unavoidable void formed during loading of the microspheres. Two digital computer programs have been developed at TRW Systems to accurately predict the creep deformation in radioisotope containment capsules. The first program, CRASH,* applies to a relatively thin-walled capsule, and was used to analyze the final IHCOS design, as discussed below. For preliminary design purposes, however, the simplified plane strain theory was used. This theory yields approximate results of creep strain at the capsule midplane, where the effect of the capsule end-caps is minimum, but it cannot be used to predict creep strain over the whole capsule body. In both the preliminary and final design studies, it was assumed that the effective stress and strain in the multiaxial condition occurring in the actual capsule wall are related in the same manner as the uniaxial stress and strain obtained in uniaxial creep tests. It was also assumed that the internal pressure forces were transmitted undiminished through the thin fuel liner to the structural strength member.

Plane strain theory: Assuming a long cylinder under internal pressure and the uniaxial creep correlation, $\epsilon = B\sigma^n t^p$, it follows that $\bar{\epsilon} = B\bar{\sigma}^n t^p$, and that (ref. 25)

$$\bar{\sigma} = \frac{\frac{\sqrt{3}}{n} P \left(\frac{r_o}{r}\right)^{\frac{2}{n}}}{\left(\frac{r_o}{r_i}\right)^{\frac{2}{n}} - 1}$$

*Creep in Axisymmetric Shells

where

ϵ = uniaxial creep strain

σ = uniaxial stress

B, n = empirical material constants

ϵ_θ = circumferential strain

σ_θ = circumferential stress

σ_r = radial stress

$\bar{\epsilon}$ = effective strain = $\frac{2}{\sqrt{3}} \epsilon_\theta$

$\bar{\sigma}$ = effective stress = $\frac{\sqrt{3}}{2} (\sigma_\theta - \sigma_r)$

P = capsule internal pressure

r = capsule radius

r_o = capsule external radius

r_i = capsule internal radius

To compute the required constants and minimize the correlation errors, a least-squares fit technique was applied to the available uniaxial data using a specially developed digital computer program. The calculated value of n was 2.19. Using the above equations, the capsule stress was computed and compared to the allowable stress for a ten-year design life using Larson-Miller extrapolations of stress rupture data. Assuming that the extrapolation technique is valid for such long times, it was determined that the strength member wall thickness of 0.100 inch, determined from impact considerations, would survive the effects of creep for a time period greater than 100 years, since maximum strains were less than one percent.

As previously mentioned, the radioisotope capsule must not only survive creep during the mission lifetime, but also survive impact in case of mission abort. Material properties strongly influence impact survival, but capsule geometry is also of great importance. Hence, an overall capsule length-to-diameter ratio of three was chosen based on extensive work performed by TRW Systems and Sandia Corporation (ref. 26) on the impact survivability of cylindrical containment capsules.

With the wall thickness and length-to-diameter ratio determined from impact considerations, the capsule design was completed with the selection of the end-cap configuration. Figure 52 presents preliminary results of digital computer study (CRASH) performed to determine the optimum type end cap and most favorable weld location. The midthickness (meridian) strains in the capsule for various contoured end-cap designs are shown in the figure. It is desirable to keep the strain at the end cap at or below that in the cylindrical wall of the strength member, and also to

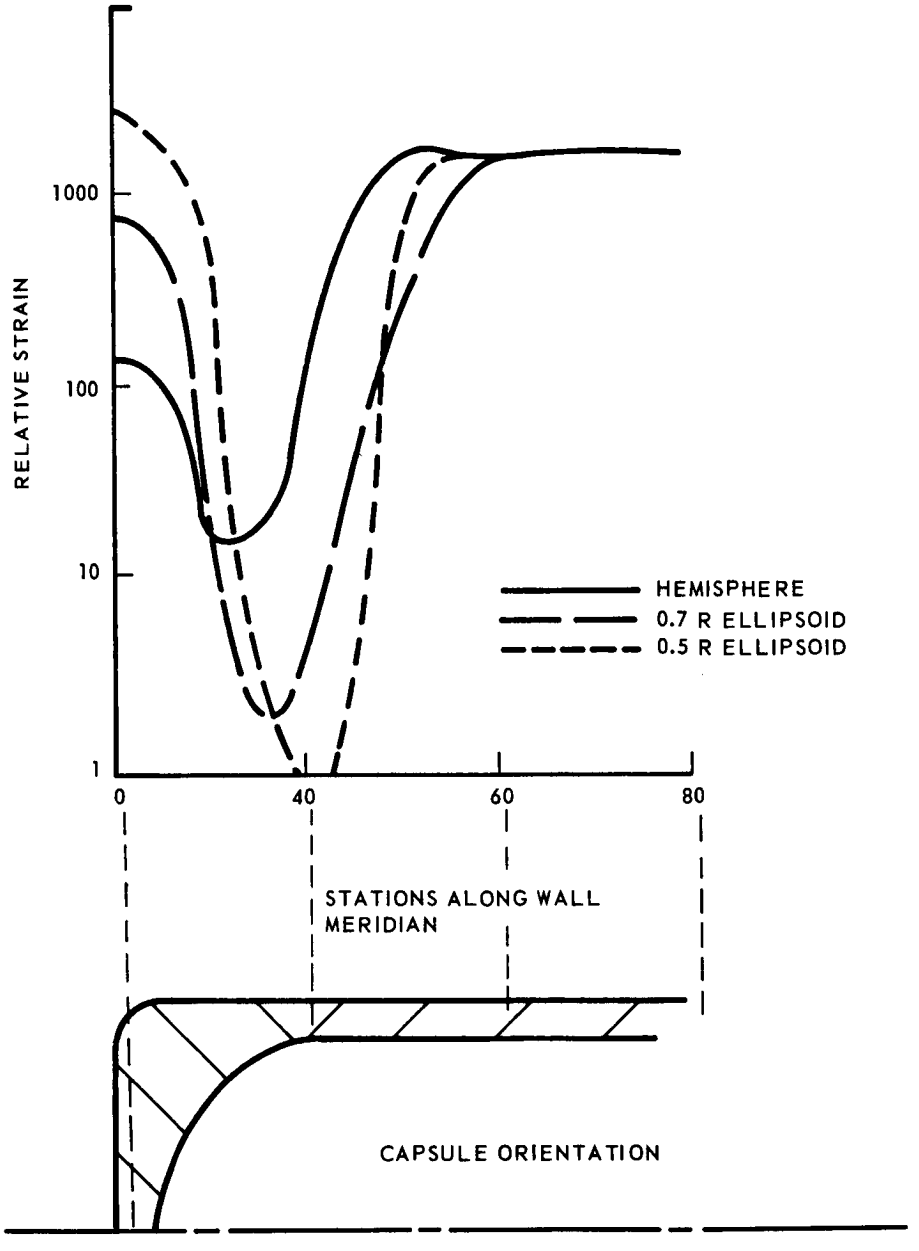

Fig. 52 Computer Predictions of Strain in a Radioisotope Capsule TZM Strength Member

maintain a low strain in the area of the end-cap joint. Consideration of both of these factors resulted in the selection of a semiellipsoidal end cap in which the semiminor axis is 0.707 times the semimajor axis.

As a further refinement to the design techniques used above and to check the creep profile of the entire capsule, the digital computer program, CRASH (ref. 27), was used to analyze the long-term creep effects on the capsule strength member. The CRASH program computes the creep in an axisymmetric two-segment shell subjected to internal pressure and axisymmetric loads, and is capable of calculating creep strains for time-varying pressure and temperatures. To calculate effective creep strains using the CRASH program, a constant temperature of 1300°F was chosen for the strength member walls. This is the highest temperature obtainable when air flow to the catalytic oxidizer is terminated for any reason. Internal pressure was varied with time to simulate the pressure profile within an actual radioisotope capsule up to a maximum value of 3500 psi at 10 years.

Since extremely low creep strain occurs within the first few months due to the very low capsule pressure, and since computer time for this phase is excessive, the time period analyzed was 10,000 to 87,000 hours (10 years). The program incorporates an automatic time step generator which bases each time step on the changes in the effective stress. Below approximately 10,000 hours, the percentage changes in stress are high (although absolute values are very small), leading to very small time steps and, consequently, high running time.

Figure 53 shows the meridian points on the IHCOS strength member at which computations of stress and strain were performed. Figure 54 shows the corresponding effective strains, obtained after 10 years, plotted against meridian wall location. The low strain present in the vicinity of the end-cap joint supports the selection of the end-cap configuration. It is seen that the amount of creep strain occurring even after ten years' operation is quite small and capsule design appears to be more than adequate to insure complete integrity.

Cladding. – The choice of the selected refractory as the capsule strength member material necessitates the use of an external cladding to provide long-term oxidation protection during system operation and in the event of mission abort. Present technology favors the use of noble metals for this application.

Experimental evaluation of a large number of noble metal alloys has been performed at TRW (refs. 19, 28), and a particular alloy was selected as the best cladding material for this application. No unusual fabrication or joining techniques are required for this alloy composition, and its high melting point (3400°F) insures material integrity at the calculated maximum reentry temperatures.

Interdiffusion between the strength member and the cladding material could be detrimental if during the life of the mission interdiffusion is sufficient to (1) alter the composition of the strength member to the point of degrading its mechanical properties, thus risking failure due to excessive creep, or (2) destroy the integrity of the clad and permit the strength member to oxidize either during normal operation or upon exposure to the atmosphere in an abort situation. Data from short-term interdiffusion

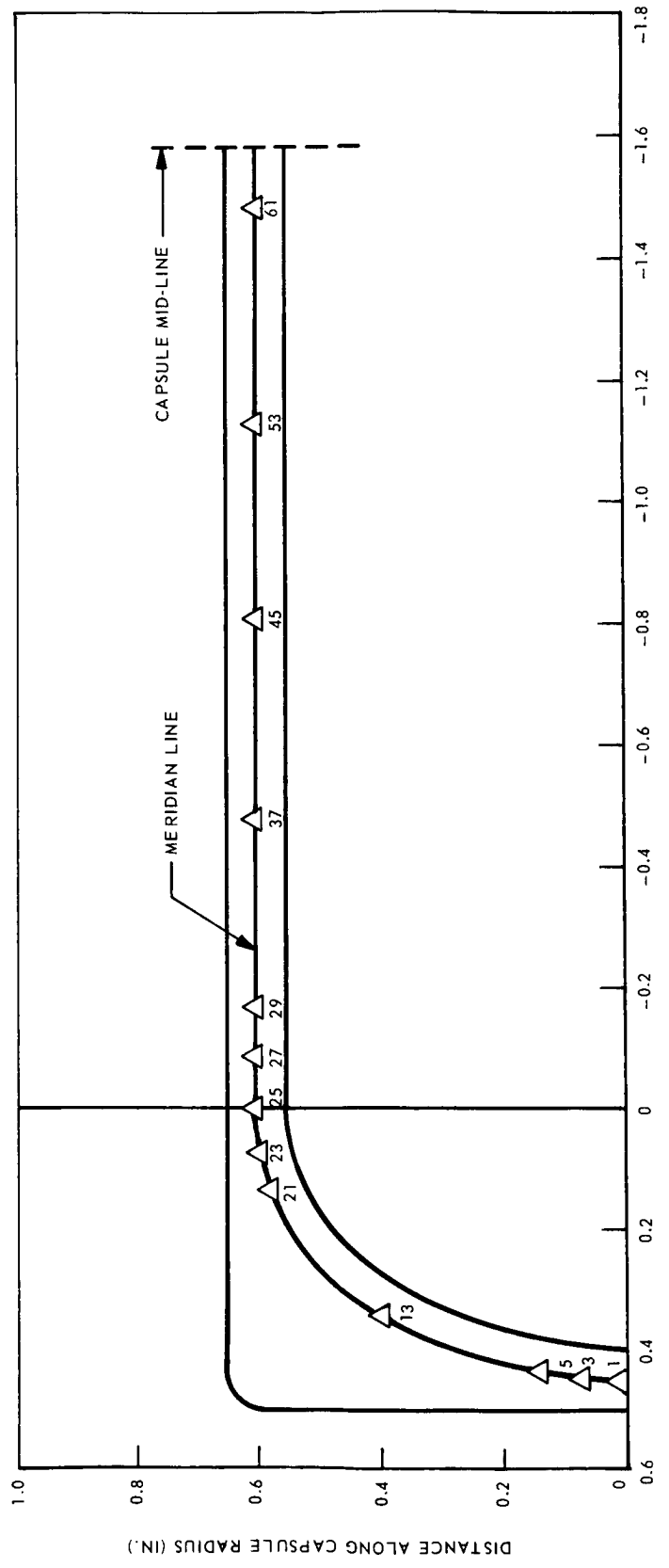

Fig. 53 Strength Member Configuration Showing Points on Meridian Line at Which Effective Strain was Calculated

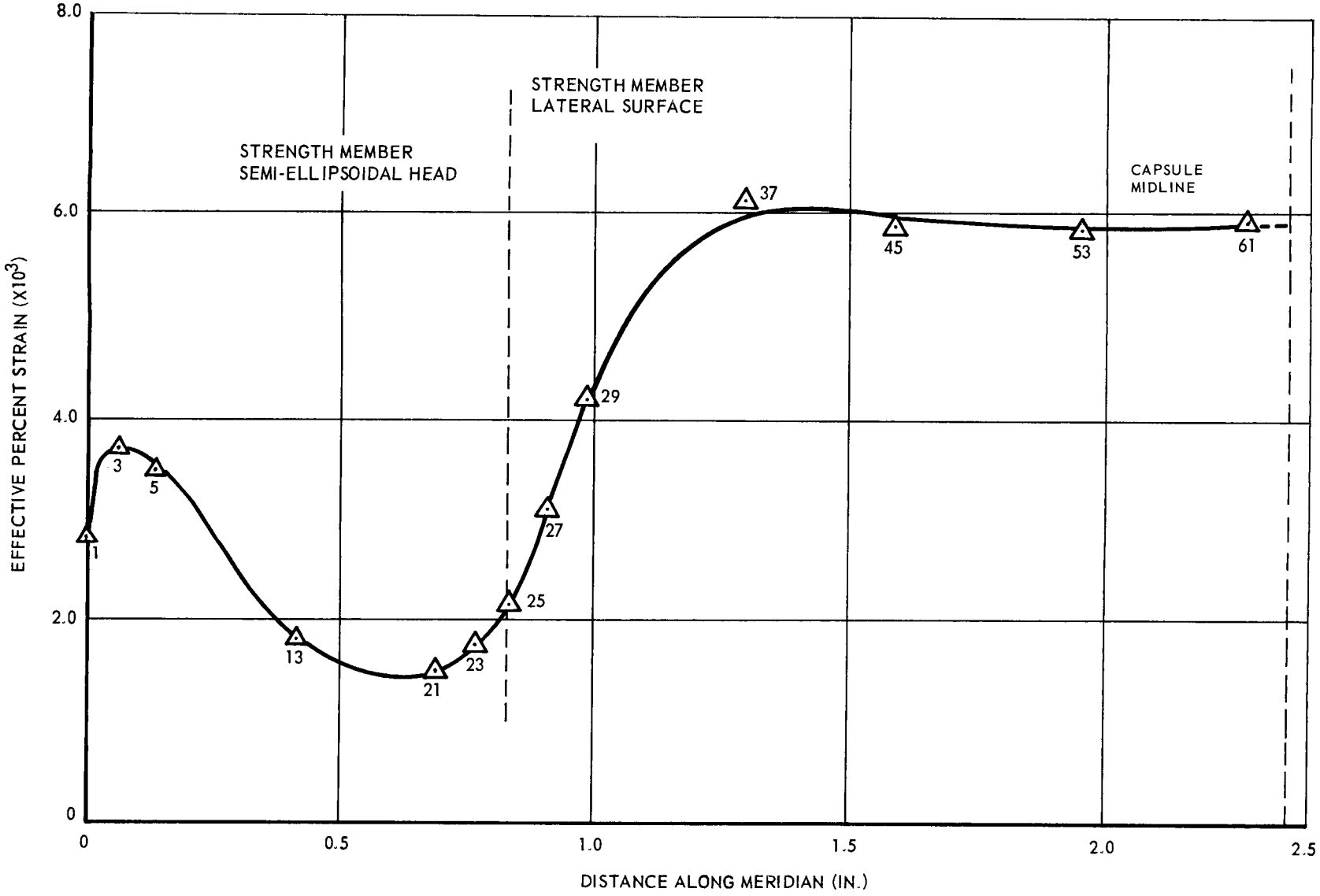

Fig. 54 Effective Strain vs Meridian Distance

studies (ref. 19) was extrapolated to longer time periods, indicating a maximum diffusion zone thickness of 8.1 mils after two years at 1300°F. Therefore, a conservative cladding thickness of 20 mils was selected and is believed to be adequate to satisfy both operational and abort requirements.

Capsule configuration and fabrication. – An assembly view of the complete heat source, including capsule and reentry module (Drawing No. X114024), showing an axial and midplane cross-section view, appears in fig. 55. This is a photographic reduction of the original drawing, and it should, therefore, be noted that scale call-outs are not valid. A 0.010-inch clearance is provided between all capsule materials to accommodate easy assembly of the capsule components in hot cell facilities, and provide for differential thermal expansion between the component materials. As shown in the drawing, an access port is provided in the liner to facilitate fuel loading. A 0.040-inch diameter hole is also provided in the strength member to enable the clearance gap between the strength member and the liner to be filled with purge gas. All other gaps are filled with purge gas from the welding process. The purpose of the purge gas is to improve heat transfer and minimize the internal capsule material temperature by reducing the temperature difference between components.

The pressure vessel end cap will be electron-beam welded, thus providing a very narrow heat-affected zone in the strength member and also minimizing the possibility of crack formation due to embrittlement. All joint configurations in the liner and strength member are of the step-butt type which facilitates remote welding in hot cell facilities, while allowing adequate weld penetration with minimum disturbance of the inner surface of the joint. This reduces possible radioisotope contamination through weld zones. The 30-degree weld zone bevel in the strength member is incorporated to reduce shear stresses at the joint in case of capsule impact.

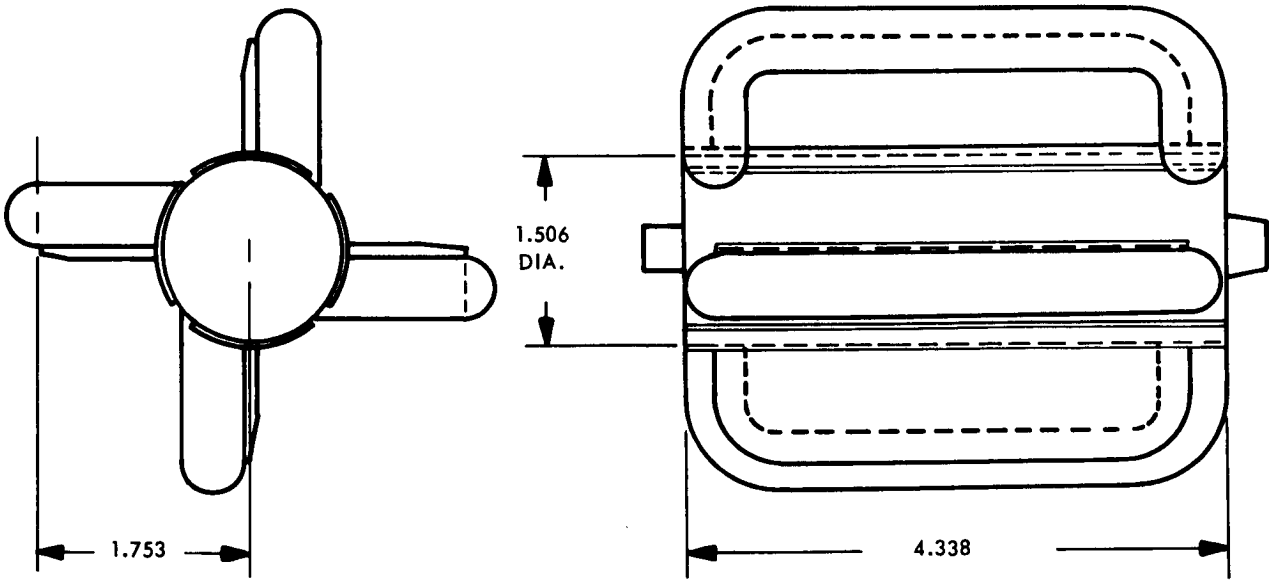

Fig. 55 Heat Source Assembly

Reentry Aid Design

As prescribed by the aerospace nuclear safety criteria described earlier, the IHCOS heat source was designed for intact reentry and containment after impact should an abort situation occur.* To accomplish this, some form of reentry aid was necessary to decrease the reentry heating and impact velocity to a point where survival upon impact could be assured. Without reentry aids, the heat generated by atmospheric reentry would be sufficient to compromise the integrity of the isotope capsule.

Reentry aid selection. – The use of an ablative heat shield to permit intact reentry of the heat source module was initially considered. Only those materials that ablate at temperatures well above 1300°F are usable. Various materials, including special refrasil composites, nickel impregnated with aluminum trifluoride, and pyrolytic graphite, were among those considered. However, assuming that an isotope capsule protected by a conical heat shield with a spherical nose would survive impact, several factors combined to effectively eliminate ablator reentry aids from further investigation. A key factor was the excessive additional weight imposed by the heat shield reentry aid on IHCOS. Typically, the ablative reentry system would weigh more than the system it is designed to protect. Another factor of considerable importance was the severe limitations imposed on the overall design and efficiency of IHCOS when using an ablative heat shield.

In order to survive reentry heating without ablative protection and to obtain a sufficiently low earth-impact velocity to guarantee containment of the isotope material, it was necessary to add aerodynamic drag area, i.e., fin surfaces, to the radioisotope capsule. Calculations performed under an extensive reentry aid design study for the POODLE program (ref. 21) have shown that a cylindrical reentry vehicle with longitudinal fins added to the external surface can be designed to maintain a spinning motion broadside to its flight path. The broadside spinning motion was later verified by experiments in which models were dropped from a hovering helicopter and their motion observed and recorded photographically. Comparative analyses have shown that a finned configuration results in a minimum weight penalty to achieve intact reentry. In the hypersonic flight regime, the aerodynamic heating is distributed and averaged over all exposed surfaces, and throughout both the hypersonic and subsonic flight regimes the vehicle presents its maximum effective drag area while spinning. Furthermore, in the catalytic oxidizer unit such a fin configuration aids in transferring the heat generated by the radioisotope to the surrounding catalytic material during normal operation.

Reentry aid design. – To ensure a spinning broadside motion as well as to reduce the local aerodynamic heating, cylindrical tubes or "beads" were located at the fin panel outboard edges. On the basis of previous calculations performed for this configuration (ref. 28) with various fin span sizes, a one-inch fin span with a 0.5-inch diameter bead was chosen. The required fin root thickness was computed assuming that the fin itself acts as a cantilever beam loaded by aerodynamic and centrifugal acceleration forces. Figure 56 illustrates the model used.

* This requirement is necessitated by the assumption that IHCOS could be flown aboard a MORL-type spacecraft which is not designed to have a reentry capability.

The stress, acting at the fin root cross-section, consists of the following:

- The stress due to the bending moment resulting from the aerodynamic loading (assumed constant) on the fin panel
- The stress due to the centrifugal acceleration of the bead
- The stress due to the fin panel centrifugal acceleration

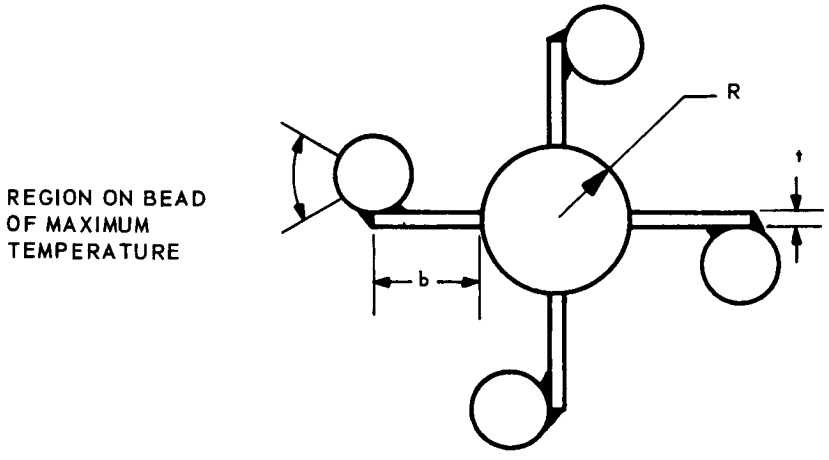

Fig. 56 Configuration Used in Computing Fin Root Thickness

Accordingly,

$$\sigma = \frac{Mc}{I} + \sigma_{cf}$$

$$\sigma = \left(P \cdot b \cdot \frac{b}{2} \cdot \frac{6}{t^2}\right) + \frac{W_B}{g} \cdot \frac{\omega^2}{t} \cdot (R + b) + \frac{W_F}{g} \cdot \frac{\omega^2}{t} \cdot \left(R + \frac{b}{2}\right)$$

where:

σ = allowable stress

σ_{cf} = axial stress due to centrifugal acceleration

M = bending moment at critical area

c = distance from outer fin surface to centroid of critical cross section, $\left(= \frac{t}{2}\right)$

I = moment of inertia of the cross sectional area about its centroid $\left(= \frac{bt^3}{12}\right)$

t = fin root thickness

P = aerodynamic pressure loading ($\sim$ 4 psi during peak heating)

b = fin span

ω = angular velocity ($\sim$ 3000 rpm)

W_F = fin panel weight per unit length = $\rho \cdot b \cdot t$

W_B = bead weight per unit length

ρ = material density (0.37 lb/in^3)

R = cylindrical body radius

Using a conservative allowable stress of 2000 psi at 3000°F, and applying a safety factor of 1.5, the fin root thickness was computed to be 0.100 inch.

A digital computer trajectory analysis was performed for the IHCOS reentry module, assuming a nominal orbital-decay type reentry in order to obtain key input parameters for the aerodynamic heating analyses described below, and predict the earth-impact velocity. Based on the present configuration and weight, an impact velocity of 150 ft/sec was computed. On the basis of results obtained under a Company-sponsored experimental program in which the effects of impact on refractory-clad capsules are being evaluated, it appears that the capsule will remain completely intact, regardless of impact angle at this velocity.

Using standard aerodynamic heating equations and the method of analysis employed in the DART program (ref. 19), it was determined that a critical region on the bead (fig. 55) could experience a reentry temperature as high as 3640°F, assuming a surface emissivity of 0.7. The maximum temperatures were computed assuming that all the input aerodynamic heat flux was reradiated from the external surfaces, i.e., equilibrium radiation temperature. However, during the design of a four-finned reentry body under the POODLE program, it was found – by performing a detailed digital computer thermal analysis – that by accounting for thermal conduction through the bead into the fin and internal radiation within the hollow bead, the maximum temperature reached was approximately 100°F lower than was predicted by the radiation equilibrium theory. Due to similarities in configuration, it is reasonable to assume that the IHCOS reentry body will experience the same 100°F temperature alleviation as indicated in the POODLE analysis. Hence, the maximum temperature attained by the IHCOS capsule would be 3540°F. Although the peak reentry temperatures are of short-time duration (less than five minutes), superalloys obviously cannot be used. Hence, a high-temperature refractory alloy is required for both capsule and reentry aids. Accordingly, the fins and beads will be fabricated from a refractory alloy.

Structural support module. – It is not possible to attach either the heat source support structure or the reentry fins directly to the cladding material. This is because it does not have sufficiently high strength at operating temperature to withstand booster vibrational environments or at reentry temperatures to support the fins (3050°F reentry surface temperature). Consequently, a refractory material was selected for a structural support module with due consideration being given to its fabricability and ease of joining to the reentry aids. Due to the oxidizing environment during both normal operating and abort situations, both the structural support member and the fins will require the application of a high-temperature oxidation-resistant coating (see following section) to protect them from the excessive oxidation.

A module thickness of 0.050 inch is sufficient to maintain structural integrity under the booster "g" loads transmitted through the structural mounting as well as the aerodynamic loading experienced during reentry. Fin mounting pads were employed on the structural member (see design drawing) to distribute the aerodynamic loads imposed on the fins over a wider lateral surface area, thereby eliminating possible shell distortions.

Oxidation resistant coatings. – Because of the choice of material for the structural support module and reentry aid material, an oxidation resistant coating is required. Such protection is required not only during reentry heating but also for normal operation, where operating temperatures are sufficiently high to allow reactions between the cabin air and the structural support module material to occur.

Two coating materials, molybdenum disilicide ($MoSi_2$) and tungsten disilicide (WSi_2), were selected for consideration on the basis of their applicability and advanced state of development as high-temperature refractory coatings. The following factors were considered in making the final coating selection:

- oxidation rate in air and space cabin environments
- emittance as a function of temperature
- compatibility between coating and catalytic material
- compatibility between coating and trace contaminants
- melting point of the coating
- techniques for application
- effect of differential thermal expansion

Data on the protective life of $MoSi_2$ above 3000°F are scarce. A Pfaudler PFR-6 coating is reported (ref. 29) to have survived for three minutes at 3400°F in a plasma environment, and indefinitely at temperatures below 1300°F. At 3450°F, a eutectic occurs between $MoSi_2$ and Mo_3Si_2, and hence this is the highest temperature at which the coating could be expected to retain its integrity, even for short periods of time. A WSi_2 coating developed by TRW survived one hour at 3600°F on a tungsten substrate in a static air environment (ref. 30). As in the case of $MoSi_2$, eutectic melting

occurs, thus limiting the application of this coating to peak temperatures lower than 3740°F.

The emissivity of the coating is very important since it affects the rate at which heat generated during reentry is radiated to space, thus controlling the maximum reentry temperature. Both coatings have an emittance range (refs. 30, 31, 32) of 0.65 to 0.75, depending on the method and type of instrument used in measurement. An average value of 0.70 was used in the reentry analyses.

Both the $MoSi_2$ and WSi_2 are diffusion coatings, i.e., during the coating process the deposited materials interdiffuse and react with the substrate material. Although the bond integrity is fairly good, differential thermal expansion resulting from very rapid heating can cause spalling and peeling. However, differential thermal expansion between the coating and the substrate (approximately 30 percent) is probably not sufficient to cause such coating failure during reentry conditions.

It has been reported that $MoSi_2$, the principal constituent of the PFR-6 coating, is rapidly attacked by chlorine at elevated temperatures (ref. 33). Compounds present in the trace contaminants, such as freon, ethylene dichloride, and trichloroethylene, may-partially dissociate at the predicted operating temperature of 600°F, providing a source of elemental chlorine for reaction with the protective coating. Additional experimental effort should be expended to determine possible reactions of the trace contaminants with the $MoSi_2$ coating. Tests conducted at TRW Systems for the Thrust Chamber Technology Program (ref. 34), indicate that silicide coatings of tungsten and molybdenum are also slowly attacked by water vapor at 2200°F, but that carbon monoxide or carbon dioxide produced no appreciable attack at this temperature. Data at lower temperature are presently not available.

After consideration of the foregoing factors, the tungsten disilicide coating was selected. Maximum reentry temperatures (approximately 3600°F) obtained from the thermal analysis, preclude the use of molybdenum disilicide for the bead coating. The WSi_2 coating will be applied to all external surfaces of the reentry module. It may be necessary, because of the lack of experience in applying a WSi_2 to a molybdenum-based substrate, to vapor deposit a thin coating (0.0005 inch) of tungsten on the support mode. The coating can then be applied to the tungsten by the two-cycle pack cementation process which TRW has perfected for this coating.

Heat Source Support

An axial support is used to locate the capsule assembly within the IHCOS. A stress analysis was performed on the structural module end caps to determine a simple structural design sufficient to withstand a loading of 30 g applied in any direction. Conical supports, having a 10-degree axial taper, were included on both end caps to aid in positioning and aligning the heat source during assembly. In addition, a standard Wooddruff key was used to eliminate angular movement. Lockheed Missiles & Space Company will design the complementary female receptacles and define the same in their Master IHCOS Assembly Drawing.

Moist Gas Design

The moist gas version of the IHCOS heat source was based on the same design criteria as the dry process gas unit with one exception. The nominal power loading for the moist gas unit is 125 watts, and the maximum power loading for the moist gas unit is 156 watts. Thus, the moist gas design was scaled up from the dry process gas design to allow for the increased fuel loading.

Of the many possible ways of resizing the heat source, two appeared most promising: (1) retain the same L/D ratio as in the dry process gas design, or (2) retain the diametral dimensions and vary the length of the capsule. The first approach resulted in a capsule configuration similar to one developed at TRW Systems for a propulsion application and which has survived creep and impact tests. However, the total heat source weight was found to be in excess of five pounds. Also, the fin span had to be increased to 1.55 inches in order to hold the peak reentry temperature at a value where the survival of the coating could be assured. In the second approach, the outside heat source diameter of 1.506 in. was retained, and the required increase in fuel-loading was accommodated by a change in the overall heat source length from 4.3 in. to 5.4 in. with a corresponding increase in the capsule L/D ratio from 3.2 to 4.1. This L/D ratio is still within the range generally desired to assure capsule survival upon impact. The total heat source weight including reentry aids was computed to be 4.78 lb. Aerodynamic analysis showed that the one-inch fin span, previously used, would be adequate to ensure survival during atmospheric reentry. Since both drag area and weight scaled nearly linearly for a fixed diameter, the ballistic coefficient and, consequently, the peak reentry temperature remained the same as previously computed for the dry gas design. Based on these considerations, the second approach (holding the diameter fixed and increasing system length) was selected. Thus, the isotope heat source for the moist gas design is identical to the dry process gas version in radial cross-section; however, it is 1.1 in. longer.

Radiation Dose Analysis

The radiation dose intensity of IHCOS is presented in a classified summary to this report. The classified summary defines the dose intensity as a function of distance from the heat source in both radial and axial directions. This is done for both the dry process gas and moist gas versions of IHCOS. Included in the following report is a discussion of the minimum average distance that would probably exist between the crew and IHCOS, and a qualitative discussion of the dose rate effects.

IHCOS spacecraft location. – A brief study was made to establish a basis for estimating the minimum probable distance between IHCOS and the spacecraft crew. One of the spacecraft configurations considered was the MORL (NAS 1-3612). This vehicle is depicted in fig. 57, including a probable location of IHCOS based on the data presented in NAS 1-3612 (ref. 35). A 1.5-meter-radius sphere is also shown on this figure. It appears from examination of this figure that a crew member would spend considerably less than 50 percent of the time within the 1.5-meter-radius sphere, and thus it would be conservative to base the average dose rate on a 1.5-meter separation distance.

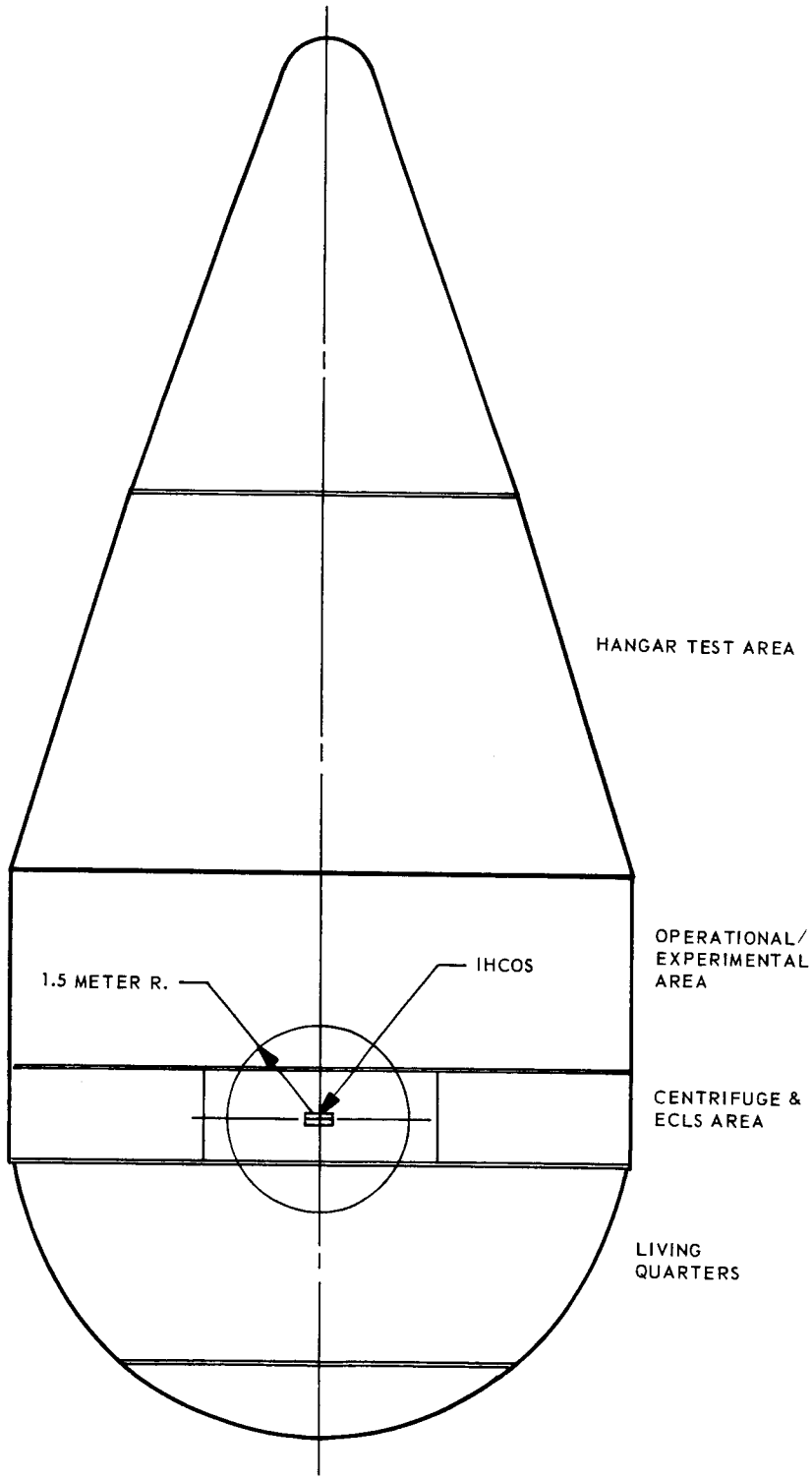

Fig. 57 Probable Location of IHCOS in MORL Spacecraft Design (NAS 1-3612)

Dose rate effects. – At 1.5 meters from either the moist or dry process gas versions of IHCOS, the accumulated dose over the 180-day mission amounts to less than 1 percent of the recommended maximum dosage to the skin. For the blood-forming organs, or abdominal viscera, the allowable dose is lower than the skin dose; however, the radiation from IHCOS (predominantly neutrons) is attenuated in reaching these dose points, and thus IHCOS radiation is responsible for less than four percent of the recommended maximum continuous dosage at 1.5 meters.

For the lenses of the eye, the relative biological effectiveness (or quality factor) for neutrons is twice that for other body organs. Applying this factor, IHCOS contributes less than 5 percent of the total mission allowable continuous eye dose. The total allowable dose rates, based on the current LMSC recommended values (ref. 36) derived in consultation with C. A. Tobias, University of California, Donnor Laboratory, for a 180-day continuous exposure are 43 mrem/hr for the lens of the eye, and 139 mrem/hr for skin.

The dose rate from the dry process gas version of IHCOS is about 80 percent of that from the moist gas version.

In considering possible maintenance requirements for IHCOS, the recommended maximum acute dosage may become the dominant criterion. An exposure period of 5 days at the surface of IHCOS would result in less than 10 percent of the recommended maximum acute hands-and-feet dose, or less than 25 percent of the maximum acute eye dose.

The closest possible approach to the radioisotope heat source is at the wall of the heat source capsule, and this point can only be reached by disassembly of IHCOS. At this location, an exposure time of 50 hours would result in less than 100 percent of the total acute dose to the hands and feet; while an exposure time of 10 hours to the eyes would result in less than 100 percent of the total acute eye dose.

Based on the foregoing data, the radiation field from the unshielded IHCOS constitutes only a minimal perturbation in the operational radiation safety situation. If maintenance operations are approached with the knowledge that the heat source is radioactive, there should be no significant effect on the crew accumulated radiation dose status.

SYSTEM DESIGN

The following subsections describe the major design features of both the IHCOS designs:

Dry Process Gas Design

The dry process gas version of IHCOS (shown in fig. 58) is 12.50 in. long, excluding end fittings, and 7.59 in. in diameter. The weight of the unit is approximately 20 lb. The unit consists of an outer shield, molded insulation, and an inner body. The inner body is made up of a regenerative heat exchanger, catalyst canister, and radioisotope heat source.

The regenerative heat exchanger is a 5-pass cross-counter flow, stainless steel plate fin heat exchanger. The cold end is bolted to one end of the cylindrical aluminum shield. The hot end of the heat exchanger terminates in a machined flange that mates with the catalyst canister. The gas ports are sealed with Parker metallic face seals.

The catalyst canister is a cylindrical unit that contains the 0.5 percent palladium catalyst and the radioisotope heat source. This unit is furnace-brazed and entirely constructed of nickel. The radioisotope is mounted in the center of the catalyst canister where it is supported by posts projecting from either end of the isotope source. One post is tapered and held in place, in a tapered socket, with a pin to prevent rotational movement of the isotope heat source. The other post is cylindrical, and fits into a socket located on the end of the catalyst canister away from the heat exchanger. Axial movement is limited with a Belleville spring placed in this socket. This spring also allows for thermal expansion of the isotope.

The catalyst material is located in eight compartments located between the fins of the isotope heat source. A perforated steel plate and screen is brazed into one end of the catalyst compartment and a screen is located at the other end to prevent the catalyst material from entering the heat exchanger. A machined flange is located at the end of the catalyst canister away from the heat exchanger to provide access to the isotope heat source and catalyst material. This flange is held in place with bolts and sealed with a Parker metal face seal.

The catalyst canister is supported from the aluminum shield assembly by 36 steel wire spokes in tension. One end of the spokes is threaded into the cylindrical wall of the catalyst canister, while the other end is supported in a cylindrical channel section with small threaded disks. The cylindrical channel section is used to support the two portions of the aluminum shield.

The entire area between the inner body and the shield is filled with molded insulation (Johns Manville Min-K 1301). The insulation is molded in four pieces, mating at the wire spokes and center line of the unit.

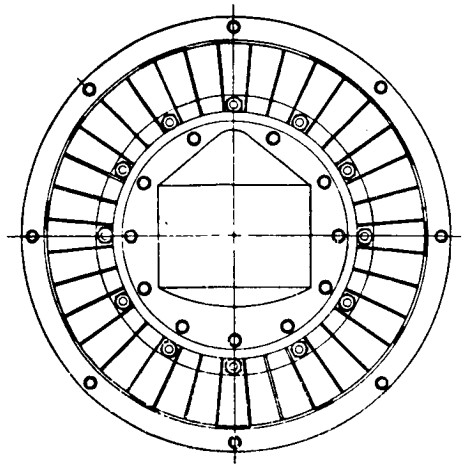

SECTION A–A

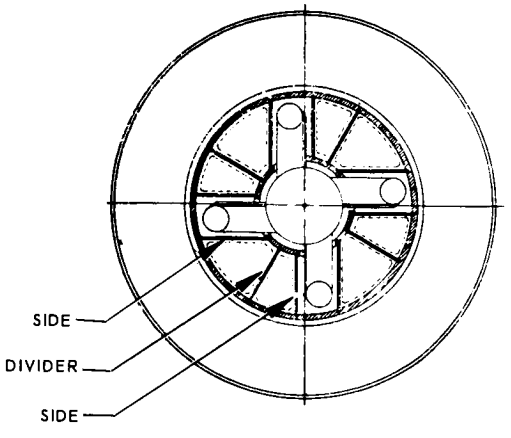

SECTION B–B

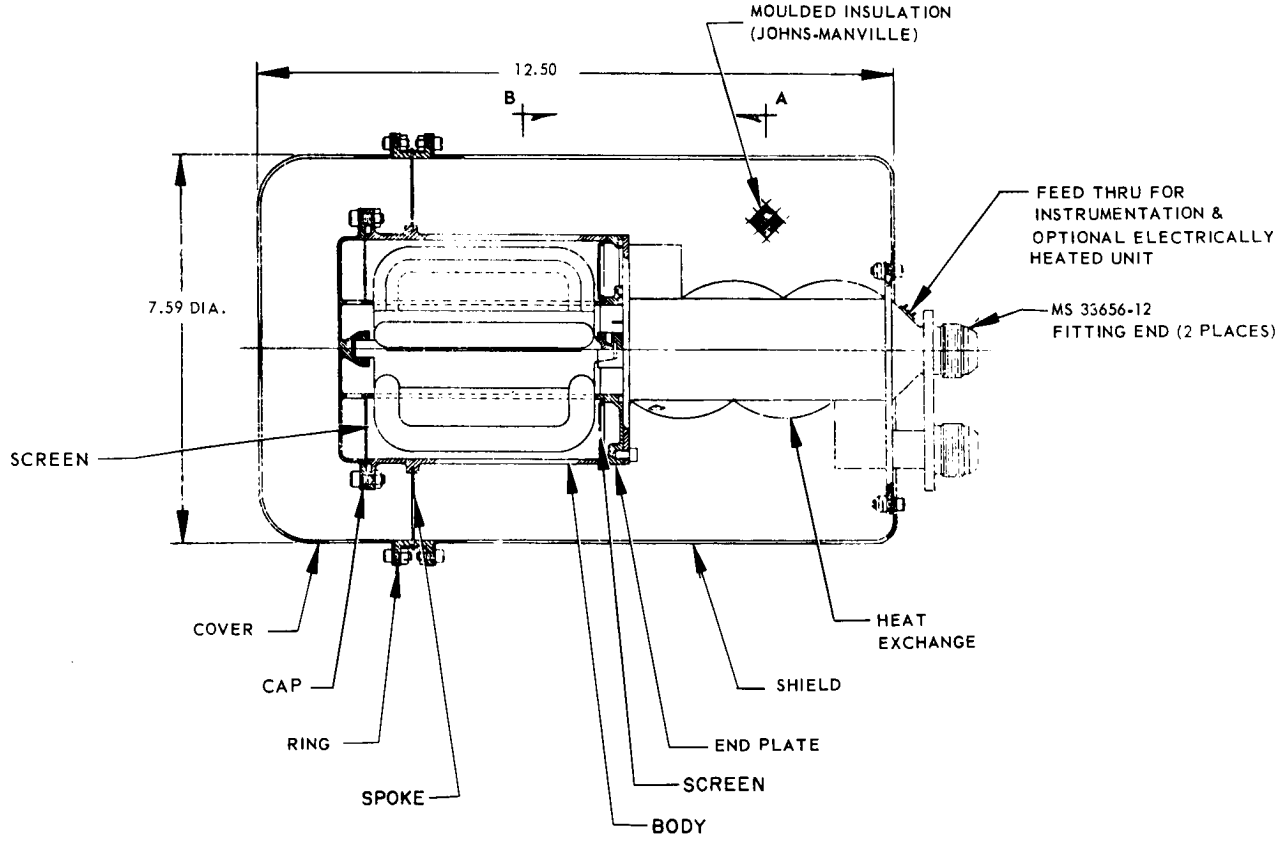

Fig. 58 IHCOS Dry Process Gas Version

The aluminum outer shield separates at the spoked supports to allow access to the insulation and inner body of the unit. The aluminum outer shield is also attached to the cold end of the regenerative heat exchanger. The shield is painted white to provide a high emittance, and thus reduce its surface temperature.

Fitting ends on the cold end of the regenerative heat exchanger are per MS33656-12, for flared tube connections. An electrical feed-through is also located at the cold end of the heat exchanger for instrumentation leads and for the electrical leads of the optional electrically heated simulated isotope. The instrumentation and electrical leads pass through the inlet gas passage of the regenerative heat exchanger. Instrumentation consists of recording gas temperatures at the inlet and outlet of the catalyst bed.

Moist Gas Design

The moist gas version of IHCOS (shown in fig. 59) is 13.6 in. long, excluding end fittings, and 6.87 in. in diameter. The weight of this unit is approximately 25 lb. The unit is similar in design to the dry process gas unit with the only differences being the type of thermal insulation and the size of the isotope heat source.

The insulation technique for this unit consists of a vacuum jacket surrounding the catalyst canister and insulated regenerative heat exchanger. The vacuum jacket is a vacuum furnace-brazed stainless steel vessel. The vessel when assembled is evacuated and sealed to maintain vacuum integrity. The inner and outer walls of the vacuum vessel are joined at a machined ring on the open end of the vessel. Thirty-six radial spokes are brazed under light preload, between the inner and outer wall, at the closed end of the vacuum vessel. The interior walls of the vacuum vessel have special coatings to achieve the desired thermal characteristics. The inner wall is gold plated to provide an emittance of 0.1, and the outer wall is silver-plated to provide an emittance of 0.05.

The surface of the vacuum vessel facing the catalyst canister, as well as the surface of the catalyst canister, are oxidized to provide an emittance of 0.8.

The catalyst canister containing the catalyst material and isotope heat source is attached to the vacuum vessel at a point adjacent to the wire spokes. The cold end of the regenerative heat exchanger is attached to an aluminum plate, which, in turn, is fastened to the machined ring in the open end of the vacuum vessel. The volume between the regenerative heat exchange and the inner wall of the vacuum vessel is filled with molded insulation (Min-K-1301).

The 156-watt sized isotope heat source for the moist gas unit is the same as the dry process gas unit in radial cross section; however, it is 1.1 in. longer.

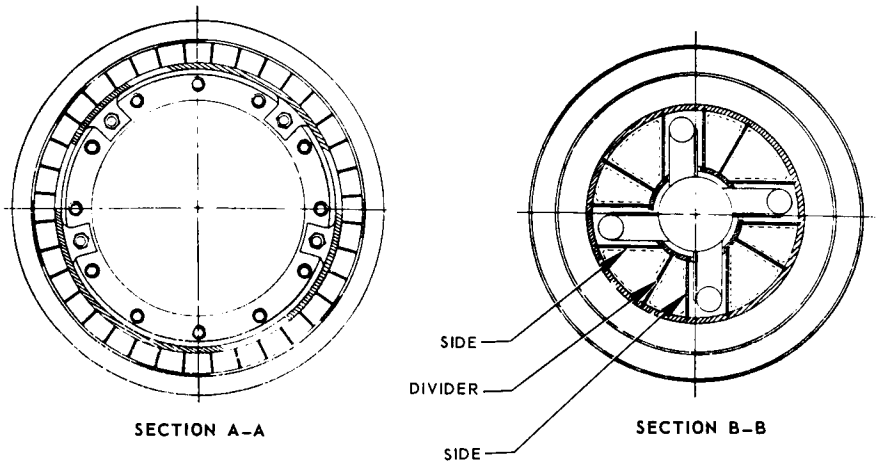

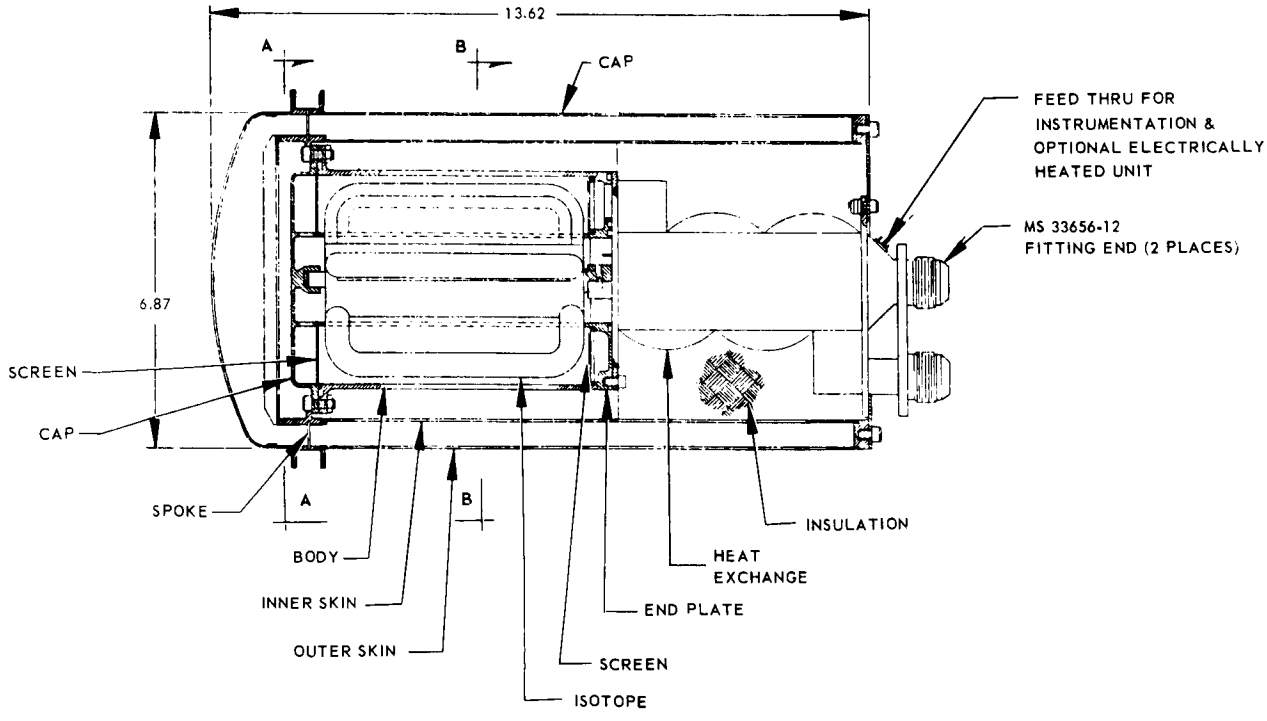

Fig. 59 IHCOS Moist Gas Version

Structural Analysis

Structural analyses were performed on the critical areas of the IHCOS design to investigate the ability of the unit to withstand the static and dynamic loads that are anticipated to be present. The designs indicated in figs. 58 and 59 were found adequate to withstand these loads.

DEVELOPMENT PLAN

The Phase I effort to develop an isotope-heated catalytic oxidizer system (IHCOS) resulted in an engineering layout drawing of the selected approach. The tasks accomplished in developing this design include the following:

- Mission Definition
- Contaminant Load Definition
- Isotope Selection
- Catalyst Selection
- Catalyst Performance Tests
- Analysis and Optimization
- Design Layout Drawing
- Development Plan

The results of the last effort are described herein. The objective of the development plan is to furnish a planning document for implementing the detailed design, fabrication, and evaluation of a space flight qualifiable isotope-heated catalytic oxidizer system. Phase II deals with a unit utilizing a resistively heated simulated isotope and Phase III describes the effort required to complete the isotopically heated unit. The development plan describes the major tasks required to complete the IHCOS development and indicates the costs, and schedule for each task.

The proposed effort in Phase II of the IHCOS development includes design and evaluation of pre- and post-sorbent beds to be included in IHCOS and the detailed design, fabrication, and evaluation of a full scale IHCOS with a resistively heated simulated isotope. This phase of the program consists of the following steps:

I. Pre- and post-sorbent bed development

- Pre- and post-sorbent contaminant load definition
- Long-term sorbent bed evaluation
- Model post-sorbent bed design and fabrication
- Full scale pre- and post-sorbent bed design

II. Detailed engineering, resistive prototype

- Material specification
- Joining and fabrication tests
- Coating evaluation
- Insulation evaluation
- Detailed design engineering

III. Fabrication and evaluation, resistive prototype

- Fabrication and evaluation test, heater
- Fabrication and evaluation, heat source
- Fabrication of complete unit
- Evaluation of complete unit

IV. AEC coordination and commitment

The proposed effort in Phase III of the IHCOS development includes nuclear qualification and testing of the radioisotope heat source and culminates in a flight-type demonstration test of an isotope heated catalytic oxidizer system. This phase of the program consists of the following steps:

I. IHCOS design evaluation

II. Heat source design

- Post demonstration test evaluation
- Reentry aid evaluation
- Detailed thermal analysis
- Stress analysis
- Evaluation and drawings

III. Chemical compatibility tests

- Capsule component compatibility tests
- Coating chemical compatibility tests

IV. Fabrication and assembly isotope test unit

V. Isotope mechanical and safety evaluation tests

- Shock and vibration loading
- Hypersonic reentry simulation tests
- Impact tests
- Post impact creep tests

VI. Final radioisotope heat source design

VII. Fabrication, assembly, and qualification test of radioisotope demonstration units

- Isotope heat source component fabrication
- Isotope heat source shipping container fabrication
- Encapsulation of radioisotope

VIII. Demonstration testing of integrated IHCOS

- System performance test
- Post demonstration test evaluation

IX. Assistance in preparation and conduct of Langley in-house program

Pre- and Post-Sorbent Bed Development

This section describes the effort related to the development of pre- and post-sorbent canisters for use with IHCOS.

Pre- and post-sorbent contaminant load definition. — The contaminants to be used during this effort will be based on the following sources: (1) the contaminants defined in the contaminant load definition in Phase I of NAS 1-6256, and (2) recent test data on closed life support systems atmospheres such as the Langley Integrated Life Support tests or the "Apollo Air Frame 8" tests being conducted at NASA/MSC. Attention will be given to those contaminants known to be poisonous to catalysts or to decompose to harmful products. A list of candidate poisons and compounds that might produce undesirable products is presented in Table 10.

Table 10

POTENTIAL CATALYST POISONS AND CONTAMINANTS
THAT PRODUCE UNDESIRABLE BY-PRODUCTS

Potential Poisonous Contaminants	Contaminants that Produce Undesirable By-Products from Catalytic Oxidizer
Sulphur containing compounds	Sulphur containing compounds
Halogenated compounds	Halogenated compounds
Cyanamide	Cyanamide
Chlorine	Dimethyl hydrazine
Nitric oxide	Hexamethylcyclotrisiloxane
Ammonia	Monomethyl hydrazine
Water	Chlorine
Inorganic acids	Ammonia
	Inorganic acids

Model presorbent bed design and fabrication. – The first step in this task is the selection of a presorbent bed material for efficient removal of compounds which are potentially poisonous to the catalyst. To accomplish this, data taken by LMSC and other industrial groups as well as Government agencies such as the U. S. Bureau of Mines and the Naval Research Laboratory will be reviewed. At the present time, it appears that a basic sorbent such as lithium hydroxide or lithium carbonate would be the most promising candidate presorbent material. After the presorbent material has been selected, the required quantity of this material will be determined. This will be accomplished by comparing the quantity and type of contaminants that are expected to reach the presorbent bed with the selected presorbent material's capacity for removal of these contaminants. The model presorbent canister will be approximately 1/10 scale.

Long-term sorbent bed evaluation. – The long-term sorbent bed evaluation will have a duration of approximately 150 days and will be divided into three time periods of approximately 30, 70, and 50 days. The test apparatus utilized will be the same as used in the catalyst tests conducted in three Phase I catalyst performance tests.

First test period: During the first test period of approximately 30 days, the system will operate with the presorbent bed located upstream of the catalytic oxidizer. The system will be operated at the nominal conditions used during the long-term catalyst test in Phase I. The contaminants introduced will be the same as those used in the Phase I test with the addition of potential catalyst poisons such as:

Sulphur dioxide

Freon 12

Freon 22

Vinyl chloride

Water vapor

Gas analyses will be performed at (1) the inlet and outlet of the presorbent bed to establish its effectiveness in removing potential poisons, and (2) at the outlet of the catalytic oxidizer to ensure that its removal efficiency has not been altered by the presence of the poisonous contaminants.

Second test period: During the next test period (approximately 31st to 100th day) the system will be operated under the same conditions as the first period except for the addition of contaminants that may produce undesirable products. These contaminants will be selected on the basis of a high probability of passing through the presorbent bed as well as being potential producers of undesirable products. These contaminants might be:

Methyl mercaptan

Freon 23

Ammonia

During this test period, the gas analyses performed will be the same as the first test period with the addition of an analysis of the catalytic oxidizer effluent to establish if any undesirable products have been formed. If the results of this analysis indicate that undesirable products are present, a postsorbent bed will be designed, fabricated, and installed in the test apparatus.

Third test period: During the final 50 days of the test, the conditions will be the same as the second test period with the exception that the postsorbent bed effluent will be monitored to establish if the postsorbent bed is effective in removing the undesirable products of oxidation.

Model postsorbent bed design and fabrication. – If the results of the long-term catalyst test indicate that undesirable products of oxidation are being formed, it will be necessary to design and fabricate a model postsorbent bed. Selection of a postsorbent material for this bed will also be based upon a review of studies performed by Government agencies and private industry. Considerations of this problem to date have indicated that all of the undesirable products formed are acidic and that a basic sorbent would be the most suitable postsorbent material. The sizing of this bed will be based on consideration of the toxic species that could be formed and the capacity of the selected postsorbent material for these compounds.

Full-scale presorbent and postsorbent bed design. – After completion of the long-term test, the results will be evaluated and a design performed for full-scale presorbent and postsorbent canisters to be used with the isotope heated catalytic oxidizer being developed under NAS 1-6256.

Detailed Engineering Resistive Prototype

This section describes the effort related to the detailed engineering of the resistively heated prototype IHCOS. The detailed engineering tasks include several material development efforts for the isotope heat source, evaluation of the selected thermal insulation, and completion of detailed engineering drawings for the entire unit.

Material specifications. – To ensure that materials of construction for the isotope heat source, with reproducible physical and chemical properties, will be used in the entire program; and to establish material selection guidelines it will be necessary to undertake a materials traceability program. The major tasks necessary to ensure an effective program are material specifications, material heat number identification, forming operation, thermal treatments, and nondestructive testing operations.

Joining and fabrication tests. – Because of the complex joint configurations characteristics of the heat source capsules and reentry-aid components, it will be necessary to study and test several fabrication and joining techniques. These tests, necessary to ensure absolute integrity of all joints will lead to a specific weld and fabrication procedure for each joint type, including necessary stress-relief thermal treatments. "T"-shaped specimens will be TIG-welded, mechanically tested, and metallographically examined for detrimental factors, such as embrittlement, excessive recrystallization, or matrix defects which could lead to premature failure. Specimens in which the reentry bead-to-fin joint is simulated, will be joined using both TIG and electron beam welding processes. As outlined above, these samples will be mechanically tested and metallographically examined.

Coating evaluation. – Regardless of the choice of materials for the outside structural support module, an oxidation resistant coating is required to protect the unit during both operation in air and during reentry into the earth's atmosphere. Molybdenum disilicide ($MoSi_2$) and tungsten disilicide (WSi_2) have been identified as the most promising coatings, but tests will be necessary to determine their survivability in the IHCOS environments. Because the survival time of these coatings at temperatures very near to the predicted maximum reentry temperature (approximately 3500°F for five minutes) is short, it will be also necessary to evaluate several other promising coating materials whose upper limit of oxidation protection is greater than 3500°F. A study of candidate coating materials which supplements the studies performed previously at TRW, will be initiated. A test program in which candidate coatings will be evaluated under simulated operational conditions will be undertaken. Tests of the selected coating under simulated reentry conditions will be performed under Phase III of this contract.

Coating technology review: A technology review will be conducted to ascertain the present state of coating development with particular emphasis on short-time survival at temperatures above 3500°F and long-term chemical compatibility in an IHCOS operating environment.

Application test and short survivability test: Based on the above, at least 16 specimens will be obtained for development of suitable application techniques using vapor deposition, electroplating, flame spraying or pack cementation. Oxidation tests of all coatings selected will be performed in a dynamic air environment at temperatures

up to 1400°F for two weeks. This will determine short-time catastrophic failures due to delamination or coating-substrate interface reactions, thereby aiding the evaluation and selection of materials for use in subsequent compatibility tests. During these tests the interface between the heat source and heat source support will be simulated. The specimens will be metallographically examined to ascertain if any degradation of material has occurred due to coating application, temperature, differential thermal exapnsion, or contact with the heat source support. It will be necessary to perform long-term coating evaluation tests in subsequent phases of this program.

Insulation evaluation. – For the moist gas version of IHCOS it is important to evaluate the integrity and thermal characteristics of the vacuum canister prior to performing the final design and fabrication of the complete unit. This will be accomplished by fabricating the vacuum canister at the outset of the program and testing it before detailed engineering of the rest of the unit is initiated. The test will consist of placing a known heat source within the canister and monitoring internal and external temperature to establish the thermal resistance of the unit at elevated temperature. This test will be continued for a period of time such as 30 to 60 days to observe if the thermal resistance of the unit degraded with time. If these tests prove satisfactory, detailed design and fabrication of the complete unit can proceed with a higher degree of confidence.

Design engineering. – A discussion of engineering design follows.

Simulated heat source: The resistively heated unit will be, insofar as possible, an exact duplicate of a radioisotope fueled heat source except that the thermal power will be obtained from an electrically-heated element located in the fuel cavity. All component closures will be identical to those of the final radioisotope heat source, except for those required or altered by the heater element leads and any required interior thermocouples.

TRW Systems has extensive experience in the design and manufacture of several different types of high-temperature electric heaters ranging from a flight-qualified sheathed heater, successfully operated in space in an electrothermal thruster, to radioisotope simulation heaters tested at 2200°C for 1000 hours under the POODLE program. A review of existing heater designs and fabrication techniques will be performed to select the approach best suited to the IHCOS design and operating requirements.

After evaluating the results obtained from the material evaluation tests, the preliminary heat source design will be modified, if necessary. This will be followed by a complete and detailed integrated resistive heater design compatible with geometric constraints imposed by the catalytic-oxidizer system. This design will be based on: (1) Phase I Preliminary Design, and (2) the results of the Phase II materials tests and the status of current technology. The design will include not only the capsule components and resistive heating elements, but also the outer support structure and reentry aids.

Overall system design: The development of the detail engineering drawings for the complete system will evolve from the preliminary design layout drawings prepared during Phase I of the IHCOS program and the detailed heat source design. The selected

configuration will enter the detail phase of design and spot layouts will be made to ensure that form and fit are assured under all operating conditions of the device.

Detail drawings will be prepared which will define all views of the part, subassembly, and top assemblies required for fabrication. The parts will be dimensioned with the tolerances given to ensure proper fit of mating parts and final assembly of the complete device. The drawings will define material requirements and call for the applicable MS and AN hardware.

Standard process specification and bulletins, which apply, will be called out on the drawings. These specifications and bulletins cover all facets of fabrication techniques, surface coatings, and handling requirements of aerospace hardware.

Envelope drawings (ED) will define requirements of vendor fabricated hardware, such as the regenerative heat exchanger or thermal insulation. These drawings specify all general requirements and define the interface between the vendor hardware and LMSC hardware. A detail specification defining performance, environmental, and test requirements becomes a part of the envelope drawing package.

The ED package will be sent to various vendors specializing in the design and manufacture of the subject hardware. Proposals from these vendors will be screened and a selection made based on design integrity, cost, and delivery schedules.

Fabrication Resistive Prototype

This section describes the effort required for fabrication and evaluation of IHCOS. The tasks include fabrication and preliminary evaluation of the heater element and then the simulated heat source. Following this, the final resistive heat source will be fabricated along with the balance of the unit and the complete system will be evaluated.

Fabrication and evaluation test heater. – Prior to fabrication of the heat source, two sheathed resistive heater elements will be fabricated to assist in evaluation of fabrication methods and to verify material selection. These units will be tested in air and vacuum to ascertain thermal performance during operation and to assist in the design and fabrication of the heater elements for the simulated heat source.

Fabrication and evaluation test heat source. – One resistive unit will be fabricated, assembled, and inspected. The heater element capsule liner, structural member, fin support, and fins will be fabricated at TRW Systems. The noble metal clad and high emissivity coatings will be obtained from an outside vendor. Assembly and welding of the prototype unit will be performed by TRW Systems. The unit will be an exact facsimile of the radioisotope demonstration unit, including structural support members and reentry aids.

This resistive heater verification unit will be used to obtain experimental thermal test data and to verify the thermal model and assumptions used in the resistive heater design. The unit will be instrumented with thermocouples at various axial and radial locations and will be tested in atmospheres simulating normal operating conditions. These tests will also provide a sound basis for the demonstration tests of the resistive

heater units at LMSC. The unit will also be used for integration tests to determine if any problems occur during normal assembly and to what extent, if any, coating integrity is jeopardized.

Fabrication final heat source. – Based on the results obtained from the verification test unit and the thermal performance tests, any required modifications of the nominal configuration will be made. The final resistive unit for demonstration at LMSC will then be fabricated, assembled, and inspected. After inspection, the unit will be shipped to LMSC for demonstration testing of the entire catalytic oxidizer system.

Fabrication of complete IHCOS prototype. – The various elements of IHCOS will be fabricated at LMSC or vendors specializing in certain aspects of the system. IHCOS consist of the following basic items: simulated isotope heat source regenerative heat exchanger, catalyst and isotope canister, insulation, and outer container. The fabrication of the isotope heat source has been described in the previous sections.

The regenerative heat exchanger will be purchased from a supplier specializing in stainless steel plate fin heat exchanger design and manufacture such as AiResearch, Stewart Warner, or Janitrol.

The catalyst and isotope canister will be constructed of nickel 200. The individual components will be machined at LMSC and hydrogen-furnace brazed at 1435°F using a silver copper brazing alloy. The brazing will be performed by the Pyromet Corporation.

The moist and dry process gas units utilize two different approaches to insulation. The dry process gas unit utilizes a molded insulation, Min-K-1301. This insulation will be purchased from Johns-Manville molded to LMSC configuration and specifications. The moist gas version of IHCOS utilizes an evacuated canister with low emittance coating for thermal insulation.

The vacuum canister is of welded construction using all stainless steel components (fig. 59). The inner skin, rings, and end plate will be machined, assembled, and welded prior to applying surface finishes required. The outer skin and ring will be machined, assembled, and welded prior to applying surface finishes. The support spokes (fig. 59) will then be installed by threading in the inner spoke ring through the outer spoke ring. The outer skin will be welded to the ring common to both inner and outer skins. Nuts will then be installed on the outer end of the spokes and each spoke preloaded to the desired load. These nuts will be welded closed to form a vacuum seal at each spoke penetration. The end cap will then be welded in place to complete the assembly. All welding will be X-rayed for integrity and a pressure check will be conducted to verify a leak-tight container. A vacuum will then be pulled on the canister at elevated temperature and it will be sealed. This work will be performed by a vacuum specialty manufacturing company such as Vacco Electronics.

The outer container for the dry process gas unit is of welded construction using all-aluminum components with the exception of the stainless steel spoke supports. These supports will be fabricated in the manner described for the vacuum canister. This portion of the unit will be fabricated at LMSC. The moist gas version of IHCOS does not require an outer canister since the vacuum canister serves this purpose.

Evaluation of the complete unit. – Evaluation of the IHCOS prototype consists of thermal and contaminant removal performance tests.

Thermal performance: The thermal performance characteristics of the resistively heated version of IHCOS must be accurately established to determine the precise fuel loading required for the isotopically heated fuel source. It will be necessary to establish operating temperature as a function of input power for several modes of operation to select the final power level. The minimum temperature is expected to occur at normal flow conditions with no contaminants present. The maximum temperature is expected to occur at the no-flow condition with a depressurized cabin. Two other conditions of interest include normal flow with contaminants and flow shutdown without a depressurized cabin.

The thermal performance test will be conducted with the apparatus shown in fig. 60. The catalytic oxidizer will be mounted in a vacuum vessel to allow accurate simulation of the heat transfer environment during simulated pressurized and depressurized cabin conditions. Instrumentation will be provided to monitor simulated isotope source power and temperatures, within the catalytic oxidizer. The temperature data will include isotope surface temperature, the regenerative heat exchanger inlet and outlet gas temperatures (both hot and cold), catalyst bed temperature, and temperatures on the insulation's inner and outer surface.

Tests will be conducted to establish the power level and thermal resistance characteristics required to (1) obtain the desired operating temperature under normal flow conditions, and (2) not exceed the maximum allowable temperature during flow shutdown with a depressurized cabin.

Contaminant removal capability: The experimental evaluation of IHCOS will include determination of the system's contaminant removal capability. This will include establishing the effectiveness of the presorbent bed, postsorbent bed, and catalytic oxidizer.

The recommended test apparatus consists of a closed-loop arrangement (fig. 60) with the presorbent bed, catalytic oxidizer and postsorbent beds connected in series. A fan is installed in the closed loop to provide the required 3 cfm circulation rate. The atmosphere in the closed loop will be controlled to the design conditions of 10 psia total pressure with 160 mm Hg oxygen partial pressure, 7.6 mm Hg carbon dioxide partial pressure, and a dew point of approximately 60°F. Vehicle leakage will be simulated by withdrawing gas from the closed loop at a known rate. Contaminants that are expected to be removed by IHCOS will be introduced at the production rates defined in the contaminant load definition. These contaminants, such as the potential producers of undesirable products of oxidation that are not expected to be removed by IHCOS, will be introduced in such a way as to maintain a given inlet concentration to IHCOS.

The tests will be conducted by stabilizing the system at design conditions and then introducing the contaminants to the system in stages. The first group of contaminants to be introduced would be methane and contaminants known to compete with methane for active catalyst sites. During the first period when the contaminants are being

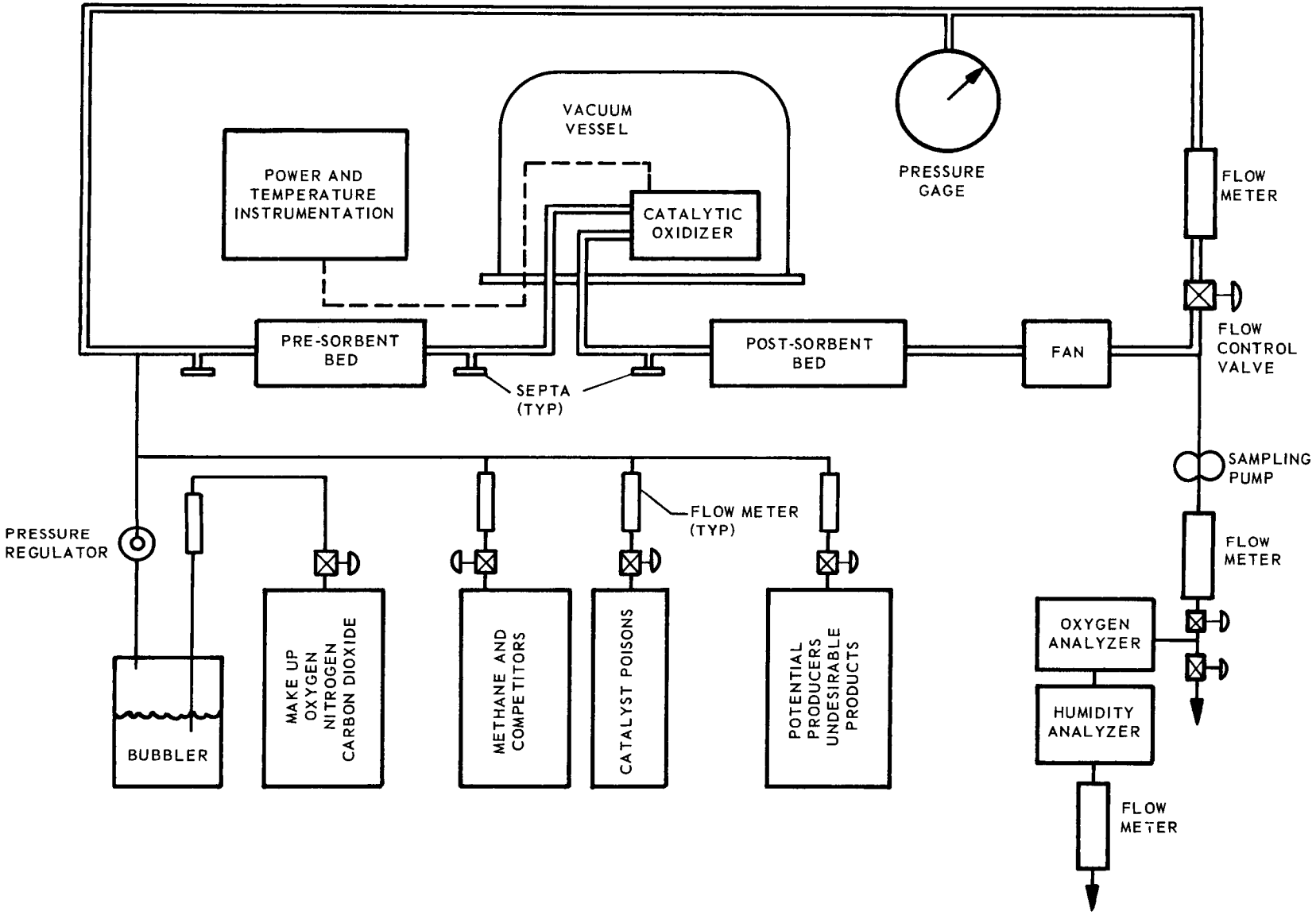

Fig. 60 Thermal Performance and Contaminant Removal Capability Test Apparatus

introduced, chemical analysis will be performed at the inlet and outlet of the catalytic oxidizer. After the first period of approximately one week, the second group of conteminants, consisting of potential catalyst poisons, will be introduced into the system in addition to methane and the competing contaminants. During this test period, chemical analyses will be performed at the inlet and outlet of the presorbent bed and at the outlet of the catalytic oxidizer. After approximately two weeks of testing, a third group of contaminants consisting of potential producers of undesirable products of oxidation will be introduced into the system in addition to the first two groups of contaminants. At this point, chemical analysis will be performed at the inlet and outlet of each of the IHCOS components.

It is desirable to continue the test for an extended period such as 120 days. This will allow assessment of the contaminant removal capability of the full scale system and also confirm the integrity of the coating material on the isotope source when at temperature and exposed to contaminants and the IHCOS materials of construction. Since long-term model tests of the system and coating evaluation tests have been made or are planned, it does not appear that a long-term full scale performance evaluation is mandatory. For this reason, two test programs, long term and short term, are presented in this plan.

During these tests both flow shutdown, and flow shutdown with depressurized cabin conditions, will be simulated. This will be done to verify the isotope coating integrity and to check catalyst behavior at elevated temperature.

Modification and retest of resistive prototype: If a functional failure of IHCOS occurs during any of the performance tests, the test will be terminated and appropriate action taken to modify and retest the hardware. Any component failure or inadequacy that prevents the system from functioning will be corrected. If, however, the system functions but at a slightly reduced capacity, the tests will be continued and the capacity of the system established.

AEC Liaison and Qualification Support

By interagency agreement, the responsibility for the development of flight qualified radioisotope heat sources resides with the Atomic Energy Commission. It will be necessary at the beginning of Phase II (to provide for sufficient leadtime) to enlist the support and commitment of the AEC to sponsor the development of the IHCOS radioisotope heat source (Phase III). AEC support will be required in the following areas:

- Nuclear qualification of radioisotope heat source, including design, fabrication, and safety evaluation
- Scheduling, production, and processing of radioisotope in accordance with program requirements
- Loading, sealing, and delivery of radioisotope heat sources to TRW for testing IHCOS
- TRW facility support, including technicians, health physics and safety personnel.

To accomplish this, LMSC and TRW will assist Langley Research Center in preparation of a document to be sent to AEC listing all pertinent details of the developmental plan. This document will be updated at the close of Phase II and will be made more specific, reflecting the progress made in Phase II. In addition, LMSC and TRW will maintain continuous liaison with the AEC in establishing the operational safety procedures and licensing requirements for preparation and testing of the radioisotope heat source in a life support system.

IHCOS Design Evaluation

Following completion of the Phase II evaluation of the resistive prototype, IHCOS will be examined to ascertain if the hardware has been adversely affected by the long term test. The system design will be reviewed in light of any findings from the post-test evaluation and any redesign and modifications required will be accomplished. At this time it would be desirable to take IHCOS with the resistively heated simulated isotope heat source and subject it to limited environmental tests. The objective of these tests would be to increase confidence in the flight qualifiable capability of the unit. These tests would be limited to those deemed critical such as vibration or shock only. The tests would be performed with the unit at maximum operating temperature. Following this effort, final design of the isotope heat source assembly will be performed.

Isotope Heat Source Design

Postdemonstration test evaluation. – After demonstration testing of the resistively heated unit by LMSC, the heat source will be returned to TRW Systems for comprehensive post test inspection and evaluation. This will consist of a detailed inspection of all components of the resistively heated unit to ascertain the effects of extended exposure to the operational environment. Parameters to be evaluated will include capsule integrity, interdiffusion between component materials, integrity of coating (resistance to abrasion and oxidation) and a review of LMSC thermal performance data generated in the demonstration test.

Reentry aid evaluation and analysis. – Based on work performed under Phase I of this program, a four-finned reentry aid configuration was chosen for the heat source to ensure intact reentry and tolerable impact velocities, should an abort situation occur. A trajectory and aerodynamic heating analysis was performed in Phase I for the dry process gas heat source; however, the moist gas design was based on an extrapolation of this data. If the moist gas unit is selected for development, the trajectory and aerodynamic heating analysis should be repeated. The results will then be used to compute impact velocities and impact temperatures – necessary data in the preparation of the Safety Evaluation Tests. A structural analysis will also be performed on the reentry aids to determine the maximum stresses induced during atmospheric reentry, and to ascertain if any weight reductions are possible.

Detailed thermal analysis. – With the reentry aid design finalized, a complete thermal analysis will be performed. The thermal model for this analysis will include all components of the integrated IHCOS and the analysis will be performed jointly by TRW and LMSC. It will rely heavily on experimental thermal data, as generated in the thermal performance testing of the resistively heated prototype units at TRW and the integrated IHCOS tests at LMSC. The results of this analysis will yield the temperature distributions within the system required for the stress analysis and chemical compatibility tests.

Stress analysis. – As discussed in Phase I, the use of an alpha-emitting fuel such as Pu-238 results in a pressure buildup within the capsule, necessitating the strength member to be properly designed to withstand the effects of long-term creep. It was established that the dry process gas heat source capsule containing a potential maximum 123 watts undergoes negligible creep in ten years at 1300°F. The moist gas design, however, although maintaining the same maximum operating temperature and design life, has a potential maximum power loading of 156 watts. Based on the new power loading and heat source temperatures, as determined in the thermal tests using electrical heaters, new creep calculations will be performed if the moist gas unit is selected for development. These calculations will be made using the TRW-developed CRASH digital computer program for creep in cylindrical capsules.

Evaluation and drawings. – Using the data generated in Phase II of this program and the results of the preceding thermal and reentry aid analyses, the radioisotope heat source design, with completely dimensioned shop drawings, will again be updated. This design will be used for the fabrication of fuel-simulated prototype test units to be used in safety evaluation tests.

Chemical Compatibility Tests

Capsule component compatibility tests. – The IHCOS heat source capsule is comprised of four concentric close-end cylinders. The innermost layer, or liner, contains the radioisotope fuel form and has been selected on the basis of compatibility tests performed by Mound Laboratory. It is planned that the second layer, the structural member, will be a refractory metal. The protective cladding for this structural member, necessary to provide long-term oxidation protection during system operation and in the event of mission abort, will, on the basis of present technology, be a noble metal alloy. Experimental evaluation of a large number of noble metal alloys has been performed at TRW. Although this cladding material is expensive, a considerable savings can be realized in reclaim value of test units, currently at about 90 percent of purchase cost.

Specimen couples will be used to establish the extent of interdiffusion between all component materials, and to verify the extrapolation of TRW's existing high-temperature interdiffusion data to lower operating temperatures. Tests will be run for six months and results will be extrapolated to the required five years. Metallographic examination of all specimens will determine whether or not diffusion barrier materials will be

required for the IHCOS system. Considerable progress has been made in perfecting these barriers for the IHCOS-type materials at higher temperatures (2000°F) where their use appears mandatory.

Coating chemical compatibility tests. – Based on the results obtained from the Phase II Coating Application Task, specimens will be fabricated for long-term compatibility tests between coatings and an atmosphere representative of that of a space cabin. These tests will be run for six months and will simulate the contaminant atmosphere insofar as possible. Emittance measurements, at various temperatures and times, will be taken on all coated specimens. Weight measurements will also be made to determine the effects of erosion, sublimation, and chemical interactions. All specimens will be evaluated metallographically and microhardness measurements will be made to ascertain the extent of interdiffusion and to determine the necessity of a diffusion barrier between the coating and substrate.

Fabrication and Assembly of Isotope Test Units

Procedures for procurement and traceability of all materials necessary to complete Phase III will be outlined, reflecting, in large part, the procedures and experience gained in Phase II. Additional quality control measures will be required because of the absolute necessity for material integrity in its function as a radioisotope containment material. Sufficient material will be ordered to enable the fabrication of the heat source assemblies required for safety evaluation tests, and for the final radioisotope-loaded heat source unit.

Using techniques developed in Phase II, the components for the test units will be fabricated at TRW. Eight complete units and two containment capsules will be assembled for shock and vibration tests, reentry simulation tests, and impact tests. Postimpact creep tests will also be carried out. Inspection of components will include visual, zyglo, and X-ray or ultrasonic testing techniques, and will be performed prior to assembly.

Isotope Heat Source Mechanical and Safety Evaluation Tests

Prior to fueling the IHCOS heat source and prior to its shipment from Mound Laboratory to TRW Systems, its integrity under normal ground transportation and complete containment of the fuel in ground transportation accidents must be demonstrated. No abort environments were simulated in tests of the capsule structure under the Phase II design of the resistively heated units. To ensure complete isotope containment in abort environments, it will be necessary to perform a number of safety evaluation tests on full-scale heat source units. Heat source integrity during normal ground transportation will be demonstrated in shock and vibration tests simulating tests of flight hardware. Fuel containment during abort conditions will be demonstrated under reentry, impact, and postimpact conditions, since these are more severe than any encountered in potential transportation accidents. All units will be exact duplicates of the final radioisotope unit except that the fuel will be simulated.

Shock and vibration loading. – Since flight-type hardware must be capable of surviving the shock and vibration loading associated with transportation, launch, and stage separation, such verification testing of the heat source must be performed. Two complete electrically heated units will be tested under vibration loads representative of launch conditions. The simulated heat source will be maintained at steady-state operating temperatures characteristic of the launch period.

Hypersonic reentry simulation tests. – One of the most severe conditions encountered by the heat source during abort occurs during reentry of the heat source module into the earth's atmosphere. Peak heating temperatures, as calculated in Phase I, approach 3500°F and last for several minutes. The severity of this abort mode requires that ground simulation tests be performed to establish the integrity of the coating during reentry and verify that internal temperatures do not exceed allowable values. To accomplish this task, two heat source assemblies will be tested in a hypersonic plasma-jet facility at TRW Systems. In these tests, time, temperature, pressure, and plasma flow velocity will be varied to simulate reentry conditions. The units will be thoroughly instrumented during the test and inspected after test to ascertain the extent of degradation.

Impact tests. – As a verification of the ability of the heat source to survive impact, four complete heat source units will be tested with a TRW-developed pneumatic impact gun. Some modifications of existing equipment will be required to accept the additional weight and size of a full-scale heat source test unit including reentry aids. The capsule structure will be impacted at the anticipated terminal impact velocity and temperature of the radioisotope source. Two of the impact test units will be inspected, sectioned, and metallographically examined to ascertain possible degradation in joints or in overall capsule integrity. The other two units will also be inspected except that the capsule strength-member will be left intact for subsequent creep testing.

Postimpact creep tests. – Capsules must not only survive impact, but must be left in a condition which assures complete containment for a specified time after impact. The continued generation of helium and sustained high temperature in weakened or deformed capsules may lead to rapid failures. Confidence in the survivability of impacted capsules and development of design features, if necessary, to preclude early creep failures, require experimental creep testing of capsules after they have been impacted.

To check the effect impact may have on subsequent creep, the two capsules tested for impact and two nonimpacted capsules will be tested. One end cap of the capsules will have been designed so that, after impact, it can be fitted with a pressurizing tube. These two capsules will then be pressurized and creep tested along with the nonimpacted capsules under identical conditions. Impact-induced degradation of creep properties will be apparent by directly comparing the results of the two experiments.

Final Radioisotope Heat Source Design

Results from the above safety evaluation tests may indicate that some modifications are necessary in the preliminary design model to ensure maximum reliability in an abort environment. Modifications, if any, will be made and the final heat source design,

along with detailed component and assembly drawings, will be completed. These drawings will be sent to LMSC to be used in final system design fo the IHCOS.

Fabrication, Assembly, and Qualification Test of Radioisotope Demonstration Units

A complete isotope-fueled heat source unit will be fabricated for demonstration testing of the integrated catalytic oxidizer system. Additional fuel-liner, strength-member and cladding components will be required as backup units for Mound Laboratory to be used in loading the heat source capsule. The capsule components will be delivered to Mound Laboratory for encapsulation prior to demonstration testing at TRW Systems.

Isotope heat source component fabrication. – Having established the final design, and using the techniques and experience gained under both the Phase II and the Phase III fabrication tasks, components for two complete radioisotope-fueled heat source assemblies and four fuel capsules will be fabricated. Although only one unit will be loaded with the radioisotope fuel, the remaining components are required by Mound Laboratory to establish handling procedures, perfect weld schedules, and provide a backup unit. Strict quality control measures will govern every phase of fabrication to assure flight-quality heat source components.

Isotope shipping container fabrication. – Concurrent with the fabrication of the heat source components at TRW, a suitable shipping container for the radioisotope-fueled heat source assembly will be procured for containment of the unit. The shipping container will be AEC-approved and will meet ICC interstate shipping regulations. The container will be used whenever the unit is transported in its fuel-loaded condition.

Encapsulation of radioisotope. – The heat source components for the demonstration test unit will be sent to Mound Laboratory for fueling and encapsulation. In accordance with established specifications, and in conjunction with the AEC, the plutonium fuel will be loaded into the capsule and all closure welds performed. After quality assurance tests, the noble metal cladding will be applied and all welds checked. The structural support member, reentry aids, and coating (the techniques for which were developed in Phase II) will then be applied.

The exact nature, duration, and extent of the radioisotope heat source quality assurance tests performed at Mound Laboratory are the sole responsibility of the AEC. These tests will include the following:

a. Weight and calorimetry measurements of fuel to ascertain exact total power

b. Surface contamination after closure welds of liner and pressure vessel and external radiation levels after addition of the reentry aids

c. Ultrasonic and/or radiographic inspection of all component closures

Demonstration Testing of Integrated IHCOS

The parameters of most interest in the IHCOS demonstration tests include the catalytic oxidizer performance, system thermal performance, and the radiation field associated with the isotope-loaded system. The demonstration testing of an integrated IHCOS system would be carried out at TRW Systems which currently holds research and development type radioactive materials licenses at both its Space Park (Redondo Beach) and Capistrano Test Site locations. Adequate facilities for the IHCOS test already exist at the Capistrano location and additional facilities are now under consideration at Space Park. The LMSC-supplied portion of the catalytic oxidizer life support system will be delivered to TRW in sufficient time to permit installation and complete checkout of the system prior to receipt of the radioisotope heat source from Mound Laboratory.

System performance test. – Based on experience gained from the thermal performance test of the resistively heated units of Phase II, temperature measurements will be taken at various internal and external locations of IHCOS. These measurements will be compared with results of the thermal analysis, and will permit determination of system thermal efficiency.

The model atmosphere will be introduced over the isotope-fueled heat source. The contaminant level will be periodically measured both upstream and downstream of the IHCOS using a gas chromatograph, and the efficiency of the unit in removing impurities will thus be determined. These tests will rely heavily on the resistively heated demonstration tests performed at LMSC.

Radiation measurements, both before and after the heat source is loaded into the catalytic oxidizer, will be taken to provide a comparison with calculated values. Background radiation counts will be taken continuously during the course of the test.

Postdemonstration test evaluation. – After the demonstration tests, the heat source must be returned to Mound Laboratory and defueled prior to inspection and evaluation. This will consist of a thorough and detailed inspection of all heat source and catalytic oxidizer components to ascertain the effects of exposure to the operational environments. Parameters to be evaluated include capsule integrity, interdiffusion between component materials, integrity of coating, resistance of coating to abrasion, and oxidation of coating and catalytic oxidizer components.

Assistance in Preparation and Conduct of Langley In-House Program

LMSC and TRW will assist Langley in preparing a test plan for their in-house testing efforts. This plan will include a description of the apparatus and test procedures necessary to evaluate IHCOS performance. Consideration will be given to those efforts required to establish good performance data as well as conducting the evaluations within the required safety constaints. Assistance will be rendered in matters pertaining to AEC licensing, facility requirements for handling and testing, and radiation safety requirements.

Program Schedule and Estimated Cost

Phase II. – The total Phase II effort can be carried out in approximately 20 months. The major tasks, schedule, and an approximate estimate of the program man hour requirements are indicated in fig. 61. A number of optional tasks are indicated for this program. These options deal with the type and number of units to be developed, the degree of performance evaluation, and the number of component developmental tests to be performed prior to fabrication and evaluation of the complete unit.

Estimates are presented for both the moist and dry process gas versions of IHCOS and for one and two deliverable units. Since a significant portion of the fabrication costs are of a nonrecurring nature it might be desirable to provide two deliverable units, since the cost of the second unit is considerably less than the first. The advantages of providing two units include (1) the ability to have a backup system in case a test failure occurs, and (2) if no design changes occur during the program, the second unit could be used for the isotopically heated system, thus providing NASA with both electrically heated and isotopically heated systems.

Phase III. – The Phase III effort can be carried out in approximately 20 months. The major tasks, schedule, and an approximate estimate of the program man hour requirements are indicated in fig. 62.

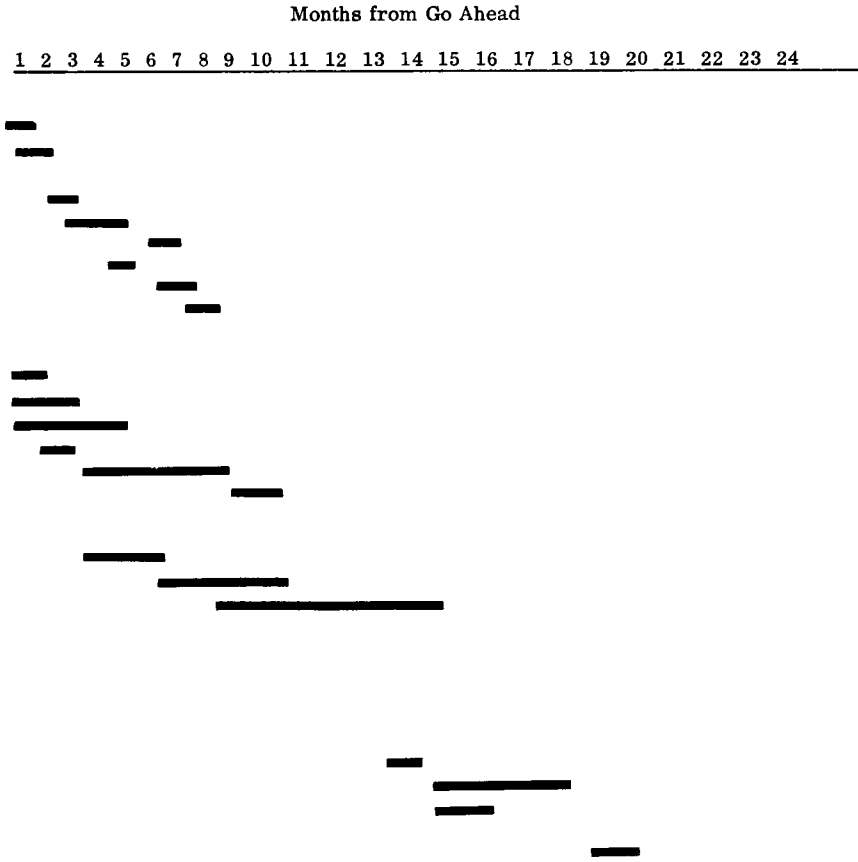

Task	Approximate Man-Hours
1.0 Pre- and Post-Sorbent Bed Development	
Contaminant Load Definition	140
Model Presorbent Bed Design and Fabrication	140
Long Term Sorbent Bed Evaluation	
Poisons – Presorbent Bed	300
Producers of Undesirable Products	900
Postsorbent Bed	650
Model Postsorbent Bed Design and Fabrication	120
Full Scale Pre- and Post-Sorbent Bed Design	140
Reports	300
2.0 Detailed Engineering Resistive Prototype	
Material Specifications	960
Joining and Fabrication Tests	300
Coating Evaluation	850
Insulation Evaluation	200
Detailed Engineering	1500
Reports	300
3.0 Fabrication and Evaluation Resistive Prototype	
Fabrication Evaluation Test Heater	320
Fabrication Evaluation of Heat Source	1800
Fabrication of Complete Unit	
Pre- and Post-Sorbent Beds	250
Moist Units (2)	500
Moist Unit (1)	340
Dry Process Units (2)	810
Dry Process Unit (1)	475
Evaluation of Complete Unit	
Thermal Performance	200
Contaminant Removal Capability (Long Term Test)	1750
Contaminant Removal Capability (Short Term Test)	500
Modification and Retest	150
Reports	300
4.0 AEC Coordination and Commitment	250

Fig. 61 Schedule and Manpower Estimate – Phase II

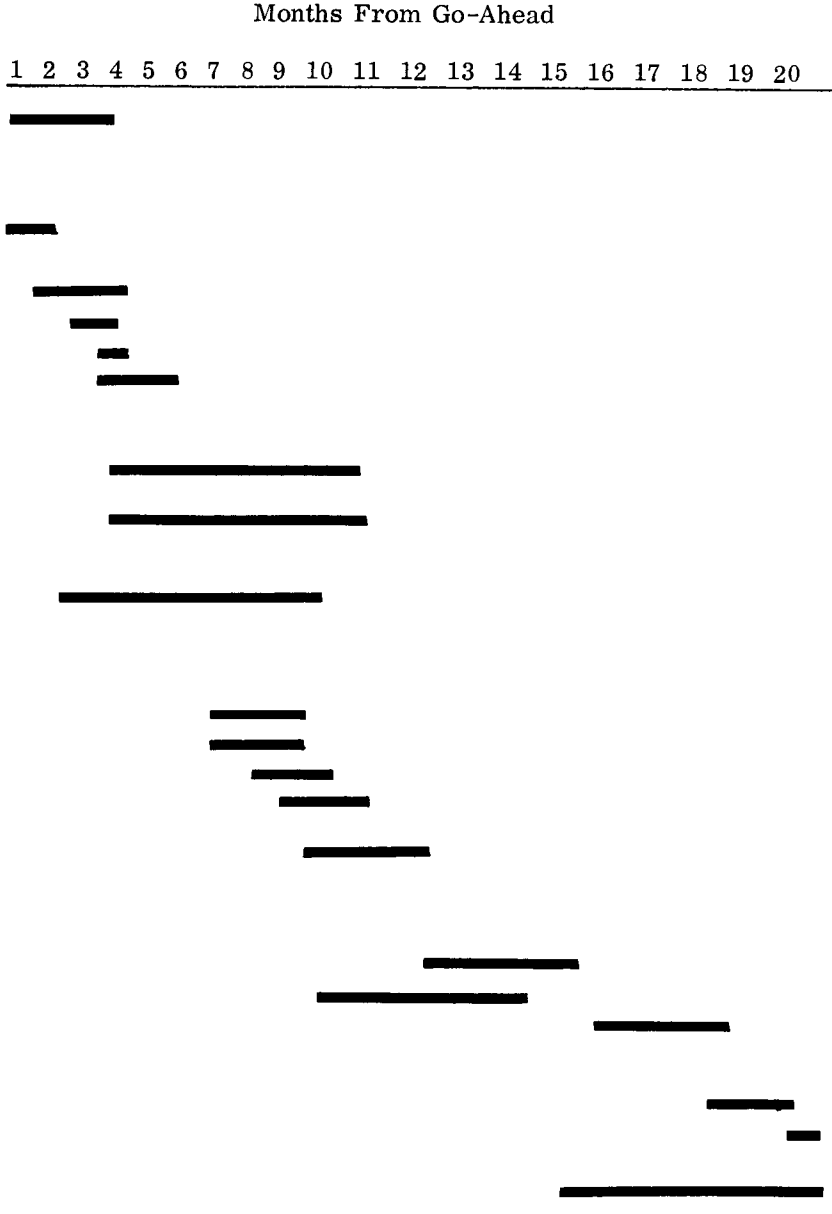

Task	Approximate Man-Hours
1.0 IHCOS Design Evaluation	1000
2.0 Heat Source Design	
Postdemonstration Test Evaluation	350
Reentry and Evaluation and Analysis	750
Detailed Thermal Analysis	150
Stress Analysis	150
Evaluation and Drawings	500
3.0 Chemical Compatibility Tests	
Capsule Compatibility Tests	450
Coating Chemical Compatibility Tests	950
4.0 Fabrication and Assembly Test Isotopes	1900
5.0 Isotope Mechanical and Safety Evaluation Tests	
Shock and Vibration Loading	450
Hypersonic Reentry Simulation	700
Impact Tests	550
Post-Impact Creep Tests	500
6.0 Final Isotope Heat Source Design	450
7.0 Fabrication, Assembly, and Qualification Test Isotope Source	
Component Fabrication	650
Shipping Container Fabrication	350
Encapsulation of Isotope	250
8.0 Demonstration Test of IHCOS	
System Performance Test	1250
Post Demonstration Test Evaluation	450
9.0 Assist Langley In-House Program	250

Fig. 62 Schedule and Manpower Estimate – Phase III

CONCLUSIONS

The IHCOS design study has indicated that an isotope-heated catalytic oxidizer can be successfully used to control a significant portion of the contaminants anticipated to be present in a typical early space station. This study was based on a crew size of 9 men and a mission duration of 180 days.

By utilizing an isotope heat source for thermal power, a substantial weight saving can be realized. The 125-watt version of IHCOS has a total equivalent weight of approximately 28 pounds. If this unit were heated electrically, the resulting total equivalent weight, including power penalty, would be approximately 69 pounds.

The isotope heat source most suitable for use in IHCOS is Pu 238, based on minimum system weight and commensurate with mission objectives, availability, cost, and safety constraints. No special radiation shielding is required and the radiation dose rate is less than 5 percent of the total allowable accumulated dose for a 1.5-meter separation distance.

The most effective catalyst of those screened for use in IHCOS is a 0.5 percent dispersion manufactured by Engelhard Industries. This catalyst was successfully tested for the full 180-day mission duration. The results of this test demonstrated that this catalyst is sensitive to the presence of water vapor. It was concluded that two humidity levels should be used for test purposes: a high level typical of that available from the ECS, 41-44°F dew point; and a very low dew point typical of that available from the predrying section of a molecular sieve CO_2 removal system. With a moist gas and the selected space velocity, the required methane oxidation occurred at a temperature of 680°F; the dry process gas system provides the required methane oxidation at a temperature of approximately 560°F.

The moist gas version of IHCOS requires 125 watts of power and is 13.6 inches long, excluding end fittings, and 6.9 inches in diameter. The dry process gas version requires 107 watts of power and is 12.5 inches long, excluding end fittings, and 7.6 inches in diameter. The weight of the dry process gas unit is about 20 lb and the moist gas unit about 25 lb.

REFERENCES

1. M. Honma and R. J. Jaffe: Thermal Degradation of Polymeric Materials – III. LMSC 65-75-66-1, Lockheed Missiles and Space Co., January 1966

2. Personal communication, W. L. Solitario, TRW Systems, May 1966

3. L. L. Bolstad et al.: Gassing and Flammability Testing of Organic Materials for Apollo A63 777A22(2), Honeywell Aero. Div., September 1963

4. Personal communication, M. L. Owen, NASA Manned Spacecraft Center, June 1966

5. S. A. Hall, et al.: Development and Test of a Prototype Advanced Biomedical System. Air Force AMD TR-66-1, April 1966

6. Toliver, W. H. and Morris, M. L.: Chemical Analysis of Permanent and Organic Gases in a 30-Day Manned Test. Aerospace Medicine, Vol. 37, No. 3, March 1966, pp 233-238

7. Adams, J. D., et al.: Study of Man During a 56-Day Exposure to An Oxygen-Helium Atmosphere at 258 mm Hg Total Pressure – II. Major and Minor Atmospheric Components. Aerospace Medicine, Vol. 37, No. 6, June 1966, pp 555-558

8. Personal communication, W. L. Solitario, TRW Systems, June 1966

9. V. M. Downey, et al.: Biological Measurement of Man in Space. LMSC M-61-64, Lockheed Missiles and Space Co., May 1965

10. LMSC R&D Staff: Design and Fabrication of a Trace Contaminant Removal System for Apollo Phase I. LMSC M-58-65-1, March 1965

11. LMSC R&D Staff: Design and Fabrication of a Trace Contaminant Removal System for Apollo Phase III. LMSC M-58-65-3, April 1966

12. Second Annual Progress Report: The Present Status of Chemical Research in Atmosphere Purification and Control on Nuclear-Powered Submarines. NRL Report 5814, 29 August 1962

13. LMSC R&D Staff: Design and Fabrication of a Trace Contaminant Removal System for Apollo Phase II. LMSC M-58-65-2, November 1965

14. Arnold, E. C.: Handbook of Shielding Requirements and Radiation Characteristics of Isotopic Power Sources, ORNL-3576, April 1964

15. TRW Staff: DART Proposal – Analytical and Experimental Investigation of a Radioisotope Heated Propellant Reaction Control System, 9778-2601-PL000, October 1965

16. Rohrman, C. A.: Radioisotopic Heat Sources. Battelle Northwest, April 1965

17. Davis, H. L.: Handbook of Nuclear Research and Technology, Section Isotope Costs and Availability, McGraw Hill

18. Schulman, Fred: Handbook of Nuclear Research and Technology, Section Generator Performance and Mission Prospects

19. TRW Systems: Radioisotope Heated Propellant Reaction Control Systems, First Quarterly Report No. 4579-6003-T5000, July 1966

20. L. J. Van Nice: Thermal Radiation from Saturn Fireballs. Volumes 1 and 2, No. 2122-6001-T0000, TRW Systems, December 1965

21. J. L. Blumenthal: Study of the Chemical Integrity of Radioisotope Containment Materials in Launch Abort Environments. No. 4510-6001-R000, TRW Systems, December 1965

22. TRW Systems: Radioisotope Applications in Space Program, Volume I, POODLE Aerospace Safety Analysis. Final Report No. STL-517-0016

23. TRW Systems: Mission Definition for Radioisotope Heated Catalytic Oxidizer, prepared under LMSC Subcontract No. 24-16088, Report No. 4642-6001-R000, June 1966

24. G. B. Bradshaw: Superalloy Capsule Study, Final Report, 1965

25. I. Finnie and W. Heller: Creep in Engineering Materials, McGraw-Hill, 1959

26. W. J. Dalby: SNAP-15A and SNAP-15B Fuel-Capsule Impact Tests, Sandia Corporation, SC-DR-65-132

27. E. S. Diamant: Analysis and Numerical Calculation of Creep in Axisymmetric Shells. In publication

28. TRW Systems: Radioisotope Propulsion Technology Program (POODLE), Quarterly Progress Report No. STL-517-0042, April 1966

29. P. J. Chao, et al.: Advanced Development of PFR-6, Pfaudler Permutit Inc., ML-TDR-64-84, May 1964

30. DMIC Report No. 195, Properties of Coated Refractory Metals, January 1964

31. Goldsmith, Waterman and Hirschhorn: Handbook of Thermophysical Properties of Solid Materials, The Macmillan Company, New York, 1961

32. The Pfaudler Co., PFR Coatings Technical Bulletin No. 6, 1964

33. O. Kubaschewski and B. E. Hopkins: Oxidation of Metals and Alloys. Academic Press, New York, 1962

34. S. J. Van Grouw: TRW Systems, Thrust Chamber Technology IR & D Program, Phase I Report, 1966

35. Report on the Optimization of the Manned Orbital Research Laboratory (MORL) System Concept, Douglas Report SM-46082

36. LMSC 4-17-67-2: Use of Food and Waste for Space Radiation Shielding, February 1967

Appendix A

CONTAMINANT LOAD FOR IHCOS DESIGN STUDY

Appendix A

CONTAMINANT LOAD FOR IHCOS DESIGN STUDY

Contaminant	Production Rates			Maximum Allowable Concentration (mg/m^3)	Data Source								To Be Removed By Oxidation	Flow Required Through IHCOS (cfm)
	Non-Biological (gm/day)	(1)* Biological (gm/day)	Total (gm/day)		Production Rates (23)							Allowable Concentration		
					A	B	C	D	E	F	G			
Acetone	10.20	0.0045	10.20	240	XX	X	XX	X	XX	X		(2)	X	1.25
Acetaldehyde	2.50	0.0018	2.50	36		X	X	X	X			(2)	X	2.07
Acetic Acid	0.25		0.25	2.5	X			X				(2)		
Acetylene	2.50		2.50	180		X	X	X				(3)	X	0.37
Acetonitrile	0.25		0.25	7			X					(2)		
Acrolein	0.25		0.25	0.25	X							(2)		
Allyl Alcohol	0.25		0.25	0.5	X	X	X		X			(2)	X	1.47
Ammonia	2.50	9.0	11.50	3.5		X	X					(2)		
Amyl Acetate	0.25		0.25	53					X	X		(2)		
Amyl Alcohol	0.25		0.25	36	X							(2)	X	0.16
Benzene	2.50		2.50	8	XX	X	X	X	XX	X		(2)		
n-Butane	2.50		2.50	180		X	X	X	XX			(3)	X	0.37
iso-Butane	0.25		0.25	180	X							(3)		
Butene-1	2.50		2.50	180	XX	X	X	X	XX			(3)	X	0.37
cis-Butene-2	0.25		0.25	180		X						(3)		
trans-Butene-2	2.50		2.50	180		X	X		X			(3)	X	0.37
1, 3 Butadiene	2.50		2.50	220	X				X			(2)		
iso-Butylene	0.25		0.25	180			X	X	X			(3)		
n-Butyl Alcohol	2.50	0.027	2.53	30	X	XX	XX	X	X			(2)	X	2.53
iso Butyl Alcohol	0.25		0.25	30					X			(2)	X	0.20
sec-Butyl Alcohol	0.25		0.25	30	X							(2)	X	0.21
tert -Butyl Alcohol	0.25		0.25	30						X		(2)	X	0.21

*Footnotes defined at end of table.

CONTAMINANT LOAD FOR IHCOS DESIGN STUDY

Contaminant	Production Rates			Maximum Allowable Concentration (mg/m^3)	Data Source								To Be Removed By Oxidation	Flow Required Through IHCOS (cfm)
	Non-Biological (gm/day)	(1) Biological (gm/day)	Total (gm/day)		Production Rates (23)							Allowable Concentration		
					A	B	C	D	E	F	G			
Butyl Acetate	0.25		0.25	71					X	X		(2)		
Butraldehydes	0.25		0.25	70					XX	X		(4)		
Butyric Acid	0.25		0.25	14				X				(5)		
Carbon Disulfide	0.25		0.25	6	X	X	X					(2)		
Carbon Monoxide	2.50	0.30	2.80	29	XX	X	XX		X	X		(6)	X	2.91
Carbon Tetrachloride	0.25		0.25	6.5	X				X	X		(2)		
Carbonyl Sulfide	0.25		0.25	25		X						(4)		
Chlorine	0.25		0.25	1.5							X	(6)		
Chloroacetone	0.25		0.25	100							X	(5)		
Chlorobenzene	0.25		0.25	35					X			(2)		
Chlorofluoromethane	0.25		0.25	24		X						(11)		
Chloroform	2.50		2.50	24	XX	X			X			(2)		
Chloropropane	0.25		0.25	84		X	X					(5)		
Caprylic Acid		X	0.25	155							X	(5)		
Cumene	0.25		0.25	25	X							(2)		
Cyclohexane	2.50		2.50	100	X	X	X		X			(2)	X	0.67
Cyclohexene	0.25		0.25	100		X						(2)	X	0.03
Cyclohexanol	0.25		0.25	20	X							(2)		
Cyclopentane	0.25		0.25	100		X						(12)	X	0.02
Cyclopropane	0.25		0.25	100	X							(7)	X	0.03
Cyanamide	0.25		0.25	45							X	(5)		
Decalin	0.25		0.25	5.0					XX			(13)		

CONTAMINANT LOAD FOR IHCOS DESIGN STUDY

Contaminant	Production Rates			Maximum Allowable Concentration (mg/m^3)	Data Source								To Be Removed By Oxidation	Flow Required Through IHCOS (cfm)
	Non-Biological (gm/day)	(1) Biological (gm/day)	Total (gm/day)		Production Rates (23)							Allowable Concentration		
					A	B	C	D	E	F	G			
1, 1 Dimethyl cyclo-hexane	0.25		0.25	120					X			(5)		
trans 1, 2, Dimethyl Cyclohexane	0.25		0.25	120		X						(5)		
2, 2 Dimethyl butane	0.25		0.25	93		X			X			(5)	X	0.03
Dimethyl Sulfide	0.25		0.25	15					X			(4)		
1, 1 Dichloroethane	2.50		2.50	40	X	X	X					(2)		
Di iso Butyl Ketone	0.25		0.25	29						X				
1, 4 Dioxane	2.50		2.50	36	XX	X						(2)		
Dimethyl Furan	0.25		0.25	3.0					X			(15)		
Dimethyl Hydrazine	0.25		0.25	0.1							X	(2)		
Ethane	2.50		2.50	180	XX	X				X		(3)	X	0.37
Ethyl Alcohol	2.50	0.09	2.51	190	XX	XX	XX	X	XX	X		(2)	X	0.35
Ethyl Acetate	2.50		2.50	140		X	XX	X	X			(2)		
Ethyl Acetylene	0.25		0.25	180		X						(3)		
Ethyl Benzene	0.25		0.25	44	X				X			(2)		
Ethylene Dichloride	0.25		0.25	40	XX	XX			X			(2)		
Ethyl Ether	2.50		2.50	120					X	X		(2)	X	0.59
Ethyl Butyl Ether	0.25		0.25	200	X							(4)		
Ethyl Formate	2.50		2.50	30				X	X			(2)		
Ethylene	2.50		2.50	180	X	X	X	X	XX			(3)	X	0.37
Ethylene Glycol	0.25		0.25	114							X	(5)		
trans 1, Methyl 3 Ethyl Cyclohexane	0.25		0.25	117		X						(4)		

CONTAMINANT LOAD FOR IHCOS DESIGN STUDY

Contaminant	Production Rates			Maximum Allowable Concentration (mg/m^3)	Data Source								To Be Removed By Oxidation	Flow Required Through IHCOS (cfm)
	Non-Biological (gm/day)	(1) Biological (gm/day)	Total (gm/day)		Production Rates (23)							Allowable Concentration		
					A	B	C	D	E	F	G			
Ethyl Sulfide	0.25		0.25	97							X	(5)		
Ethyl Mercaptan		X	0.25	2.5		X			X			(2)		
Freon 11	2.50		2.50	560		XX		X	XX			(2)		
Freon 12	2.50		2.50	500		X	XX					(2)		
Freon 21	0.25		0.25	420							X	(2)		
Freon 22	0.25		0.25	350		X			XX			(9)		
Freon 23	0.25		0.25	12		X						(11)		
Freon 113	0.25		0.25	700					X	X		(14)		
Freon 114	2.50		2.50	700		XX	XX		X			(2)		
Freon 114 unsym	0.25		0.25	700	X	X						(2)		
Freon 125	0.25		0.25	25		X			X			(4)		
Formaldehyde	0.25		0.25	0.6		X		X				(2)		
Furan	0.25		0.25	3					X			(15)		
Furfural	0.25		0.25	2	X							(2)		
Hydrogen	2.50	0.45	2.99	215	X							(5)		
Hydrogen Chloride	0.25		0.25	0.15							X	(6)		
Hydrogen Fluoride	0.25		0.25	0.08							X	(6)		
Hydrogen Sulfide		0.0007	0.0007	1.5		X						(2)		
Heptane	0.25		0.25	200	X				X			(2)		
Hexene-1	0.25		0.25	180	X	X						(3)		
n-Hexane	2.50		2.50	180	X	X			X	X		(2)		
Hexamethylcyclotri-sihexane	0.25		0.25	240	X	X						(5)		

CONTAMINANT LOAD FOR IHCOS DESIGN STUDY

Contaminant	Production Rates			Maximum Allowable Concentration (mg/m^3)	Data Source								To Be Removed By Oxidation	Flow Required Through IHCOS (cfm)
	Non-Biological (gm/day)	(1) Biological (gm/day)	Total (gm/day)		Production Rates (23)							Allowable Concentration		
					A	B	C	D	E	F	G			
Indole	0.25	0.9	1.15	126			X					(5)		
Isoprene	0.25		0.25	140	X			X	X			(4)		
Methylene Chloride	2.50		2.50	21	X	X			X			(2)		
Methyl Acetate	2.50		2.50	61	X				X			(2)		
Methyl Butyrate	0.25		0.25	30					X			(16)		
Methyl Chloride	0.25		0.25	21	X	X						(2)		
2-Methyl – 1 Butene	0.25		0.25	1430	X							(4)		
Methyl Chloroform	2.50		2.50	190		X			X			(2)		
Methyl Furane	0.25		0.25	3					X			(15)		
Methyl Ethyl Ketone	2.50		2.50	59	X	X	XX		XX	X		(2)	X	1.25
Methyl Isobutyl Ketone	0.25		0.25	41					X	X		(2)	X	0.14
Methyl Isopropyl Ketone	2.50		2.50	70	X	X			X			(8)	X	1.03
Methyl Cyclohexane	0.25		0.25	200	X				X			(2)		
Methyl Acetylene	0.25		0.25	165	X							(2)		
Methyl Alcohol	2.50	0.09	2.59	26		X	XX		XX	X		(2)	X	2.90
3-Methyl Pentane	0.25		0.25	295		X			X			(2)		
Methyl Methacrylate	0.25		0.25	41					X			(2)		
Methane	29.5	5.4	34.9	1720	XX	X	XX			X	X	(5)	X	(22)
Mesitylene	0.25		0.25	2.5	X							(4)		
mono Methyl Hydrazine	0.25		0.25	0.035							X	(2)		

CONTAMINANT LOAD FOR IHCOS DESIGN STUDY

Contaminant	Production Rates			Maximum Allowable Concentration (mg/m^3)	Data Source								To Be Removed By Oxidation	Flow Required Through IHCOS (cfm)
	Non-Biological (gm/day)	(1) Biological (gm/day)	Total (gm/day)		Production Rates (23)							Allowable Concentration		
					A	B	C	D	E	F	G			
Methyl Mercaptan		X	0.25	2			X		X			(2)		
Naphthalene	0.25		0.25	5.0					X			(2)		
Nitric Oxide	0.25		0.25	32		X						(5)		
Nitrogen Tetroxide	0.25		0.25	1.8							X	(5)		
Nitrogen Dioxide	0.25		0.25	0.9			X					(6)		
Nitrous Oxide	0.25		0.25	47							X	(5)		
Octane	0.25		0.25	235					X			(2)		
Propylene	2.50		2.50	180	XX	X	XX	X	XX			(3)	X	0.37
iso-Pentane	2.50		2.50	295		X			X			(2)	X	0.21
n-Pentane	2.50		2.50	295	X	X			X			(2)	X	0.21
Pentene -1	0.25		0.25	180	X							(2)	X	
Pentent -2	0.25		0.25	180	X							(2)		
Propane	2.50		2.50	180	X	X						(2)	X	0.37
n-Propyl Acetate	0.25		0.25	84					X			(2)		
n-Propyl Alcohol	2.50		2.50	75	XX	X			XX	X		(9)	X	0.97
iso-Propyl Alcohol	2.50		2.50	98	X	X	XX		XX	X	X	(2)	X	0.73
n-Propyl Benzene	0.25		0.25	44						X		(17)		
iso-Propyl Chloride	0.25		0.25	260					X			(20)		
iso-Propyl Ether	0.25		0.25	120					X			(19)		
Proprionaldehyde	0.25		0.25	30	X							(4)		
Propionic Acid	0.25		0.25	15				X				(4)		

CONTAMINANT LOAD FOR IHCOS DESIGN STUDY

Contaminant	Production Rates			Maximum Allowable Concentration (mg/m^3)	Data Source								To Be Removed By Oxidation	Flow Required Through IHCOS (cfm)
	Non-Biological (gm/day)	(1) Biological (gm/day)	Total (gm/day)		Production Rates (23)							Allowable Concentration		
					A	B	C	D	E	F	G			
Propyl Mercaptan		X	0.25	82					X			(5)		
Propylene Aldehyde	0.25		0.25	10						X		(18)		
Pyruvic Acid		3.4	3.4	0.9								(21)		
Phenol	0.25	3.4	3.65	1.9							X	(2)		
Skatol		X	0.25	141			X					(5)		
Sulfur Dioxide	0.25		0.25	0.8							X	(10)		
Styrene	0.25		0.25	42	X							(2)		
Tetrachloroethylene	0.25		0.25	67		X		X	X			(2)		
Tetrafluoroethylene	0.25		0.25	205		X						(4)		
Tetrahydrofurane	0.25		0.25	59					X			(2)		
Toluene	2.50		2.50	75	X	XX		X	XX	X		(2)		
Trichloroethylene	2.50		2.50	52	XX	X	XX	X	X			(2)		
1,2,4 Trimethyl Benzene	0.25		0.25	49	X							(4)		
1,1,3 Trimethyl cyclohexane	0.25		0.25	140							X	(5)		
Valeraldehyde		X	0.25	70							X	(4)		
Valeric Acid		X	0.25	110			X					(5)		
Vinyl Chloride	2.50		2.50	130	X	XX	X		X			(2)		
Vinyl Methyl Ether	0.25		0.25	60						X		(19)		
Vinyldene Chloride	0.25		0.25	20		X						(6)		
O-Xylene	2.50		2.50	44		X			XX		X	(2)		
m-Xylene	2.50		2.50	44	X	XX					X	(2)		
p-Xylene	2.50		2.50	44	X						X	(2)		

NOTES FOR APPENDIX A

1. Metabolic production rate based on 9 men, production per man from Bioastronautics Data Book, NASA SP-3006. Contaminants noted by check mark have been reported, but without rate estimate.

2. Limit taken as 0.1 of the Threshold Limit Value (TLV) for 1965, American Conference of Governmental Industrial Hygienists, May 1965.

3. Limit derived by analogy to 1965 TLV for propane, butadiene, and LPG (liquefied petroleum gas).

4. Limit taken as that estimated by R. H. Edgerly, North American Aviation, October 7, 1964.

5. Limit taken as concentration that results in a vapor pressure of 0.02 torr, except for hydrogen and methane for which vapor pressure of 2.0 torr is used.

6. Limit taken as the allowable 90-day continuous exposure limit for submarines as published in Submarine Habitability Handbook, Navships 250-649-1, and from personal communication, Capt. J. Siegel, Naval Toxicology Unit.

7. Limit derived by analogy to 1965 TLV for cyclohexane.

8. Limit derived by analogy to 1965 TLV for methyl propyl ketone (pentanane-2).

9. Limit taken as 0.1 of TLV suggested by H. B. Elkins, Chemistry of Industrial Toxicology, 1959.

10. Limit taken as adverse level limit set by State of California.

11. Limit derived by analogy to 1965 TLV for chloroform.

12. Limit derived by analogy to 1965 TLV for ethyl butyl ketone.

13. Limit derived by analogy to 1965 TLV for naphthalene.

14. Limit derived by analogy to 1965 TLV for Freon-114.

15. Limit taken as 0.1 of Sax's suggested value for furan.

16. Limit derived by analogy to 1965 TLV for lower esters.

17. Limit derived by analogy to 1965 TLV for ethyl benzene.

18. Limit derived by analogy to 1965 TLV for acetaldehyde.

19. Limit derived by analogy to 1965 TLV for ethyl ether, plus divinyl ether data.

20. Limit derived by analogy to 1965 TLV for ethyl chloride.

21. Limit derived by analogy to 1965 TLV for formic acid.

22. The removal efficiency required for methane with a flow of 3 CFM is 27%

23. Listed contaminants have been reported in connection with materials screening or atmospheric analysis as follows: (an "X" indicates reported, a double "X" means found in large amounts)

    A. = Outgassing products of space cabin qualified materials as determined by LMSC studies, as reported by Apollo C/M contaminant control studies, and as cited in Honeywell report A63 777A 22(2).

    B. = Detected as contaminants in charcoal desorption tests of samples from Mercury and Gemini (up to GT-7) ECS. (R. Saunders, Naval Research Lab.).

    C. = Detected by LMSC as contaminants in Air Force Biosatellite 30-day ground test (chimpanzee subject) (AMD TR-66-1, April, 1966).

    D. = Reported in 30-day manned experiment conducted by Aerospace Medical Research Lab. (W. H. Toliver and M. L. Morris, Aerospace Medicine, 37, 3, 233, March 1966).

    E. = Reported in 56-day manned experiment conducted by School of Aerospace Medicine (J. D. Adams, et. al., Aerospace Medicine, 37, 6, 555, June 1966).

    F. = Reported as present in Apollo C/M ECS breadboard testing.

    G. = Contaminants likely to result from experiments conducted onboard space stations.

PERTINENT CHEMICAL SYNONYMS FOR APPENDIX A

2-Butanone = Methyl ethyl ketone

Chlorodifluoromethane = Freon 22

Crotonaldehyde = Propylene aldehyde

Decahydronaphthalene = Decalin

1, 2 Dichloroethane = Ethylene chloride = Ethylene dichloride

Dichlorodifluoromethane = Freon 12

Dichlorofluoromethane = Freon 21

Dichlorotetrafluoroethane = Freon 114

p-Dioxane = 1, 4 Dioxane

2-Methyl butanone-3 = 3-Methyl 2-Butanone = Methyl isopropyl ketone

Methoxyethane = Vinyl methyl ether

Propene = Propylene

Propyne = Propine + Methyl acetylene

Pentafluoroethane = Freon 125

Perchloroethylene = Tetrachloroethylene

Trichlorofluoromethane = Freon 11

Trichlorotrifluoroethane = Freon 113

Trifluoromethane = Fluoroform = Freon 23

1, 3 5 Trimethyl benzene = mesitylene

Appendix B

CONVERSION EFFICIENCIES

Appendix B-1

METHANE CONVERSION EFFICIENCY

Day	Date	Temperature °F	Inlet Concentration mg/m^3 at 10 psia	Outlet Concentration mg/m^3 at 10 psia	Conversion Efficiency %
1	9-12-66	535	1720 ± 0	1260 ± 27	26.8 ± 2.2
2	9-13-66	575	1700 ± 7	1260 ± 45	26.0 ± 3.6
3	9-14-66	613	1700 ± 21	1280 ± 21	25.4 ± 1.7
4	9-15-66	668	1700 ± 7	1150 ± 26	32.6 ± 2.3
5	9-16-66	657	1760 ± 49	1225 ± 16	30.6 ± 1.3
8	9-19-66	665	1715 ± 9	1184 ± 17	31.0 ± 1.4
9	9-20-66	675	1740 ± 0	1380 ± 0	20.4 ± 0
10	9-21-66	675	1740 ± 17	1260 ± 7	27.9 ± .4
11	9-22-66	675	1810 ± 6	1290 ± 0	23.9 ± 0
12	9-23-66	688	1760 ± 22	1180 ± 15	32.9 ± 1.3
15	9-26-66	692	1730 ± 32	865 ± 17	50.0 ± 1.0
16	9-27-66	670	1790 ± 0	1330 ± 18	25.5 ± 1.0
17	9-28-66	685	1730 ± 19	1125 ± 3	35.0 ± .3
18	9-29-66	683	1720 ± 18	1210 ± 28	29.8 ± 1.6
19	9-30-66	683	1750 ± 28	1170 ± 14	33.0 ± .8
22	10- 3-66	683	1750 ± 87	822 ± 4	52.8 ± .2
23	10- 4-66	685	1680 ± 22	1090 ± 12	35.1 ± .7
24	10- 5-66	685	1820 ± 24	1010 ± 13	44.4 ± .7
25	10- 6-66	685	1750 ± 23	962 ± 7	45.0 ± .4
26	10- 7-66	685	1795 ± 28	1150 ± 27	36.2 ± 1.5
29	10-10-66	685	1780 ± 14	815 ± 13	54.2 ± .7
30	10-11-66	682	1720 ± 14	1270 ± 14	26.1 ± .8
31	10-12-66	683	1730 ± 28	1200 ± 15	30.5 ± .9
32	10-13-66	683	1710 ± 0	1140 ± 7	33.3 ± .4
33	10-14-66	683	1710 ± 14	1110 ± 19	35.0 ± 1.1
36	10-17-66	683	1800 ± 27	870 ± 27	51.7 ± 1.5
37	10-18-66	678	1690 ± 15	1150 ± 18	32.0 ± .5
38	10-19-66	684	1780 ± 3	1120 ± 23	37.3 ± 1.3
39	10-20-66	683	1760 ± 3	1080 ± 23	38.7 ± 1.3
40	10-21-66	683	1650 ± 30	1000 ± 3	39.7 ± .2
43	10-24-66	676	1730 ± 20	1050 ± 10	39.3 ± .6
44	10-25-66	678	1700 ± 0	1050 ± 10	38.5 ± .6
45	10-26-66	676	1660 ± 11	1030 ±12	37.7 ± .7
46	10-27-66	676	1730 ± 12	1060 ± 35	39.0 ± .2
47	10-28-66	681	1710 ± 0	1080 ± 12	35.7 ± .7
50	10-31-66	673	1790 ± 6	945 ± 11	47.2 ± .6

Methane Conversion Efficiency (continued)

Day	Date	Temperature °F	Inlet Concentration mg/m^3 at 10 psia	Outlet Concentration mg/m^3 at 10 psia	Conversion Efficiency %
51	11- 1-66	675	1780 ± 0	1200 ± 0	32.6 ± 0
52	11- 2-66	682	1780 ± 26	1160 ± 4	35.0 ± .2
53	11- 3-66	683	1795 ± 15	1160 ± 30	35.5 ± 1.7
54	11- 4-66	673	1785 ± 40	1210 ± 14	32.5 ± .8
55	11- 5-66	675	1910 ± 11	970 ± 12	49.2 ± .6
56	11- 6-66	~673	1795 ± 14	924 ± 14	48.5 ± .8
57	11- 7-66	~675	1820 ± 16	1030 ± 16	43.5 ± .9
58	11- 8-66	~678	1680 ± 15	953 ± 29	43.2 ± 1.7
59	11- 9-66	~678	1700 ± 30	1170 ± 15	32.3 ± .9
60	11-10-66	~679	1770 ± 15	1140 ± 0	35.5 ± 0
61	11-11-66	~680	1760 ± 28	1090 ± 28	37.9 ± 1.6
64	11-14-66	~678	1765 ± 52	947 ± 9	46.3 ± .5
65	11-15-66	~678	1740 ± 49	1025 ± 24	41.1 ± 1.4
66	11-16-66	~680	1810 ± 35	986 ± 9	45.6 ± .5
67	11-17-66	~681	1790 ± 27	980 ± 15	45.3 ± .8
68	11-18-66	~682	1780 ± 41	985 ± 31	39.7 ± 1.5
71	11-21-66	~680	1705 ± 7	845 ± 27	50.5 ± 1.6
72	11-22-66	~681	1760 ± 36	1052 ± 30	40.2 ± 1.7
73	11-23-66	~680	1780 ± 24	1260 ± 18	29.2 ± 1.1
78	11-28-66	~675	1870 ± 0	1140 ± 24	42.4 ± 2.8
79	11-29-66	~680	1650 ± 17	1070 ± 37	35.0 ± 2.2
80	11-30-66	~683	1700 ± 10	1180 ± 26	30.7 ± 1.5
81	12- 1-66	~678	1785 ± 32	1295 ± 20	27.4 ± 2.2
82	12- 2-66	~674	1770 ± 36	1375 ± 28	22.2 ± 1.8
85	12- 5-66	~679	1770 ± 12	1115 ± 8	37.0 ± .8
86	12- 6-66	~678	1745 ± 16	1220 ± 11	30.0 ± .6
87	12- 7-66	~680	1710 ± 9	1310 ± 7	23.5 ± .4
88	12- 8-66	~680	1735 ± 20	713 ± 8	58.8 ± .3
89	12- 9-66	~683	1780 ± 28	626 ± 10	64.8 ± .1
92	12-12-66	~675	1795 ± 16	746 ± 7	58.6 ± .9
93	12-13-66	~678	1810 ± 19	655 ± 7	63.8 ± .4
94	12-14-66	~680	1800 ± 29	1105 ± 16	44.2 ± .7
95	12-15-66	~680	1692 ± 34	729 ± 14	57.0 ± .7
96	12-16-66	~680	1680 ± 18	875 ± 10	48.0 ± .3
99	12-19-66	~680	1720 ± 26	689 ± 10	60.0 ± .2
100	12-20-66	~678	1720 ± 36	799 ± 17	53.6 ± .8
101	12-21-66	~680	1710 ± 22	855 ± 11	50.0 ± .2
102	12-22-66	~678	1835 ± 16	734 ± 7	60.5 ± .3
107	12-27-66	~667	1810 ± 34	630 ± 12	65.2 ± .2
108	12-28-66	~680	1815 ± 18	647 ± 7	64.3 ± .3
109	12-29-66	~680	1820 ± 23	674 ± 9	62.9 ± 1.4
110	12-30-66	~675	1860 ± 42	643 ± 12	65.4 ± 2.0

Methane Conversion Efficiency (continued)

Day	Date	Temperature °F	Inlet Concentration mg/m^3 at 10 psia	Outlet Concentration mg/m^3 at 10 psia	Conversion Efficiency %
114	1- 3-67	~675	1865 ± 20	626 ± 7	66.4 ± .2
115	1- 4-67	~675	1868 ± 18	660 ± 12	64.7 ± 1.0
116	1- 5-67	~675	1725 ± 27	654 ± 10	59.8 ± .5
117	1- 6-67	~675	1695 ± 23	664 ± 9	60.8 ± .3
120	1- 9-67	~678	1660 ± 10	614 ± 3	63.0 ± .7
121	1-10-67	~675	1740 ± 15	737 ± 7	57.6 ± .2
122	1-11-67	~655	1688 ± 2	1055 ± 1	37.6 ± 1.8
123	1-12-67	~660	1725 ± 17	1005 ± 10	41.8 ± 1.0
124	1-13-67	~660	1730 ± 25	374 ± 6	79.5 ± .2
127	1-16-67	~610	1745 ± 18	1075 ± 10	38.4 ± .7
128	1-17-67	~610	1750 ± 24	780 ± 11	55.4 ± 1.4
129	1-18-67	~585	1650 ± 6	1250 ± 45	23.3 ± .4
130	1-19-67	~585	1760 ± 8	1410 ± 6	20.6 ± .9
131	1-20-67	~585	1715 ± 34	1170 ± 23	31/7 ± .6
134	1-23-67	~590	1700 ± 29	863 ± 10	43.6 ± .6
135	1-24-67	~590	1620 ± 10	995 ± 70	38.6 ± .8
136	1-25-67	~587	1730 ± 4	1150 ± 2	33.5 ± .8
137	1-26-67	~585	1750 ± 36	1295 ± 27	25.9 ± .6
138	1-27-67	~585	1740 ± 22	1395 ± 18	19.8 ± .3
141	1-30-67	~588	1750 ± 11	1400 ± 35	20.6 ± 1.9
142	1-31-67	~585	1670 ± 11	1013 ± 3	39.3 ± .2
143	2- 1-67	~582	1740 ± 10	950 ± 19	44.2 ± 1.1
144	2- 2-67	~587	1750 ± 9	970 ± 19	44.5 ± 1.1
145	2- 3-67	~585	1730 ± 12	958 ± 12	44.7 ± .7
148	2- 6-67	~585	1745 ± 34	800 ± 3	54.2 ± .2
149	2- 7-67	~587	1730 ± 32	776 ± 2	55.4 ± .1
150	2- 8-67	~560	1785 ± 30	1150 ± 60	35.5 ± 2.2
151	2- 9-67	~560	1790 ± 61	1110 ± 51	38.1 ± 2.9
152	2-10-67	~560	1735 ± 33	1160 ± 33	33.3 ± 1.9
155	2-13-67	~560	1700 ± 4	1160 ± 9	31.8 ± .5
156	2-14-67	~557	1740 ± 26	1180 ± 9	32.3 ± .5
157	2-15-67	~560	1660 ± 16	1100 ± 24	34.0 ± .9
158	2-16-67	~560	1740 ± 45	1045 ± 18	30.1 ± 1.1
159	2-17-67	~560	1790 ± 43	1260 ± 15	29.8 ± .8
162	2-20-67	~560	1750 ± 23	1100 ± 23	37.0 ± 1.3
163	2-21-67	~560	1770 ± 14	1120 ± 39	37.0 ± 2.3
164	2-22-67	~560	1800 ± 27	1270 ± 18	29.3 ± 1.0
165	2-23-67	~560	1735 ± 43	1060 ± 4	38.8 ± .3
166	2-24-67	~560	1745 ± 11	1000 ± 48	42.8 ± 2.7
169	2-27-67	577	1680 ± 40	1200 ± 23	28.4 ± 1.4
170	2-28-67	557	1720 ± 20	1220 ± 25	29.0 ± 1.5

Methane Conversion Efficiency (continued)

Day	Date	Temperature °F	Inlet Concentration mg/m^3 at 10 psia	Outlet Concentration mg/m^3 at 10 psia	Conversion Efficiency %
171	3- 1-67	~560	1680 ± 24	1135 ± 24	32.4 ± 1.4
172	3- 2-67	~560	1730 ± 14	1200 ± 4	30.5 ± .2
173	3- 3-67	~560	1670 ± 49	1060 ± 26	36.5 ± 1.5
176	3- 6-67	~560	1725 ± 46	1155 ± 23	32.9 ± 1.3
177	3- 7-67	~560	1780 ± 20	1270 ± 20	28.5 ± 1.1
178	3- 8-67	~560	1720 ± 66	1160 ± 5	32.7 ± .3
179	3- 9-67	~560	1710 ± 58	1200 ± 14	30.2 ± .8

Appendix B-2

CARBON MONOXIDE CONVERSION EFFICIENCY

Day	Date	Temperature °F	Inlet Concentration mg/m^3 at 10 psia	Outlet Concentration mg/m^3 at 10 psia	Conversion Efficiency %
1	9-12-66	535	29.0 ± .6	0	100
2	9-13-66	575	29.0 ± 1.0	0	100
3	9-14-66	613	29.0 ± .5	0	100
4	9-15-66	668	28.7 ± .7	0	100
5	9-16-66	657	29.8 ± .4	0	100
8	9-19-66	665	29.0 ± .4	0	100
9	9-20-66	675	29.3 ± .5	0	100
10	9-21-66	675	29.3 ± .2	0	100
11	9-22-66	675	30.5 ± .5	0	100
12	9-23-66	688	29.7 ± .4	0	100
15	9-26-66	692	29.0 ± .6	0	100
16	9-27-66	670	30.2 ± .4	0	100
17	9-28-66	685	29.2 ± .1	0	100
18	9-29-66	683	29.0 ± .7	0	100
19	9-30-66	683	29.5 ± .4	0	100
22	10- 3-66	683	29.4 ± .1	0	100
23	10- 4-66	685	28.3 ± .3	0	100
24	10- 5-66	685	30.7 ± .4	0	100
25	10- 6-66	685	29.5 ± .2	0	100
26	10- 7-66	685	30.3 ± .7	0	100
29	10-10-66	685	30.0 ± .5	0	100
30	10-11-66	682	29.0 ± .3	0	100
31	10-12-66	683	29.0 ± .4	0	100
32	10-13-66	683	29.0 ± .2	0	100
33	10-14-66	683	29.0 ± .5	0	100
36	10-17-66	683	30.4 ± 1.0	0	100
37	10-18-66	678	28.5 ± .4	0	100
38	10-19-66	684	30.0 ± .6	0	100
39	10-20-66	683	29.7 ± .6	0	100
40	10-21-66	683	27.9 ± .1	0	100
43	10-24-66	676	29.0 ± .3	0	100
44	10-25-66	678	28.6 ± .3	0	100
45	10-26-66	676	28.0 ± .3	0	100
46	10-27-66	676	29.0 ± .2	0	100
47	10-28-66	681	29.0 ± .5	0	100
50	10-31-66	673	30.0 ± .1	0	100

Carbon Monoxide Conversion Efficiency (Continued)

Day	Date	Temperature °F	Inlet Concentration mg/m^3 at 10 psia	Outlet Concentration mg/m^3 at 10 psia	Conversion Efficiency %
51	11- 1-66	675	30.0 ± .5	0	100
52	11- 2-66	682	30.0 ± .4	0	100
53	11- 3-66	683	30.3 ± .2	0	100
54	11- 4-66	673	30.1 ± .6	0	100
55	11- 5-66	675	32.2 ± .2	0	100
56	11- 6-66	~673	30.3 ± .2	0	100
57	11- 7-66	~675	30.3 ± .2	0	100
58	11- 8-66	~678	28.3 ± .2	0	100
59	11- 9-66	~678	28.7 ± .5	0	100
60	11-10-66	~679	29.8 ± .3	0	100
61	11-11-66	~680	29.7 ± .6	0	100
64	11-14-66	~678	29.8 ± 1.0	0	100
65	11-15-66	~678	29.4 ± 1.0	0	100
66	11-16-66	~680	30.5 ± .7	0	100
67	11-17-66	~681	30.2 ± .4	0	100
68	11-18-66	~682	30.2 ± .4	0	100
71	11-21-66	~680	28.7 ± .6	0	100
72	11-22-66	~681	29.7 ± .2	0	100
73	11-23-66	~680	30.0 ± .4	0	100
78	11-28-66	~675	31.5 ± .4	0	100
79	11-29-66	~680	27.8 ± .5	0	100
80	11-30-66	~683	28.7 ± .2	0	100
81	12- 1-66	~678	30.1 ± .6	0	100
82	12- 2-66	~674	29.9 ± .7	0	100
85	12- 5-66	~679	29.9 ± .3	0	100
86	12- 6-66	~678	29.4 ± .3	0	100
87	12- 7-66	~680	28.8 ± .2	0	100
88	12- 8-66	~680	29.3 ± .4	0	100
89	12- 9-66	~683	30.0 ± .5	0	100
92	12-12-66	~675	30.3 ± .3	0	100
93	12-13-66	~678	30.5 ± .4	0	100
94	12-14-66	~680	30.4 ± .6	0	100
95	12-15-66	~680	28.5 ± .6	0	100
96	12-16-66	~680	28.4 ± .3	0	100
99	12-19-66	~680	29.0 ± .4	0	100
100	12-20-66	~678	29.0 ± .6	0	100
101	12-21-66	~680	28.8 ± .4	0	100
102	12-22-66	~678	31.0 ± .3	0	100
107	12-27-66	~667	30.5 ± .6	0	100
108	12-28-66	~680	30.9 ± .3	0	100
109	12-29-66	~680	30.7 ± .4	0	100
110	12-30-66	~675	31.4 ± .7	0	100

Carbon Monoxide Conversion Efficiency (continued)

Day	Date	Temperature °F	Inlet Concentration mg/m^3 at 10 psia	Outlet Concentration mg/m^3 at 10 psia	Conversion Efficiency %
114	1- 3-67	~675	31.5 ± .4	0	100
115	1- 4-67	~675	31.5 ± .3	0	100
116	1- 5-67	~675	29.0 ± .4	0	100
117	1- 6-67	~675	28.6 ± .4	0	100
120	1- 9-67	~678	28.0 ± .2	0	100
121	1-10-67	~675	29.4 ± .3	0	100
122	1-11-67	~655	28.6 ± .1	0	100
123	1-12-67	~660	29.0 ± .3	0	100
124	1-12-67	~660	29.4 ± .4	0	100
127	1-16-67	~610	29.4 ± .3	0	100
128	1-17-67	~610	29.5 ± .4	0	100
129	1-18-67	~585	27.5 ± .2	0	100
130	1-19-67	~585	29.7 ± .2	0	100
131	1-20-67	~585	28.9 ± .6	0	100
134	1-23-67	~590	28.7 ± .4	0	100
135	1-24-67	~590	27.3 ± 1.9	0	100
136	1-25-67	~587	29.2 ± .1	0	100
137	1-26-67	~585	29.5 ± .6	0	100
138	1-27-67	~585	29.4 ± .4	0	100
141	1-30-67	~588	29.5 ± .2	0	100
142	1-31-67	~585	28.2 ± .2	0	100
143	2- 1-67	~582	29.4 ± .2	0	100
144	2- 2-67	~587	29.5 ± .2	0	100
145	2- 3-67	~585	29.2 ± .2	0	100
148	2- 6-67	~585	29.4 ± .1	0	100
149	2- 7-67	~587	29.4 ± .1	0	100
150	2- 8-67	~560	30.1 ± 1.0	0	100
151	2- 9-67	~560	30.2 ± .9	0	100
152	2-10-67	~560	29.2 ± .6	0	100
155	2-13-67	~560	28.7 ± .1	0	100
156	2-14-67	~557	29.3 ± .2	0	100
157	2-15-67	~560	28.0 ± .3	0	100
158	2-16-67	~560	29.3 ± .7	0	100
159	2-17-67	~560	30.2 ± .7	0	100
162	2-20-67	~560	29.5 ± .4	0	100
163	2-21-67	~560	29.8 ± .2	0	100
164	2-22-67	~560	30.4 ± .5	0	100
165	2-23-67	~560	29.2 ± .7	0	100
166	2-24-67	~560	29.4 ± .2	0	100
169	2-27-67	~557	28.3 ± .7	0	100
170	2-28-67	~557	29.0 ± .5	0	100
171	3- 1-67	~560	28.3 ± .4	0	100

Carbon Monoxide Conversion Efficiency (continued)

Day	Date	Temperature °F	Inlet Concentration mg/m^3 at 10 psia	Outlet Concentration mg/m^3 at 10 psia	Conversion Efficiency %
172	3- 2-67	~560	29.0 ± .1	0	100
173	3- 3-67	~560	28.2 ± .8	0	100
176	3- 6-67	~560	29.0 ± .8	0	100
177	3- 7-67	~560	30.0 ± .3	0	100
178	3- 8-67	~560	29.0 ± 1.1	0	100
179	3- 9-67	~560	29.0 ± .4	0	100
180					

Appendix B-3

Acetylene Conversion Efficiency

Week	Date	Temperature °F	Inlet* Concentration mg/m^3 at 10 psia	Outlet Concentration mg/m^3 at 10 psia	Conversion Efficiency %
1	9-16-66	668	195 ± 5	0	100
2	9-23-66	675	185 ± 2	0	100
3	9-29-66	683	183 ± 2	0	100
4	10- 6-66	685	183 ± 3	0	100
5	10-13-66	683	180 ± 0	0	100
6	10-20-66	683	182 ± 1	0	100
7	10-27-66	676	181 ± 1	0	100
8	11- 3-66	683	187 ± 2	0	100
9	11-10-66	~679	185 ± 2	0	100
10	11-17-66	~681	186 ± 3	0	100
11	11-23-66	~680	186 ± 3	0	100
12	12- 1-66	~678	186 ± 3	0	100
13	12- 8-66	~680	182 ± 2	0	100
14	12-15-66	~680	180 ± 4	0	100
15	12-22-66	~678	192 ± 2	0	100
16	12-29-66	~680	190 ± 2	0	100
17	1- 5-67	~675	181 ± 3	0	100
18	1-12-67	~660	181 ± 2	0	100
19	1-19-67	~585	183 ± 1	0	100
20	1-26-67	~585	182 ± 4	0	100
21	2- 2-67	~587	183 ± 1	0	100
22	2- 9-67	~560	186 ± 1	0	100
23	2-16-67	~560	182 ± 5	0	100
24	2-23-67	~560	182 ± 5	0	100
25	3- 2-67	~560	180 ± 1	0	100
26	3- 8-67	~560	179 ± 6	0	100

*SMAC: 180 mg/m^3 at 10 psia

Appendix B-3 (continued)

n-Butane Conversion Efficiency

Week	Date	Temperature °F	Inlet Concentration mg/m^3 at 10 psia	Outlet Concentration mg/m^3 at 10 psia	Conversion Efficiency %
1	9-16-66	668	195 ±5	5.8 ± .1	96.0 ±1.3
2	9-23-66	675	185 ±2	9.3 ± .1	95.0 ±1.3
3	9-29-66	683	183 ±2	7.3 ± .1	96.0 ±1.6
4	10- 6-66	685	183 ±3	4.9 ± .1	97.3 ± .4
5	10-13-66	683	180 ±0	7.2 ± .1	96.0 ± .4
6	10-20-66	683	182 ±1	5.5 ± .1	97.0 ±1.3
7	10-27-66	676	18p ±1	4.7 ± .2	97.4 ± .2
8	11- 3-66	683	187 ±2	6.9 ± .2	96.3 ±1.7
9	11-10-66	~679	185 ±2	5.6 ±0	97.0 ±0
10	11-17-66	~681	186 ±3	3.4 ± .1	98.2 ± .8
11	11-23-66	~680	186 ±3	6.9 ± .1	96.3 ±1.1
12	12- 1-66	~678	186 ±3	8.9 ± .1	95.2 ±2.2
13	12- 8-66	~680	182 ±2	3.6 ± .1	98.0 ± .3
14	12-15-66	~680	180 ±4	2.9 ± .1	98.4 ± .7
15	12-22-66	~678	192 ±2	5.8 ± .1	97.0 ± .3
16	12-29-66	~680	190 ±2	1.9 ± .1	99.0 ±1.4
17	1- 5-67	~675	181 ±3	3.6 ± .1	98.0 ± .5
18	1-12-67	~660	181 ±2	8.5 ± .1	95.3 ±1.0
19	1-19-67	~585	183 ±1	2.2 ± .1	93.8 ± .9
20	1-26-67	~585	182 ±4	9.1 ± .2	95.0 ± .6
21	2- 2-67	~587	183 ±1	2.7 ± .1	98.5 ±1.1
22	2- 9-67	~560	186 ±1	15.0 ± .1	92.0 ±2.9
23	2-16-67	~560	182 ±5	7.3 ± .1	96.0 ±1.1
24	2-23-67	~560	182 ±5	4.7 ± .1	97.4 ± .1
25	3- 2-67	~560	180 ±1	4.1 ± .1	97.7 ± .2
26	3- 9-67	~560	179 ±6	4.8 ± .1	97.3 ± .4

Appendix B-3 (continued)

Ethane Conversion Efficiency

Week	Date	Temperature °F	Inlet Concentration mg/m^3 at 10 psia	Outlet Concentration mg/m^3 at 10 psia	Conversion Efficiency %
1	9-16-66	668	195 ±5	40.0 ± .5	79.5 ±1.3
2	9-23-66	675	185 ±2	37.0 ± .5	80.0 ±1.3
3	9-29-66	683	183 ±2	31.1 ± .7	83.0 ±1.6
4	10- 6-66	685	183 ±3	32.0 ± .2	82.5 ± .4
5	10-13-66	683	180 ±0	43.2 ± .3	76.0 ± .4
6	10-20-66	683	182 ±1	33.7 ± .7	81.5 ±1.3
7	10-27-66	676	181 ±1	35.8 ±1.2	80.2 ± .2
8	11- 3-66	683	187 ±2	29.0 ± .8	84.5 ±1.7
9	11-10-66	~679	185 ±2	34.7 ±0	81.3 ±0
10	11-17-66	~681	186 ±3	30.7 ± .5	83.5 ± .8
11	11-23-66	~680	186 ±3	43.7 ± .6	76.5 ±1.1
12	12- 1-66	~678	186 ±3	51.2 ± .8	72.5 ±2.2
13	12- 8-66	~680	182 ±2	20.9 ± .2	88.5 ± .3
14	12-15-66	~680	180 ±4	25.7 ± .5	85.7 ± .7
15	12-22-66	~678	192 ±2	29.8 ± .3	84.5 ± .3
16	12-29-66	~680	190 ±2	15.2 ± .2	92.0 ±1.4
17	1- 5-67	~675	181 ±3	27.2 ± .4	85.0 ± .5
18	1-12-67	~660	181 ±2	50.7 ± .5	72.0 ±1.0
19	1-19-67	~585	183 ±1	36.3 ± .2	70.2 ± .9
20	1-26-67	~585	182 ±4	34.2 ± .7	71.2 ± .6
21	2- 2-67	~587	183 ±1	29.3 ± .6	84.0 ±1.1
22	2- 9-67	~560	186 ±1	47.4 ±2.2	74.5 ±2.9
23	2-16-67	~560	182 ±5	45.4 ± .8	75.0 ±1.1
24	2-16-67	~560	182 ±5	37.8 ± .2	79.2 ± .1
25	3- 2-67	~560	180 ±1	44.2 ± .2	75.4 ± .6
26	3- 9-67	~560	179 ±6	39.3 ± .5	78.2 ±2.5

Appendix B-3 (continued)

Propylene Conversion Efficiency

Week	Date	Temperature °F	Inlet Concentration mg/m^3 at 10 psia	Outlet Concentration mg/m^3 at 10 psia	Conversion Efficiency %
1	9-16-66	668	195 ±5	0	100
2	9-23-66	675	185 ±2	0	100
3	9-29-66	683	183 ±2	0	100
4	10- 6-66	685	183 ±3	0	100
5	10-13-66	683	180 ±0	0	100
6	10-20-66	683	182 ±1	0	100
7	10-27-66	676	181 ±1	0	100
8	11- 3-66	683	187 ±2	0	100
9	11-10-66	~679	185 ±2	0	100
10	11-17-66	~681	186 ±3	0	100
11	11-23-66	~680	186 ±3	0	100
12	12- 1-66	~678	186 ±3	0	100
13	12- 8-66	~680	182 ±2	0	100
14	12-15-66	~680	180 ±4	0	100
15	12-22-66	~678	192 ±2	0	100
16	12-29-66	~680	190 ±2	0	100
17	1- 5-67	~675	181 ±3	0	100
18	1-12-67	~660	181 ±2	0	100
19	1-19-67	~585	183 ±1	0	100
20	1-26-67	~585	182 ±4	0	100
21	2- 2-67	~587	183 ±1	0	100
22	2- 9-67	~560	186 ±1	0	100
23	2-16-67	~560	182 ±5	0	100
24	2-23-67	~560	182 ±5	0	100
25	3- 2-67	~560	180 ±1	0	100
26	3- 9-67	~560	179 ±6	0	100

LIBRARY CARD ABSTRACT

This report describes the results of a design study for an isotope-heated catalytic oxidizer. This program included a study of all critical aspects of an isotope fuel element with selection of a preferred isotope, catalyst screening tests with selection of a preferred catalyst, and a 180-day test of this catalyst under expected operating conditions to determine if performance degradation occurs. Additional tasks included design of the isotope heating element and an analysis and optimization to determine the system configuration having the minimum weight penalty. The final design was documented with layout drawings. A development plan was also prepared describing the steps leading to flight qualifiable hardware.